AGARD-LS-103

AGARD

ADVISORY GROUP FOR AEROSPACE RESEARCH & DEVELOPMENT

7 RUE ANCELLE 92200 NEUILLY SUR SEINE FRANCE

AGARD LECTURE SERIES No. 103

Non-Destructive Inspection Methods for Propulsion Systems and Components

NORTH ATLANTIC TREATY ORGANIZATION

UNITED STATES DEPARTMENT OF COMMERCE
National Technical Information Service
5285 Port Royal Road
Springfield, Virginia 22161

Date 5 June 1974 NTIS Control # 154 C10

TO: Defense Documentation Center - DDC/TC
Cameron Station
Alexandria, Virginia 22314

FROM: NTIS, Input Branch
5285 Port Royal Road
Springfield, Virginia 22161

Report # Agard - LS - 103 ADA # _____

Title: Non-Destructive inspection methods for...

Subject report is ☒ Standard Process ☐ STG report. STG - Special Technology Group. ☐ Computer Product. ☐ Follow up date _____.

☐ The report will be accessioned by DDC. The form noting the ADA number is returned.

☐ The report has been assigned the ADA number noted above and is returned to NTIS for processing.

☐ DDC will not process the report. It is returned to NTIS.

Mag Tape Price _____
PC & MF Price _____
Stock Quantity 4
Comments: Bin - 148

Source DODSD
Source Share _____

_____
Signature (for billing)

Copy when completed to
Finance Branch.

DOD Report Action Request
(Replaces NTIS-164 5-72)

Dottie Adams
Processor

UNITED STATES DEPARTMENT OF COMMERCE
National Technical Information Service
5285 Port Royal Road
Springfield, Virginia 22161

Date 8 June 1979 NTIS Control # 159 C10

TO: Defense Documentation Center - DDC/TC
Cameron Station
Alexandria, Virginia 22314

FROM: NTIS, Input Branch
5285 Port Royal Road
Springfield, Virginia 22161

AD A069901

Report # Agard - LS - 103 ADA #

Title: Non. Destructive Inspection Methods for.

Subject report is ☒ Standard Process ☐ STG report. STG - Special Technology Group. ☐ Computer Product. ☐ Follow up date .

☐ The report will be accessioned by DDC. The form noting the ADA number is returned.

☐ The report has been assigned the ADA number noted above and is returned to NTIS for processing.

☐ DDC will not process the report. It is returned to NTIS.

Mag Tape Price
PC & MF Price
Source DOD SD
Stock Quantity 4
Source Share
Comments: Bin - 148

Signature (for billing)

Copy when completed to
Finance Branch.

DOD Report Action Request
(Replaces NTIS-164 5-72)

Dottie Adams
Processor

NORTH ATLANTIC TREATY ORGANIZATION

ADVISORY GROUP FOR AEROSPACE RESEARCH AND DEVELOPMENT

(ORGANISATION DU TRAITE DE L'ATLANTIQUE NORD)

(7)

AGARD Lecture Series No.103

(6)

NON-DESTRUCTIVE INSPECTION METHODS FOR PROPULSION SYSTEMS AND COMPONENTS.

(11) Apr 79 (12) 256p.

The material in this publication was assembled to support a Lecture Series under the sponsorship of the Propulsion and Energetics Panel and the Consultant and Exchange Programme of AGARD and presented on 23–24 April 1979 in London, UK, and on 26–27 April 1979 in Milan, Italy.

THE MISSION OF AGARD

The mission of AGARD is to bring together the leading personalities of the NATO nations in the fields of science and technology relating to aerospace for the following purposes:

- Exchanging of scientific and technical information;
- Continuously stimulating advances in the aerospace sciences relevant to strengthening the common defence posture;
- Improving the co-operation among member nations in aerospace research and development;
- Providing scientific and technical advice and assistance to the North Atlantic Military Committee in the field of aerospace research and development;
- Rendering scientific and technical assistance, as requested, to other NATO bodies and to member nations in connection with research and development problems in the aerospace field;
- Providing assistance to member nations for the purpose of increasing their scientific and technical potential;
- Recommending effective ways for the member nations to use their research and development capabilities for the common benefit of the NATO community.

The highest authority within AGARD is the National Delegates Board consisting of officially appointed senior representatives from each member nation. The mission of AGARD is carried out through the Panels which are composed of experts appointed by the National Delegates, the Consultant and Exchange Programme and the Aerospace Applications Studies Programme. The results of AGARD work are reported to the member nations and the NATO Authorities through the AGARD series of publications of which this is one.

Participation in AGARD activities is by invitation only and is normally limited to citizens of the NATO nations.

Published April 1979

ISBN 92-835-0237-X

Printed by Technical Editing and Reproduction Ltd
Harford House, 7–9 Charlotte St, London, W1P 1HD

PREFACE

This Lecture Series No.103 on the subject of Non-Destructive Inspection Methods for Propulsion Systems and Components is sponsored by the Propulsion and Energetics Panel of AGARD and implemented by the Consultant and Exchange Programme.

The safety in use of mechanical systems is dependent on the identification of possible defects in their component parts. This particularly applies to turbine engines, certain components of which, especially turbine and compressor discs and blades, are subjected to particularly severe stresses; creep, low cycle fatigue, thermal fatigue.

These potential defects must be detected, on the one hand when the parts are at the manufacturing stage and, on the other, during periodic inspections in service.

It is, therefore, essential to have available non-destructive inspection methods which, while they are accurate and sensitive, can be used in the workshop for the detection of even minor defects and cracks.

A considerable amount of research work has been done throughout the world in this field and has led to the development of various methods; ultrasonic, magnetometer, X-ray. New procedures, which are complementary to these now conventional methods, are in process of development or optimization; acoustic emission, laser holography, eddy current etc.

The aim of this Lecture Series is to survey the means currently available, with particular emphasis on the intrinsic possibilities and present limitations of the non-destructive inspection methods most widely applied to turbine engines, and to describe the state of progress of research on more recent methods.

LIST OF SPEAKERS

Lecture Series Director: l'Ingénieur en Chef de l'Armement
G.Bessonnat
Direction des Recherches,
Etudes et Techniques pour l'Armement
26 Boulevard Victor
75996 Paris Armées
France

Mr J. de Belleval
Office National d'Etudes et de Recherches Aérospatiales
29 Avenue de la Division Leclerc
92320 Châtillon-sous-Bagneux
France

Mrs D.M.Comassar
NDT Operations
General Electric Company
Aircraft Engine Group
Cincinnati, Ohio 45215
USA

Mr P.Dumousseau
Centre d'Etudes Techniques des Industries Méchaniques
BP No.67
60304 Senlis
France

Dr R.E.Green
Mechanics and Materials Science Dept
The John Hopkins University
Baltimore, Maryland 21218
USA

Dr T.J.Moran
AFML/LLP
Wright-Patterson Air Force Base
Dayton
Ohio 45433
USA

Mr R.W.Parish
Atomic Energy Research Establishment
Harwell
Oxfordshire
UK

Mr N.Parr
2 Surbiton Court
St Andrew's Square
Surbiton, Surrey
UK

Mr J.Ritchie
Ministry of Defence (Procurement Executive)
Materials Department
Royal Aircraft Extablishment
Farnborough
Hampshire
UK

CONTENTS

	Page
PREFACE	iii
LIST OF SPEAKERS	iv
	Reference
INTRODUCTION (in English and French) by G.Bessonnat	1
STATE-OF-THE-ART OF NON DESTRUCTIVE INSPECTION OF AIRCRAFT ENGINES by D.M.Comassar	2
HIGH RESOLUTION RADIOGRAPHY IN THE AERO-ENGINE INDUSTRY by R.W.Parish	3
WEAR DEBRIS ANALYSIS by N.L.Parr and J.Ritchie	4
HIGH RESOLUTION ULTRASONIC NON-DESTRUCTIVE TESTING OF COMPLEX GEOMETRY COMPONENTS by T.J.Moran	5
NON-DESTRUCTIVE METHODS FOR THE EARLY DETECTION OF FATIGUE DAMAGE IN AIRCRAFT COMPONENTS by R.E.Green, Jr	6
CONTROLE IN SITU PAR EMISSION ACOUSTIQUE DE SOUDAGES PAR BOMBARDEMENT ELECTRONIQUE par P.F.Dumousseau	7
TRANSDUCTEURS ULTRASONORES A LARGE BANDE POUR LE CONTROLE NON DESTRUCTIF DE PIECES AERONAUTIQUES par J. de Bellevil	8
BIBLIOGRAPHY	B

INTRODUCTION

Cette Lecture Series N° 103 est établie dans le cadre de l'activité du "Propulsion and Energetics Panel", et du "Consultant and Exchange Programm" de l'AGARD.

Elle a pour but d'examiner et de commenter l'état actuel de l'art, et les progrès prévisibles ou attendus des méthodes de contrôle non destructif appliquées aux pièces de turbomachines et autres moteurs thermiques.

La réalisation de ces turbomachines ou moteurs thermiques de hautes performances nécessite la mise en oeuvre de matériaux et techniques de plus en plus sophistiqués. De plus, le niveau de sécurité exigé sur les composants de ces matériels exige des techniques de contrôle non destructif de plus en plus évoluées.

Les défauts à détecter sont de nature et d'origine diverses :

- défauts de fabrication :
  - géométriques : soufflures, porosités, retassures, manques de liaisons,
  - métallurgiques : inclusions, précipitations grossières ;
- défauts apparaissant en utilisation : essentiellement criques ou fissures de fatigue, de fluage, éventuellement zones de corrosion.

Une unique méthode de contrôle ne peut prétendre à elle seule révéler ou identifier avec la même efficacité ces différents types de défauts ; il est donc important de pouvoir disposer d'une gamme de méthodes, faisant appel à des principes physiques différents, pouvant être utilisées conjointement ou non suivant le type de défaut à détecter, et le degré de sécurité exigé pour le composant ; et ceci sans perdre de vue le coût de ces opérations de contrôle.

Certaines de ces méthodes sont déjà anciennes, mais font souvent l'objet de perfectionnements incessants ; on peut citer en particulier :

- ultra-sons : si le principe général de cette méthode est maintenant bien connu, des nouveautés apparaissent soit au niveau du palpeur : largeur de bande utilisée, amortissement de l'élément sensible, soit dans la définition même de la méthode de contrôle ; imagerie acoustique, diffraction ultra-sonore ;
- radiographie : cette méthode également très ancienne connait différents perfectionnements récents : amélioration du pouvoir séparateur par utilisation de matériel microfocal, augmentation de la sensibilité des films.

D'autres méthodes sont apparues plus récemment, en particulier :

- émission acoustique : la difficulté essentielle de cette méthode réside dans l'interprétation des signaux sonores recueillis ; un traitement approprié de ces signaux devrait remédier en partie à cet handicap ;

.../...

- courants induits : cette méthode est de plus en plus utilisée pour la vérification des alésages ;

- holographie laser dont la mise en oeuvre en atelier reste encore délicate.

Dans le cas des défauts apparaissant en service, il serait évidemment souhaitable de pouvoir détecter leur apparition le plus tôt possible, afin de réduire le risque de rupture par développement de la fissure, et également d'alléger la fréquence des opérations de contrôle ; une analyse fine des anomalies métallurgiques précédant l'apparition de fissures macroscopiques semble pouvoir ouvrir une nouvelle philosophie de contrôle.

Enfin, le suivi en utilisation de la dégradation par usure des organes mécaniques peut être effectué en analysant la nature et la forme des débris d'usure recueillis dans les circuits hydrauliques et de lubrification ; cette technique, qui permet de prévoir les ruptures d'organes mécaniques après un taux d'usure déterminé, est déjà utilisée pour les boîtes de transmission d'hélicoptères, et peut être étendue aux pièces de moteurs.

Il est évident que les procédés de contrôle décrits dans cette Lecture Series ne s'appliquent pas seulement uniquement aux composants de moteurs, et turbomachines, et peuvent présenter ou présentent de l'intérêt pour d'autres applications, essentiellement dans le domaine aérospatial.

Leur efficacité et leurs éventuels progrès constituent un très important facteur de la sécurité d'utilisation de ces matériels.

L'Ingénieur en Chef de l'Armement BESSONNAT
Lecture Series n° 103's Director.

INTRODUCTION

This Lecture Series N° 103 is sponsored by the "Propulsion and Energetics Panel" and implemented by the "Consultant and Exchange Program" of AGARD.

Its aim is to examine and comment on to-day's state of the art, and the foreseeable or hoped progress of the non-destructive inspection methods applied to the turbine or pistons engine. The manufacturing of these kinds of mechanical systems needs the use of more and more sophisticated materials and processes.

The defects it's necessary to detect are of various kinds and various origins :

- manufacturing defects :
  - geometrical defects : blow holes, pores, shrinkages, voids ;
  - metallurgical defects : inclusions, coarse precipitations ;
- defects occurring in use : mainly fatigue cracks, creep cracks, occasionnally corrosion areas.

Only one method can't claim to detect or identify all these kinds of defects with the same effectiveness ; so, it is particulary important to have one's disposal a large range of methods with different physical bases ; these testing techniques must be used together or not according to the type of defect, and the safety level required for the component ; last but not least, it's opportune to take the cost of these operations into consideration !

Some of these proceduces are already established, but are incessantly improved upon :

- ultrasonic emission : this technique seems wellknown to-day, but is still in improving, either the transducer : broad of the band, damping of the piezo-electric wafer, or the process itself : acoustic imaging, ultrasonic diffraction ;
- radiography : this technique although very old is also continually being revised : improvement of the resolution, in using a microfocal X-ray equipment, and raising of the sensibility of the films.

Other methods have been born more recently :

- Acoustic emission : the main difficulty is not to listen, but to understand the sound signals ! So, a probable new processing of the signals could add to this disadvantage ;

- Eddy currents : this technique is more and more used for the inspection of holes ;

- Laser holography : the possibility to use it in a workshop still presents some difficulties.

Concerning the defects arising in service there is evidence leading to detection of defects as soon as possible, in the aim to decrease the possibility of rupture after the growth of a crack, and also to reduce the weight of the periodic inspections ; this seems possible with a fine analysis of the metallurgical phenomenal occurring just before the growth of macroscopics cracks.

At last, the control in service of the wear damaging of the mechanical components can be done in analysing the kind and the geometry of the wear debris collected in hydraulic or lubricant fluids ; with this technique, it is possible to foresee the break of these components after a defined level of wear ; this procedure is already used about the gear-boxes of helicopters, and seems to be extended at the engine components.

Of course, the N.D.I. methods described in this Lecture Series are not only available to the engine parts or pieces, but are sometimes applied to other mechanical composents, mainly in the aeronautical or space technology field.

The future improvements in safety level of aircraft propulsion systems will be gained through the efficiency and progress of these N.D.I. materials.

L'Ingénieur en Chef de l'Armement BESSONNAT
Lectures Series N° 103's Director.

STATE-OF-THE-ART OF NONDESTRUCTIVE INSPECTION OF AIRCRAFT ENGINES

by
D. M. Comassar
Manager, Aircraft Engine Quality Technology
General Electric Company
Cincinnati, Ohio 45215
Mail Drop E-45

The continuing emphasis on high performance aircraft engines over the past 20 years has required that nondestructive inspection methods keep pace with the resulting technology growth associated with the design and manufacture of these power plants. The use of higher strength alloys, the need for longer life components and the emphasis on lower life cycle costs all require that the components in the power plant be more fault free than past generation engines.

New and engine-run hardware requirements are such that not only is the detection of smaller flaws in the range of .010" (.256 mm) required, but also more reliable detection. This has both basic process as well as equipment implications. It has been our experience that an improved understanding of the basic NDI processes coupled with the identification of necessary technology extensions is required in order to reduce the gap between the desired and actual flaw detection capabilities. Additionally, new manufacturing technologies continually provide a motivation toward more effective NDI processes for hardware quality control. This is the environment we are dealing with as an aircraft engine manufacturer. Specifically, this discussion is aimed at describing where we stand today in applying state-of-the-art inspection techniques to engine components. Focus is on major engine components where the demands are more stringent.

There are five basic NDI disciplines which are more commonly applied to engine components, namely ultrasonic, eddy current, fluorescent penetrant, radiographic and magnetic particle inspection. There are a number of recent advancements in the ultrasonic and eddy current processes as well as improvements in the fluorescent penetrant process that will be discussed. These advancements are primarily in the equipment area and in the automation of the inspection process both of which provide improved capability, more reliable inspections and also a reduction in inspection costs. Major advancements have not been seen in the application of radiographic and magnetic particle inspections as they apply to aircraft engine hardware. Thus, this discussion will focus on improvements in the ultrasonic, eddy current and fluorescent penetrant processes. Several nonconventional techniques used for inspection of development hardware will also be discussed.

Ultrasonic Inspection

Typically, all major rotating hardware is ultrasonically inspected as it enters the manufacturing cycle. This is done after the forging has been rough machined into rectilinear shapes with a specified envelope to accommodate the inspection. Current production systems are designed to handle a 0.125" (3.2 mm) envelope.

A typical system in use today is shown in Figure #1. Note that the basic motion control of the system is provided by a numerical control machine. Experience has shown improved inspection consistency with the use of this equipment. The numerical control tapes which direct the system provide the following controls:

- Constant water path.
- Transducer angulation to allow longitudinal and shear inspection modes.
- Part contour following.
- All required scans both in quantity and type.

All flaw indications are recorded for each part on a strip chart recording. Accept/reject decisions are on the basis of signal amplitude. The system just described has been in successful operation since 1974.

Several innovative improvements have been introduced into these systems within the past year and one-half. These include replacing the previously used APT (Automatic Programmed Tools) numerical control language with one which better describes the ultrasonic inspection process. This new language is called WRIPP - which stands for Wrenn's Interactive Parts Programming. Figure #2 shows a comparison between the APT and Wripp systems. There are a number of features of the WRIPP system which are shown in Figure #3. With the APT approach, numerical control (N/C) machine programmers prepared the N/C tapes in a batch process mode which took an average of one week. The tapes were checked-out with the part in the tank as in an inspection. Correction of the tape errors, which typically ran ~30%, were very time consuming.

The WRIPP system utilizes a graphics terminal which has been linked to the electronic part definition in the Computer Aided Design (CAD) and Computer Aided Manufacturing (CAM) systems. Through this linkage, the numerical control tape, plus the inspection scan plan and complete operator instructions, are generated. This is done interactively in approximately two hours. The WRIPP system features simple software routines which describe the ultrasonic process as well as tape checkout routines as part of the inspection planning package. Experience since introduction of the WRIPP system has been excellent with less than 1% of the tapes generated requiring correction.

The system just described utilizes advancements in the manufacturing and design areas through Computer Aided systems (CAD and CAM) and interfaces the inspection requirements to achieve maximum benefits.

In addition to newer programming techniques, such as WRIPP, advancements have been made in part contour following techniques, which have allowed ultrasonic inspection technology to keep pace with advanced material process technology. This material processing technology is now presenting shaped (nonrectilinear) hardware to the inspection process. From an inspection standpoint there are significant technology implications. These lie in both the instrumentation and transducers required to achieve near surface

resolution in the range of 0.050" (1.28 mm) as well as improved process understanding which relates the lens effects of the ultrasonic beam to part radii down to 0.500" (12.7 mm). Such an advanced system is currently under development and is shown in Figure #4. This system features advanced instrumentation and part following techniques as well as the following capabilities:

- Automatic

  - o System calibration.
  - o Distance amplitude correction.
  - o Correction for lens effects of radii.
  - o Flaw angulation technique to maximize signal response.
  - o 0.050" (1.28 mm) near surface resolution.
  - o Contour following of radii down to 0.500" (12.7 mm).

In addition to new inspection capability and the inherent benefits of an automatic inspection, there is a projected reduction in inspection time of ~40% when this system is introduced in early 1980.

The advancements in ultrasonic technology coupled with computer technology have led the way for similar advancements in other NDI processes. The visible gains from advancement of the ultrasonic process have provided an impetus for similar work with both the fluorescent penetrant and eddy current inspections.

Fluorescent Penetrant Inspection (FPI)

Probably the most widely applied nondestructive inspection in the aircraft engine industry is fluorescent penetrant inspection. While this technique has not experienced the advancements in basic process technology that ultrasonic inspection has, major improvements have been made. These improvements have made this process a viable candidate for automatic inspection techniques.

One of the more recently applied improvements is in the area of hydrophilic removers. These removers are now in wide application in the aircraft engine industry. Experience has shown the following improvements through application of these removers.

- Improved process tolerance.
- Less background fluorescence.
- Cost effective dilute solutions.

The reduced background fluorescence obtainable with hydrophilic removers has contributed greatly to improved inspectability while enhancing the opportunity for automated inspection techniques.

Recent improvements in water washable penetrants have indicated their suitability for certain engine components. These improvements include improved process tolerance which allows application in a production environment.

Over the past several years, a number of studies were conducted to determine the best penetrant system for different hardware types and materials. These studies were conducted on test blocks of different material types containing a range of low cycle fatigue cracks generated for test purposes. The block configuration is shown in Figure #5. Tests were run on iron, nickel and titanium based alloys. These blocks were used to generate relative flaw detection capability over a range of fluorescent penetrant systems. The following generic penetrant material types were tested.

- Penetrants

  - o High sensitivity post emulsification
  - o Ultra-high sensitivity post emulsification

- Emulsifiers

  - o Hydrophilic
  - o Lipophilic

- Developers

  - o Dry
  - o Nonaqueous

Figures #6 and #7 exemplify the type of data obtained. Figure #6 shows the relative effect of part base material on detection efficiency using an ultra-high sensitivity penetrant system. Figure #7 shows the effect of developers on detection efficiency by material type using an ultra-high sensitivity penetrant system. This type of information allows the best match of FPI system and part inspection needs.

Eddy Current Inspection

The two previously discussed inspection processes are broadly applied to newly manufactured hardware. However, eddy current inspection has been found most suitable for service-run hardware. There are a number of reasons why eddy current inspection has been successfully applied to service-run hardware; these stem from differences in the basic requirements for new and service-run hardware. Typical differences include:

	NEW	SERVICE-RUN
- Where the process is applied	In-process shapes	Final part shape
- The type and size of flaws	Material and process related flaws - typically larger flaws	Fatigue cracks - small cracks in compression
- Location of the flaws	Subsurface and surface flaws	Surface flaws
- Inspection coverage required	Bulk - Ultrasonic - FPI	Local inspection of critical areas and bulk - FPI

In considering the requirements for service-run hardware, eddy current inspection has been found by experience to be the most readily adaptable method to meet the majority of the requirements.

A number of more recent advancements have occurred in eddy current inspection. A major motivation for these improvements has been the increasing widespread application of this technique to aircraft engine hardware. This coupled with the continuing demand for improved flaw detection has provided impetus for improved capacity.

Eddy current inspection has demonstrated relatively high flaw detection capability in comparison with other NDI processes. Figure #8 depicts the relative capability of surface inspection techniques as demonstrated on low cycle fatigue (LCF) cracked specimens of titanium material. These cracked specimens were the same as described in the FPI studies.

While eddy current is very geometry-adaptable as shown in Figures #9, #10 and #11, the signal response can be affected by geometry. This geometry condition, which in earlier work impeded clear interpretation of the signal response, led to advancements in the area of signal processing. Figures #12 and #13 show signal response on several types of flaws before and after signal processing. Note the clarity of flaw interpretation after the signal has been electronically processed to remove low frequency components.

The instrumentation found most suitable to our applications is the impedance plane type. A typical vector diagram is shown in Figure #14. This type of instrumentation facilitates separation of flaw information as shown in the two channel strip charts in Figures #12 and #13.

Like ultrasonic inspection, there are many opportunities for improvement of the eddy current process as it is currently manually applied. Technology advancements are required to achieve these improvements. These reside in such things as having a computer compatible eddy current instrument, automated motion control, computer controlled steup, inspection and data analysis as well as a better understanding of eddy current field and flaw interpretations.

Development Inspection Methods

Several development inspection methods used primarily on nonproduction hardware are laser holography and infrared thermography. The holographic technique is typically applied as in Figure #15 to determine vibrational patterns of development hardware. The infrared technique can be used as in Figure #16 to determine unbond conditions. Also, microfocus X-ray and high frequency ultrasonic presents methods of flaw detection for special cases where very small flaws ($<$.010", .256 mm) must be found.

In summary, over the past several years, nondestructive inspection has received ever increasing emphasis at General Electric - Aircraft Engine Group. This emphasis is driven by new material and process technology, the need for longer life engine components and the emphasis on lower life cycle costs. Productivity provides another driver and further impetus toward automatic inspection features. While automation endeavors are for the most part still in their infancy, significant advancements in inspection process technology have been made. These advancements predominate in the ultrasonic process with major gains in the eddy current and fluorescent penetrant processes.

REFERENCES

1. Technical Memorandum #75-516, "Statistical Capability of Optimum Fluorescent Penetrant Methods for Detection of LCF Cracks" by T. Bantel
2. Technical Memorandum #76-18, "The Effect of Preheating Parts on the Detection Capability of LCF Cracks During FPI" by T. Bantel
3. Technical Memorandum #76-487, "Statistical Capability Studies of Eddy Current and Immersed Surface Wave Inspection for Detection of Low Cycle Fatigue Cracks" by R. Cammett
4. Technical Memorandum #77-523, "Eddy Current Process for LM2500 Blade Quality-Task II-The Establishment of Improved Methods of Eddy Current Signal Analysis" by K. Oelker
5. Technical Memorandum #78-431, "Titanium LCF Blocks for Airline Service Engineering NDT Field Testing" by T. Bantel
6. Technical Memorandum #78-496, "Fluorescent Penetrant Detection Capability of LCF Cracks in Powder Metallurgy Rene 95" by T. Bantel
7. 11/3/77, "The Introduction of Signal Processing Techniques to Eddy Current Testing" by EE Weismantel at National Bureau of Standards Conference on Nondestructive Testing, Gaithersburg, Maryland

8. 4/3/78, "The Application of Advanced Eddy Current Techniques to the Control of Cast Turbine Blade Quality" by EL Weismantel at 1978 ASNT Spring Conference, New Orleans, Louisiana

9. 7/18/78, "The Test Bed Concept as a Means of Introducing New Technology" by AL Thompson, EE Weismantel and DM Comassar at ARPA/AFML Conference on Quantitative NDE, LaJolla, California

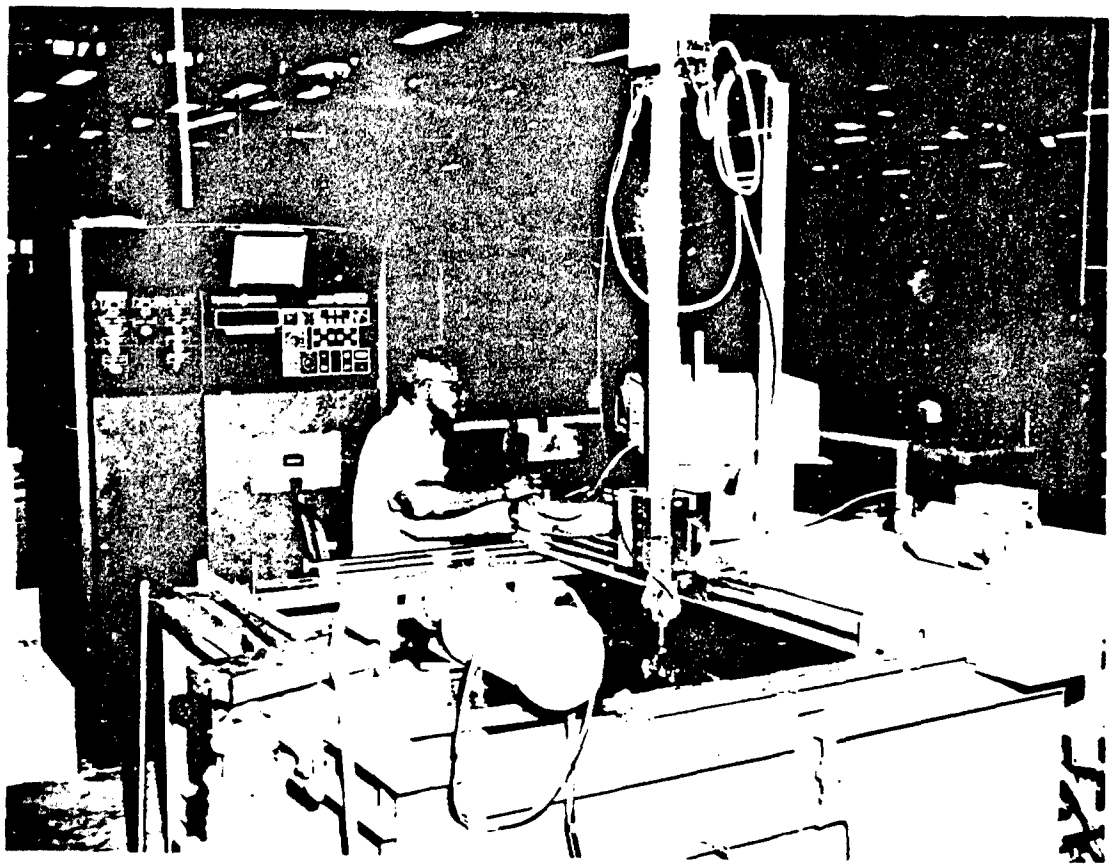

Figure 1

	APT	WRIPP
o Ease of Application	- Motion defined based on conic sections	- Scans defined by simple start and stop points
	- All motions must be specifically defined	- Only speed and mode required
o Planning	- Generated by hand	- Automated scan plans, operating sheets, planned times
o Process Verification	- Output checked by calculations or trial with part in tank	- Output displayed and verified graphically
		- Immediate feedback via graphics display

Fig.2 Comparison of APT and WRIPP in key areas

- o Interactive Graphics System for:
  - Definition of part configuration via CAD/CAM or interactively
  - Definition of scanning requirements
  - Generation of numerical control tape image
  - Generation of operator paperwork
- o Additional System Features:
  - Graphic display of manipulator motion for tape verification
  - Ready access for tape corrections or additions
  - Interfaced with overall CAD/CAM system

Fig.3 Features of WRIPP system

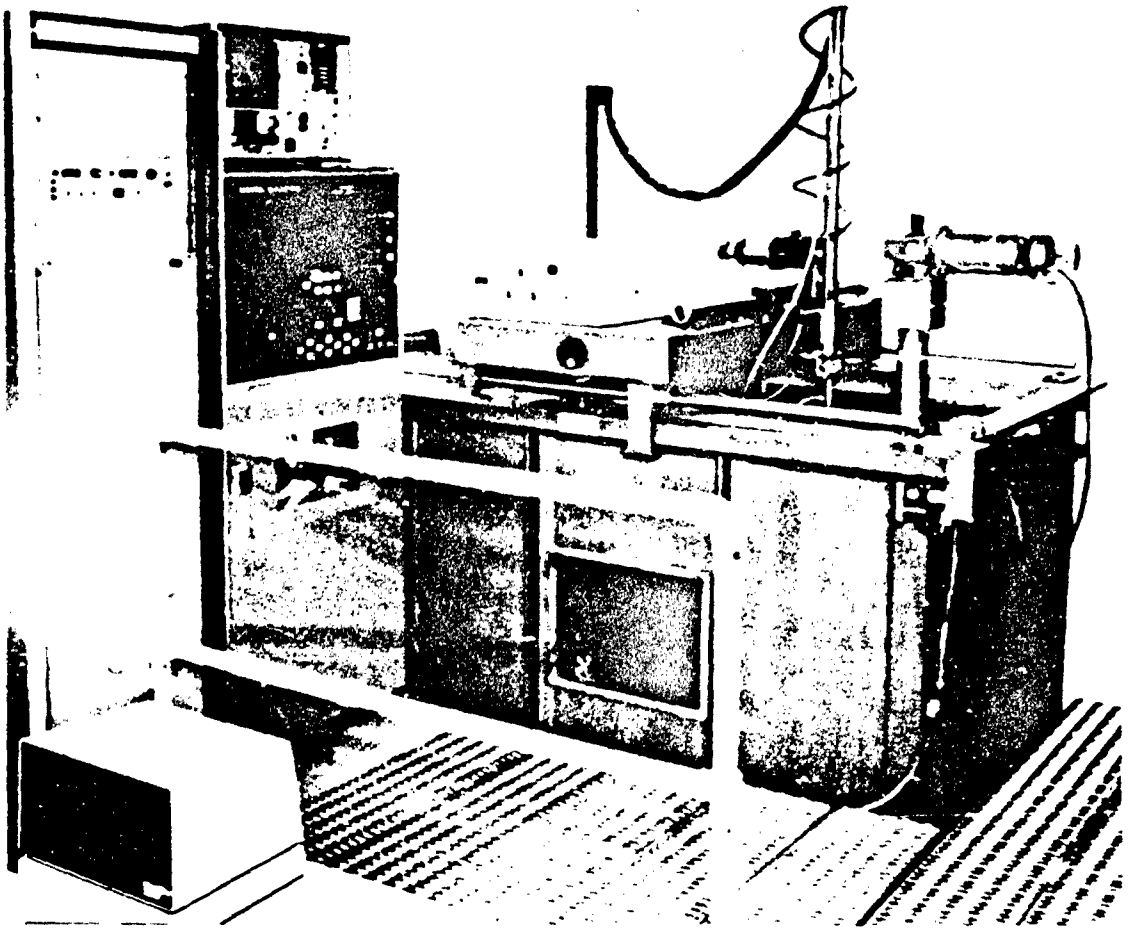

Figure 4

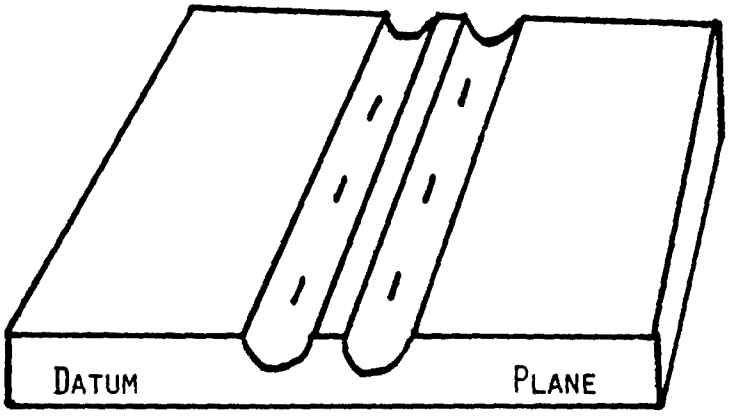

Fig.5 Fatigue crack test block

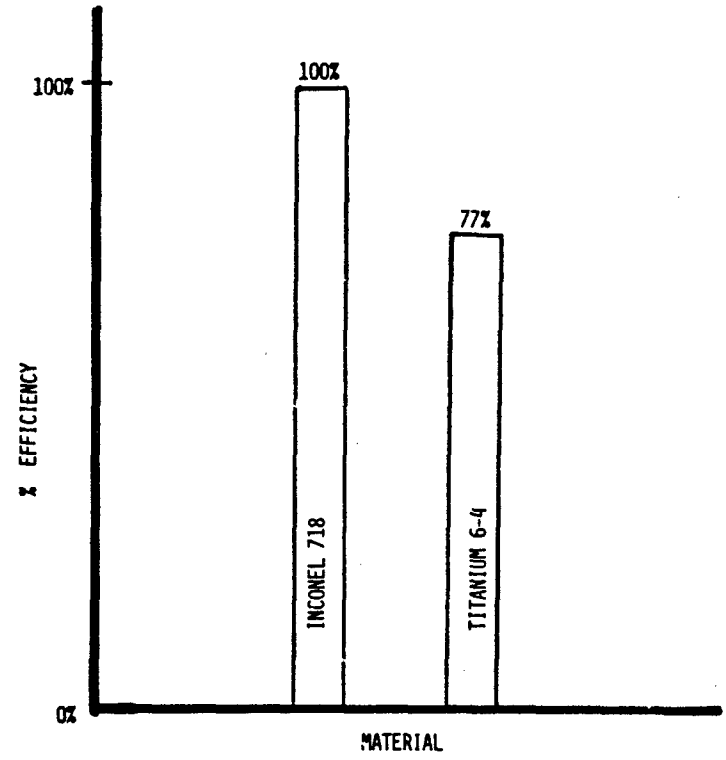

Fig.6 Efficiency of an ultra-high sensitivity penetrant system relative to alloy

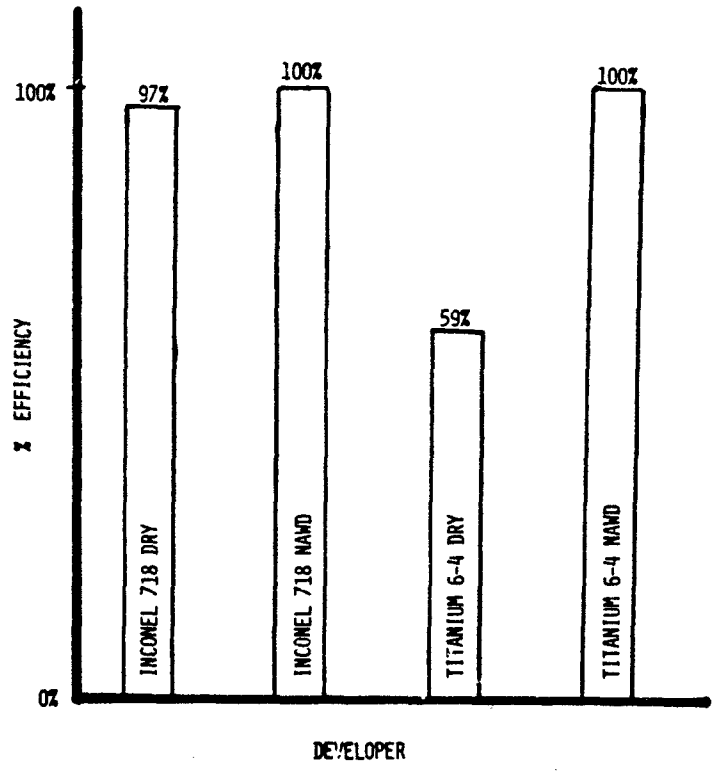

Fig.7 Efficiency of dry powder developer versus nonaqueous wet developer (NAWD) using an ultra-high sensitivity penetrant system

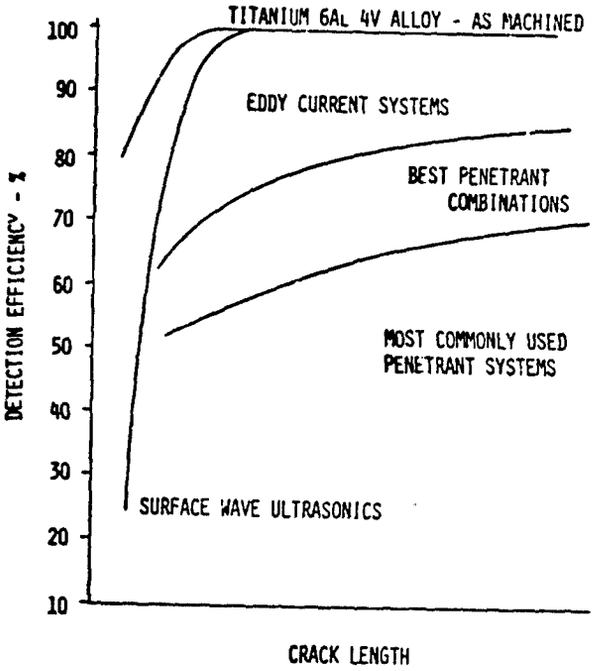

Fig.8 Comparsion of the typical detection performance of eddy current inspections with other surface sensitive processes

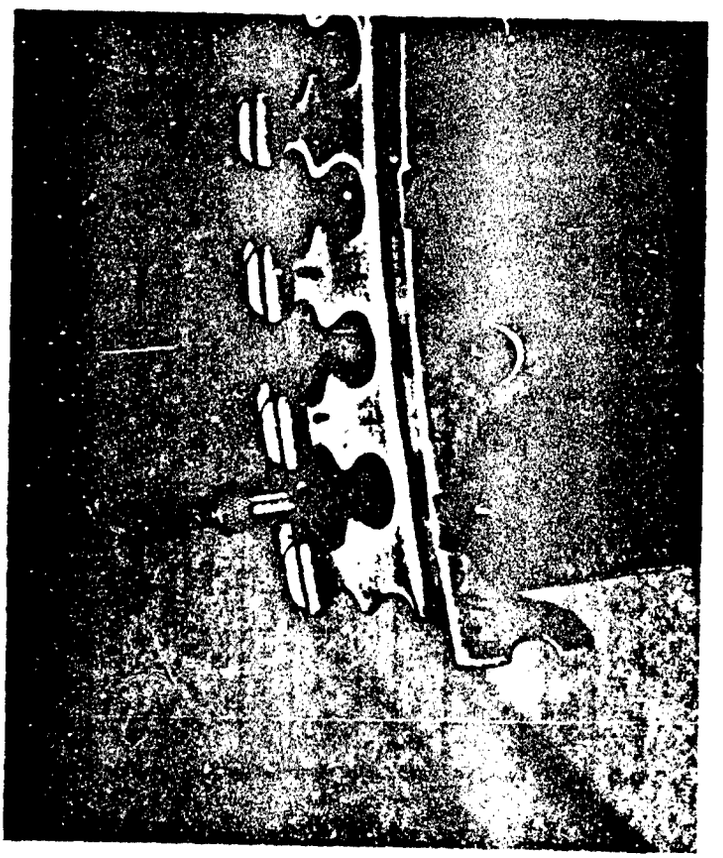

Figure 9

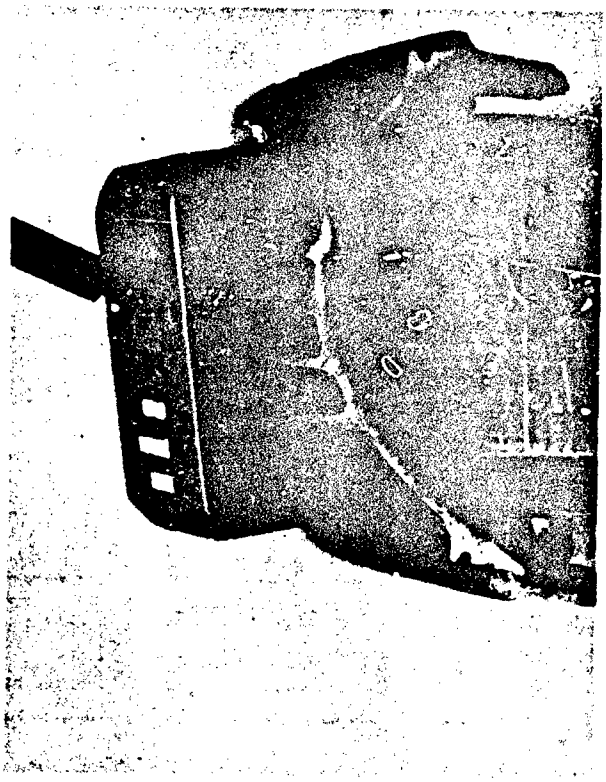

Figure 10

Figure 11

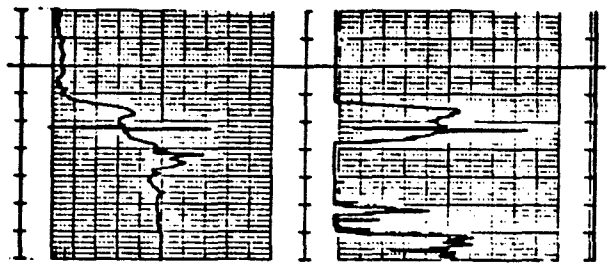

0.070" LONG CRACK (NATURAL FLAW)

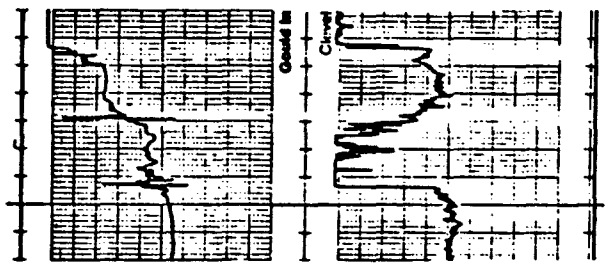

0.006" DIAMETER x 0.080" LONG HOLES - 0.003" BELOW THE INSPECTION SURFACE

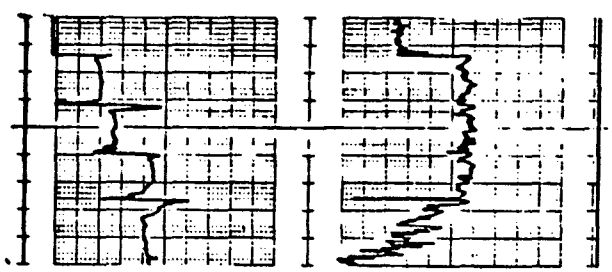

FOUR EDM NOTCHES - 0.020" x 0.010"

Fig.12 Illustration of typical eddy current response on turbine blade edges without signal processing

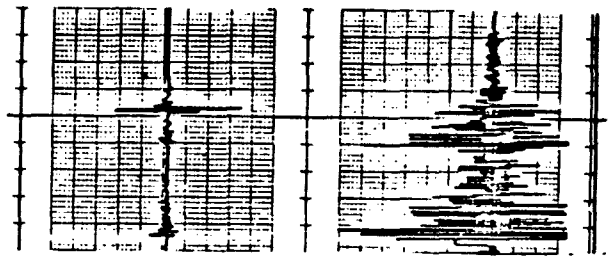

0.070" LONG CRACK . (NATURAL FLAW)

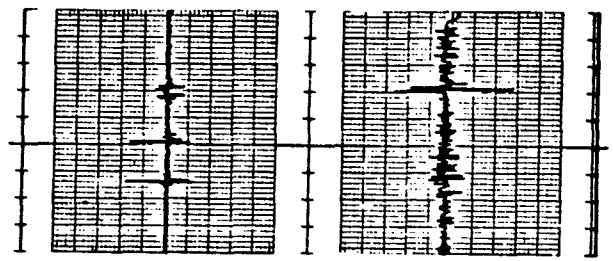

0.006" DIAMETER x 0.080" LONG HOLES

0.003" BELOW THE INSPECTION SURFACE

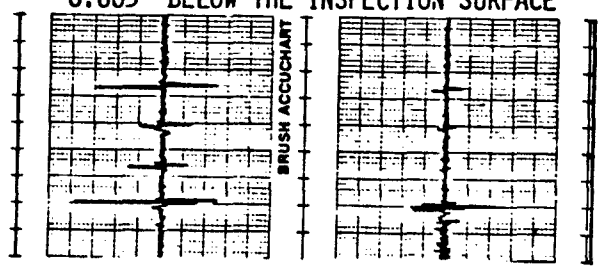

FOUR EDM NOTCHES - 0.020" x 0.010"

Fig.13 Illustration of typical eddy current response on turbine blade edges with signal processing

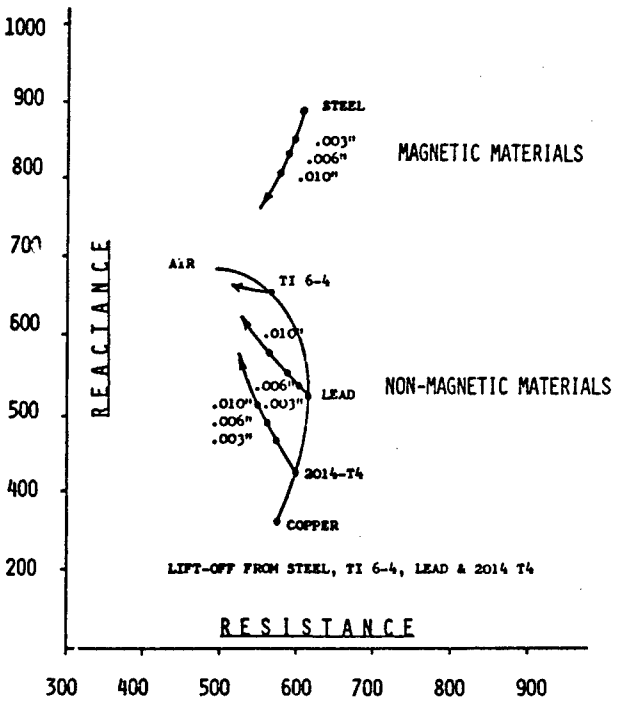

Fig.14 Impedance plane or vector diagram of electrical conductivity

Fig.15 Epoxy graphite blade nickel cladding

Fig.16 Nickel base alloy lap braze joint

HIGH RESOLUTION RADIOGRAPHY IN THE AERO-ZNGINE INDUSTRY

R.W. Parish, T.ENG.(C.E.I.) Member INST.NDT.

Manager, Advanced Application Unit,
Non-Destructive Testing Centre,
Material Physics Division,
A.E.R.E.,
Harwell,
Oxon. OX11 ORA

SUMMARY

This paper examines the practical problem of achieving adequate resolution in the broad field of radiography (x-rays, gamma rays and particle radiations) in the aero-engine industry. The interpretation of any industrial radiograph is a subjective process, involving the human eye and the experience and skill of the viewer. Although many automated and programmed interpretation systems have been postulated, there still remains a basic need to produce radiographic images which are sharply defined, so that the information contained in them can be analysed more readily by either man or machine.

Microfocal x-ray equipment which in certain circumstances can achieve considerably enhanced resolution is discussed and emphasis in the paper is placed on the application of these small x-ray sources to aero-engine components. These newer techniques allow small defects to be resolved which hitherto have been undetectable when using conventional x-ray techniques.

1. INTRODUCTION

These lecture notes are concerned with the interaction between two successful scientific and technological stories; the explosive development in aero-space design and the impact of x-radiography. The former has developed from the crude beginnings of the flying machine at the turn of the century to the technological achievements of supersonic flight. The latter concerns the accidental but brilliant discovery of x-rays in the same era which, apart from providing a vital tool in medicine, now contributes significantly in maintaining the low incidence of failure experienced with modern air transportation.

Radiography was used on aircraft as long ago as [1] the 1914-1918 war when wooden propellors were examined for the presence of cracking and other flaws. When in the 1920's aluminium alloys were first used for casting pistons, cylinder heads and crank cases, radiography had arrived into the industry. It was not until the 1940's however that radiography was rightfully acknowledged, by the inauguration of written codes and standards, as a useful and practical technique to ensure the soundness of components used in aero-engines.

In the UK a system was initiated in 1939 by the then named Aeronautical Inspection Directorate (AID) now named Aeronautical Quality Assurance Directorate (AQD) which examined and approved those engaged in the radiography of aircraft components. Part of the same approval scheme evoked the requirement not only of assessing the man but also the equipment and facilities at his disposal. The correct application of an appropriate and meaningful x-ray technique was realised even then to be of paramount importance if castings and weldments are to be confidently examined for the presence of internal flaws. Not only is assurance needed that the correct technique is applied but also that the sampling frequency is commensurate with the importance of the component.

For many components today a 100% radiographic inspection is mandatory. Modern practice in the aero-engine manufacturing industry is that radiographic acceptance standards are only established after agreement has been reached by teams comprising many disciplines within the industry. These include representatives of the development, engine design, stress, quality control and production departments. The metallurgial laboratory is also involved and (often belatadly) the non-destructive testing department; this latter often, in the event, provides the best communication link between the disciplines.

The inspection role of industrial radiography in the manufacture of components is well known in the industry but radiography has other lesser known but important roles. It features from the conception of the design of an engine, through the many scheduled maintenance inspections and is often used as an investigatory tool in the unhappy event of premature failure.

These stages which are presented in Table 1, are indicative of the scope and worth of radiography in the aircraft industry.

Table 1

Scope of radiography in the aero-engine industry

Stage	Applications
1. Design/Development	Dynamic radiography of engines Fluoroscopy of casting processes
2. Materials & Component Research & Development	Metallurgical samples. Special welding techniques. Assemblies
3. Manufacture	Quality Control of weldments, castings and assemblies
4. Maintenance	Detection of corrosion & cracking at inaccessible sites within an engine
5. Failure analysis	Examination prior to destructive tests etc.

A modern gas turbine consists of many thousands of individual components. These can be manufactured in a wide variety of materials, they vary considerably in size and complexity and are built using many differing manufacturing processes. Many of the components are highly stressed and the operating temperatures range from -40°C to greater than 1000°C. Critical crack lengths can vary from a few millimeters down to a few microns. Acceptable porosity levels or any other flaws in castings and weldments can also vary considerably.

Many of these components are successfully examined for the presence of defects with standard x-ray or other non-destructive testing methods but there are some that require more specialised techniques and work is still continuing on their development and introduction.

Other NDI methods of course play an important part but the role of radiography is still a considerable one despite the emphasis sometimes placed on the development of its alternatives. The components that are radiographed during the manufacture of an engine are listed below so that the extensive role of radiography in this sphere can be appreciated.

Table 2

Aero engine components

	Static Components
Casings	Welds in structural members, large complex fabrications, wrought and cast materials.
Combustion chambers	Welded fabrications in nickel based heat resistant alloys.
Guide vanes	Castings and fabrication weldments. Materials: Composites, aluminium titanium, steels, nickel/cobalt alloys.
	Dynamic Components
Turbine blades	Investment castings with complex cooling channel configurations.
	Auxiliary Components
Auxiliary Components	Welds and brazes in fuel and hydraulic systems. Cast tee and elbow joints. Electrical assemblies etc.

X-rays and gamma rays have established themselves in industry because of their ability conveniently to penetrate solid objects and to produce a two dimensional pictorial record. Their wide acceptance for inspection in the aircraft industry is not only due to this recording ability but, for many applications, they can be more economic than complementary techniques. As, for instance, an alternative to stripping down an assembly to allow visual inspection; thereby saving many manhours.

When the simple arrangement of radiography is considered (i.e. a radiation source, an object and a film) there is little wonder that radiography is acclaimed as the foremost method of examining interiors. Although to produce a radiograph is a relatively simple operation, the demands of obtaining a radiograph of adequate defect sensitivity are such that a large number of variables (Fig.1) has to be considered and where possible controlled. Radiography also demands a knowledge of the components and

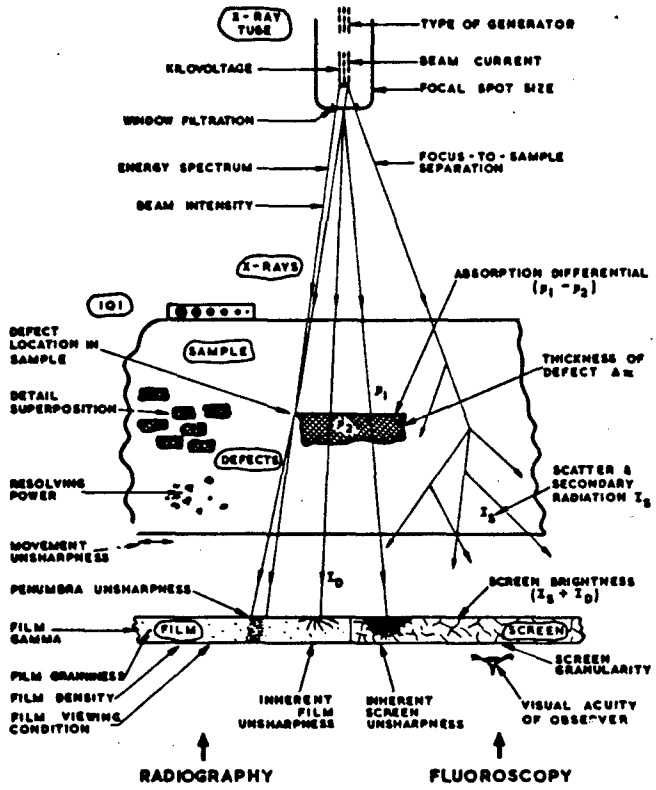

FIG. I. VARIABLE FACTORS IN RADIOGRAPHY & FLUOROSCOPY.

the processes that are used in manufacturing the component to decide on the type and the possible locations of defects that may occur. In maintenance inspections the conditions that may lead to wear, corrosion or cracking also should be known so that the sites are identified where defects may be found. Without a broad knowledge of these problems the conditions of the radiographic technique cannot be properly optimised.

The quality and standards of radiographic inspection used in the aircraft industry are such that it could be claimed that high resolution radiography is the norm rather than the special case. All radiographs must obviously be of an adequate quality to allow sensible interpretation. The resolution therefore must also be adequate for the purpose intended, i.e. it must be capable of resolving the desired details in the component or assembly. Another definition of resolution will be given later in photographic or radiographic terms, but in general terms resolution can also mean simply the resolution of a flaw in a component. Achieving adequate resolution in all aspects of aero-engine radiography is both an art and a science and should be recognised as such. These notes will therefore review and comment on the general problem, but emphasis will be on the application of minute sources of radiation and the results that have been obtained using them. It must be realised that there are many applications of radiography both in the production, and particularly in the maintenance, of aero engines when the results achieved are anything but high resolution, but can be useful nevertheless. A few examples will be given where radiographs need sometimes to be taken under unfavourable conditions; even so, with due consideration to the principles involved, adequate resolution can often be achieved thereby making radiography a viable technique.

High definition radiography will be specifically discussed because it is an x-ray technique which has recently emerged and is gaining ground as a viable inspection tool used to ensure the quality of some aero-engine components.

2. PRINCIPLES

At this stage some of the well known (and relevant in this context) principles of radiography should be briefly reviewed and also some of the terms that are used should be defined to allow the problems of producing high resolution radiographs to be explained.

Electromagnetic radiation (such as x and gamma rays) travel in straight lines, they are attenuated by matter depending on the types of material and the thickness of the material and they can be detected, usually by film. When the latent image on the film, caused by the photons emerging from the sample, is developed by a chemical process a radiograph is produced. The radiograph is then a two dimensional array of varying photographic densities revealing structural details within a solid specimen. The sharpness of the shadows thus produced depend on the effective size of the target (focal spot) within the x-ray tube (or, in the case of a radiographic isotope, the effective size of the metallic pellet).

The sharpness (Fig.2) also depends on the relationship between the ratio of distances a/b where;

a the distance from focal spot to object
and b the distance for object to film.

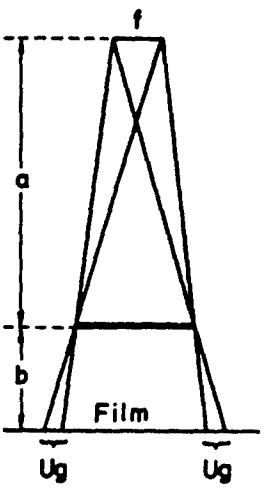

Unsharpness (Ug)
$= \frac{b\ f}{a}$

Figure 2

It is desirable therefore for the designers of conventional x-ray equipment to minimise the effective size of the focus but this can only be achieved by a subsequent reduction in intensity. Limits on tube loading are imposed by the melting temperature of the target material. Using excessive distances between the focus and the film (FFD) to improve sharpness leads to longer exposure times, as the intensity (I) decreases inversely with the square of the distance. Conventional x-ray sets for industrial use normally have effective focal spot sizes of between (1.5 mm x 1.5 mm) to as high as (6 mm x 6 mm). Radioisotopes from (0.5 mm x 0.5 mm) to (17 mm x 17 mm).

Sharpe [2] has pointed out that "although the maximum current of electrons which produce the x-ray beam is necessarily lower with extremely small spots the current density, or brilliance, of the source can be made very much greater without damaging the target by overheating". The loading of a wide range of x-ray tubes is graphically presented in Fig.3.

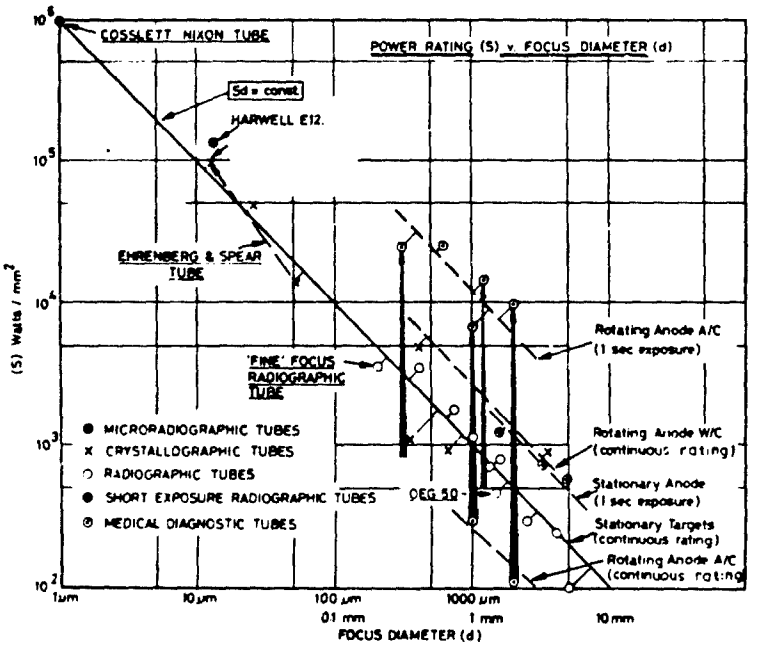

Figure 3

Relative power ratings to focal spot diameters for various types of X-ray tube.

2.1 Magnification

Enlarged images can be obtained by placing the specimen away from the film, at some position between the focus and the film. The magnification (m) is given by:

$$m = \frac{a + b}{a}$$

As the distance from the film to the specimen increases so also does the unsharpness (Ug) due to geometry increases. As a consequence the limit on the degree of projective enlargement, whilst retaining good definition of detail, is imposed by the large foci of conventional x-ray tubes. Therefore the smaller the focal spot can be made, the greater the amount of primary magnification possible (see Fig.2).

2.2 Image quality

In the field of optics, resolution is used as a term to describe the ability of a system to separate similar adjacent objects. The British Standard which defines radiographic terms [3] quotes specific resolution as:

"The smallest distance between recognisable images on a film or screen. It may be expressed as the number of lines per millimeter which can be seen as discrete images."

Definition is another term that is used in radiography. It is used qualitatively and refers to the sharpness of image detail on a radiograph.

In industrial radiology circles, radiographic contrast is understood to be, the relative brightness of two adjacent areas in a radiograph. Whereas film contrast is the effect of the film's characteristics on radiographic contrast, which is given by the slope of the characteristic curve of the film at the relevant density.

2.3 Radiographic contrast

X-rays and gamma rays are both electromagnetic radiation having wavelengths shorter than 10^{-7}cms. X-rays are extranuclear in their origin, and they are produced by accelerating a stream of electrons on to various metal targets (usually tungsten) thus producing photons by deceleration and other interactions with electrons that orbit the nucleus of the target atoms.

Gamma rays however are emitted by atomic nuclei in a state of excitation and often occur in association with the emission of alpha and beta particles.

Thus, on the one hand we have x-ray machines and on the other hand gamma ray sources (radioactive isotopes), which are small encapsulated metallic pellets which have been irradiated with neutrons and, so excited, give off gamma rays.

There are various scattering and absorption processes which account for the total attenuation of these radiations but it is only necessary here to consider that both x-rays and gamma rays are attenuated by matter exponentially and that the intensity (I) is usually written:

$$I = I_o e^{-\mu/\rho \rho x}$$

When I_o = intensity of original beam
and μ/ρ = mass attenuation coefficient (cm^2/gm).
ρ = density (gm/cm^3)
x = section thickness.

The x-ray spectrum can be considered continuous Fig.4 and the minimum wavelength (λ min) can be varied, through the operating range of the x-ray device, by varying the potential (kilovoltage) between the cathode and the anode (electron emitting filament and the target). Therefore, attenuation coefficients can be varied, thus affecting the intensity differentials with small incremental thickness variations - introducing either an increase or decrease in radiographic contrast.

The energy spectrum from a radioactive source unlike that of the x-ray source spectrum, is not continuous Fig.5 . Each radioactive isotope is characterised by spectral lines of fixed energies. Therefore it is only possible to alter the radiographic contrast by changing the film (or the processing technique) or more fundamentally, by selecting a different isotope within a limited choice, Table 3. Gamma-ray sources are also less intense than x-ray sources and exposure times can be considerably longer than x-ray exposures.

By the foregoing it is obvious that the contrast obtained on a radiograph depends on the energy of the radiation. With the normal range of thicknesses encountered on engine components greater radiographic contrast can usually be attained using x-rays. The energy can be conveniently varied to suit the particular thickness at hand.

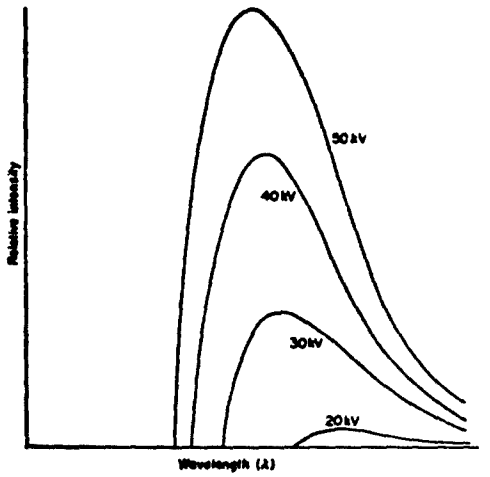

Figure 4

Illustrating the continuous spectrum of X-rays and the distribution of intensity with wavelength for differing x-ray tube voltages

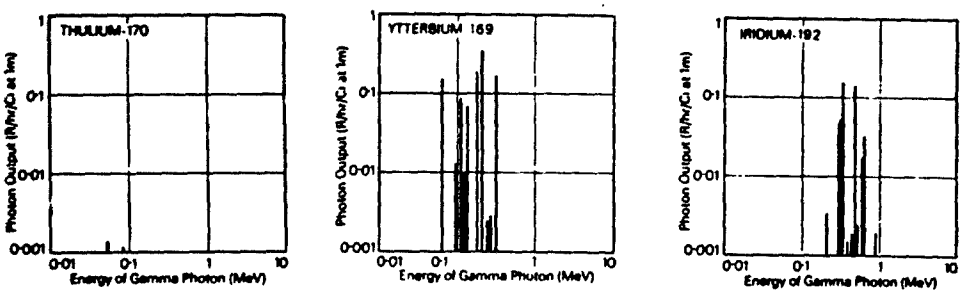

Figure 5

Energy spectra of 3 gamma-emitting radioisotopes used in industrial radiography

Table 3

Isotopes available for industrial radiography

Radioisotope	Cobalt 60	Iridium 192	Thulium 170	Ytterbium 169
Half life	5.26 years	74 days	127 days	31 days
Gamma energies (MeV)	1.17, 1.33	0.3 - 0.61	0.052 - 0.084	0.063 - 0.3
Thickness for radiography				
Steel (mm)	50 - 150	10 - 70	2.5 - 12.5	2.5 - 25
Other materials g/cm^2	40 - 130	8 - 50	5 - 12.0	5 - 20

The image contrast in a radiograph can be written as:

$$\text{Contrast} = \frac{0.43\,(\mu_1 - \mu_2)\,\Delta x.G}{1 + I_S/I_D}$$

Where μ_1 = attenuation coefficient of sample
μ_2 = attenuation coefficient of defect
Δx = thickness of defect in direction of beam
G = film gradient.

The build-up factor $(1 + I_s/I_D)$ is non-image forming scattered and secondary radiation generated within the sample.

3. ADVANTAGES OF PROJECTION RADIOGRAPHY

The case for projective radiography is made by Reynolds [4] in which the increase in radiographic contrast, which is attained by increasing the distance between specimen and the film, is expressed as a quantifiable term.

The smallest separation x resolvable is limited by the penumbral effect and in a sample irradiated by a source of diameter f is given by

$$x = f \frac{b}{a+b}$$

where the focus to object distance is a and the object to film distance is b. Thus the highest attainable resolution is achieved for the case of $b \longrightarrow 0$, i.e. for a contact radiograph. In fact the resolution can be made as fine as we please by increasing a to the limits imposed by the strength of the source and the time allowed for the exposure.

For projection systems where $a \longrightarrow 0$, the penumbral effect limits the resolution x to the value of f and the use of microfocus sources becomes necessary. What requires further explanation is that projection radiographs frequently reveal more detail than enlarged contact prints.

Two factors at least are involved. The resolution which can be attained in the contact case is also limited by the grain size of the film. Details which cannot be resolved in a contact radiograph may nevertheless be revealed in projection because of the magnification factor a+b/a which increases the apparent size of the whole sample and its structure.

A second effect occurs through the related medium of contrast. General discussions of absorption and scattering processes [5] show that most of the scattering in the energy range of interest is due to the inelastic Compton effect, and that much, if not most, of this scattering is in the forward direction, as described by the Klein-Nishnia Law.

$$Id(\theta) \propto \frac{I_o}{r^2} \quad K(\theta)\, d\theta$$

where the intensity $Id(\theta)$ is measured at a distance r from the scattering centre at angles between θ and $\theta + d\theta$ to the straight through direction. $K(\theta)$ is a function called the differential scattering cross section. The behaviour of the coherent scattering is somewhat similar.

Thus, for a contact exposure, much of the scattered energy will still reach the film and serve to blur the image and reduce contrast. In projection systems, only those x-rays scattered at angles small enough to intersect the film will be available to reduce the effective contrast in this way, and a large portion, depending on the energy of the beam and the angle of collimation, will be completely lost. Thus, other things being equal, a projection radiograph of a given defect can provide better contrast than a contact shot and fine details will appear to be more highly resolved.

In terms of the well known expression for contrast (see Page 6) the value of I_S/I_D is effectively decreased and the value of contrast enhanced accordingly.

4. IMAGE QUALITY INDICATORS

Numerous methods are currently used to evaluate the image quality of a radiograph. These include devices incorporating a series of wires of varying diameters; others use drilled holes in stepped wedges, or plaques with holes of differing diameters (Fig.6). They are known as image quality indicators (IQI's) or penetrameters in the US. These devices are placed on the weld or casting at a position nearest to the source of radiation and the radiographic sensitivity is usually expressed as a percentage, thus;

$$\text{Sensitivity \%} = \frac{\text{Thinnest wire or step hole visible X100}}{\text{Thickness of specimen}}$$

A small percentage sensitivity therefore indicates a radiograph of high image quality.

As an attempt to separate the radiographic effects of the image forming characteristics of contrast and unsharpness a duplex system of IQI has been designed [6]. Two components are required, one incorporating a series of pairs of wires, each wire in each pair being separated by the diameters of the wires in that particular pair. The diameters increase in a geometrical progression and to

establish the image quality one selects the smallest wire pair visible, that does not merge into one image when viewing. The percentage sensitivity is calculated using the diameter of this pair and the method described above. The contrast element is calculated by reference to the second component of the system, which is a plain step wedge.

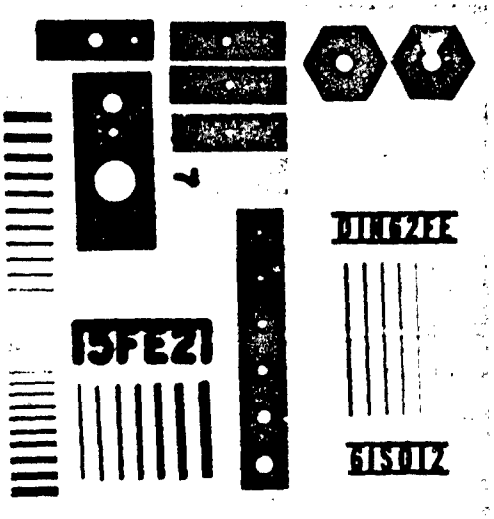

Figure 6

A radiograph of a collection of Image Quality Indicators (IQI's)

The relationship between the sensitivities obtained by using the various types of IQI device is complex. In practice it therefore is best to use the correct one specified and quote the sensitivity and the type of IQI used otherwise the information is confusing.

5. UNSHARPNESS

When considering the resolution of a radiographic system the causes of unsharpness need to be established and the relationship between the causes and the image quality accounted for.

Unsharpness of the radiographic image can often be caused by vibration of the equipment during exposure. The unsharpness here will be directly related to the amplitude of the vibration and particular care should be taken when small sources of radiation are used and when large projected enlargements are made, as this blurring will increase with magnification (m). This, and the unsharpness due to bad film/screen contact can usually be remedied and in all cases should be dealt with. There remain the other three contributors to unsharpness of a sharp edge feature, which are:

1. Geometric unsharpness (Ug)
2. Film unsharpness (Uf)
3. Screen unsharpness (Us).

The total unsharpness which could be a combination of all three is generally abbreviated to (U_T).

5.1 The geometric unsharpness (Ug) is identical to the penumbral effect in light, which is the imperfect shadow cast of a sharp edge and arises from the finite size of the source. This is also illustrated in Fig.2 and the magnitude of (Ug) is calculated by simple geometry

$$Ug = \frac{b.f}{a}$$

Primary x-ray enlargement is possible by moving the sample nearer to the source, with the source of radiation and the film remaining in the same positions. As the magnification is increased, so the attendant increase in (Ug) becomes apparent when a large (f) is used.

5.2 Film unsharpness (Uf) is caused by the scattering of the photon-induced electrons in the film emulsion, and with the normal range of conventional films used in industry this unsharpness is

dependent on the energy of the radiation irrespective of the speed of the film. The unsharpness at 100 kV is approximately 0.01 mm increasing to 0.06 mm at 200 kV.

5.3 Screen unsharpness (Us) which is due to the scattering of light by the crystals of the fluorescent materials used in intensifying screens. It has been suggested that this may be partly due to the shadows of crystals at the layer nearest to the film, as cast by fluorescent light from crystals behind the first layer.

Quantum mottle resulting from the spatial fluctuations of photon quanta absorbed on the screen has been postulated as also contributing to the loss of definition.

Typical unsharpness values are from 0.2 mm for high definition medical salt screens to 0.4 mm for similar high speed screens and both would be totally unsuitable for the radiography of engine components when conventional x-ray equipment is used. According to Klasens [7] the combination of two causes of unsharpness relate to the total unsharpness (U_T) thus

$$U_T = (U_1^3 + U_2^3)^{\frac{1}{3}}$$

Unsharpness values calculated in this way have been compared with experimental unsharpness curves and for most practical cases provide the basis for optimising the radiographic conditions.

6. FOCAL SPOT SIZE

The literature abounds with theoretical and experimental data on the subject of the measurement of focal spots [8,9 & 10]. This topic is so relevant to the potential resolution of a radiographic system, that a brief resume of the methods and the problems involved in obtaining meaningful measurements is worth relating.

Pinhole radiography is used throughout the medical and industrial fields to establish a practical appreciation of the size of focal spots. What is obtained however, is an image of the spatial distribution of the intensity across the spot. A small pinhole in an opaque material is placed usually midway (to arrive at a simple 1:1 relationship) between the focus and the detecting film and an exposure made. The size of the pinhole affects the enlargement of the image and must be accounted for (Fig.7).

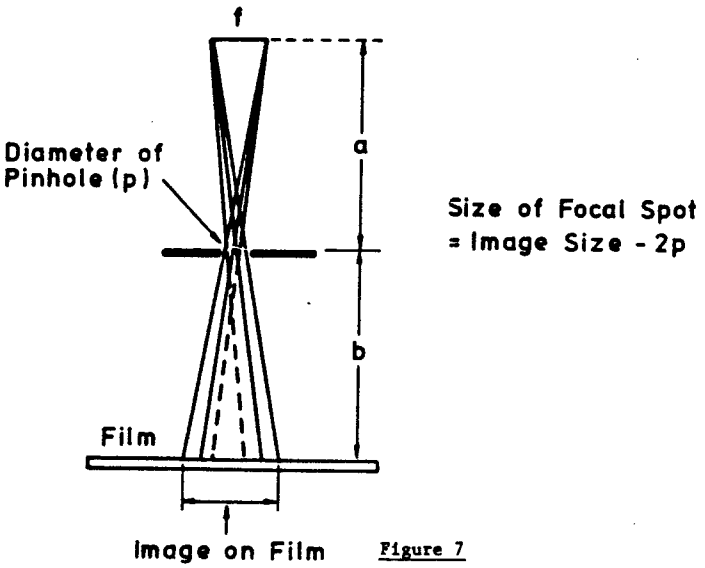

Figure 7

How disappointing to the novice radiographer when the result is an overexposed blur or an underexposed (some would say correctly exposed) image varying in density across the image. Where is the measurement to be made? This is analogous but not identical to the measurement of the unsharpness of a radiographic edge image. Exposure times for imaging through a pinhole are prohibitively long when small foci are to be compared, but for foci of approximately 0.5 mm and above, a working result can be obtained. The image of the focus can be traversed with a microdensitometer for a graphical film density/distance curve or displayed for comparison using an electronic image analysis system.

Comparative measurements of foci can also be made by inference from the shadow cast on the film by a sharp opaque edge; two edges at 90° in the plane of the film when radiographed simultaneously conveniently provide information of the focus dimensions in two directions at 90°. This is a useful method for evaluating the dimensions of foci of approximately 50 μm and when fine grained film is used with large projective distances and therefore when the inherent unsharpness of the film (Uf) is minimal.

7. MEASUREMENT OF RESOLUTION

Unsharpness gradients at edges can be also displayed graphically (Fig.8) by a microdensitomer of

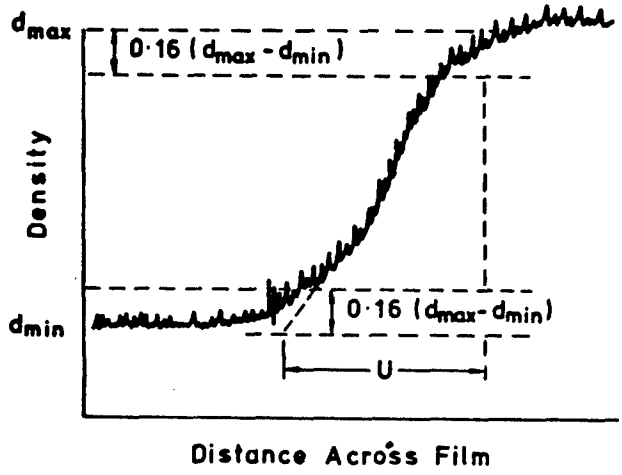

Figure 8

A microdensitometer trace of a radiographic image of an edge, illustrating Klasens equivalent blur. The granularity of the film, which shows as noise on the trace, can be measured by calculating the standard deviation of a number of microdensity readings, by traversing a measuring spot across the film.

the Joyce-Loebel type. The instrument produces a film density/distance curve, with the distance axis greatly amplified (typically X500). Much information can be obtained from these curves on the performance of the imaging system and can conveniently provide the means of comparing one system with another.

However, for analytical purposes, a method that separates the effect of the many variables involved in the radiographic process may be desirable. Such a method of assessing the image forming capability of a complete radiographic system has been intoduced into industrial radiography by Halmshaw [11]. This application of modulation transfer functions (MTF) which came to industrial radiography via the electrical communications industry via researchers in the medical radiological circles, has now been adapted to suit the photographic materials used in industrial radiography. A modulation transfer curve describes the ability of a system, and more importantly, any part of a system, to transmit information in terms of amplitude, phase and spatial frequency. For instance, the MTF of a focal spot, the film, and the microdensitometer can be evaluated independently. In the case of the total radiographic system Halmshaw used the line spread function (LSF) of a radiographic image of a slit (approx. 1 μm) in an opaque material. By a mathematical process known as convolution this can be transformed to determine the result that would be obtained of a bar/space object which is usually used in determining MTF.

An MTF of 1.0 indicates that all the information is correctly transmitted in terms of phase, amplitude and spatial frequency. These principles were used by Halmshaw to establish values for a number of film/screen combinations that are used in industry and he concludes that because they do not take full account of the effects of film granularity or the performance of the human observer, they do not yet provide the complete answer to enable the detail recording capability of a radiographic system to be specified.

When high resolution systems are to be evaluated in the practical situation, reliance is still placed on the well-tried comparative techniques using details within the specimen, images of fine wires, meshes, step holes etc. As the wire diameters of standard IQIs are too large for high definition work on turbine blades, which is described later, one has been constructed with four wires measuring; 0.025 mm (0.001 inches), 0.05 mm (0.002 inches), 0.076 mm (0.003 inches) and 0.1 mm (0.004 inches) and sometimes smaller individual wires are used.

8. RADIOGRAPHIC FILMS

Radiographic film, unlike photographic film, usually has light sensitive emulsions coated on both surfaces, which effectively reduce x-ray and gamma exposures to one half. Single-sided emulsion films are available and can improve resolution when the resultant increase in exposure time is acceptable.

All photographic films are extemely convenient detectors of x-rays and gamma rays, they can be used with low intensity sources simply by integrating the image through larger exposure times. They are available with a wide variety of characteristics of speed, contrast and graininess (Fig.9). In general, when fine detail is to be resolved it is achieved by using a fine-grained film with high contrast. Conversely high-speed films are relatively coarse-grained and are of a lower contrast. Gradients in excess of 6 (density/log exposure) can be achieved if the radiographic conditions are

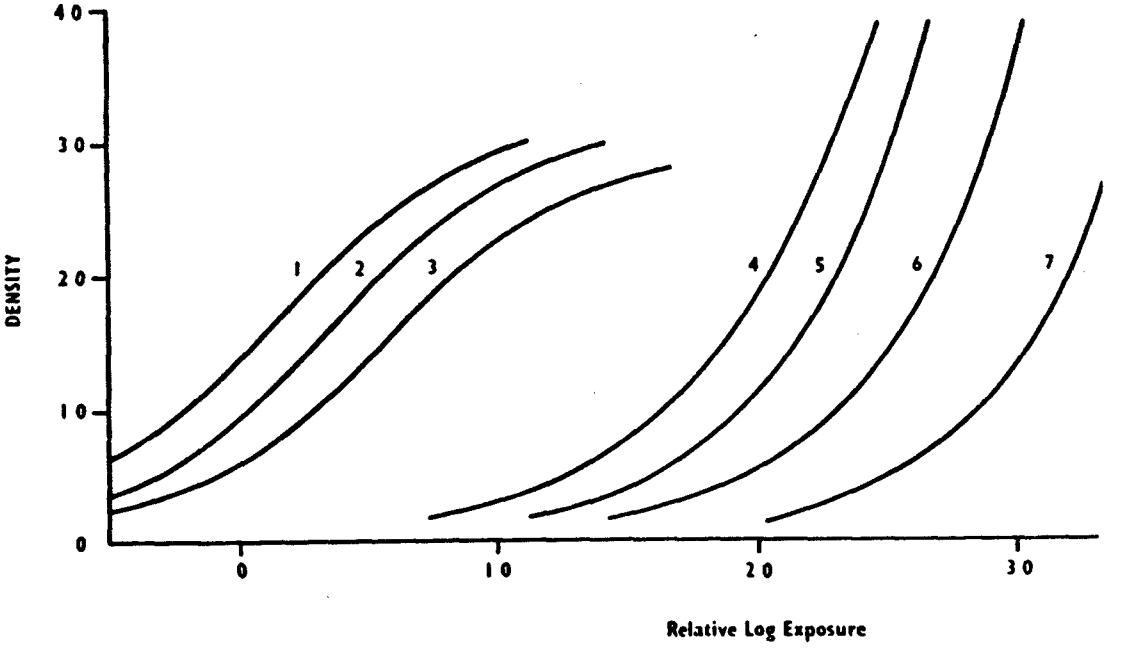

Figure 9

Characteristic curves of radiographic films.
Curves 1, 2 and 3 are fast salt/screen films, whereas
4, 5, 6 and 7 are curves of non-screen films of differing speeds and contrast

correctly selected, resulting in the recording of small changes in radiation intensity as large differentials in light intensity when the film is viewed. The high gain in sensitivy of film is achieved during the chemical development process which ideally ensures that the film provides sharp images of minimal incremental thickness changes of the specimen which is the objective in most radiographic tasks. Radiographic films can be broadly divided into two groups.

8.1 Non-screen films, although so named, are more often used with lead screens (typically 0.1 mm front and 0.15 mm back) particularly on aero engine parts when energies of greater than 120 kV are used. Lead screens have an image intensifying effect above this energy and exposure times are reduced. The screens also reduce the effects of the non-imaging forming scattered radiation of lower energy, whih emerge from the specimen.

8.2 Screen films

These films are used with fluorescent intensifying screens, (salt screens) and have wide application in medical radiography where there is a need to reduce the x-ray dose to the patient. They are extremely fast.

Until recently, the role for these film/screen combinations in the aero-engine industry was infinitesimal. Since the advent of dynamic radiography and high definition radiography the use of these materials have increased, in particular when large numbers of specimens are involved where the advantage of the reduced exposure time can be exploited. The speed advantage could not be utilised for conventional x-ray work when fine detail is to be resolved because of the unsharpness (Us) attributable to the film/screen combination.

By using high definition projective techniques however, the lack of photographic resolution due to the screen unsharpness (Us) and that caused by the particulate nature of the phosphors need not be a serious limiting factor. Indeed the screen and film unsharpnesses remain unchanged with an increase in projected enlargmenet when a virtual point source of radiation is used, thereby reducing these unsharpnesses in comparative dimensional terms, relative to the enlarged image, until they become insignificant.

Silver halide emulsions are normally used for radiographic films and the film images are made up of a number of developed grains, and when viewed, a granular structue is apparent. This granularity is the result of the 'clumping together' of individual grains and can be evaluated by using a microdensitometer. (See Fig.8).

Within a year of the discovery of x-rays, it was known that calcium tungstate ($CaWO_4$) was an effective phosphor for intensifying x-rays. Up to the present time ($CaWO_4$) has maintained its lead in medical radiography. The light emitted is predominantly in the blue region of the spectrum (420 nm) and films have evolved over the years that are spectrally sensitive to the blue emissions. More recently, new phosphors have become available which are terbium activated rare earth oxysulphides based on the rare earths, gadolinium and lanthanum [12]. They have high photon absorption and x-ray-to-light

conversion characteristics and when coated on thin cards make very efficient intensifying screens for x-radiography. Screens made from these new phosphors emit mainly green light and matching films that are green sensitive must be used to gain the speed advantage (Fig.10).

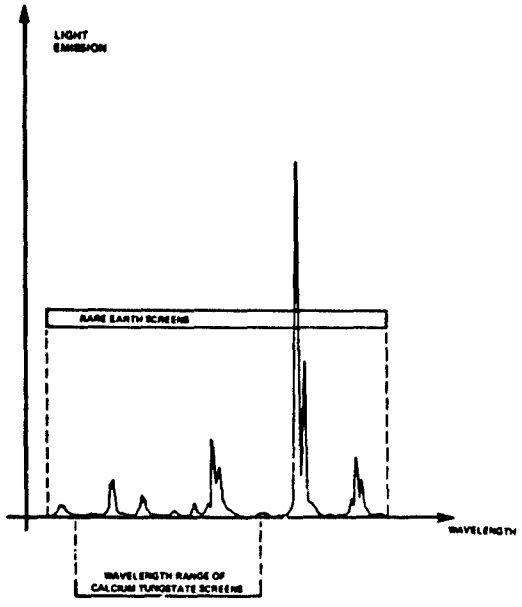

Figure 10
Spectral characteristics of rare-earth intensifying screens

8.3 Darkroom practice

Methodical and correct darkroom practices are essential for high resolution results, particularly when extremely fast film/screen techniques are used. Correct lighting, cassettes which ensure good film/screen contact and careful film handling are areas that need special attention. Automatic film processing equipment also ensures that consistent results are attained. This is particularly important when large batches of components, such as turbine blades, are to be examined for micro details using high definition projection radiography.

9. DYNAMIC RADIOGRAPHY OF AERO-ENGINES

In the main, the wide range of standard x-ray equipment that is available commercially fulfil the needs the manufacturing and maintenance sections of the aero-engine industry. When large thicknesses of material are to be penetrated however, linear accelerators of 8 MeV have been brought into use. They are currently being used to enable the design clearances of components to be determined whilst the engine is under power [13] [14]. Relative movements of components can thus be measured under the various running conditions of the engine which, before the radiographic technique had been developed, were impossible to measure. Improvements in resolution have enabled these engaged in dynamic radiography to make more accurate measurements and have thus allowed designers to adjust the design clearances with greater precision.

Normally, radiographers in the aero-industry are concerned with the detection and evaluation of flaws in components but the technique of dynamic radiography is an excellent example when a radiographic system can provide designers with information which leads to improvements in the "running efficiency" of aero engines. This important development was initiated as a joint Rolls Royce/NDT Centre Harwell venture in 1970. Others had previously considered that x-ray exposures of a few nanoseconds were needed to record the relative movements of static and rotating components inside an engine under power. Flash radiography had been tried but the combination of short-pulsed exposures and the obligatory fast films and screens, did not provide the resolution necessary. In fact for the first trials in 1970 a cobalt 60 isotope was used and exposure times were up to 2 hours duration. The results obtained were encouraging and lead to the use of the linac. The technique was used on "the view obtained of a wheel on a rotating shaft" principle. With a view normal to the shaft, the periphery and one side face of the wheel will be seen as a profile and a straight line; and will remain so irrespective of the speed of motion. Stop motion was therefore necessary. Techniques have been tried which strobe the pulses emitted from the linac with features, such as an individual turbine blade; this may be a useful technique for the future.

The linac exposures are typically 0.3 - 2.0 seconds for transient exposures, that is when the engine is accelerated or decelerated. For the steady state exposures, when the engine is rotating at a constant speed, exposures up to several minutes are normal. Some improvement was achieved by reducing the focal spot from 2 mm to 1 mm diameter, particularly in the radial plane when radical gaps are to be measured. For axial gaps the source size can appear to be less critical as the narrow gaps tend to auto-collimate the beam (Fig.11) and gap dimensions have been recorded down to 0.15 mm in width,

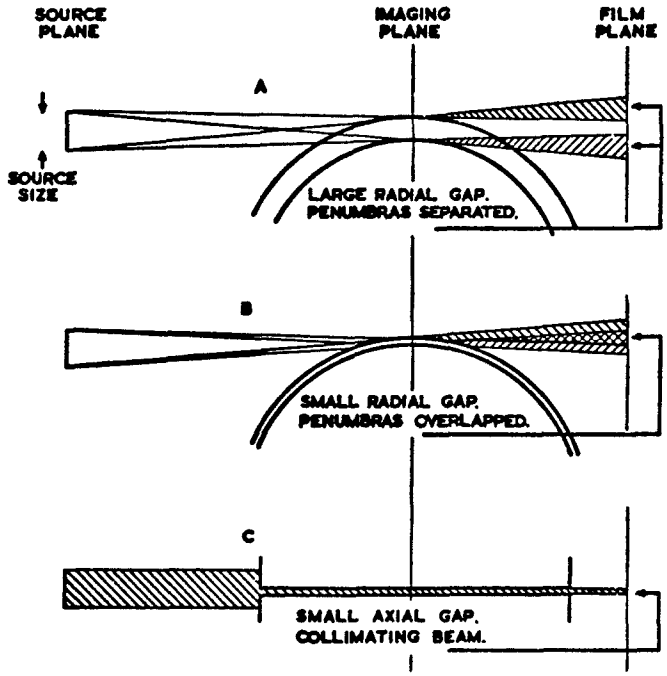

Figure 11

Radiography of seal clearances in gas turbines.
Note difficulty with small radial gaps at B.
No clear images recordable.

despite using a focal spot of 2 mm. typically, thickness paths are usually between 75 and 250 mm of Nimonic alloy (or equivalent in titanium alloy). In steady state exposures, fine-grained film can be used with lead screens but for the transient exposures extremely fast films and screens are needed to obtain a working density.

The major factors limiting the production of radiographs of high resolution in this situation are: the geometric unsharpness (Ug) due to the focal spot size and the unfavourable a/b ratios that are sometimes used, and also film unsharpness due to the energy (Uf) which has been described earlier. Unsharpness due to vibration is not, surprisingly, considered a major factor although alignment of the beam, along the axial faces, has to be accurate to within 1 mm. The 8 MeV linac on site at an airfield at Hucknell in Derbyshire is shown, see Plate 1. Plates 2 and 3 illustrate typical results obtained when using the linac.

10. CONVENTIONAL X-RAY EQUIPMENT

We move from the high energies of the 8 MeV linac to the low energies of the beryllium windowed x-ray equipment (approx. 20-50 kv). The low inherent filtration of these x-ray units allows the longer x-ray wavelengths to emerge from the tube and thus radiographs of the highest contrast are possible. When used with fine grained film, and with the right subject, high resolution radiographs are produced. These units are used extensively to detect corrosion and cracking and are more useful for scheduled maintenance inspections. However, they have inspection roles in the manufacturing sector and are used for testing welds in sheet fabrications, radiographing investment casting wax cores and the thinner metallurgical laboratory samples.

The bulk of component radiography however, is carried using x-ray equipment between 100-300 kV. Turbine blades, nozzle guide waves, segments, weldments and many of the other components and assemblies that make up aero-engine propulsion units are successfully examined using conventional radiographic equipment. The geometric complexity of many of these components which offer varying thicknesses in the path of the x-ray beam, requires that a compromise in the technique which sometimes emphasises latitude (by covering many thicknesses with one exposure) rather than contrast. It is not suggested here that this situation, brought about by the understandable pressures of deliveries and costs, should change. Sometimes however, a lot more could be done to resolve small flaws by bringing to bear the science (always available) and the art (not always available) of radiography and by using conventional x-ray equipment.

However, as operating conditions change, usually due to design changes which increase the performance of an engine, it sometimes becomes necessary to detect flaws even smaller than those considered detectable hitherto and beyond the scope of conventional x-ray equipment. Therefore, more specialised equipment has to be utilised which can resolve to a higher sensitivity.

11. EVOLUTION OF SMALL FOCUS X-RAY EQUIPMENT

Within two years of the discovery of x-rays a microradiograph had been produced [15]. This type of x-ray imaging has improved to make it a useful technique for research since modern materials have become available.

Microradiography requires that a specimen is placed in contact with a fine-grained photographic plate, or film, and exposed to x-rays emanating from a normal tube. The enlargment of the image is produced optically and therefore the resolution is limited by; the graininess of the photographic emulsion, fogging due to photoelectrons given off by the specimen and the optical system of the enlarger. Sometimes these limitations can be overcome by using a small x-ray source and projecting the image (Fig.12) and so obtaining a primary enlargement thus reducing the enlargement of the film grain and imperfections due to particles of dust etc. (Plate 4).

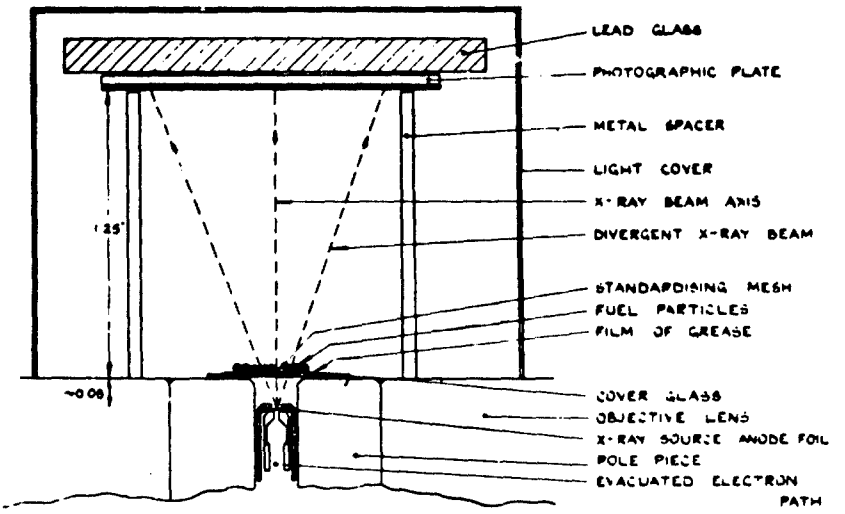

Figure 12

Projection micro-radiography of small nuclear fuel particles

Although work continues to produce a viable x-ray microscope which emphasises the focusing x-rays to achieve a small effective focus, it is not intended here to enlarge on this subject; the application of focused x-rays in industrial radiography is minimal, indeed if it exists at all. Small x-ray foci can, however, be conveniently formed by the focusing of electron beams, producing a small irradiated target in the anode, and thus a small focus is achieved. The ability to focus electrons by an electromagnetic lens or electrostatically is now utilised by all modern microfocal x-ray equipment. A focusing system for an x-ray microscope using an electromagnetic lens was first made at Cambridge [16]. It was constructed with two lenses and the transmission target was a thin metal foil, which also provided the vacuum seal. Whilst the electrons were focused within the vacuum the x-ray beam was conveniently at atmospheric pressure. Small specimens can be placed close to the target and with the photographic plate positioned some distance away, thus producing enlarged images. X-ray magnifications up to 1000 times have been produced and these have been further enlarged optically to achieve a resolution of 0.1 - 1 μm depending on the specimen, kilovoltage and target material.

This technique is called Projection microradiography and apart from a few specialised instances, is not a technique that is particularly suited to problems in the aircraft industry. It is more often used as a complementary technique to optical micrography and confined to the laboratory. Wafer thin samples which require special preparation are necessary and the field size is minute. The interest in projection microradiography stimulated the associated development of micro-focus x-ray sources with diameter from 20-100 μm.

The transmission foil, of the projection microradiographic system, was replaced with a variable solid target (VST) (Plate 5). With this system the electron beam is focused on to a selected position on an assembly of detachable rings of a variety of target materials (i.e. tungsten, molybdenum and copper). The anode assembly is massive when compared with the spot size and this aids the dissipation of the heat produced at the target which is also water-cooled. The required target can be selected

without breaking the tube-head vacuum system. The whole target assembly can also be rotated and thus a fresh target area can be selected when required, also without breaking the vacuum. The minute size of the focal spot is impossible to measure accurately. Estimates of between 1 μm - 10 μm have been inferred from the enlarged images cast by fine metal meshes etc. The vacuum window from which the x-rays emerge into atmosphere is made of aluminium (12 μm thick) and this inherent filtration is acceptable for the electron acceleration range of between 5-30 kilovolts. The limitations of this equipment, imposed by the peak voltage and the maximum beam current of 250 μA, confines the applications to thin samples (typically 0.25 - 1.0 mm) of light alloy or other low attenuation materials. The field of coverage is generally limited to approximately 50 mm diameter and only samples (or areas of samples) smaller than the beam can be radiographed completely with one exposure as the low beam intensities mandates short focus-to-film distances. So far, the application of the equipment described here have not penetrated into the production areas of the aero-engine industry, although they have been successfully applied to small metallurgical samples.

A further development of the VST has resulted in a design which has however found many applications in the aircraft manufacturing industry.

It is the Harwell E12 high definition x-ray unit (Fig.13) [17] which derived from a series of designs developed over the years by Ely [18]. The common features and the principles involved with the E12 and its antecedents will be discussed, and comparisons made on both the construction and application of the various types.

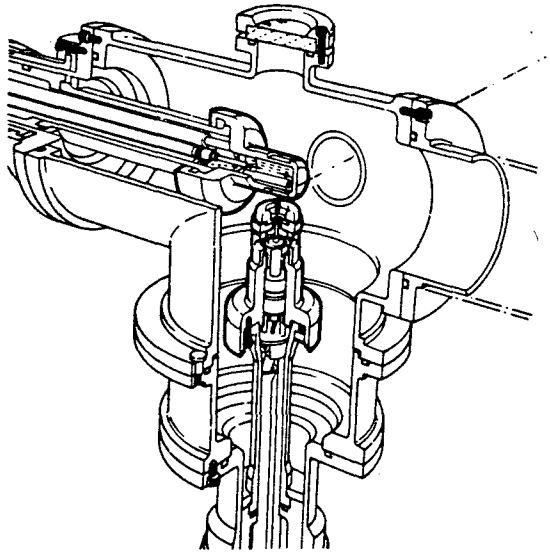

Figure 13

Schematic drawing of the tube head of the Harwell E12 high definition x-ray unit

The operating range of the E12 is between 30 - 85 kV with a maximum current of 1.0 mA at 50 kV, reducing to 0.5 mA at 85 kV. The equipment has been designed to operate continuously if required and it can be used intermittently at 100 kV.

Many of the features are common with the previous Ely designs but basically it has been designed to achieve a focus of approximately 15 μm diameter. Unlike the models already discussed however, the focusing is achieved electrostatically. It has proved more difficult, with the alternative electromagnetic focusing systems, to achieve the necessary stability that allows a consistent focus that is reproducible when many similar parts are to be radiographed, without considerable adjustment for each exposure. The source of electrons, in common with the earlier types, is a heated tungsten filament formed from tungstem wire (0.1 mm thick) bent into a sharp "vee". The top of the "vee" protrudes through the aperture in the bias cup effecting a minute primary electron source and thus the single stage focussing suffices. The tube current is regulated by the voltage applied to the bias cup. Electrostatic focusing in this case depends on the principle that a negative charge in the biasing cup repels the electrons as they are accelerated towards the target (by the potential, between the anode and cathode). As the electrons pass through the annular electrostatic field (produced by the bias voltage and effected by the shape of the cup) they are pinched. Thus the conditions can be optimised so that the electrons arrive onto a small area of the target producing the minute focus.

The single stage electrostatic focusing of the E12 not only simplifies the design, leaving the tube housing uncluttered and more robust but allows for maximum adjustment of the spatial arrangement between the filament and the target. Focusing is readily achieved by controlling the variables:

a) spacing between filament to target

b) protrusion of the filament through the aperture of the biasing cup

c) bias voltage applied to the cup.

The effect of the interplay between the variables can be observed directly on a television monitor. The TV camera has been adapted so that the lens system is replaced with a fibroptically coupled phosphor. The primary enlarged image of a fine calibrated mesh is adjusted approximately and final optimisation is achieved by trial radiographs.

The x-ray tube head, in common with the other types, requires a continuously pumped vacuum system attaining pressures of 10^{-5} torr. The E12 system however, is constructed to allow greater flexibility of working without breaking the vacuum seal. It is possible to manipulate the conditions and so optimise an accelerating voltage, bias voltage, tube current, distance between focusing cup and target, target position and the position of the filament tip relative to the bias cup, whilst maintaining vacuum. All these variables, except the selection of the target position, which is made by rotating a knurled wheel at the tube head, can be operated remotely from the console. The x-ray beam emerges from the tube head via a beam-defining window formed from 0.05 mm aluminium foil and the effective beam divergency is 14°. A useful facility to aid focussing is a silver mesh (20 lines/mm) which can be inserted between the target and the exit window, whilst the unit is under vacuum, with the x-rays on.

The vacuum systems (Fig.14) are similar in principle for all the microfocus equipment. Diffusion pumps, backed by GDR rotary pumps are used and care has to be taken to reduce vibration as the effective focus will increase with the amplitude of any vibration of the tube head. The vacuum system is designed to allow the rapid replacement of a filament. Normally the filaments last from 30-60 working hours and although the replacement takes but a few minutes, pumping down to 10^{-5} torr may take a further 10 minutes.

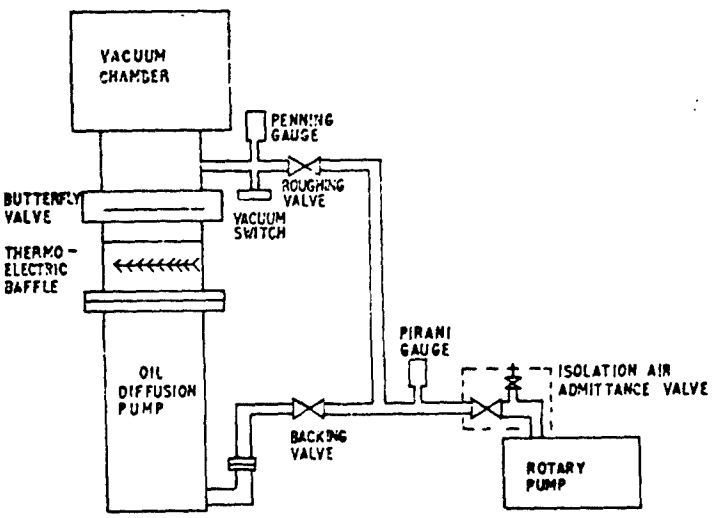

Figure 14

Schematic diagram of the E12 Vacuum System

The electron gun assembly is similar to the earlier types and to those of electron microscopes. The E12's electron gun and the anode are supplied with negative and positive EHT respectively from two Brandenburg 858R power units, which provide variable stabilised voltage outputs. Opposing the outputs of the two power units, (with the centre common connection 50 kV above earth) allows for up to 100 kV operation and yet restricts stressing of any components more than 50 kV to earth. The EHT supply to the bias cup is provided separately and is isolated from earth by insulating pillars.

12. RADIOACTIVE ISOTOPES VERSUS ROD ANODE UNITS

12.1 Radioactive isotope sources are used to radiograph aero-engine components in situ and their main application is in the maintenance area. They sometimes offer a considerable advantage in that they are intrinsically small and can be conveniently inserted in places inaccessible to normal x-ray equipment.

With the more intensive sources that are available today, unsharpness due to geometric considerations can be minimal even with short FFD's. They have limited application in production because;

a) the energy from a particular element is characterised by the element and therefore the facility for improving contrast (apart from using a film of higher gamma) and therefore improving the resolution, does not exist.

b) the intensity of the radiation is low compared with x-radiographic sources, leading to larger exposure times.

They are however particularly useful for maintenance work when components within the complete assembly can be radiographed without stripping out. The isotope, iridium 192 has been used to examine, in situ, the fir-tree assemblies for cracking or other damage and for the detection of wear on exit guide vanes. Indeed, engine designs have been influenced by this requirement, holes through rotary shafts have been introduced to allow access for the source to enable a panoramic technique, whereby a complete ring of blade roots or exit guide vanes can be radiographed simultaneously [19].

The isotope, thulium 170 (Tm 170) is readily available and when required can be as small as 0.5 mm x 0.5 mm diameter with activities up to 1 curie. These are suitable for use on weldments of relatively thin gauge (up to 6 mm) and the source-to-film distance, with an acceptable geometric unsharpness for unprojected radiographs can be in the order of 1 cm or less. A typical application is illustrated by the tube-to-tube plate welds used in heat exchangers for power stations and is shown in Fig.15.

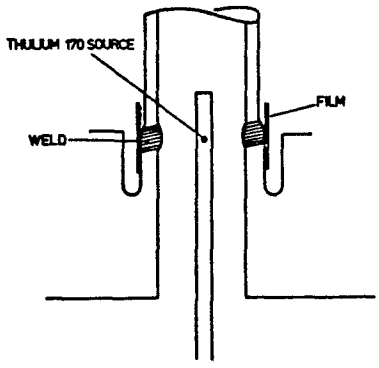

Figure 15

Panoramic technique using the isotope Thulium 170
Source to film distance, 10 mm
Source size, 0.5 mm x 0.5 mm diameter

This technique is successfully applied to the inspection of welds attaching vapouriser units in aero-engines, when a panoramic arrangement such as illustrated in Fig.15 is possible. Gas pores of 0.177 mm diameter (0.007 inches) in welds can be detected in thicknesses of 2.5 mm with a source-to-film distance of 0.8 cms. This represents a 'spherical pore' sensitivity of 7%, which does not approach the more sensitive x-ray technique for similar thicknesses but is useful nevertheless. Ytterbium 169 which produces radiographs of similar contrast to those produced by Tm 170 is a more intense source and can be considered as an alternative when shorter exposures are needed.

12.2 Rod anode x-ray units are also used not only when an accessibility problem exists such as with electron beam welds or diffusion bonds joining cylindrical components but often when considerable economic savings can be made. Certainly, when welds of rocket motors or combustion chambers are joining parts of circular cross section they do allow panoramic techniques. The target assembly of a rod-anode device is at the extremity of a rod and the x-rays emit radially for 360°. The focal spots for these devices are elliptical, and two dimensions are specfied for geometric calculations. They are usually too large (typically 0.5 mm x 1.5 mm) to allow short focus-to-film distances without increasing the geometric unsharpness unduly.

12.3 Fine focus rod-anode x-ray units

X-ray equipment has been developed to examine the tube-to-tube plate weld mentioned earlier. These are now under consideration for use in the aero-engine production sector for the examination of joints in small diameter cylindrical components. This will no doubt lead to much wider application of rod anode techniques in both the production and maintenance scenarios.

The equipment, which has been developed in Holland by, Technische Physische Dienst-(TNO-TPD) uses miniature magnetic lenses built into small diameter extension rods, which focus the electrons on to the target at the end of the rod [20].

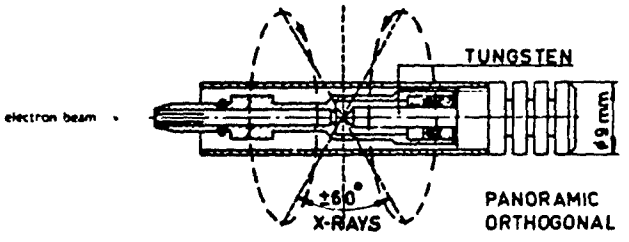

(T.P.D.)

Figure 16

The target assembly of a rod-anode x-ray unit
The electron beam is focused, with the mini magnetic lens, onto the target, which in this case is conical, with a flat conetip (0.2 mm diameter) allowing the emission of x-rays normal to the electron optical axis

Several 80 kV and 150 kV microfocus units are currently in use testing welds on heat exchangers, and a unit of 250 kV is planned. The major source dimension is claimed to be 0.1 mm and the peformance is compared with isotopes in Table 4.

Table 4

Comparison of exposure rate values for radioactive isotopes and rod anode micro-focus equipment

Source	Activity	Exposure Rate
Thulium 170 (0.5 mm x 0.5 mm dia.)	1 Ci	0.025 R/hr/m^{-1}
Ytterbium 169 (0.6 mm x 0.6 mm dia.)	2 Ci	0.24 "
Iridium 192	1 Ci	0.48 "
X-ray Source	kV at 1 mA	
0.1 x 0.005 mm	80	3 "
0.1 x 0.015 mm	150	9 "
0.1 x 0.050 mm	250	20 "

Extension rods incorporating the minimagnetic lenses have been made with useful lengths of 450 mm x 9 mm diameter; with lengths of 915 mm the outer diameters increase to 12 mm. A typical exposure, when radiographing a cylindrical weld, with an outside diameter of 50 mm, and a thickness of 9.5 mm is; 150 kV 7.2 mA seconds (target current 2 μA, time 180 seconds) achieving a film density of 2. (Agfa Gaveart D4 film). All seven wires of an Fe IQI (0.4 - 0.1 mm wires) could be seen indicating a DIN-IQI sensitivity of approximately 1%. An improved design, incorporating a high voltage cable connection between the generator and the electron gun, is under consideration. This will greatly improve the versatility of the unit and will no doubt lead to wider application in the aero-engine industry and thus improve the resolution of some radiographic examinations.

12.4 Fine focus sealed x-ray unit

Another comparative newcomer is the Magnaflux MxK100M. This is a variable-focus sealed x-ray unit which, it is claimed, has a variable focus from 0.5 mm to 0.05 mm, varied by adjusting an electrostatic biasing device. The maximum tube current for the larger focus is limited to 1 mA and when the smaller spot is used, somewhat lower. Comparison radiographs of an aluminium weld have been made with this unit, conventional x-ray unit and the Harwell E12 and these are shown in Plate 6. The comparison was made at 80 kV with a projected enlargement of X6 which obviously favoured the E12 unit because of the much smaller focus (15 μm). Nevertheless at lesser projected enlargements, the MxK100 unit will have

considerable advantage as the tube-head is small, and connected to the generator via an HT cable. The tube head can also enter an opening of 88 mm diameter, a convenient feature for some aero-engine maintenance work.

13. THE DEVELOPMENT OF A HIGH DEFINITION RADIOGRAPHIC TECHNIQUE

By far the most widely appreciated application of high definition radiography, on an engine component to date has been the inspection of the first stage turbine blades of the Pegasus engine, manufactured by or for Rolls Royce [22][23]. The blades are complex in shape, with cooling holes which run parallel to the longitudinal axis of the blade. They are manufactured using the 'lost wax' investment casting process which is an attractive and economic process for the precision casting of components for parts of this type. Indeed, it would be difficult to imagine a component of this type being manufactured in any other way. With investment castings which are complex, particularly if long range freezing materials are used such as In 100, microporosity can be a problem.

Conventional radiographs will reveal the presence of some porosity and other grosser shrinkage defects that may occur. However, when an increase in the output of an engine is demanded, the operating conditions of a component may change, particularly temperatures, and hence smaller micropores in the casting may lead to failure under the more strenuous conditions of service. Specifications exist which mandate that sample blades must be sectioned, polished and etched and so allow the incidence of microporosity to be evaluated. This method of quality control can be far from ideal because only a relatively small sample is evaluated and even then the results are only relevant to the polished exposed surfaces of the sectioned blocks. Information is available that relates the microporosity content with the performance of the blade in service.

The small and possibly non-representative samples can be evaluated with measurements made by a microscopic device such as the 'Quantimet' system. Another major and obvious snag is that the test destroys the blade. Other nondestructive testing inspection methods have been tried to replace the destructive sampling tests and so far results have not been encouraging.

High definition projection radiography, because of previous experience in inspecting the condition and geometry of fine spark-eroded cooling holes at the trailing edge of some blades, was tried and is now a routine inspection method.

X-radiography, using conventional equipment, had previously been rejected as a means of detecting and evaluating microporosity because:

a) the individual micropores were too small to detect (0.03 - 0.01 mm)

b) individual crystallites of the alloy produce a diffraction pattern on the radiographic image, obscuring details of the micropores.

The Harwell E12 x-ray unit was used and initially projected radiographs (X5) were used with fine grain film and the exposures were 10 minutes, for an aero-foil thickness of 6 mm. Eventually a technique using high definition salt screens with X12 projected enlargements the exposure has been reduced to 75 seconds. A further reduction to 20 seconds is possible, by using the rare-earth screen films, if required. A parallel programme of destructive testing, when many samples were sectioned, polished and etched etc. (Plate 7), to establish the relationship between the radiographic results and the measurements obtained using the 'Quantimet' 720 system.

The system provides data on the percentage of microporosity of an area of the sectioned sample with dimensions of 1.25 mm x 0.7 mm. With enlarged projections of X12 the whole blade could not be covered so an area chosen as typifying the incidence of microporosity of the blade, was chosen by the evidence of the X5 enlargements and the related destructive tests. The sample area measured 30 mm x 12 mm, the largest dimension along the major axis of the blade. Properly engineered lead masks (Plate 8) are essential for this work not only correctly to position and align the blade but to reduce the irradiated field area and thus restrict the non-imaging forming scatter from the blade which emanates from outside the area of interest. The ad-hoc masking device shown in Plate 9 is to allow the radiography of the thicker blade section.

Initially radiographic interpretation presented some difficulties. The 40 cm x 35 cm films contained so much information, including details of individual grains, that the normal industrial radiographer had to adapt his viewing and acceptance techniques. This is analogous to the confusing array of densities found on normal chest radiographs but with experience and knowledge of the subject subtle and significant details can be diagnosed and appraised.

Individual pores of 0.03 mm have been detected (Plate 10) and subsequently confirmed by sectioning the blade. Some radiographic results are illustrated in Plates 11 and 12. A Quantimet microporosity level of 1.5% can now be detected readily by experienced staff. A system could be envisaged that could reduce the sectioning to an occasional cross-check. It may be possible to evaluate the porosity in terms of volume by using an x-ray stereo system and when used with an image analysing, present the information directly.

13.1 Facility design

The facility illustrated in Fig.17 is suitable when large scale production radiography is required. Operating as a slide projector, the blades can be placed in the exposure position from outside the irradiated area. The films can be replaced in the same way. The shielding requirements for the E12 with a maximum energy of 100 kV, can be accommodated with steel sheet (4 mm thick) on all the sides of the compartment except in the forward position, when 10 mm of lead in the core area is adequate. The beam angle of 14°, which is limited by the tube window, ensures that the primary beam does not impinge on to the sides of a correctly dimensioned compartment.

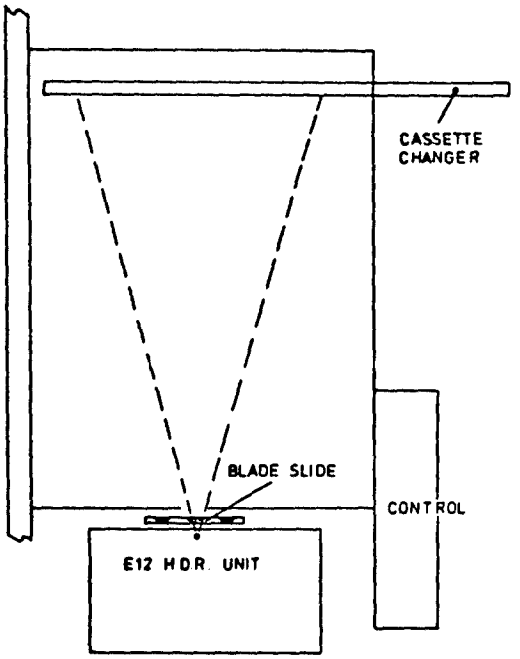

Figure 17

Facility for the high definition projection radiography of turbine blades. Note that all operations can be carried out without entering the irradiated area

To date, E12 units have been installed in production areas, one is even equipped with a pneumatically operated blade changing device to speed up the process. They are applied when the requirement of defect resolution is beyond that achieved by conventional radiography, which started with the Pegasus blade and is now an established method of examining many other similar components.

14. LOW TEMPERATURE RADIOGRAPHY

Since the introduction of salt screen techniques the need to radiograph even thicker sections of blade castings has arisen. This has lead to the development of a low temperature exposure technique 24 which utilises the rare-earth intensifying screens which were discussed earlier. The screens have already extended the use of the E12 to allow thicknesses of 8 mm (Ni alloy) to be radiographed at 90 kV with exposures of 10 minutes. The present design of the E12 does not allow an increase in energy or radiation output and therefore the possibilities of low temperature exposures have been investigated and a working technique has evolved which extends the upper thickness to 20 mm.

When radiographic film is directly exposed to x-rays, that is without intensifying screens, there is a direct reciprocal relationship between the time of the exposure and the intensity of the radiation. But when image intensification is achieved by using phosphor screens the film density is attributable mainly to the light emitted from the phosphors and the reciprocal relationship no longer exists.

This means, in practice, that extending the exposure time no longer results in a continuing increase in film density. The reciprocity failure [25] thus determines the limit in thickness that can be radiographed using low intensity sources.

It is also known that photographic emulsions are less sensitive at low temperatures but a reduction in temperature also reduces the reciprocity failure. Indeed, Berry and Mendlsohn [26] have observed that some emulsions at -183°C do not suffer reciprocity failure at all.

Special film cassettes with compartments packed with dry ice (CO_2) which reduces and maintains a low temperature during the exposure period and this technique is now used on turbine blade root sections. Liquid nitrogen was tried but has proved more difficult to apply and caused damage to films and screens. The effect of film temperature on the resultant density is plotted in Fig.18. Conveniently the temperatures achieved by CO_2 apparently overcame the reciprocity failure. A comparison between radiographs taken of turbine blades with and without low temperature cooling is given in Plate 13. It is not certain what proportion of gain is attributabe to the reduction in the reciprocity failure as the efficiency of the phosphors probably also improves with a reduction in temperature. Nevertheless, the desired effect of increasing the thickness that can be radiographed with a comparatively low intensity x-ray source such as the E12 and provides the thicker sections of blades to be radiographed, with a high resolution technique (X8) revealing porosity which normal radiography can not.

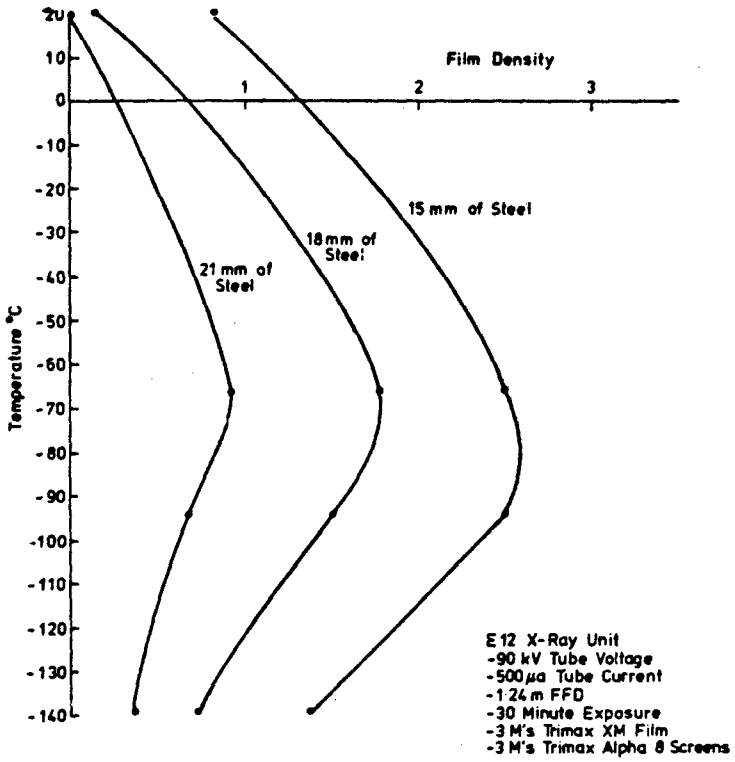

Figure 18

Effect of film temperature on film density

The technique however, is time consuming, typically a cycle of 1 hour is required for cooling and exposure and it is more suitable for the examination of small batches of experimental castings.

15. HIGH RESOLUTION FLUOROSCOPY

A rudimentary fluoroscope consists of a thin screen coated with a suitable phosphor, a conventional x-ray unit with suitable protective shielding. The coated screen replaces the film and thus a direct viewing system is possible. This arrangement can be used to scan assemblies and detect the grosser defects in castings and weldments etc. A small area of screen brightness differences can often be detected more readily when the image is moved but because the images are produced with a minimal integration of time, the sensitivities either of contrast or resolution are much lower than all but the extremely fast radiographic techniques using salt screens and when standard x-ray equipment is used.

Image intensifiers greatly extend the scope of 'real time' radiological imaging and they have many applications in medicine and industry. Not only do they produce greater screen brightness and hence higher sensitivity but they can also enhance contrast, and enlarge the image electronically and are more convenient as less time is required for 'dark adaption'.

A typical image intensifier assembly is encased in a glass envelope and a primary fluorescent screen which is backed with a photoelectric layer. The conversion process is: photons to phosphor - light to electrons (via the photoelectric backing). The electrons emitted by the photoelectric layers are accelerated and focussed onto a secondary fluorescent screen where the electrons are reconverted to light. The energy imparted to the electrons during acceleration, and by the reduction in size of the secondary screen, results in the high gain in brightness available for viewing, when compared with the rudimentary fluoroscope described hitherto.

The image on the secondary screen of the I.I. can be optically magnified. Alternatively a television camera is sometimes fibroptically coupled to allow a magnified image to be presented on to a TV monitor.

However, in the system described are two particulate phosphors, which can cause, in a similar way to the fluorescent screens in radiography, degradation of image detail due to energy unsharpness, (Uf), screen unsharpness, (Us), etc.

In addition, the integrating time of a true real-time system is 0 and thus the phosphors need to be fast and non-persistent, which they are not. A compromise results in a workable system, but lacking in resolution when compared with standard industrial x-radiography.

It is recorded that the sensitivity of real time image devices improves as the primary (x-ray) magnification increases [27] to a limit when the effect of the geometric unsharpness (Ug) predominates in the combination of the effects of all the unsharpnesses in the system. This implies that ultimately the resolution of such a system as in radiography will be limited by the size of the focal spot and when these are very small (10-50 μm) a large magnification can be used and thus an improvement in resolution is to be expected. Unfortunately other limitations are imposed by the low screen brightners, associated with the relatively low radiation intensities available from such small foci at large magnification distances, particularly after further attenuation by the specimen. A clumpy graininess appears on the screen known as 'quantum mottle' when the sensitivity is not improved by increasing the intensification to this level, or further. High resolution fluoroscopy is therefore currently limited to relatively thin sections. However, photographs of TV presentations showing the images of the trailing edge of a turbine blade illustrates the potential of this technique on aero-engine components (Plate 14).

16. XERO-RADIOGRAPHY using the Rank Xerox, system 125 has become an important method of graphic reproduction in the medical field. The basic xerographic process is versatile and allows the light source to be replaced with an x-ray source, thus xero-radiographs are produced. The process replaces photographic film with an aluminium plate coated with a layer of amorphous selerium. This semi-conducting layer is sensitised by imparting an even electrical charge to its surface by passing over an air-ion generating device. When exposed to x-rays the charge leakage depends on the intensity of the radiation reaching any point on its surface. The thicker (or denser) regions of an object will absorb most of the x-rays and the plate under these areas will retain most of the original charge. Areas under the less dense regions will allow more x-rays to the plate with a consequent leakage away from these areas. Thus a latent image is built as a pattern of the remaining charge on the plate. Development of the image is achieved by blowing charged powder on to the plate which is attracted to any area in proportion to the charge and therefore proportional to the x-ray exposure. A further ion emitting device is used to transfer the image to a paper carrier which is fixed by heating. The system can operate in a positive or negative mode. The plate is also re-usable and in some circumstances is a convenient and economic alternative to photographic film.

One well established use is in the radiography of the core assemblies of investment castings, when the presence of cracks in the silica tubes and the correct placement of the air cooling duct assemblies can be checked rapidly and economically (Plate 15). For high resolution work the process has some advantages. The technique for detecting microporosity, which has already been described, utilises film but the xero-radiograph of a similar turbine blade is shown in Plate 16. This technique proved to be superior and revealed details with greater resolution than the film techniques but the considerably longer exposure times were prohibitive (8 minutes as opposed to 20 seconds). The interesting edge enhancement found at the intensity steps is a characteristic which is peculiar to the xero process and may well be capitalised on in future x-ray techniques applicable to aero engines. For fine detail work however, the system that was tried at Harwell was not completely reproducible, a requirement that must be satisfied when large numbers of components are to be examined with confidence when flaws of micro size are to be detected and evaluated.

17. RADIOGRAPHY USING PROTONS

Proton radiography was first proposed by Koehler [28] who pointed out that the sensitivity to thickness variations was very high. At an energy of 160 MeV the limiting sensitivity is about 0.2%, with the range 32 mm of steel, which compares favourably with the sensitivities achieved using x-rays. The principles were demonstrated mainly with medical samples [29] but were first used on aero-engine components by West [30] when thick sectioned turbine blades were examined for the presence of microporosity. Unfortunately the apparently unavoidable unsharpness, caused by the multiple Coulomb scattering of the particles, does not permit images of high resolution, except when the detail is close to the film.

However, this marginal range technique (Fig.19) is capable of attaining contrast, which is not possible with x-rays, which can sometimes compensate for the lack of definition of detail. The high thickness sensitivity, achieved by matching the energy with the thickness to be radiographed, produces radiographs of minimal latitude and therefore the varying sectional thicknesses of a turbine blade require equalising masks (anti-blades) to compensate. The technique has been used to examine a large number of experimental blades and its use has lead to improvements in blade manufacturing and inspection techniques.

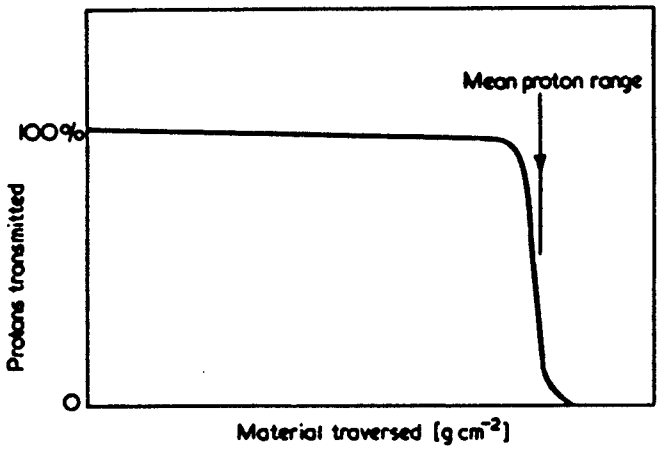

Transmission of protons of a given initial energy

Figure 19

18. NEUTRON RADIOGRAPHY

Radiography using thermal neutrons is an established technique for examining for the presence of residue core material in turbine blades and nozzle guide vanes etc. These components may have complex cooling galleries within the aerofoil sections since, like many other aero-engine components, they are also made using the lost wax investment casting process. After casting, a chemical process is used to remove the core material which consists of silica-zircon ceramics. Because, in some cases, it is not possible to view inside the galleries, assurance that all the core material is removed is needed before these components are used in an engine. A local temperature gradient or even incandescence can occur at positions where core material remains and thus may lead to a forshortening of the life of the component or even premature failure.

For some components, neutron radiography can fortuitously detect the presence of core material whereas x- and gamma-radiography can not. The quality of a neutron radiograph is determined primarily by the flux of neutrons available. Most neutron radiography to date has been carried out using thermal neutrons (0.025 eV) although cold neutrons (<0.005 eV) have been used for some applications. Neutrons sources emit a range of energies well above the thermal energies and they must be moderated or reduced in energy to become useful for radiography; because the attenuation coefficients of the higher energies are too low for most materials to produce radiographic contrast.

In a similar way to the x-ray case, the resolution of a neutron radiographic facility ultimately depends on the geometry. This however is expressed as the L/d ratio where L = length from aperture to the detector/film, d = diameter of the aperture from which the neutrons emerge, and this ratio determines the potential resolution of the system.

Other factors such as the neutron scattering produced by the sample and the inherent unsharpness of the film and foil will also affect the resolution. So also does the gamma radiation that is present when neutrons are generated. This will decrease the contrast thereby reducing the resolution. The presence of gamma radiation limits the capability of low intensity sources and generally it is not possible to produce a neutron radiograph by excessively long exposures because the gamma ray image may then predominate and thus the advantage of favourable contrast, obtained by using thermal neutrons, would be nullified.

A comparison between the attenuation of thermal neutrons and 120 kV x-rays is shown in Fig.20. It can be seen that in the case of x-rays the increase is steady and smooth with an increase in atomic numbers. The neutron attenuation coefficients however vary markedly from element to element. Whilst x-rays interact with the electrons orbiting the nucleus, neutrons interact with the nucleus of atoms. This means that low density elements such as are in the residue core material can present a greater barrier to a beam of thermal neutrons than heavy metals (e.g. turbine blades made of nickel-based alloys).

Nuclear reactors are prolific sources of thermal neutrons and they can provide a facility (Fig.21) that produces radiographs of high quality, with short exposures. For subjects with suitable contrast the resolution can be similar in quality to that of radiographs taken with low energy x-rays (Plate 17). Consequently, up till the present time, most neutron radiography of engine components has been carried out using reactor sources.

Alternative transportable or mobile sources may be convenient to apply on the premises of the blade manufacturer, and indeed the operating costs may be lower. So far the alternatives have yet to be proved viable as regards either coping with the numbers of samples involved or producing the quality of radiograph which is currently desired for most aero-engine components.

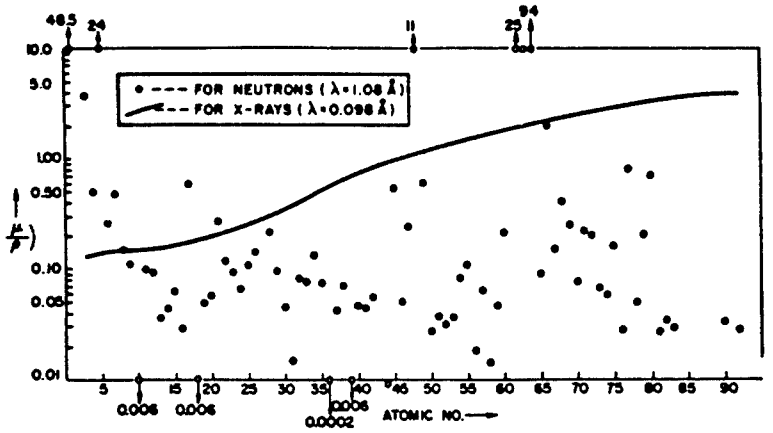

Figure 20

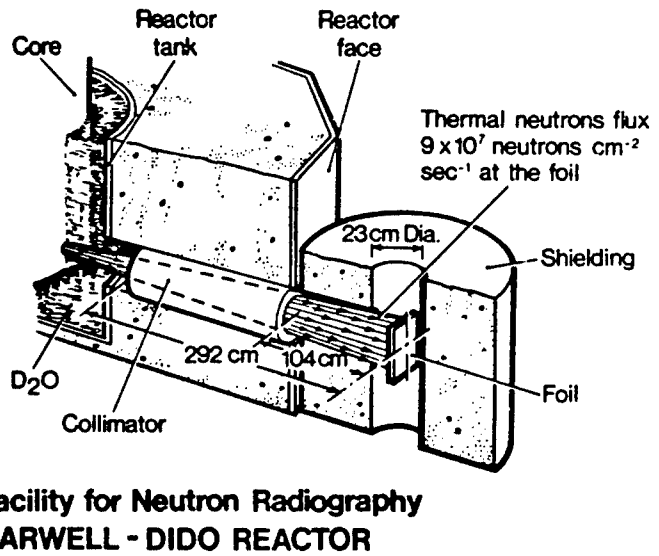

Figure 21

18.2 Types of detector

An intermediate thin foil of material is required to convert the neutrons into the gamma radiation or beta particles which can then be recorded on a photographic film in the normal way. Thin foils of rare earth metals are used to overcome the inability of neutrons to form their own latent image and basically two techniques are used to overcome this limitation. In one, the transfer technique (Fig.22) a metal foil is placed into the exposure position and after a predetermined time, the foil is removed then placed into intimate contact with a photographic film for a further exposure period. Thus the image is transferred. The foils which are rendered radioactive by the neutrons and the activity of the foil depends on the number of neutrons impinging on the foil. The activity from point to point across the foil is thus proportional to the variation of opacity to neutrons of the component being radiographed. The transfer technique is particularly useful for the radiography of radioactive specimens in the nuclear industry, which emit their own radiations that causes serious fogging of the film if x-radiography is used. The transfer foil is not affected by the gamma radiation from the active specimen and the remote position of the film eliminates the fogging. Foils of indium and dysprosium are used and these materials have half lifes of 54 minutes and 2.3 hours respectively. The

energies of the beta particles emitted by indium and dysprosium are approximately 1 MeV and thus an unsharpness due to this energy is apparent. An increase in unsharpness, as in the x-ray case, which has been previously stated, is evident as the energy is increased.

TRANSFER METHOD

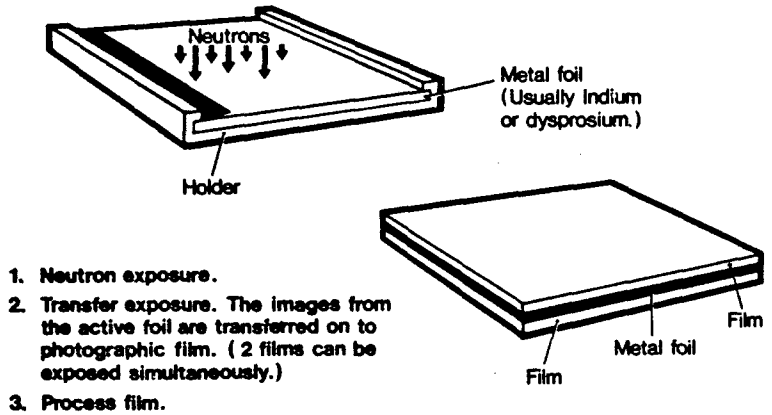

1. Neutron exposure.
2. Transfer exposure. The images from the active foil are transferred on to photographic film. (2 films can be exposed simultaneously.)
3. Process film.

Figure 22

The best results for residual core detection in castings however are obtained using the direct technique. The rare earth gadolinium is used and a thin foil is loaded together with the photographic film into a cassette and exposed directly (Fig.23).

DIRECT METHOD

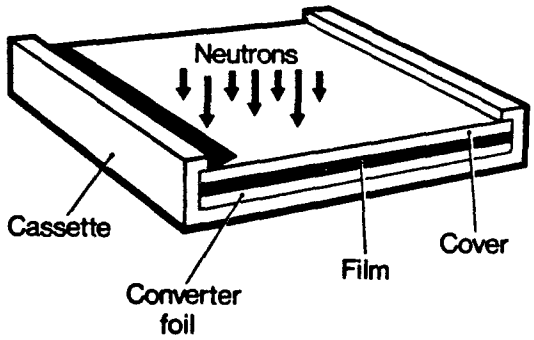

1. Neutron exposure
2. Process film

Figure 23

When neutrons collide with the foil the nuclear reactions (I.C. β_1^- 71 KeV min) taking place in it lead to emissions of beta particles (electrons). The electrons react with the photographic film to produce an image. Electrons produced from gadolinium have energies of approximately 7 keV and are promptly emitted when a neutrons is absorbed by the foil. The low energy electrons are thus capable of producing a sharp image and they have the resolution potential similar to that of low kV x-radiography. This is due to the short path length of the low energy electrons in the silver compounds of the photographic material.

18.2 Alternative sources

It is necessary to discuss alternative sources to enable conclusions to be drawn on the potential resolution of each type and to make comparisons between the results achieved by these and the high flux reactor sources.

1. Nuclear reactors
2. High voltage neutron generator tubes
3. Isotopic sources
4. High energy x-ray/beryllium sources.

All neutron sources produce energies much higher (fast neutrons) than the thermal level and must be moderated (reduced in energy) before they are suitable for radiography. Neutrons lose their energy by multiple collisions with atoms of moderating materials, particularly graphite, paraffin wax and water. Moderating materials are integral parts of nuclear reactors and allow thermalised beams, with more than adequate collimation (L/d ratio) directly. The alternatives, which also require moderation and collimation, are so reduced in flux that the radiographic resolutions do not approach that attained using a reactor source.

18.3 Generator tubes

Neutrons are produced by deuteron-deuteron or deuteron-triton reactions and the beams have fluxes of 10^5 - 10^6 neutrons cm^{-2} sec^{-1}. These fluxes can only be achieved with some relaxation in the collimation. In consequence the picture quality suffers and the results are rather like coarse grained fast salt-screen radiographs.

18.4 Isotopic sources

The flux of collimated thermal neutrons obtained by using these sources are also of a relatively low order. Composite sources have been considered which are constructed basically of 2 parts. One an alpha or gamma emitter and the other a beryllium component. The alpha particles or the gamma radiation interact with the beryllium component to produce neutrons. The most promising source for mobile work appears to be californium 252 (Cf 252).

The radiographs produced by the high energy x-ray/beryllium route are also lacking in quality for the same reason - the neutron flux is insufficient. Plate 18 presents illustrations of a typical turbine blade which has been radiographed using a variety of techniques [31]. Although the photographic resolution varies with the particular technique that is used, all reveal the presence of the core material indicating that neutron radiographs can be produced with low fluxes and providing the subject presents suitable contrast; the results are not high resolution from the photographic sense but can be useful nevertheless.

When the flux is so diminished due to moderating and collimating the beam, special detectors are required. These consist of a neutron scintillating plate containing small particles of lithium fluoride and zinc sulphide. The lithium converts the neutrons to alpha particles which act on the zinc sulphide, which emits flashes of light. These in turn are imaged on the photographic film. More recently the rare earth screens of gadolinium oxysulphide have been found to be useful in the same way. Use of both of these devices result in a considerable reduction in the exposure time required - at the expense of image quality. They do however enable radiographs to be obtained when the rare earth foils are unsuitable, as in the case when only a low flux source of neutrons is available.

18.5 Resolution

When considering the image forming capabilities of neutron radiography account must be taken of the contrast, which is effected by, variations in specimen thickness, differing materials and the energy of the neutrons. The scattering produced by the specimen contributes to image degradation although in practice this is serious only on the larger sectional thicknesses or with materials of high scattering cross section. Unsharpness, due to foil or films, which originates from the isotropic nature of neutrons and electrons can be improved by using thinner convertor foils, which are typically 0.1 mm when using the direct technique. A gadolinium coating 0.01 mm thick is sometimes used for high quality work. Single emulsion films, which effectively halve the effects of any gamma radiation in the beam, also improves the resolution.

The resolution achieved, using neutron radiography varies with the particular application and the technique that is used. The only advantage of using scintillators is a reduction in exposure time, since it can be 100 times faster than the metal screens but the resolution is in the order of 1 mm.

Using the transfer technique with indium or dysprosium foils this is improved to 0.3 mm. For maximum resolution the direct technique, using a neutron flux of 10^8 neutrons cm^{-2} sec^{-1}, a resolution of 0.01 mm is possible. Therefore with a suitable sample this would qualify as a high resolution radiographic technique.

18.6 Direct viewing

Image intensifiers, with phosphors adapted to convert neutrons to light, have been used to form a direct viewing system. These may find applications in imaging dynamic events, for instance for observing the distribution of oils within an aero-engine whilst running.

Although most of the neutron radiography in the aircraft industry has been applied to the 'residue core' problem there are others which should be mentioned here. Mobile equipment using the isotope Cf 252 has been used to detect corrosion in airframes [32], when radiographs of 'high resolution' were not a requirement.

Neutron radiography has also been applied to the examination of brazed joints, detection of adhesives in honeycomb sections, detection of organic compounds such as paper washers, rubber 'O' rings in thick metallic assemblies and the measurement of a component within an assembly.

18.7 Measurement using neutron radiography

Neutron radiogaphic measurement techniques have yet (to the author's knowledge) to be applied to aero-engine parts. It has however been used in the nuclear industry to measure the progressive swelling of samples undergoing irradiation 33 . Tell-tale devices are incorporated into the rig which are made of materials of high neutron cross sections such as dysprosium. The devices are spring-loaded against the component to be measured and the relative positions of the tell-tale can be measured and related to progressive increases in size. Accuracies of $\pm$ 0.025 mm have been achieved and the technique may also find application in dynamic radiography of aero-engines, when contrast and thus resolution is lacking, as sometimes is the case when x-rays are used. Similar tell-tales could be introduced providing silhouettes of extremely high contrast and resolution within large sectional thickness of a complete engine, and so measurements could be made of dimensional changes with greater precision.

19. CONCLUSIONS

Microfocal x-ray units are now established as viable radiographic inspection tools. They can consistently produce high resolution radiographs of aero-engine components and they can be operated by the normal radiographer employed in the aero-engine industry. These units can be installed in shielded compartments on the shop floor which cost a fraction of exposure cells having conventional x-ray equipment.

Microfocal/direct viewing systems can produce results of higher resolution than normally achieved but unless the radiation output from microfocal units is increased considerably their use will be limited to metallurgical specimens.

Neutron radiography can produce radiographs of high resolution. Indeed, the technique of detecting the residue core material in aero-engine investment castings is used on both sides of the Atlantic. Although mobile neutron sources can produce results, which may not in the strictest sense be claimed to be of high resolution, they can however sometimes resolve conditions such as 'core residues' and will be applied when it is not practical or economic to use reactor sources.

APPENDIX

Radiographs are difficult to reproduce with any printing process and there is no doubt, despite the skills of the printer, that some details in the plates will be inferior to the originals. However, included in this appendix are examples of high definition radiographs which can be compared with conventional radiographs and hopefully the advantages of using microfocal sources will be demonstrated.

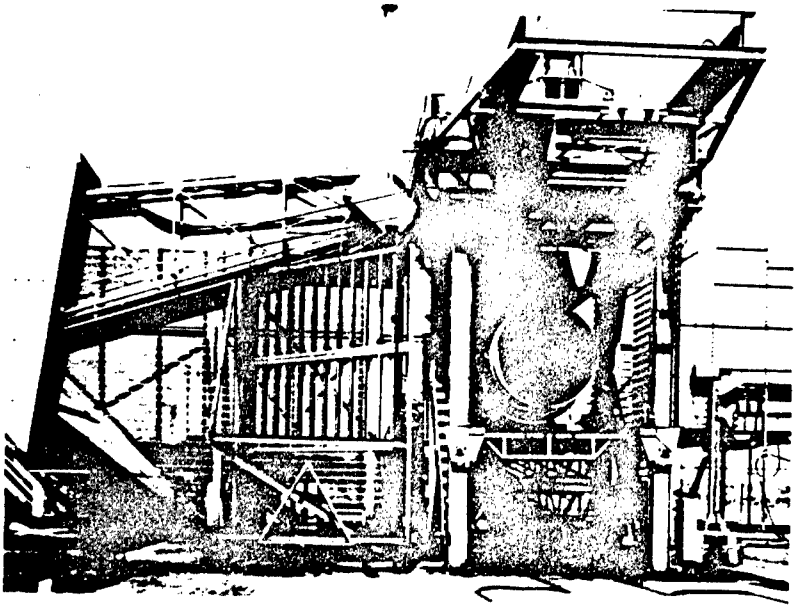

Plate 1

Linear accelerator set up to radiograph the RB211 Turbofan at Rolls Royce, Hucknall (Photo courtesy Rolls Royce Ltd.)

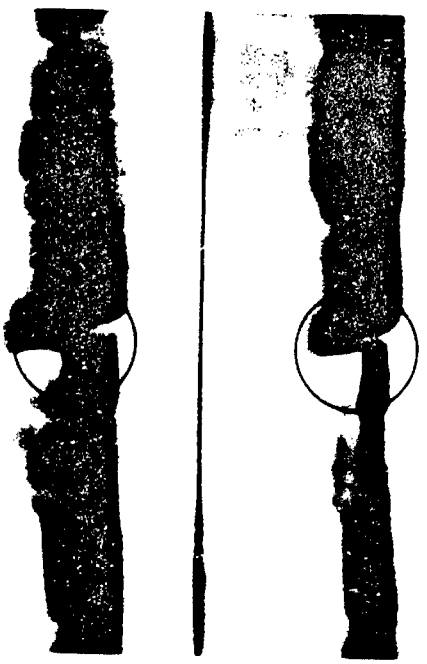

Plate 2

Radiographs comparing the engagement of a turbine seal under different engine running conditions The rotary component is on the right of each radiograph

Plate 3

Radiographs of low pressure turbine showing variations in vertical gaps between starter and rotor components, under different engine running conditions

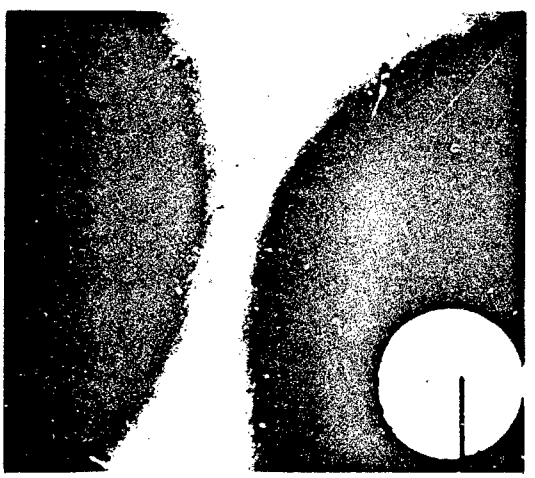

Plate 4

Comparison between a contact radiograph (inset) of a small nuclear fuel particle and a projected x-ray enlargement

The projected enlargement reveals flaws in the particle coating
For the contact radiograph, the particle (approx. 0.5 mm dia.) is positioned at the tip of a hyperdermic needle

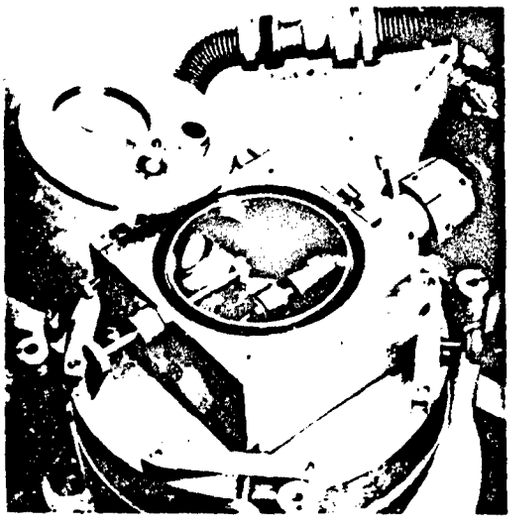

Plate 5

Variable solid target. Note the detachable target rings and the focussing mesh device

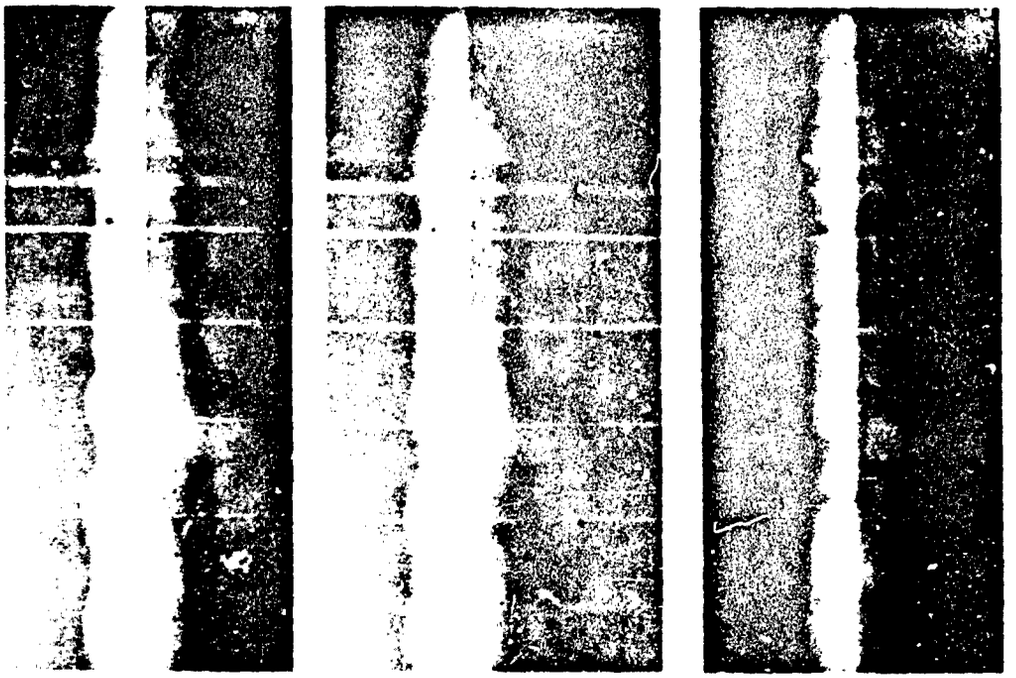

Plate 6

Comparison radiographs of an aluminium weld
From left to right, the Harwell E12, Magnaflux MxK100M and a conventional x-ray unit
Primary x-ray enlargement X6 (80 kV)

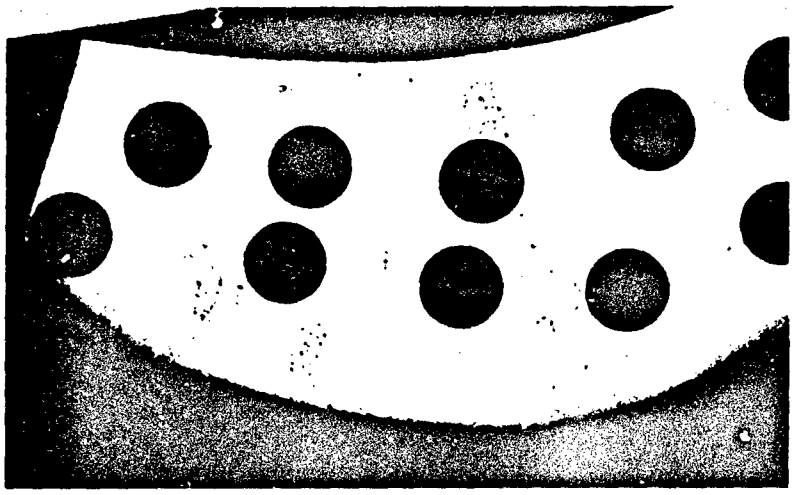

Plate 7

Section of blade aerofoil revealing bands of microporosity (Photo courtesy Rolls Royce Ltd.)

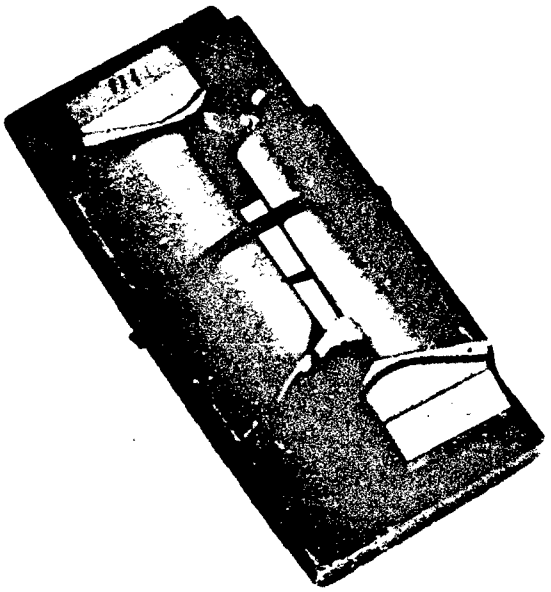

Plate 8

Coated lead mask constructed to precisely position and to mask the blades from extraneous radiation from outside the area of interest

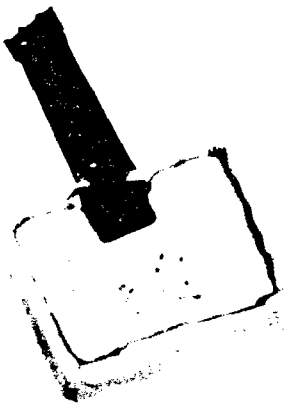

Plate 9

Ad hoc mask, used to enable the thick section of a turbine blade to be radiographed using a high definition projection technique

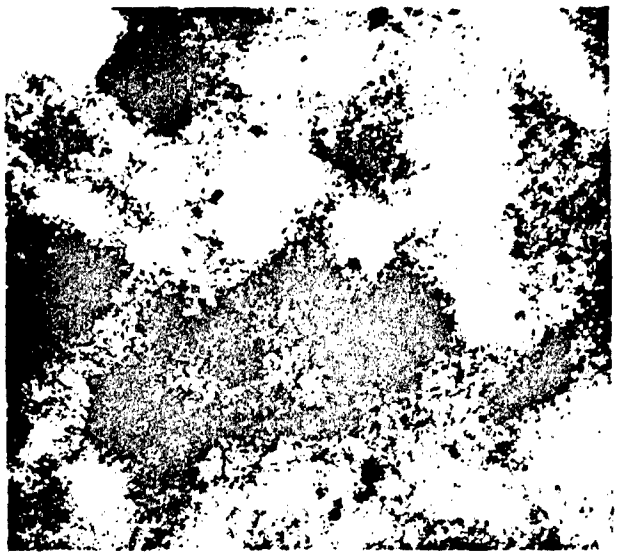

Plate 10

Enlarged projected radiograph showing
pores (0.03 mm diameter) in the presence of
'mottling' due to individual crystallites of the alloy

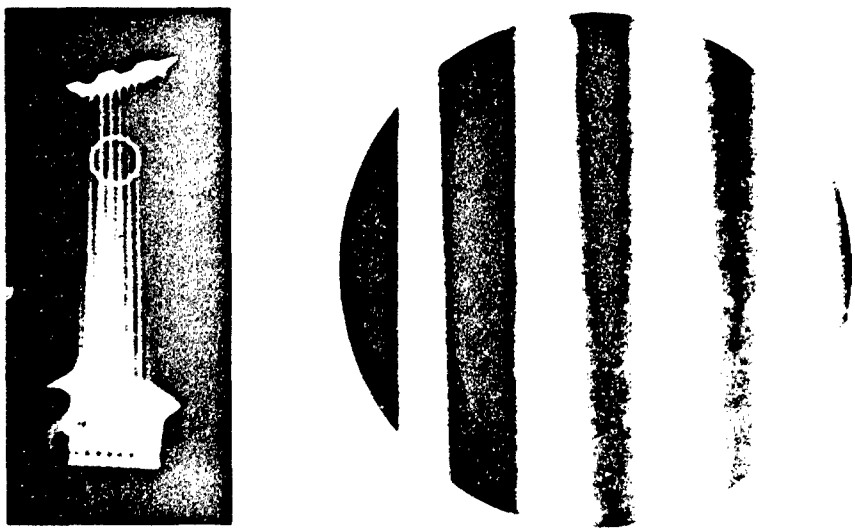

Plate 11

Conventional radiograph of a turbine blade
compared with a high definition projection radiograph
Note bands of microporosity

Plate 12

High definition radiograph
(Magnification X15)
Blade material 9 mm thick showing individual dendrites
90 kV 0.5 mA - 4 minutes.
Trimax film/screens

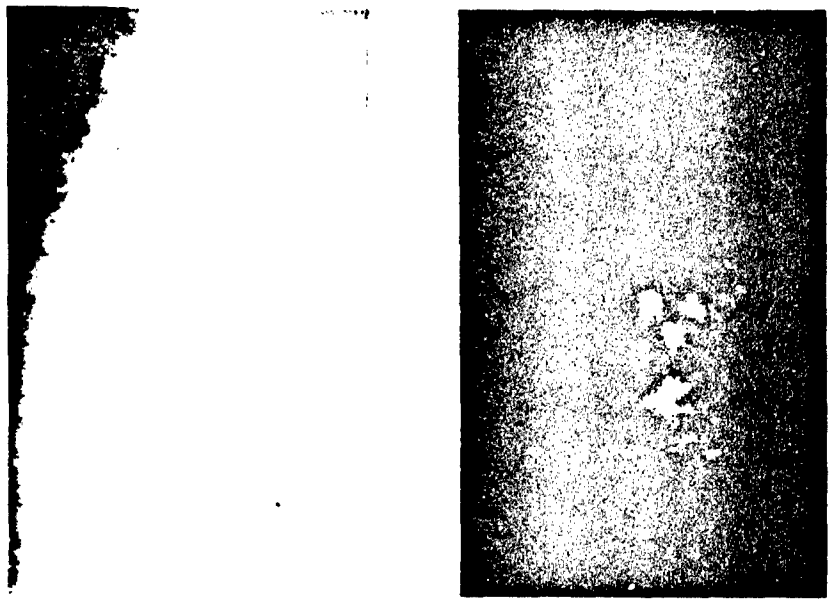

ROOM TEMPERATURE COLD

AERE - M 2871 Fig. 5
Turbine blade section

Tube voltage	85 kV
Tube current	500 μA
Film-to-focal spot distance	2.21 metres
X-ray magnification	x 12
Exposure time	8 minutes
Film and screen	3 M's Trimax

Plate 13

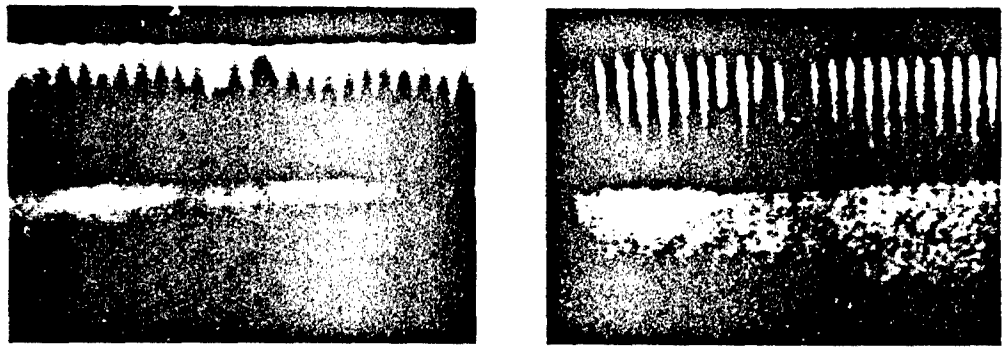

Focal spot size - 0.3 mm Focal spot size - 0.015 mm

Plate 14

Photographs of the screen of a T.V. monitor
illustrating two high definition direct viewing systems

Note: Blockages in the spark eroded holes (0.25 mm dia.).
'Quantum mottle' also evident on the lower output x-ray tube

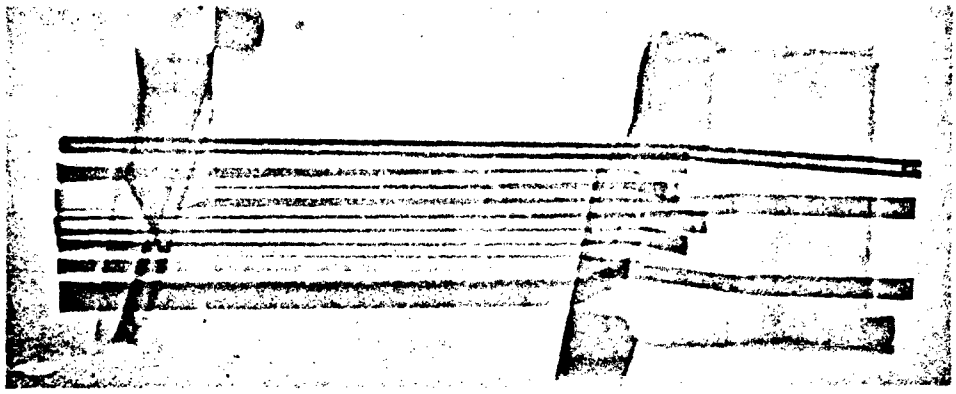

Plate 15

Xeroradiograph of air cooling duct assembly

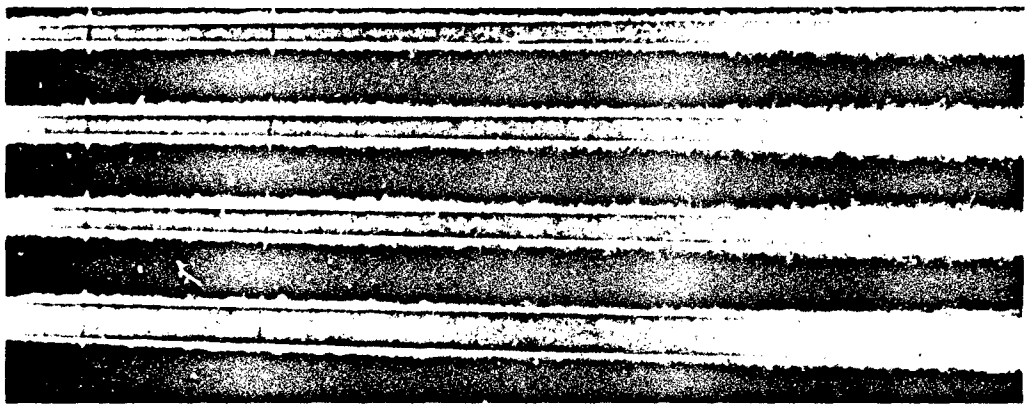

Plate 16

Xeroradiograph of a Pegasus turbine blade
Thinnest wire (Fe) visible os 0.02 mm

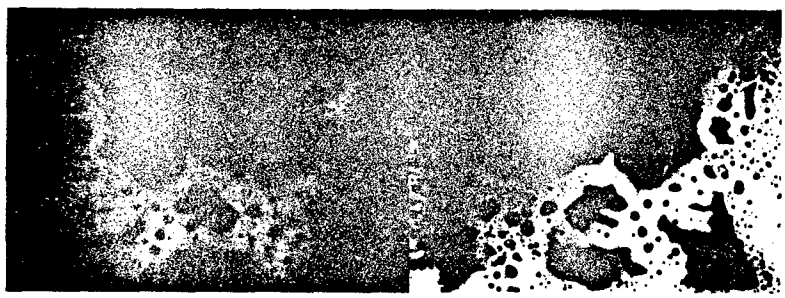

Plate 17

Neutron radiograph of a brazed joint (right)
compared with an x-radiograph material, Brass 12.5 mm thick
The contrast, resulting in excellent resolution, is due to traces of cadmium in the brazing material

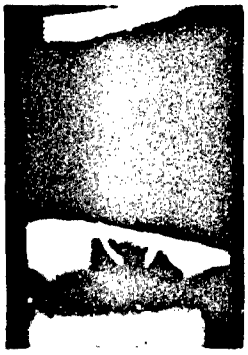

Cold Neutrons
DIDO Reactor
Gadolinium Nitrite
Enhancement

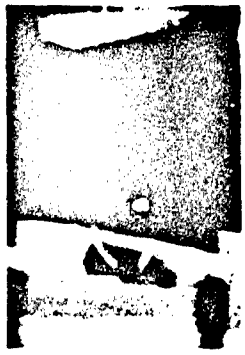

Thermal Neutrons
DIDO Reactor
Water Enhancement

Thermal Neutrons
GLEEP Reactor
Gadolinium nitrate
enhancement

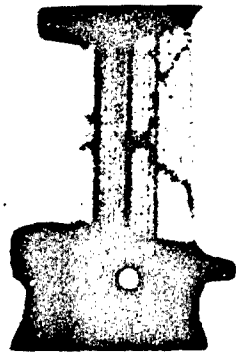

Thermal Neutrons
Cf-252 Source
Gadolinium nitrate
enhancement (Print)

Plate 18

Illustrating various neutron radiography techniques applied to the detection of residue core material within the galleries of a turbine blade Although the resolution varies with each technique, all are capable of detecting the presence of the core material

REFERENCES

1. Knox, R. and Kaye, G.W.C. The examination of aircraft timber by x-rays. Proc. Faraday Soc. Vol.15, Pt.2, 1918, pp.60-65.

2. Sharpe, R.S. High definition radiography. Proc. 6th Symp. of Physics. DAYTON OHIO, 1965.

3. Glossary of terms used in radiology. B.S.2597, 1955.

4. Reynolds, W.N. Private communication, 1978.

5. Halmshaw, R.

6. Carson, H.L., Feaver, M.J. An improved means for the measurement of weld radiograph image quality. International Inst. Welding, Annual Assembly, 1972.

7. Klassens, H.A. Measurement and calculations of unsharpness combinations in x-ray photography. Phillips research report 1, 4. (1946).

8. Robinson, A and Grimshaw, G.M. Measurement of the focal spot size of diagnostic x-ray tubes. Brit. Journal of radiology. Vol.48, No.571, (1975), pp.572-580.

9. Milne, E.C.N. Effective focal spot size. Investigative radiology, Vol.7, No.2 (1972), pp.124-128

10. Bernstein, F. Specification of focal spots and factors affecting their size. Proc. Soc. Photo-optical instrumentation engineers, Maryland, U.S.A., Vol.56, (1974), pp.159-163.

11. Halmshaw, R. Measurements of the modulation transfer function of radiographic films at different x-ray energies. 5th Int. Symp. Industrial Radiography, Belgium (1969).

12. Buchanan, R.A., Finkelstein, I. and Wickersheim, K.A. X-ray exposure reduction using rare earth oxysulphide intensifying screens. Radiology, 105:185 (1972).

13. Pullen, D.A.W. Radiography applied to determine dynamic conditions inside aero-gas turbines. Brit. Journal N.D.T., Vol.13 (1971), pp.42-45.

14. Stewart, P.A.E. Radiography of gas turbines in motion, Chartered Mechanical Engineer, Vol.19, (1972), pp.65-67.

15. Heycock, C.T. and Neville, F.H. Journ. Chem. Soc. L73 (1898) 714.

16. Cosslett, V.E. and Nixon, W.C. Nature, 168 (1951) 24.

17. Beirne, T. and Taylor, A. The E12 High definition x-ray unit. U.K. Atomic Energy Authority A.E.R.E. 7247 (1972) 13 pp.

18. Ely, R. Micro and enlargement radiography, Ilford Publication, Focus (1967) (1) p.14.

19. Walker, H.D. Inspection of jet engines by radioisotopes. Proc. Conf. Dayton (1966).

20. Fontijn, L.A. Mini magnetic lenses for microfocus x-ray applications, J. Vac. Sci. Technol., Vol.12, No.6, (1975).

21. Ridder, H.J. Developments in high resolution radiography. 8th World Conf. N.D.T. Cannes (1976) 3.E.10.

22. Parish, R.W. and Cason, J. Evaluation of incidence of microporosity in cast turbine blades using high definition radiography. N.D.T. International, I.P.C. Publication (1977).

23. Parish, R.W., Kear, P.E., Simmonds, L.R. Private Communication

24. Kear, P.E. The possibilities of low temperature radiography, AERE-M 2871

25. Hamilton, J.F. Reciprocity failure. The Theory of the photographic process. Macmillan (1942) Chapt.7, p.132.

26. Berg, W.F. and Mendelssohn, Proc. Roy. Soc. (London) Ser.A, 168 (1938).

27. Halmshaw, R. Recent Developments in industrial radiography. Fluoroscopy and screen processes. Progress in N.D.T. Stanford and Feavon (1958) pp.1-31.

28. Koehler, A.M. Proton radiography, Science 160, 303 (1968).

29. Koehler, A.M. and Berger, H. Proton radiography research, Techniques in N.D.T. research, Editor R.S. Sharpe, Academic Press, Vol.II (1973).

30. Stafford, P., Sherwood, A.C., West, D. Proton radiographic detection of microporosity in aero engine turbine castings. N.D.T. International I.P.C. Vol.8, No.5 (1975), pp.235-240.

31. Hawkesworth, M.R. Mobile equipment for neutron radiography using a Californium 252 source. Dept. of Physics, Birmingham, U.K. (To be published)

32. John, J. Californium-based neutron radiography for corrosion detection in aircraft. Proc. Symp. ASTM (1975) pp.168-180.

33. Matfield, R.S. The creep measurement of irradiated specimens using neutron radiography. U.K. Atomic Energy Authority, A.E.R.E. R 6822 (1972).

ACKNOWLEDGEMENTS

I wish to acknowledge colleagues at Harwell and at other establishments for allowing me to use material and for contributing generally by encouragement and discussion.

In particular I acknowledge the considerable help given by W. Reynolds and R.S. Sharpe both of the N.D.T. Centre, Materials Physics Division, Harwell. My thanks are also due to V.S. Crocker (Division Head, M.P.D.) and to the United Kingdom, Atomic Energy Authority for allowing me to prepare and present this work, and for allowing me to include figures and illustrations which unless otherwise indicated, remain the copyright property of the U.K.A.E.A.

WEAR DEBRIS ANALYSIS

by
N L Parr, C,Eng, FIMechE, FIM, FICeram
Management Consultant, ex Ministry of Defence
The Adelphi
John Adam Street
London WC2N 6BB, UK

J Ritchie, BSc
Procurement Executive, Ministry of Defence
Royal Aircraft Establishment
Farnborough, Hampshire, GU14 6TD, UK

SUMMARY

Factors controlling the cost of ownership of expensive military equipment are outlined with specific reference to the role of wear on scheduled and unscheduled maintenance. The value and limitations of established condition monitoring techniques and procedures, based on study of the particulate debris carried by the lubricating fluid, are explored for engine, gearbox and hydraulic systems. An account is given of current effort to improve these techniques and of research to evolve meaningful monitoring measures for a more scientific approach to the development and operation of new machinery incorporating advanced engineering designs and materials. An idealised research and development programme, centred on gear profile failure demonstrator facilities, including a number of supporting scientific, technological and design exercises, is presented.

1. INTRODUCTION

In absolute terms, the cost of ownership of an aircraft is directly related to the time it is available for operation against that originally planned at the design and specification stage, and this is shown in detail in Fig 1 from which it can be seen that maintenance costs represent an important and vital element. With increasing sophistication of design and construction there has been a continual increase in maintenance costs and it is not unusual for these to represent a third of the total ownership cost, hence any improvements in the ability to predict and control deterioration is likely to have a profound influence on life costs.

The normal procedure for improving both reliability and performance is to accumulate experience from field operations and then to apply this knowledge retrospectively to iterative development of design and construction processes. This is, however, a laborious process and a number of statistical surveys to highlight the major causes of unreliability and high maintenance costs have merely indicated the need for a more scientific approach involving research activity to improve knowledge of material behaviour, to reveal the true nature of loadings and environments, and to evolve more accurate means for assessing future satisfactory performance and residual safe-life. Such information is required both for a more accurate scheduled component replacement programme, and for quantifying defects and their significance in terms of fitness for service. Implicit in the acquisition of such knowledge is the need to provide more effective means for transferring this knowledge between design, production and operation, as each problem area will require attention and support from technology, management and data retrieval. Such an approach involving the integration of a number of disciplines and responsibilities to achieve maximum life performance has received much attention recently in the UK under the general term Terotechnology, or in its simplest terms, the Science of Care[1].

The three interrelated major elements of Terotechnology as applied to complex engineering systems shown in equilibrium in Fig 2 are:

i Improved management by the development of means for increased awareness, and for stimulating individual responsibilities within the complex management involved in the control of costs in large enterprises.

ii Improved technology transfer for enhancing the quality of technical knowledge along the lines of decision by harnessing relatively unoriented research, development and experience to the reduction of ownership cost.

iii Evaluation of more cogent means for generating pertinent data and systems for the automatic feedback to the design stage of more critical information on the factors dominating maintenance and residual safe life of expensive and strategically important aircraft.

An effective scheme for achieving such information and thereby to enhance and improve the Design and Specification process is outlined in Fig 3 which emphasises the need for degradation demonstrator exercises upon which to evolve more effective health sensing and safety monitors. Such a demonstrator programme requires to take a number of design variables into account aimed specifically at factors controlling cost rather than performance and would provide both on-line, or periodic, residual health and safety indicating monitors for equipment either under development, or in full operation.

Such demonstrator exercises are required to study and provide information on each of the six major forms of degradation experienced in aircraft and outlined in Fig 4, some of which are interdependent. The value of such an approach to all factors influencing the cost of aircraft can be seen from Fig 5, but the concept relies heavily on the existence of highly effective and meaningful health sensing techniques. Those required for monitoring strain damage and corrosion damage rates are outside the scope of this paper, which is concerned principally with wear damage rate.

$$\text{Anticipated achievement factor} = \frac{\text{Initial cost} + \text{total maintenance cost} + \text{operating cost}}{\text{Estimated annual cost} \times \text{estimated life (years)}}$$

$$\text{Actual achievement factor} = \frac{\text{Initial cost} + \text{total maintenance cost} + \text{operating cost}}{\text{Estimated annual cost} \times \text{estimated life (years)}} \times \frac{\text{Actual availability}}{\text{Estimated availability}}$$

Constituent elements

Initial cost	— Concept and feasibility studies, design, development and specification, airworthiness certification, production and quality assurance, handover and training
Maintenance cost	— Scheduled replacements, inspection, major strip and repair post design improvements, unscheduled replacements (i e defect rectification) manpower
Operating costs	— Logistic support, manpower, disposal
Availability	— Reliability and maintainability
Reliability (principally war-time requirement)	— Confidence in extended use. Mainly governed by retrospective experience
Maintainability	— Principally subject to good engineering practice, design and production

Fig 1 Principal elements of the cost of ownership appropriate to military aircraft

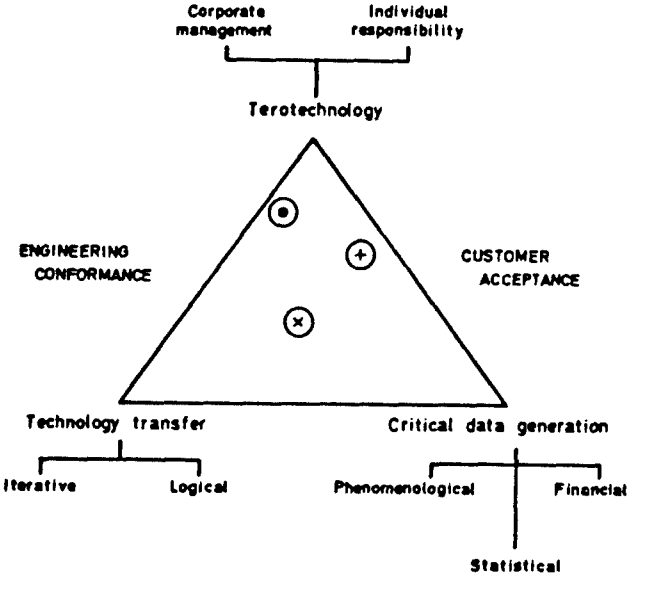

⊙ Case I Requires improved management of existing data

⊕ Case II Demands close management of critical data

⊗ Case III Requires generation and technical interpretation of critical data with strong management support

Fig 2 The principle elements of life cost control in design and development

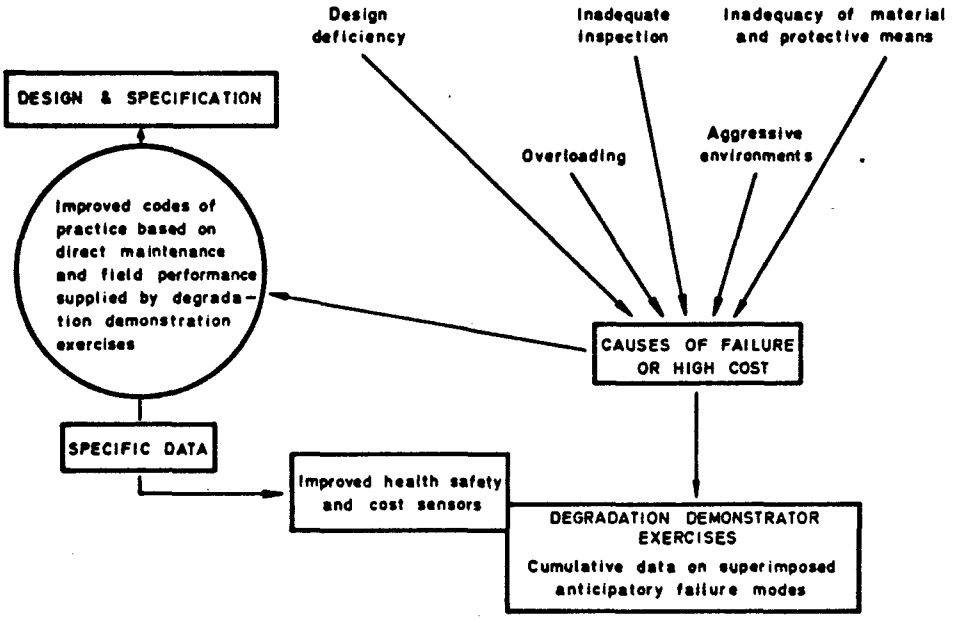

Fig 3 Means for acquiring more specific information and codes of practice to control ownership costs

STRAIN DAMAGE RATE	Flaw location and incidence	Surface Sub-surface	Criticality of position
	Flaw growth	Fatigue crack growth Criticality of position and size	
	Bulk material changes	Creep Strain damage (ageing and fatigue)	
WEAR RATE	Surface damage	Non-linear surface reactivity Increased roughness Fretting Fatigue	
CORROSION RATE	Wastage	By electro-chemical attack By oxidation By chemical reduction and biodeterioration	
	Selective attack	Stress corrosion Corrosion fatigue Hydrogen embrittlement	

Fig 4 Principal forms of material degradation

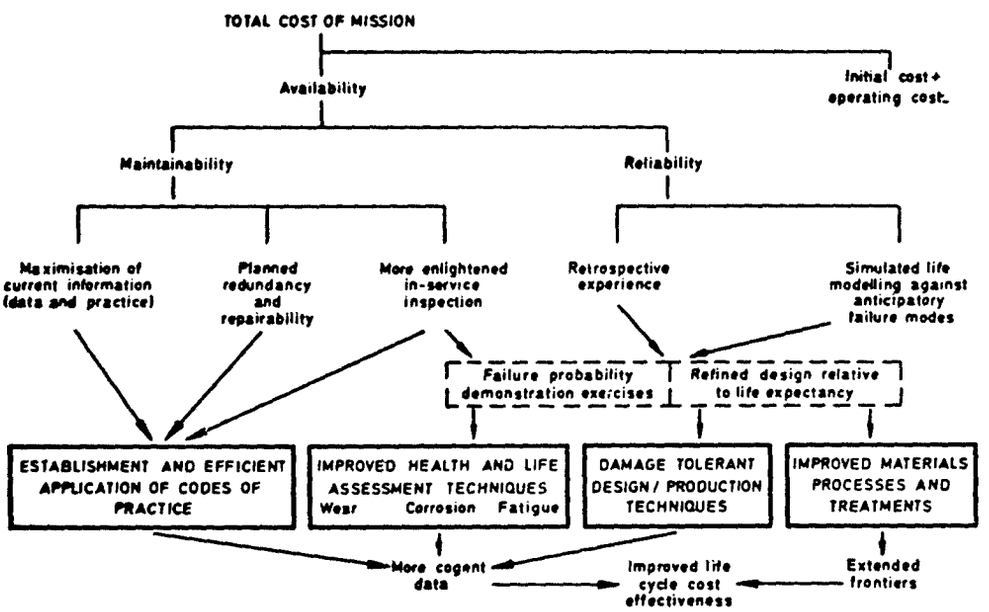

Fig 5 Derivation of pacing factors and arising areas of opportunity to control ownership costs of military aircraft

The effect of wear in bearing and sealing systems on both scheduled and unscheduled maintenance costs is considerable and spans a wide range of tribophysical and tribochemical science and technology. The whole span of scientific and technological discipline covering the subject of Tribology has been the subject of considerable academic and technological activity in the UK over the past two decades[2]. However, improvements to bearing surfaces has, and continues to be, largely empirical, but in advanced aircraft systems, for example in helicopter gearing and power transmission, it is now essential to identify more clearly those design, material and loading interactions governing changes in critical surface condition leading to a sequence of deterioration processes, sometimes culminating in catastrophic failure.

2. THE NATURE OF WEAR AND ITS CONSEQUENCES

As in the case of the gap between dislocation theory and fracture mechanics in the scientific and technical understanding of strain hardening and crack behaviour in metals, so a similar gap exists between the study of microsurface phenomena and characterisation of surfaces and the visual appearance of macro-degradation upon which engineering experience and design in bearing systems are based. The performance and improvement of bearing surfaces has evolved historically from iterative development of materials and systems within specific loading and environmental conditions, frequently to a high degree of satisfactory performance. The surface geometry, superimposed vibration, and above all the nature and continued integrity of the lubricant under time and environmental degradation are thus major influences on changes to optimum surface condition, and hence to a possible increase in the rate of wear.

Under ideal operating conditions the first stages of wear are likely to be dominated by a burnishing of asperities between the surfaces in relative motion with a consequent shedding of a small quantity of particular matter. This then leads increasingly to burnishing and passivation of the surfaces, and under ideal conditions of lubrication, prolonged operation with low wear rates. Such conditions are, however, not always obtained and highly localised micro-galling may follow from the presence of impurities in the lubricant, mechanical reasons for the breakdown of hydrodynamic lubrication, or from work hardening of mating surfaces, particularly under heavy loading conditions.

Different influences operate in gas, and dry bearings, and in seals where mating materials are often of widely different composition, and operate under lighter load bearing pressures. For instance, quite recently the nature of seal performance and wear has been observed as a distinct three concentric band phenomena[3] across the width of the seal. Thus, immediately adjacent, and in contact with the sealed fluid there is usually a circumferential band due to interaction of the sealing surfaces with the fluid. A similar effect is observed on the other outer band but the centre band is usually highly discoloured due to the effective sealing action associated with a local surface temperature rise causing a high temperature and pressure gas band with highly effective sealing and minimum surface contact and wear. This effect is due to the local surface conditions within the centre band approaching the critical temperature and pressure of the fluid being sealed, thereby generating a highly effective and minimum wear gas band condition, virtually independent of the sealing material pairs. The effect is most marked in graphite silicon carbide systems.

This paper is, however, concerned principally with the wear particles in fluid lubricated bearing systems, and the main categories of wear have been classified in engineering terms as Abrasion, Erosion, Fretting, Scuffing and Contact Fatigue. Each of these forms relate mainly to the nature, velocity and load intensity of the particular systems, to the quality of the initial design and specification, and to the care and integrity of subsequent operation and maintenance.

Abrasion is mainly a function of the nature of the initial, or developing, surface conditions, or the presence and effect of foreign particles in generating a cutting action. This condition then becomes self-generating and takes the form of progressive scoring to the point where lubrication becomes ineffective with ultimately complete surface breakdown. Time-scales involved in such processes depend much upon surface load intensity, superimposed vibration, and the degree of aggression introduced by the contaminants in the lubricating fluid, but the rate of wear always increases exponentially towards the end of the life of the bearing.

Surface degradation by erosion resulting from the imposition of localised high energy release by vapour bubble collapses, or by high microturbulence, is not usually encountered within bearing surfaces, but may occur at some locations within a total dynamic lubrication system with consequent material shedding and harmful contamination and deleterious effect to bearing surfaces.

Fretting constitutes surface breakdown through a combination of mechanical and oxidative reactions, sometimes with minimum oscillatory sliding motion. It is particularly sensitive to temperature and environmental aggression and somewhat similar to stress corrosion and corrosion fatigue in its effect upon fatigue crack initiation and growth. It arises as a result of highly localised bearing pressures associated with lubrication impoverishment or starvation. The nature of the associated debris is usually associated with a high state of oxidation of the bearing material surfaces.

Scuffing is a gross form of fretting resulting from work hardening and shedding of metal from surfaces in sliding motion and is exemplified by flakes of debris arising from local seizures.

Contact fatigue is probably the most undesirable form of wear as it can herald sudden catastrophic failure. Surface degradation by highly localised strain hardening and loss of ductility can occur under both sliding and rolling motions, although it is most common under rolling contact conditions in ball and roller bearings, gear flanks and cam surfaces. It arises as a result of orthoganal shear stress concentration causing lattice dislocation movements with micro-fracture and shedding of work hardened material and the formation of surface pitting. The presence of such surface flaws may be associated with material inhomogeneity or the existence of surface breaking impurities and inclusions. A consequential effect may be the generation of pockets of high pressure fluids under rolling contact conditions with further stress concentration and fatigue crack growth. The mechanism is accelerated by the presence of a corrosive environment, in particular where hydrogen can be generated by electrochemical activity with its consequent mobility and embrittlement effect on the material, in particular in steel.

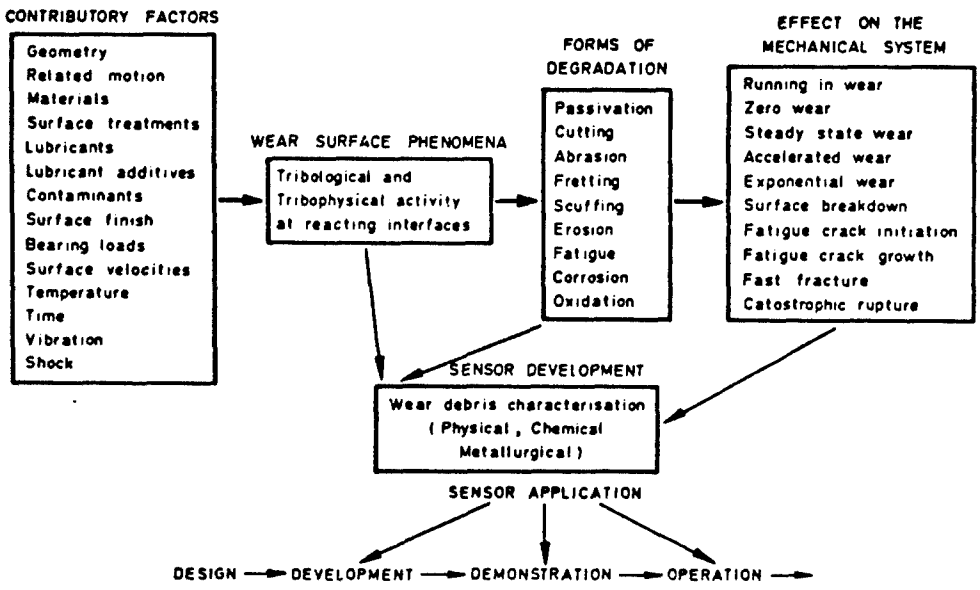

Fig 6 The origin, progression and characterisation of deterioration at tribological interfaces

Initial passivation conditioning, steady state and exponentially rate wear is invariably accompanied by the generation of debris whose chemical constitution and physical concentration must be related directly to the phenomena existing on the tribological surfaces. Thus, scientific and technological interpretation of wear debris in terms of its origin and generation provides direct intelligence of conditions existing at wear interfaces, and this gives diagnosis and prognosis of current and projected wear surface deterioration as shown in Fig 6.

Each of the major wear and degradation processes can operate independently in bearing systems according to the geometrical nature, operating loads and environmental influences concerned, but it is more likely that two or more interact simultaneously or in sequence. For instance, abrasive wear may lead to assymetry of operation with changes in hydrodynamic lubrication permitting direct contact of bearing surfaces and the onset of contact fatigue. Conversely, rolling or sliding contact fatigue may shed hardened particles which will then increase the abrasive content of particulate matter in the oil with increase in wear rate. Erosion or Fretting wear products may have a similar effect.

Once a fatigue crack situation has been established by undesirable tribological effects at the surface of components, then other more conventional metallurgical phenomena will begin to operate. This involves progressive crack development by a series of strain hardening steps, so that strain age embrittlement takes place in material immediately beyond the crack front. A situation will be reached where the crack length is critical to the working stress load on the component when fast fracture and sudden catastrophic failure will take place. The rate of crack growth, and critical crack length is a function of the bulk properties of the material but the vital trigger mechanism is frequently the tribological conditions at the surface.

It is thus highly desirable to be able to identify the nature and concentration of wear debris in terms of its origin, and the engineering conditions giving rise to its occurrence. Further, if numerical values can be given to the phenomena, then the designer and operator of equipment has data which can be used with resultant economy at the design and development stage, and as a basis for highly meaningful health monitoring systems during the operation of equipment. Ultimately, this would lead to a "Safe Life" of "Fail Safe" philosophy of extreme importance to extremely costly and highly rated aircraft equipment including main and auxiliary power units, transmissions, hydraulics and avionic systems. Such information would have a direct effect upon the precision in specifying more cost effective scheduled replacement of components, and thus upon the nature and frequency of maintenance schedules.

This then sets the scene for the next section of this paper which deals with the state of present knowledge and activity with wear debris characterisation monitoring systems of a wide variety of tribological conditions involving many metallic bearing materials in oil lubricated systems. However, ultimate calibration of wear by characterisation of debris matter can only be achieved by fully integrated scientific and technical demonstration exercises, rather than by random statistical field experience and a model system for accumulating logical and progressive data will be postulated in the final section of this paper.

3. STATE OF THE ART

The basis for the use of wear debris analysis to provide diagnosis and prognosis of surface wear has been illustrated in Fig 6. Details of current techniques and experience with them will now be outlined.

3.1 Method for Wear Debris Analysis

A variety of methods[4] can be used to evaluate wear debris in lubricating oil and thereby provide information on the condition of rubbing machine components. Those methods can be classified into three types:

On-line determinations

Debris collection and subsequent inspection

Lubricant sampling and subsequent inspection

The on-line determination with continuous read-out from a detector fitted into the system is very convenient as instant, continuous information is available without the need for any administration or possibility of error. However, equipment costs tend to be fairly high with separate units required at each point of interest. The main type of commercial instruments available are based on light scattering by the particulate matter. Vibration can cause problems and the sensors detect all particles present, for instance lubricant degradation products as well as the more critical wear debris, and this can cause interpretational difficulties. Another type is a filter which signals the quantity of conducting debris collected. Alteration of filter mesh size can change the size of debris collected, but normally this is selected to catch large particles only. Other principles that have been explored for use in such devices are electrical inductance or capacitance. These are better suited for the detection of the larger particles and both have problems ensuring adequate temperature compensation.

Debris collected by units such as magnetic plugs, filters or centrifuges can be subsequently examined to provide information on the debris collected[5,6]. Considerable information is obtainable from this source, however, the data is not continuous but only available after examination from the removal device. Equipment costs are low, although units are required at each point of interest, and effective interpretation requires considerable experience. Filters and centrifuges need to be fitted immediately downstream of critical components if evidence is not to be lost by settling. A great deal of information on the condition of the machine can be obtained by examination of accumulated debris as this contains all the contaminant present, ie the non-ferrous as well as the magnetic material.

The most common devices of the debris collection type are magnetic plugs or chip detectors. These consist of a magnetic probe fitted into the oil flow to collect magnetic debris particles. They are generally provided with self-sealing fittings so that the plug may be withdrawn for inspection without oil

loss. Only ferrous material is caught and detected but since most of the loaded components of machines are manufactured of magnetic steels, ie gears and bearings, this is not much of a limitation, although debris from some high quality stainless steels and paramagnetic material may escape collection. These equipments are cheap and easily inspected and can provide a great deal of information on machine condition to a skilled operator. The collected debris, like that collected on a filter, is representative of the whole time since the last inspection not some particular instance in time. Separate units are required at each point of use and each requires individual attention at the selected operating periods. The mode of installation has a major influence on particle catch efficiency but the necessary conditions have now been thoroughly explored. A variety of designs and magnetic plug and chip detector are available from simple units where the plug has to be removed for operator inspection and interpretation of the collected debris to sophisticated indicating units with facilities for indication at a distance.

Lubricant sampling methods have the advantage that only a single sample is required withdrawn from a convenient source whilst the machine is being operated, or sufficiently soon after it has been shut down, so that the debris particles have not settled out. The analysis is generally best carried out in a central laboratory with the associated problems of sample transport and the return of information to the equipment operator for decisions on whether or not the machine should be removed from service. Just as with the debris collection methods information is only available at periods corresponding to the intervals between sampling, and the reading obtained reflects the history since the last complete oil change. An additional factor that needs to be allowed for is the effect of top-up with new oil which has the result of reducing the concentrations of wear debris particles on the lubricating oil. The method involves two separate steps:

(1) taking a representative sample from the lubricated

(2) analysis of this sample to determine debris and contaminant materials present

The sample should preferably be taken from the machine whilst it is running or very soon afterwards, otherwise the particles present may settle from suspension thus removing the evidence. The oil samples may be obtained in a variety of ways but care is needed to ensure that dead lines or valves are thoroughly flushed. If for instance a sample is collected from a drain an unrepresentatively large quantity of debris may be obtained. The subsequent analysis may be by chemical means to determine the nature and concentration of contaminants in the lubricant or by physical means to determine quantity, size and shape of the contaminants. In either case it is usual for the analysis to be carried out by a specialist in a laboratory so the lubricant sample suitable identified as to its source has to be transported to the analysis centre. After the appropriate analysis has been completed results have to be compared with previous history before useful assessment of the condition of the particular machine is possible. The usual techniques employed to determine chemical nature of wear debris involve spectrometric analysis (SOAP) of the oil sample either by atomic absorption or atomic emission spectroscopy. These can both determine most of the metals likely to be found in used lubricating oils such as iron, copper, zinc, cobalt, chromium, nickel, tin, lead and silver. Atomic absorption uses relatively low cost equipment determining the concentration of one element at a time whereas atomic emission, which involves expensive equipment, can make instantaneous measurements for numerous elements. In both types of instrument the oil sample plus debris is vapourised, in a flame or electric arc respectively, so that the characteristic spectral lines of the contaminating metals are emitted. In practice the results produced tend to be representative of the smaller particles present, namely those up to about 8 microns in major dimension. Physical methods which have been used to analyse used oil include particle size spectrum determination and Ferrography. Particle size distribution analysis is conveniently carried out in automatic counters such as HiAc and Coulter instruments which provide a size distribution in terms of equivalent spheres. This may give useful information on wear occurring but can be confused by the presence of particulate matter from sources other than the wear and which is also counted by these instruments. A measure of the cleanliness levels and particle size spectrum may also be obtained by filtration of the fluid through a fine filter, typically a Millipore Filter, followed by microscopic examination. This tends to be wearing on the operator and somewhat inaccurate. Debris can also be separated by other techniques such as with a magnet or an ultracentrifuge. Such simple methods may be useful for a particular system. A recent more sophisticated technique is Ferrography[7,8,9] which separates wear debris from the oil sample by the action of a magnetic field. The Analytical Ferrograph arranges debris according to size on a glass slide, permitting detailed examination by visual or electron microscopy. This technique shows considerable promise for research applications but the equipment costs and the time required to examine a sample appear to rule out widespread field use. A second version of the equipment, the Direct Reader, collects particles in plastic tubes assessing the relative quantities of 'large' and 'small' from optical density readings. The results frequently being expressed as a Severity Index such as

$$I = D_L^2 - D_S^2$$

or

$$I = D_L (D_L - D_S)$$

where D_L is fractional area covered by large particles (greater than 5 microns) and D_S is the fractional area covered by small particles (1-2 micron range).

3.2 Interpretation of Wear Debris Measurements for Machinery Health Monitoring

Wear debris concentration and type can provide indications of wear and therefore of machinery condition. When interpreting the analysis results it is important to rember that the debris was collected over a period of machine operation and that it does not represent an instantaneous effect, that any new components fitted may produce running-in debris and that contaminants present from the machine build, present in the new lubricant or introduced from the environment, may tend to hide changes in the wear debris. It is generally desirable to observe the trends in wear debris generation for each particular machine and appropriate storage and retrieval of the information is necessary.

Different factors can be used to assess machine wear or failure. If machine elements produce increasing quantities of wear debris as they approach failure than the amount of debris can be used to provide an indication of the condition. Trend plots are frequently employed to indicate the cumulative amount of wear debris and any rate of change of wear debris generation with time, thus identifying the change of wear severity or the start of new processes see Fig 7.

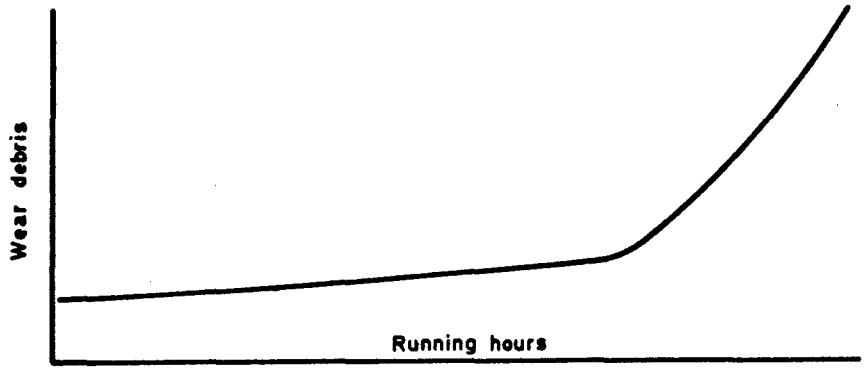

Fig 7 Trend Analysis

The fact that the size of debris normally increases from running-in through normal operation to the wear out or failure situation, can also be used to assess machinery condition, see Fig 8.

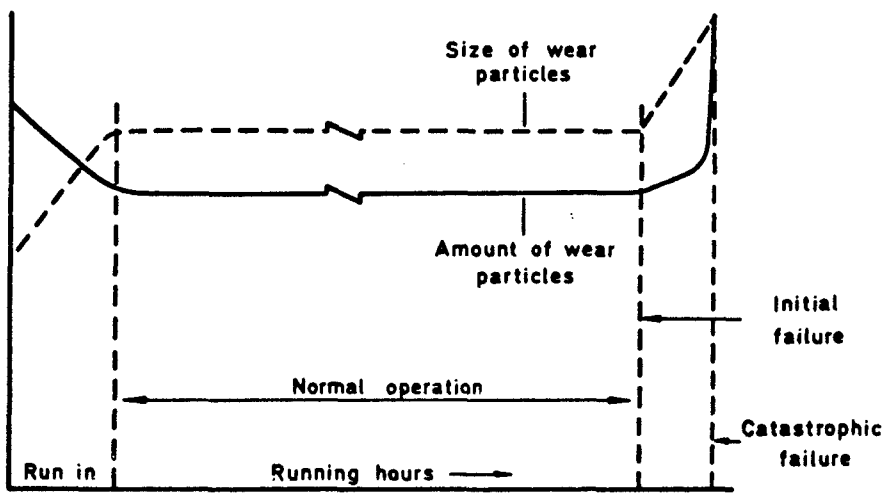

Fig 8 Variation of Wear Debris Size and Amount with Running Hours

Detection of the production of larger debris particles may provide improved lead time to failure over determination of quantity of debris. One-line systems based on comparison of amounts of large and small particles by optical methods and on the detection of large particles in electrical conducting filters are available. Similar information can also be obtained from magnetic plug inspections or Ferrography, both these latter of course depending on selection of suitable sampling intervals. Also dependant on oil sampling are the automatic counting methods which can give detailed size distribution data on particles present in a liquid. This method is frequently used with hydraulic systems which can be very sensitive to particulate matter. In the UK a Ministry of Defence Standard[10] has been published giving contamination classes for different types of hydraulic system. The standard was developed from particle size distributions determined on engineering system and thus the relative proportions in different size ranges are consistent with findings from practical systems. This avoids difficulties in classification because for instance the large particles are within the permitted numbers whilst totals of small particles are outside the limits.

Chemical analysis of wear debris can frequently help to pinpoint the components that are actually wearing. Very sensitive methods are needed, and the determination is therefore normally carried out by a suitably equipped specialist. Analysis may be by spectroscopic methods on oil samples, or by electron probe analysis of the larger particles separated by any suitable device. This approach is particularly valuable when the element determined is not the major engineering material used in the particular machine, such as steel in a gearbox, but is a contaminant such as silica or a specialist constituent such as silver from a rolling bearing cage or indium from the overlay of plain bearings. Iron is of course, very common since at least one of a rubbing pair is generally ferrous, but sometimes the simultaneous presence of alloying elements such as chromium, nickel, molybdenum, vanadium, etc can help to identify stainless steel or alloy steel components.

Physical methods of examining debris can also be used to obtain information about wear modes. Optical and electron microscopy of separated debris can yield considerable information about the source and mode of

machine surface deterioration. The essential first step is for the operator to recognise background material which has no significance for failure prediction, as for instance, metallic debris, sealing compounds, paint, fluff and other extraneous material left in the machine on build or overhaul, or the very fine ferrous debris produced in normal wear. The recent development of Ferrography has lead to considerable study of debris particles and their identification. The Wear Particle Atlas[11] produced under funding by the US Naval Air Systems Command "provides information for the identification of various wear particle types, the description of wear modes that generate these particles, and as a guide to the prediction of machine conditions based on the identified modes". This Atlas intended to be the first of a group covering identification of particles formed by the motion of steel on steel under loaded conditions and discusses the free metal particles generated. It divides wear modes into 5 types:

1. Rubbing Wear

The normal usually benign wear of sliding surfaces.

2. Cutting Wear

Abnormal abrasive wear due to interpenetration of sliding surfaces.

3. Rolling Fatigue

The fatigue wear of rolling contact bearings.

4. Combined Rolling and Sliding

The abnormal wear regimes of fatigue and scuffing as associated with gears.

5. Severe Sliding Wear

Excessive load and high speed wear of sliding surfaces.

Rubbing or normal wear particles are generated in normal sliding wear in a machine. They typically are platelets ranging in size from 15 microns down to 0.5 microns in the major dimension, between 0.15 microns to 1 micron in thickness and have a smooth surface. Abrasive contaminants such as sand can cause marked increase in the production of rubbing wear particles and the rapid wear of the system. Particulate analsis of the lubricant from such a system will of course reveal the contaminant particles as well as the wear debris. Cutting wear particles are generated as a result of one surface penetrating another, much as a lathe tool creates machining swarf but on a microscopic level. Particles can be relatively coarse and large, namely 2-5 microns wide by 25 to 100 microns long caused by a hard component penetrating a softer one, or fine wire-like material with a thickness of 0.25 microns caused by abrasive particles embedded in a soft surface and cutting the opposing wear surface. Cutting wear particles are abnormal, their presence suggesting either contaminants, or imminent component failure. Rolling fatigue particles are found in three types: fatigue spall particles, spherical particles and laminar particles. Fatigue spall particles are flat platelets with a major dimension to thickness ratio of approximately 10:1. They have a smooth surface and a random irregularly shaped circumference. The spall particles consist of the actual material removed as a pit or spall opens up. They range in size from 10 microns to 100 microns. The spherical particles have diameters ranging between one and five microns, and are believed to be generated in the bearing fatigue cracks. However, spherical metallic particles can also be present in lubricating oil as contaminants. New lubricating oil supplied by manufacturers frequently contains a few metal spheres and metallic spheres can also be formed by welding and grinding processes, so care is needed to ensure that spheres detected in a lubricant do arise from the wear process. Laminar particles are very thin 20 to 50 microns in major dimension with a thickness ratio of approximately 30:1 and frequently contain holes.

The gear wear particles caused by combined rolling and sliding arise from pitch line fatigue and scoring or scuffing. Fatigue particles from a gear pitch line are similar to rolling bearing fatigue particles. They generally have a smooth surface and are irregularly shaped, the major dimension to thickness ratio is between 4:1 and 10:1. The particles produced by scuffing tend to have a rough surface and a jagged circumference. Quantities of oxide are usually present and particles may show evidence of partial oxidation.

Severe sliding wear particles range in size from 20 microns upwards. They frequently have straight edges and a length to thickness ratio of approximately 10:1. They may show surface striations due to sliding.

3.3 Service Experience

There has been considerable experience in the application of wear debris analysis to the early detection of mechanical distress. Certain technologically advanced industries have built up experience with particular techniques for specific applications but the overall position is somewhat patchy with different techniques being applied for different operations.

The process industries have found on-line direct readers satisfactory for their purposes but this type of device has not yet been proven or accepted for aircraft use, where the weight, space and vibration requirements are more onerous.

Debris monitoring methods are widely used through a variety of industries and applications, frequently with relatively unsophisticated inspection, analysis and interpretation procedures. Table 1 lists the main methods in current use in aircraft systems. In the aircraft industry, many commercial airlines rely on debris collection methods to assess the conditions of engines in service. In military aircraft magnetic plugs and chip detectors are installed in virtually all helicopter transmissions and engines and in many propulsion and drive systems of fixed wing aircraft. Although these units are basically simple and cheap they have proved reliable indicators of incipient failure. Chip detectors, that is units including a remote warning signal, activated by debris particles closing the gap between two electrodes, have also tended

to give a large number of nuisance indications. These 'rogue' signals have tended to cause suspicion or disbelief in the indication thus reducing the value of the device to the operator.

The oil analysis methods have had the widest application in the aircraft industry with spectrometric analysis of engine and transmission lubricants and particle counting on hydraulic fluids. Military users have had high success rates with spectrometric analysis particularly of engine lubricants, by frequent oil sampling often daily, or even between each flight for engines under development, and careful plotting of trends, allowance for oil top-up etc. Commercial airlines are not unanimous as to the cost effectiveness and are concerned about the necessary administration with sample transport to the analysis laboratory and return of information to the responsible engineers. However, for many mechanical systems a suitably organised spectrometric oil analysis programme can provide a highly effective indication of impending failure.

In sophisticated hydraulic systems the contamination has to be maintained at a very low level if reliability problems due to blockage of oil ways and silting of valves are to be avoided. The total particulate content is therefore, of interest and not only the wear debris content. This data is obtained by determination of the numbers of particles preferably broken down to give a spectrum of the particle size distribution. Manual counting methods are time consuming and inaccurate but good results have been obtained with automatic particle counters. As with spectrometric methods the analysis is best reserved for a specialist in a laboratory thus necessitating transport of samples and effective administration.

The main limitations to these methods arise from the need for despatch of samples to a laboratory with the resultant loss of immediate control by the equipment operator.

3.4 Performance of Different Techniques

A number of studies have included assessment of wear debris from machinery experiencing failures by different techniques thus permitting evaluation of the different monitoring and predictive capabilities. An interesting study carried out by the Canadian Defence Research Establishment Pacific concerned oil samples taken from a Sea King helicopter gas turbine engine over the course of a bearing failure. The engine had been on an oil analysis monitoring programme using spectrometric analysis with an atomic absorption spectrometer. The results of this analysis had revealed an increasing wear trend which did not appear alarming, until failure of the number one bearing occurred. The oil samples collected over the critical period were then reexamined to determine the accuracy of the absorption spectrometric analysis and to assess the potential for improvements that alternative procedures might provide. Detailed examinations of the wear debris from the synthetic ester engine oil, to specification MIL-L-23699, were made by atomic absorption spectroscopy, X-ray fluorescence analysis, microfiltration techniques and Ferrography. The choice of methods being to provide a check on the original atomic absorption analysis, to see what additional information might be obtained from determination of all the particulate metal present in the oil and to assess the promise of Ferrographic analysis.

The atomic absorption spectrometer substantially confirmed the results obtained previously, with increases in iron and copper contents not reaching the guideline levels employed. Collection of virtually all the wear debris on a microfilter, followed by X-ray examination of the deposits and atomic absorption analysis of the deposits dissolved in hydrochloric acid gave substantially higher metal figures over the period of the failure. The Ferrographic analysis by microscopic examination of the separated debris and by the Direct Reader technique also provided early indications of abnormal wear. The analytical ferrography examination permitting recognition of particle morphology consistent with fatigue spalling.

These results imply that in this particular case the diagnostic capability of spectrometric oil analysis was limited by its ability to determine only the small wear particles and that the use of supplementary techniques permitting consideration of the larger wear particles also would provide improved diagnostic capability.

A recent UK study applied a number of condition monitoring techniques to a helicopter gear box during seven fatigue substantiation trials. The gear-boxes were run in a back to back rig and oil samples withdrawn from a magnetic plug fixture every five running hours were split and circulated to cooperating laboratories for spectrometric analysis using both atomic absorption and emission instruments, Ferrography and particle counting in addition to the vibration analysis and magnetic plug inspections carried out by the trials operator. Close agreement was obtained by the two spectrometric techniques for iron and copper but a much more sensitive failure detection was provided by the magnetic plug and by Ferrography which gave good promise of predictive capability. The trial gear boxes were driven at approximately 28% above normal operating power for 140 hours in the first four trials and at approximately 41% overload for 70 hours for three more with regular monitoring by the different techniques. On termination of the trial, or when distress was recognised, the box was stripped and the various components given an engineering appraisal. On the first trial a number of failures occurred almost simultaneously so it was impossible to identify different monitoring technique signals with particular failures but the later trials were not confused in this way and shim gear and bearing damage occurred. The vibration analysis and the spectrometric analysis had proved successful in identifying the various examples of surface damage. Particle counting gave a confused picture sometimes apparently dominated by the contaminants present in the new oil, although Pocock has shown[12] that the particle counts from the first trial can be treated to yield iron figures agreeing closely with those obtained by spectrometric analysis. Magnetic plug and Ferrography gave good indications of the various surface breakdowns with both giving indications of the failure mode being experienced. Magnetic plugs was successful at identifying shim wear with Ferrography giving particularly early signals of gear damage, perhaps showing promise as a predictive tool.

A US Army survey[17] over a two year period on one type of helicopter involving comparison of magnetic plugs with spectrometric methods on both engines and transmission systems showed a high success rate for both spectrometric analysis and chip detectors with the chip detectors reliability comparable to the spectrometric analysis overall and considerably better for the transmission.

3.5 Efficiency of Different Monitoring Techniques

Tauber[14] has produced an illuminating model for the development of the debris spectrum for a typical fatigue type failure (bearing or gear spalling), Fig 9. The diagram shows debris production rate plotted against time and debris particle size. If no failure occurs the amount and size of debris particles will not alter with time and the debris spectrum will therefore, remain unchanged along the time axis. The diagram illustrates the position as a failure develops and both increasing numbers and increasing sizes of debris particles are produced. Spectrometric methods which detect particles smaller than about 10 microns, will reflect the increasing numbers of small particles only whilst magnetic plugs permit preferential identification of the relatively large particles, typically 100 to 300 microns.

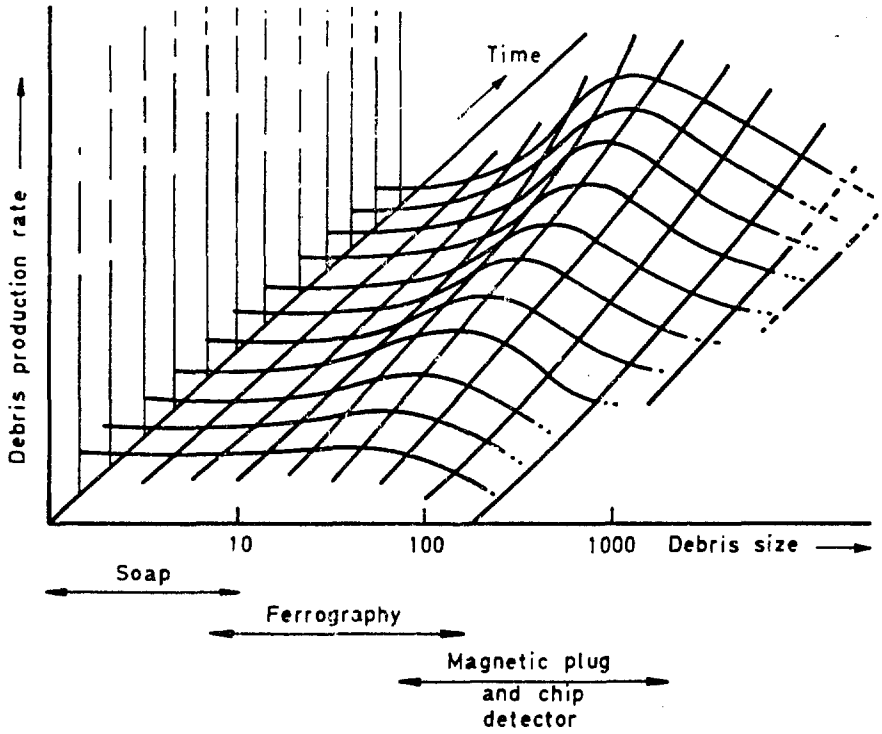

Fig 9 Wear Debris Particle Spectrum

Thus where failures occur by different mechanisms, and the relative quantities and particle size ranges of the wear debris differ, the responses of the two condition monitoring techniques would be expected to differ also. Failure mechanisms producing predominantly small particles will be most effectively monitored by spectrometric methods whilst if the mechanism generate particles in to 100-300 micron range then the magnetic plug will be the most effective.

Pocock[15] reasons that wear debris type condition monitoring sensors need to be matched to the particular wear mode because the various sensors/techniques are each sensitive to only a range of debris particle sizes. A wear mode generating particles in the size range 100-300 microns will, therefore, not be detected by a technique which is only sensitive to particles smaller than say 15 microns. And that it is often desirable to use more than one sensor to successfully monitor a particular piece of machinery. He illustrates the problem with Fig 10 which shows the efficiency/particle size relationship for three sensors. The established techniques of spectroscopic oil analysis and magnetic plugs have optimum efficiencies for debris particles of up to 15 microns and between 100-300 microns respectively. Thus whilst they complement each other there is a particle size range, between approximately 15 and 100 microns to which both are insensitive. Ferrography fits into this gap and although it is relatively new technique has already shown some success and offers promise for the future.

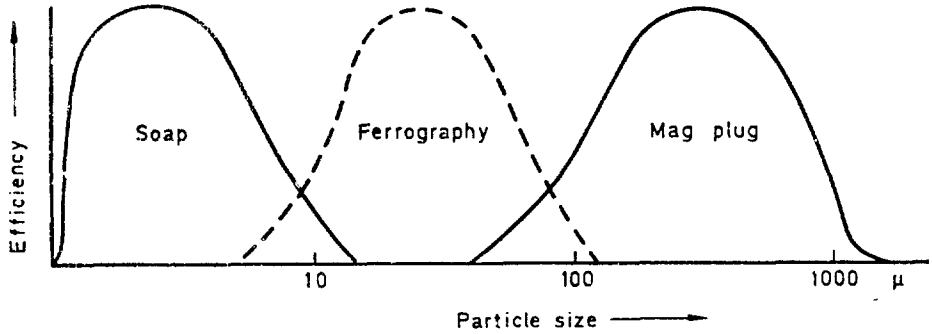

Fig 10 Sensor Efficiency - Particle Size Relationship

4 HIGHLIGHTS FROM CURRENT RESEARCH

It will be appreciated from the above that the ability to predict failures of machine components is uneven between different industries and between different types of machine. Fortunately research workers in several countries are contributing to improving understanding of the relationships between wear, surface failure and machine life, and to developing existing and new techniques. This section of the paper presents an overview of the current research. A summary of those condition monitoring techniques most likely to be of value in aircraft applications is included as the second part of Table 1.

4.1 Wear Debris and Surfaces

The US Naval Air Engineering Centre has made a major study of the correlation between particle characteristics and component surface wear[16] with the aim of providing a firm technical basis for the use of debris analysis for machinery condition monitoring. The programme involved two phases; a laboratory phase and a systems application phase. The laboratory phase consisted of bench testing of selected oil lubricated components and the systems application phase involved the verification of the laboratory findings by application to service or field conditions.

Bench testing was carried out for gears, sliding contacts, tapered roller bearings and ball bearings. Wear particle characteristics have been defined with respect to, quantity, size, elemental composition, morphology. It was concluded that severe wear can be effectively detected by monitoring wear particle quantity and size distribution. Particle quantity, as well as the ratio of large to small particles, normally increases substantially during an abnormal wear situation. Further information can frequently be obtained by elemental analysis of the debris which can be directly related to component material. Wear particle morphology (ie shape, size, colour) can also give information on wearing components and the relevant wear mode.

A separate US Navy review of literature and experience of both military and civilian personnel with spectrometric methods used for machinery health monitoring[17] concluded that they were effective in determining the amount and composition of contaminants present as particles smaller than 8 microns in jet engine lubricating oils. The identification of the composition of these particles, as for instance iron, copper, lead, etc, was of assistance in finding the failing component. Spectrometric analysis could give a good correlation with normal wear which provides a gradual build up of small particles, but a number of other wear mechanisms produce large particles prior to failure, and spectrometric analysis, because it is limited to the determination of particles smaller than 8 microns, cannot detect these larger wear particles, and is therefore less effective at predicting these types of failures. A number of other techniques were appraised for ability to supplement the spectrograph by analysis of the larger particles. A variety of devices were considered, including magnetic chips, oil filter analysis, in-line X-ray techniques, in-line light attenuation, atomic fluorescence, colorimetric methods and ferrography. It was concluded that ferrography was the only practical method available for supplementing spectrometric analysis. The major attraction of ferrography being its capability to recognise larger particles and to determine particle shape.

In a more fundamental study, Winer et al[18] analysed wear debris generated in a sliding elastohydrodynamic contact using ferrography. The contact was a steel ball rotating against a sapphire flat. Balls of three different finishes, smooth, medium rough and rough, were employed and experimental conditions included a range of loads at constant sliding speed and test duration at room temperature. Oil film thickness was determined optically for the smooth balls and the values used for the medium rough and rough series where surface roughness prevented optical measurement of film thickness. A single naphthenic mineral oil was used for all tests in a once through system to avoid particle contamination. It was found that: the total amount of wear debris correlated well with the ratio of film thickness to composite surface roughness (Λ ratio); a transition from low to high wear rate occurred as the ratio fell to about 1; wear particles were metallic and almost exclusively of the normal rubbing wear type; the Ferrograph was more sensitive in detecting the wear debris than the emission spectrograph.

In a discussion of results from a helicopter gearbox trial Pocock and Jones[19] point out that instances of gear damage gave rise to small (about 10 microns) fatigue platelets in the oil, which were recognised by ferrography some time before large (about 300 microns) fatigue particles were detected on the magnetic plug. This appears consistent with ideas from Godet, Berthe et al[20,21] that micropitting can lead to more severe forms of wear. These authors suggest that discrete asperity contacts occurring when the ratio of surface roughness to film thickness (Λ ratio) is less than unity, can produce micropits about 10-20 microns deep and as these become more extensive they join up to form large damage areas, still of the same depth, and subsequently lead to gross wear and spalling with deep pits typically 100 microns deep. Further investigation of the relationships between debris size and type of surface damage formed under these conditions should be rewarding.

4.2 Debris Studies in Specific Systems

Fodor[22] has used gamma-ray spectrometry of wear debris to monitor the behaviour of internal combustion engines. It was possible from the debris analysis to determine the amounts of wear in normal engine operation, seizure in a faulty engine, the depletion of oil additives and the contamination level in the system.

Hofman and Johnson[23] used ferrographic techniques in a laboratory study of wear of a Cummins VT-903 diesel engine. The Ferrographic Severity Index I detected slight changes in wear rate due to change of operating condition. Application of heated Ferrogram analysis (HFA) identified the parts suffering wear. The HFA (heating the Ferrogram for 90 seconds at 330°C) turns low carbon and alloy steels blue, cast iron brown and does not affect the lead from the bearings. This technique permitted identification of debris particles from the test engine as originating from the cylinder liner/piston ring or crankshaft/main bearing areas, the quantities of each present on the Ferrogram providing information on changes in wear rates of engine components with alteration of engine operating conditions.

Jones et al[24] have also determined wear in a diesel engine using ferrographic techniques. The running-in process for a Perkins Research V8 540 engine was studied showing that high initial wear fell to a low equilibrium rate after only 10 hours of running. The rubbing wear particles produced during the early running-in stage were large, typically 20 x 20 microns, and were not detected by spectrometric analysis.

A programme of trend analysis of gas turbine engines by ferrography has been reported by Scott et al[25]. Oil samples, as for spectrographic oil analysis, obtained from gas turbine engines of one type both from service and on test beds were subjected to DR Ferrograph analysis. A number of methods of plotting the results to indicate trends were tried. These included severity of wear index, $D_L^2 - D_S^2$, the total wear $D_L + D_S$ and severity of wear $D_L - D_S$ against time. An interesting way of presenting the data was recommended. This involves plotting cumulative total wear and severity of wear totals on the same graph. Data for satisfactory engines gave two curves well separated and each increasing steadily. Engines where abnormal wear was occurring gave curves which tended to converge or even to cross. Case histories on a number of gas turbine engines are included and it is noted that in some instances trend analysis of wear of lubricated components reflected failure of components in the gas stream.

Fitch at the Fluid Power Research Centre, Oklahoma State University has conducted tests over a number of years into contaminant-induced wear. Initially the measure of damage caused by particle contamination was performance degradation only. Recent work[26] has also employed the Ferrograph in contaminent wear tests on several components used in hydraulic systems and on basic hydraulic mechanisms.

4.3 Equipment and Techniques

It has been suggested, of the false indications from chip detectors approximately 60% are due to wear-fuzz, 25% to electric failure, 5% each to moisture in the lubricating oil system and contamination and unknown causes. Wear fuzz occurs in systems with fairly coarse filtration as ferrous particles slowly accumulate in the oil and are deposited on the chip detector. Eventually as the quantity of fine debris particles builds up a conductive path is formed across the gap between the two electrodes thus activating the chip detector. The Technical Development Company[14] now market a new type of chip detector which deals with the wear fuzz problem by passing a strong current pulse through the gap every time there is electrical continuity. This causes local melting of the small particles that make up the wear fuzz, whereas larger particles conduct the pulse unharmed so continuity remains. The unit may be arranged for automatic current pulse discharge every time continuity occurs with the chip light not activated unless the debris survives unchanged. This results in a system free from the wear fuzz type indication. Alternatively the current pulse can be initiated manually, when prognostic information about a failure can be obtained if the chip light comes on again after a short time thus indicating the continuing generation of fine debris particles, perhaps from a damaged bearing or gear. Although some American helicopters are using these pulsed chip detectors in their transmission systems opinion in the UK is that they could possibly represent a hazard. They have so far, therefore, not been adopted for use in British aircraft.

A new approach being explored at the Fulmer Research Institute under UK Ministry of Defence funding assesses the abrasion of a sensitive resistor by the particulate matter present in the lubricating oil. The device depends on measurement of the change in resistance of a suitable resistor as the lubricating oil, containing contaminating debris, is pumped over it. The response is related to relative hardness of debris and resistor. Laboratory tests have demonstrated the principle using alumina particles and work is proceeding to optimise conditions and to ensuring that adequate life can be obtained with sufficient sensitivity to determine changes in wear mode.

The new technique of Ferrography has been widely welcomed for its ability to provide additional insight of the wear mechanism over that available from the more conventional techniques of spectrometric analysis, magnetic plugs etc. However, it does suffer from certain limitations, including the requirement for a skilled operator, and the fact that results are not immediately available. The US Navy initiated a programme some years ago to remedy these shortcomings by the development of an automatic version of the Ferrograph that could give flight deck information. This led to the production of the Real Time (RT) Ferrograph[27,28]. The RT Ferrograph circulates the test lubricant from a reservoir through a glass tube within which wear particles are precipitated magnetically according to particle size. Readings dependent on the amount of light transmitted are taken at both the small and large particle ends of the tube with automatic compensation for the oil colour. The overall sampling system recycles automatically when all the oil in the reservoir has drained out; the electromagnet is shut off, the precipitation tube cleaned out and the reservoir recharged automatically. Comparison of the RT Ferrograph with an on-line X-ray Wear Metal Monitor, spectrometric analysis, analytical ferrography and a light scattering/attenuation device were made on laboratory disc scoring and rolling element bearing fatigue tests to simulate gear and bearing damage. Tests were run on one lubricant, a MIL-L-23699 jet engine turbine oil, with filtration at various levels from zero to 10 micron, nominal filtration. The various oil monitors clearly signalled surface failures at the coarser levels of filtration and as the level of filtration became finer the ability of all lessened. The light scattering/attenuation instrument and spectrometric analysis were effective over the widest filtration range. The RT Ferrograph was ineffective below the 40 micron filtration level. There were indications that the sensitivity could perhaps be affected by the volume of oil flow and it was recommended that further development be undertaken with emphasis on incorporating features which allowed for a variable oil volume sampling rate.

Considerable effort has recently been expended on extending the applications of Ferrography[8,29] with the recognition of friction polymers of several types from different formulations of aircraft engine lubricants, lubricant filter selection, biological fluid and jet engine gas stream analysis being some of the new areas described. It is likely that cross fertilisation from these areas will benefit the studies in the lubricating oil system field.

Another way in which the ferrographic technique is being extended is by the use of temper colours as a means of extracting further information from a ferrogram. Barwell et al[30] have demonstrated that a simple heat treatment of ferrograms on a laboratory hotplate can provide a useful means of identifying the different materials present. The magnetic particles based on iron or nickel alloys generate temper colours which can be used to divide them into four types - carbon steels, cast iron, nickel and stainless steel. The majority of non-magnetic engineering alloys such as aluminium, magnesium, chromium, cadmium and silver do not form colours under the recommended procedure. The copper based alloys may form temper colours but can, of course, be readily identified by their yellow bronze colours prior to the heat treatment. The recommended procedure is to heat the ferrogram for 90 seconds on a laboratory hotplate and photograph the large particles in the entry zone on cooling. A four-stage process is described, first the ferrogram is heated to 330°C, the carbon steels then turn blue and the cast irons a straw or bronze colour, with no change to the nickel or the stainless steel. A second heating step at 400°C results in the carbon steels becoming light grey, the cast irons deep bronze with some mottled blueing, no change to the nickel and possibly slight yellowing of stainless steel. A further heating step at 480°C leaves the carbon steel and cast iron grey, the nickel turns bronze coloured with some blueing whilst the stainless steel turns straw to bronze coloured. A final heating to 540°C leaves the carbon steel and cast iron grey, the nickel blue and the stainless steel still straw to bronze coloured with some mottled blueing. The grouping of the debris particles that this provides will normally permit identification of the particular components in machinery that are being worn and thus provide an insight into the wear processes occurring.

The technique of ferrography is also being developed by applying quantitative analysis to ferrograms. Roylance et al[31] have described a technique developed for analysing the wear debris collected on a ferrogram using a Quantimet. The ferrograph can be scanned over its whole area using reflection and transmission light sources and the variations in light density and contrast used to distinguish different particle types. The ferrogram can also be analysed in terms of dimensional parameters. The extensive range of contrast settings in the Quantimet permit particles of different materials to be distinguished thus permitting a breakdown of the total numbers of debris particles into say free metals, oxides, and polymeric materials. Use of this facility together with the temper colours produced by heating the ferrogram slides has permitted a numerical assessment of the amounts of steel and cast iron to be made in a case study of the running-in of a diesel engine. In a later paper[32] the application of the Quantimet to ferrograms prepared from oil samples collected from a helicopter gear box during fatigue trials is described. The Quantimet assessed the ferrograms in terms of particle size distribution as well as the concentration and shape of particles. The size distribution plots were of interest. The particles in the < 1, 1-2 and 2-5 micron ranges all showed a slow reduction in the number of particles from start up to 20 running hours with run-in. A gear-box inspection then revealed breakdown of several teeth on the port pinion. On reassembly after partial rebuild of the gearbox a peak in the number of particles occurred due to further running in. However, the plot of variance appeared of greater promise as a machinery health monitoring aid, definite peaks seen at the 20 and 45 running hour periods appearing to correlate well with the gear damage found on strips at 20 and 70 hours. These preliminary findings certainly justify continuation of the research into the quantitative analysis of ferrograms.

In a related approach Pocock[12,33] has shown that the complicated particle size distributions obtained during a helicopter gearbox trial can be described by the distribution function

$$P(d) = \exp - [b/(d-d')]^n$$

where $P(d)$ is the probability of a particle being smaller than d, d' is a lower particle size limit, and b and n are independent parameters adjusted to fit the experimental results. The parameter 'b' shows promise as an indication of wear since at constant 'n' it reflects a change of relative numbers of large particles. In particular examples given 'b' showed excellent agreement with the measured iron content, and the severity of wear index from DR Ferrography.

5. A RESEARCH PROGRAMME TO UNDERPIN EQUIPMENT DEVELOPMENT

The value of wear debris analysis as a powerful means for controlling ownership costs of aircraft and their sub-systems is indisputable. Realisation of the potential of this analysis, can, however, only be accomplished if the results are fully meaningful to the design, specification and maintenance authorities. The present, somewhat diffuse, situation must therefore be improved and this could best be achieved by establishing suitable demonstrator programmes in which the scientific, technical and managerial aspects are fully integrated and expressed. The following describes such an ideal programme which is based upon the study of a highly rated gearing involving a programme of integrated metallurgical, metrological, lubricant and design factors.

The heart of such a programme relies on the ability to reproduce surface degradation modes identical to those that will be important in the service application. Decisions as to which modes will be critical have in practice to be derived from past experience. On this assumption and once such a capability to reproduce the critical modes has been established, it would be possible to evaluate a span of controlled metallurgical and tribological variables, to explore causes of failure and from thence to establish more effective design and specification. Such facilities would also provide an ideal background for studying the basic scientific phenomena involved, for calibration of existing health monitoring techniques, and provide a facility on which to evolve new sensor possibilities.

Such a Critical Failure Demonstration Programme is shown as Stage II in Fig 11 and in more detail in Fig 12. Each particular test unit would need to be arranged to reproduce as simply as possible a selected critical bearing surface failure mode yet be fully representative of practical design operating under realistic rates of surface sliding and rolling over a range of loads and speeds. Other variables which would need to be investigated include a range of steel compositions, surface hardening techniques, lubricants, additives, surface finishes and temperatures. The cause of degradation would require to be followed by all available techniques including careful engineering inspection involving periodic stripping with visual and detailed surface topographical examination and assessment, but also more systematically by continual vibration and stress wave analysis and by frequent observation of the chemical, physical and metallurgical

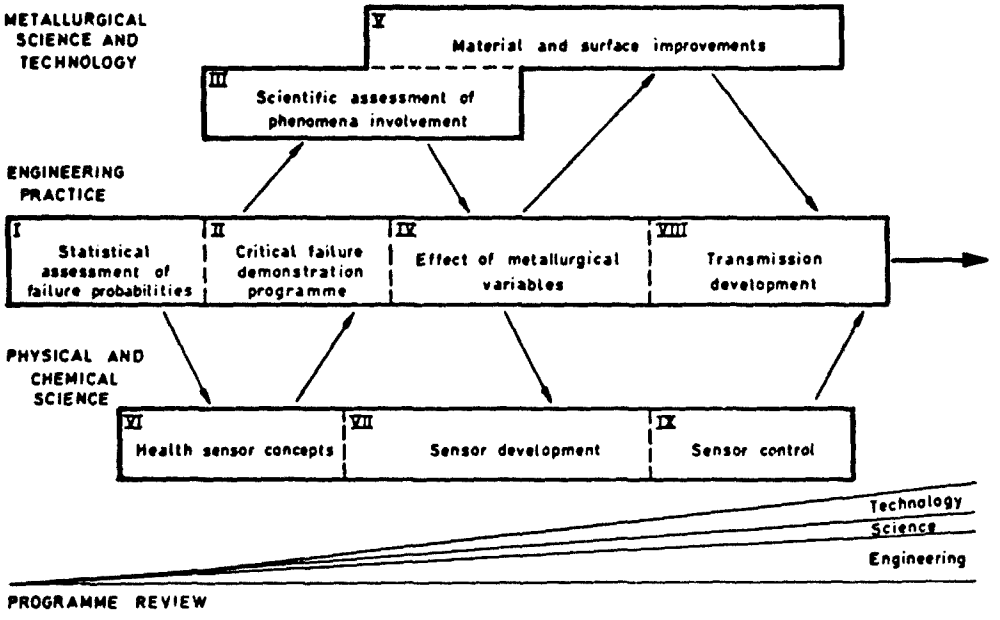

Fig 11 Interdependent elements of an improved health sensor programme for power transmission systems

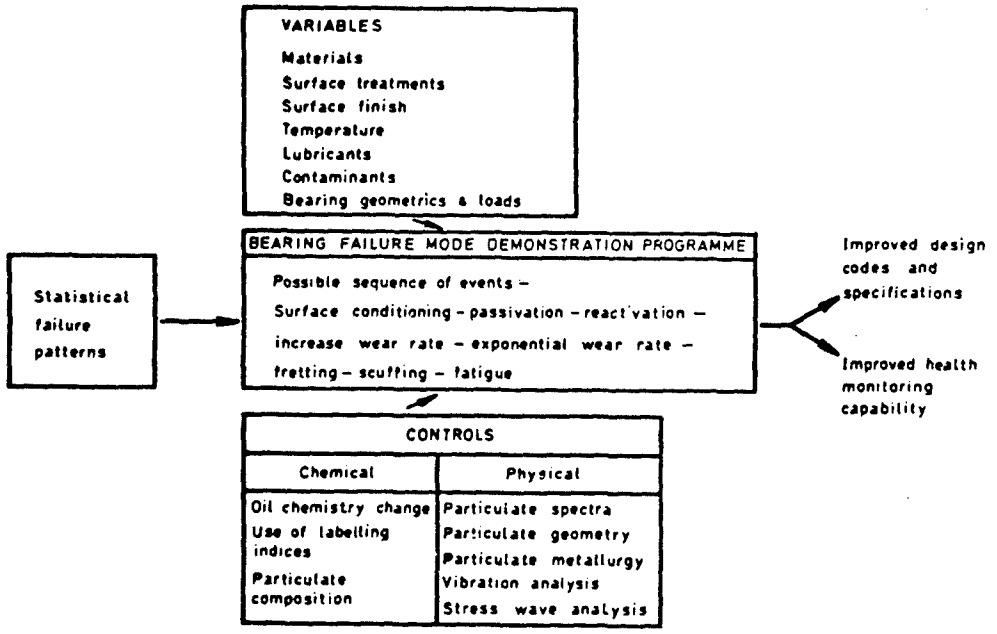

Fig 12 Interrelationship of research elements to characterise wear condition of gear bearing surfaces

DEMONSTRATOR EXERCISE	SURFACE CHARACTERISATION	ANTICIPATED FAILURE MODES
Gears	Rolling contact	Scuffing and fatigue cracking
	Sliding contact	Pitting spalling and fatigue cracking
Ball and roller bearings	High point or line contact stress	Skid wear, spalling and cracking
Plain journal bearings	Continued hydro-dynamic separation of bearing faces	Accelerated wear, galling and seizure

Fig 13 Principal types of demonstrator exercises for oil washed surfaces

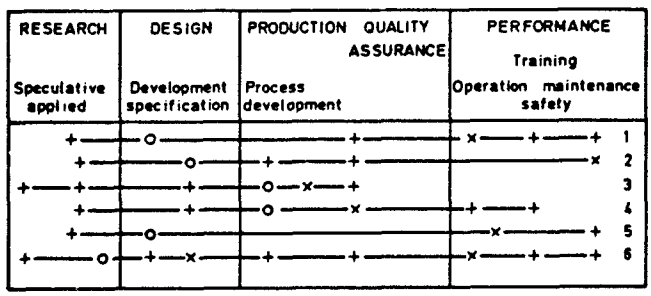

1 Performance and failure analysis
2 Maintenance data
3 Optimised material production process controls and quality assurance
4 Specification deviation and flaw incidence
5 Use and available log
6 Component and system health monitors

Management criteria :

(I) Sponsorship responsibility (O)
(II) Point of introduction (×)
(III) Intercommunication stages (+)

Fig 14 Overall use and management of health monitoring systems based on wear debris analysis

nature of debris accumulating in the lubricating fluid. It would also be essential to employ all available monitoring methods simultaneously since each reflects a somewhat different aspect of the surface condition. Ultimately it may be possible to rely on continuous mechanical monitoring methods such as vibration analysis but under the present state of knowledge, debris monitoring methods have a great deal to contribute and show considerable prognosis capability.

The parallel but interdependent activities of developing new materials, surface treatments, lubricants etc and improved sensor development are seen as separate but linked activities in Fig 11. The principal objective of the interdisciplinary programme is to achieve a capability for a less random gear development programme, by an improved wear monitoring capability leading to a greater reliability and reduced ownership costs. Another aspect that would need to be studied in such a demonstrator programme would be optimum materials for emergency dry operation in the event of temporary loss of lubricant.

Separate demonstrator exercises would be required for the principal tribological systems, in particular for gears, high speed ball and roller bearings and plain journal bearings in which controlled variables would have to be selectively imposed in order to vector onto appropriate critical surface wear or failure modes, some of which are outlined in Fig 13.

Means for ensuring the efficient use and deployment of information arising from wear debris characterisation is essential, necessitating mandatory and sympathetic management arrangements along the technology transfer route. Tribological systems usually involve a span of differing engineering activities and responsibilities, sometimes involving long time scales, distances and varying logistical arrangements. Hence a special management system is required fo the introduction of health monitoring systems and for the feedback of meaningful data to needful points along the technology transfer route and its reactive interfaces. One possible scheme for achieving this is shown in Fig 14 whereby the responsibility for, and the point of intrpduction of, wear health sensors has to take into account the whole spectrum of responsibility under an overall management control. For example, Item 6 involves the introduction of a research motivated component wear health monitoring systems at the development stage or in fully operating equipment, with the nature of the exercise and the resulting information being meaningful and utilised simultaneously by Design, Production and Maintenance authorities. While such a scheme may be idealistic and achievable only in part, it represents the optimum use and effect of wear debris analysis.

6 CONCLUSIONS

Because of the complexity of tribological factors surrounding load bearing surfaces in engineering systems, future improvements will continue to be empirical and follow iterative processes using retrospective experience on which to base improvements. However, it is believed that vigorous exploitation of the potentialities of wear debris analysis, together with other condition monitoring techniques, will in future assist in producing a more scientific approach to this important engineering technology. Significant benefits should result in improved design codes, reduced development costs and lower maintenance effort with improved availability. It is therefore concluded that research into all aspects of wear debris analysis should be prosecuted vigorously in order that the realisable benefits and improved understanding of failure mechanism should be gained at the earliest opportunity.

REFERENCES

1 Terotechnology Handbook. Department of Industry, Committee for Terotechnology. Published by Her Majesty's Stationery Office, London, 1978.

2 Tribology Handbook Edited by M J Neale. Published in association with the Committee on Tribology of the Department of Trade and Industry by Butterworth, London, 1973.

3 A Theory for Mechanical Seal Face Thermodynamics - Barnard and Weir. Proceedings of the 8th International Conference on Fluid Sealing, Durham, 1978.

4 Michael Neal and Associates. A survey of Condition Monitoring in British Industry and its Potential for Wider Application. Report TRD 187 prepared for the Department of Industry.

5 Wiggins R A 'Equipment Reliability Through Oil Monitoring' Vactric Control Equipment Ltd. 1968.

6 Hunter R C 'Engine Failure Prediction Techniques' Aircraft Engineering - March 1975.

7 Seifert W W and Westcott V C 'A Method for the Study of Wear Particles in Lubricating Oil Wear 21, p27-42, 1972.

8 Scott D, Seifert W W and Westcott V C Ferrography, an Advanced Design Aid for the 80's, Wear 34, p251-260, 1975.

9 Bowen R, Scott D, Seifert W W and Westcott V C Ferrography - Tribology International 9, p109, 1976.

10 DEF STAN 05-42 Particle Size Distribution.

11 Bowan E R, Westcott V C, Foxboro Trans-sonics Inc - Wear Particles Atlas, July 1976.

12 Pocock G 'Particle Size Analysis for Machinery Health Monitoring' - Nature 270, December 1977.

13 Johan O, Samudra S V, Corvin I, Staschke J 'Mechanisms of Wear in Helicopter Hydraulic Systems' - American Society of Mechanical Engineers, p265-273, 1977.

14 Tauber T 'A New Chip Detector' - Aircraft Engineering p4-6 October 1977.

15 Pocock G 'Wear Debris Analysis for Machinery Health Monitoring' - British Institute of Non-Destructive Testing. In the Press.

16 Dalal H and Senholzi P 'Characteristics of Wear Particles Generated During Failure Progression of Rolling Bearings' American Society of Lubrication Engineers Transactions 20, p233-242 July 1977.

17 Chandler C W 'An Investigation of the Navy Oil Analysis Program (NOAP) Naval Aviation Integrated Logistic Support Center, Report 03-41.

18 Jones W R, Nagaraj H S and Winer W O 'Ferrographic Analysis of Wear Debris Generated in a Sliding Elastohydrodynamic Contact' ASLE Montreal Meeting May 9-12, 1977.

19 Pocock G and Jones J B 'An Application of Ferrography and Magnetic Plug Inspections to the Development of New Machinery' - ASME. In the Press.

20 Berthe D, Michan B, Flamond L and Godet M 'Effect of Roughness on Pits and Micropits in Pure Rolling Lubrication' - Leeds-Lyon Symposium, Lyon.I MechE 1977.

21 Flamand L and Berthe D 'A Brief Discussion of Different Forms of Wear Observed in Hertzian Contact at Low Slide/Roll Ratios' - Leeds-Lyon Symposium, Lyon. IMechE, 1977.

22 Fodor J 'Tribodiagnostics in Internal Combustion Engines using Gamma-Ray Spectrometry of Wear' I MechE, Swansea Conference 3-4 April 1978.

23 Hofman M V and Johnson J H 'The Development of Ferrography as a Laboratory Wear Measurement Method for the Study of Engine Operating Conditions on Diesel Engine Wear' Wear 44 p183-199, 1977.

24 Jones M H, Sastry V R K and Youdon G H Leeds-Lyon Conference, Lyon. I MechE 1977.

25 Scott D, McCullough P J and Campbell G W 'Condition Monitoring of Gas Turbines - An Exploratory Investigation of Ferrographic Trend Analysis' Wear 49 p373-389, 1978.

26 Tessmann R K and Fitch E C 'Contaminant Induced Wear Debris for Fluid Power Components' I MechE Conference, Swansea, 3-4 April 1978.

27 Westcott V C and Wright R W 'Real Time Ferrograph for Application on Jet-Engines in a Test Cell Environment' Naval Air Propulsion Test Center, Trenton NJ 08628. July 1974.

28 Popgoshev D and Valori R 'Effectiveness of the Real Time Ferrograph and other Oil Monitors as Related to Oil Filtration' Naval Air Propulsion Center, Trenton NJ 08628, November 1977.

29 Scott D and Westcott V C 'Recent Advances in Ferrography and the Applications' I MechE Conference, Swansea 3-4 April 1978.

30 Barwell F T, Bowen E R, Bowen P J and Westcott V C 'The use of Temper Colours in Ferrography' Wear 44 p163-171, 1977.

31 Roylance B J, Jones M H and Price A L 'Quantitative Analysis in Ferrography' I MechE Conference, Swansea 3-4 April 1978.

32 Pocock G, Price A L and Roylance B J 'Monitoring Wear and Lubrication Conditions in Gear Systems using Ferrography' Leeds-Lyon Conference, Leeds, September 1978.

33 Pocock G 'Machinery Health Monitoring and Particle Size Distribution' I MechE Conference, Swansea 3-4 April 1978.

TABLE 1

A REVIEW OF CURRENT AND PROJECTED WEAR DEBRIS MONITORING TECHNIQUES FOR AIRCRAFT SYSTEMS

CURRENT TECHNIQUES

Method	Scope	Limitations	Remarks
Filter and Centrifuge Debris Collection.	All particulate matter available	1. Not continuous reading. 2. Interpretation requires experience. 3. Administration required.	Widely used by commercial airlines.
Mag Plugs and Chip Detectors	Coarse particles	1. Not continuous reading. 2. No response to non-magnetic debris.	1. Widely used in aircraft systems by both Military and civil operators. 2. Good detection of scuffing type failures.
Spectrometric Methods (SOAP)	Small particles	1. Not continuous reading. 2. Expensive equipment and specialist analysts required. 3. Administration necessary.	1. Widely used for monitoring all types of aircraft systems. 2. Good detection and prediction of failures by normal rubbing mechanism.
Automatic Particle Counters	All particulate matter determined	1. Not continuous reading. 2. Expensive equipment and specialist analysts required. 3. Administration necessary. 4. Findings can be confused by extraneous matter.	Frequently used with hydraulic systems.

PROJECTED TECHNIQUES

Improved Chip Detectors	Coarse Magnetic Particles	1. Not continuous reading. 2. No detection of non-magnetic debris.	Reduced number of rogue readings.
Quantitative Ferrography	Quick numerical rating of machine condition	1. Not continuous reading. 2. Little indication of failure mode.	Perhaps will prove a useful maintenance tool.
Automatic Ferrography	Not operator dependent	Equipment expensive.	Possibility that sophisticated data handling can give good predictions of different failure mechanisms.
Real Time Ferrography	Automatic reading Flight Deck Monitor	Equipment expensive.	Further development required.
Improved Analytical Ferrography	Capability of determining source of debris and mode of failure	1. Not continuous reading. 2. Dependent on expensive equipment and specialist operator.	Promise of predictive capability for several modes of failure including fatigue mechanism.
Sensitive Resistor	Determination of abrasiveness of particulate matter	Not selective for wear debris only.	Very early in development process.
Vibration and Acoustic Emission	Automatic survey of the effect of changes in bearing surface condition on system behaviour.	Segregation of critical signals for complex background noise.	Ultimate system borne complete health sensing capability equating surface condition, wear debris shedding and failure with noise and vibration analysis.

HIGH RESOLUTION ULTRASONIC NONDESTRUCTIVE TESTING OF COMPLEX GEOMETRY COMPONENTS

T. J. Moran
Air Force Materials Laboratory
Wright-Patterson Air Force Base, Ohio, USA

ABSTRACT

Research in ultrasonic nondestructive inspection methods in the USA has undergone a major change in philosophy in the last four years. Previous emphasis had been on the detection of flaws, while present work concentrates on the characterization of the flaw and the material state. The background of events leading to this change will be discussed. Along with the change in direction of research, developments efforts have concentrated on improving the reliability of the detection of defects. Major programs have been directed toward the goal of a completely automated ultrasonic inspection system which would effectively remove the human factor. Several systems which have been designed for the inspection of complex shapes will be described.

Work being done for the Air Force Materials Laboratory and the Defense Advanced Research Projects Agency by Rockwell International Science Center and its subcontractors aimed toward the development of a quantitative capability will be described. This program has taken the lead in developing the basic theoretical models and experimental techniques which would be necessary. Early work concentrated on developing approximate scattering models for simple flaw shapes such as spheres and ellipsoids at long wavelengths. The success of these efforts led to the current direction of the program which is to go from a knowledge of the scattered ultrasonic field to a description of the source (the inverse problem). Several inverse techniques have been developed which show promise. In addition to the work in the long wavelength limit, studies have been made of imaging techniques which can be used to give a direct picture of the flaw. Theoretical studies of diffraction effects have been made to allow processing of signals from an imaging system to remove spurious signals and produce an image which accurately reflects the shape of the target. The intermediate frequency range where the flaw dimensions become comparable to the acoustic wavelength is a problem both theoretically and experimentally. An attempt has been made to circumvent this by training computer based adaptive learning or pattern recognition networks on the approximate scattering theories. To date, the results have been excellent when data from ellipsoidal voids were input to the networks. In most cases void orientation and dimensions were measured with accuracy on the order of 10%.

The promising results in the development of quantitative nondestructive inspection techniques for metals have led to a more recent effort to extend this work to ceramic materials which are currently under consideration for small gas turbine applications. The predicted small size of critical flaws in materials such as Si_3N_4 required the development of a high frequency (100-500 MHz) ultrasonic testing capability. Due to the short wavelengths involved, the water coupling medium had to be eliminated in favor of a pressure contract. Complex shape parts are inspected using buffer materials machined to mate with the part under test. Current results of this program will be discussed.

I. Introduction

Ultrasonic nondestructive testing has undergone a major change in emphasis at the research level in the United States in the last few years. Prior to this change, the goal of most research and development programs had been to improve the sensitivity and reliability of ultrasonic inspection instruments and techniques. Present efforts are more concerned with extracting quantitative information from the inspection data as well as insuring that no flaws above a critical size are missed than they are with finding smaller flaws. This shift in emphasis is a result of the change from the zero defects philosophy of design and manufacturing to one which assumes the presence of flaws from the time of manufacture and designs the structure to tolerate those flaws. This new philosophy puts a tremendous burden on the nondestructive testing research community. Each improvement in capability can now be translated into more efficient design with attendant improvements in performance and economics. Unfortunately the converse is also true. If the inspection technique proves incapable of finding and identifying defects at the level desired by the designer, the structure must be strengthened with the price being a degradation in performance and an increase in cost.

This paper will attempt to cover the area of ultrasonic testing (UT) as applied to engine components, however, most of the techniques which will be discussed are of a general character and are applicable to structural components as well, where the same design constraints have been imposed and similar inspection requirements prevail. Improvements currently being made in standard UT methods applicable to engines in terms of the goals of the efforts and limitations will be discussed. In addition, I plan to outline the goals and results of a program being jointly managed by the Air Force Materials Laboratory (AFML) and the Defense Advance Research Projects Agency (DARPA) which has the Rockwell International Science Center as the prime contractor, entitled the Interdisciplinary Program for Quantitative NDE (Contract F33615-74-C-5180). The program began in 1974 and has taken the lead in changing nondestructive testing (NDT) to nondestructive evaluation (NDE), the difference being that in addition to finding the flaw, the nature and severity of the flaw must also be established. While this goal has not yet been attained, a great deal of progress has been made and some quantitative techniques have been

developed. The impact of this program on future engine designs and inspection procedures will be noted and a proposed program which depends very strongly on the development of quantitative NDE will be described. This future effort is aimed at increasing the service life of engine components by combining results from NDE, fracture mechanics and structural analysis. It is hoped that components may be kept in service even if a flaw has been detected provided that it can be shown that the flaw will not grow to critical size before a selected number of inspection intervals. As the techniques improve, the safety margin can be reduced with attendant savings in cost.

A final topic to be covered will be inspection of advanced materials, such as ceramics, which have been proposed for used in aircraft engines. At the present time these materials are not in use due to a lack of ability to ensure that they are sufficiently defect free to survive a desired length of time in service. The small critical flaw size in these materials has required the development of a UT capability in a frequency range over an order of magnitude greater than used with current techniques.

In the final summary, I will try to put into perspective the role of ultrasonics in engine component inspection and discuss its advantages and disadvantages as compared to other current and proposed techniques.

II. Current Ultrasonic Testing Capabilities

In discussing ultrasonic inspection of engine components, we first must identify which part of the component's life we are referring to, manufacture or service, due to the differing requirements at each stage. Presently in the U.S. Air Force there is virtually no ultrasonic testing of in-service components being done. This is due to the fact that at the present time most in-service failures arise from surface connected cracks and fluorescent penetrant or eddy current inspections are considerably more effective at detecting these defects. At the manufacturing stage, ultrasonic testing is used to detect internal defects. For parts which have complex finished shapes, the inspection is performed before final machining when the part has a sonic shape to avoid the blind spots which occur in the finished part due to refraction effects.

In the future, parts will be manufactured closer to the final shape to conserve materials and reduce machining costs. This near net shape manufacturing philosophy leads to an increase in the complexity of the inspection process. It is no longer satisfactory to perform an ordinary c-scan where the transducer is scanned over a grid corresponding to the dimensions of the part with no alteration in transducer orientation. New inspection systems have been developed by U.S. engine manufacturers which incorporate computer control of the scan pattern [1]. These systems require a detailed specification of the part geometry which is stored in the computer and used to determine the optimum scan pattern.

In conjunction with the development of these systems there was also work done to improve the basic ultrasonic inspection equipment. With the advent of near net shapes, near surface imperfections assumed a greater importance. In the past, even rather large defects could be machined off since there was a large excess of material in the sonic shape, albeit there was some danger of tool damage. In the near net shape component, the amount of material to be removed in final manufacture is rather small, thus there is a narrowing of the tolerance variations allowable in the ultrasonic transducers and system response. To find near surface defects, the transducer must be sufficiently broadband that there is little ringing after the first 1½ cycles and receiver must have sufficient dynamic range to be able to display the front surface reflection and a very small defect signal occurring very close to it in time. While significant progress has already been made in this area, there are presently no commercial instruments available with state of the art capabilities. This is probably due to the limited market and corresponding limited development resources of the manufacturers. To correct this, the Air Force Materials Laboratory, through its Manufacturing Technology Division, has undertaken the development of the next generation of ultrasonic instrumentation. While aimed at Air Force needs, this new instrumentation should significantly improve the capability of ultrasonics to address engine inspection problems.

III. Future Directions

In 1974 the Air Force Materials Laboratory (AFML) and the Defense Advanced Research Projects Agency (DARPA) recognized that the science base in the area of nondestructive evaluation (NDE) was woefully inadequate to provide the technology needed for future needs. AFML and DARPA jointly funded a program with the Rockwell International Corporation Science Center division to develop a science base. During the four years of the ARPA/AFML program's existence, significant progress has been made [2]. Beyond the technical advances, the assembly of a multidisciplinary research group from the university and industrial communities devoted to the development of the NDE science base has been a major achievement. This is in contrast to the research along disciplinary lines which was the norm prior to the inception of this program.

From its inception, the primary goal of this program has been the development of a true quantitative ultrasonic NDE capability. To illustrate the importance of this effort, I would like to take a detailed look at a potential application area where a quantitative NDE capability is essential to the success of the proposed program. The effort is referred to as Retirement for Cause. It's primary goal is to extend the service life of engine components, such as disks, which are now retired after a fixed number of fatigue cycles, independent of any detection of a rejectable flaw, at a point where the probability of

failure is 0.02%. This number of fatigue cycles is derived from design life calculations which assume the largest flaw likely to go undetected is actually present in the part. Figure 1 shows how the service life of the part can be extended if reliable, quantitative NDE is available. If all detectable cracks have length less than A_o at each inspection, the part can be returned to service with confidence that the remaining life should be at least equal to the original design life. As techniques improve, it may even be possible at some point to put parts back into service with cracks just slightly smaller than A* with the confidence that these cracks will not reach the critical size, A_c before the next inspection.

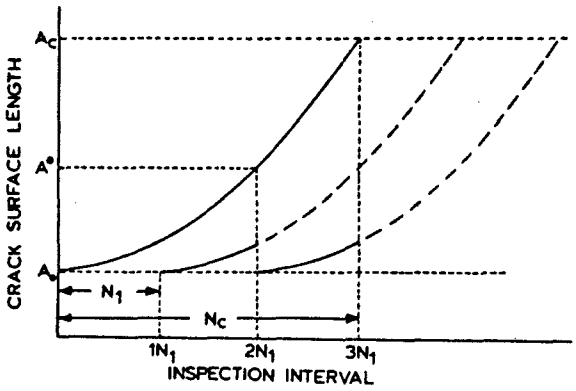

Figure 1. Crack growth - NDE relationship for Retirement for Cause program.

The simple relationship between the crack surface length and the component lifetime implied by Figure 1 is valid only for those cases where the aspect ratio ($^a/_{2c}$ = crack depth/surface length) is a constant. In the real world of the alloys found in engines, the aspect ratio is a variable which must be taken into account. This is illustrated in Figure 2 where the crack growth as a function of number of flights is plotted for bolt hole cracks in the third stage turbine disk in the TF-33 engine. From this figure one immediately comes to the conclusion that crack depth must be accurately measured as well as surface length.

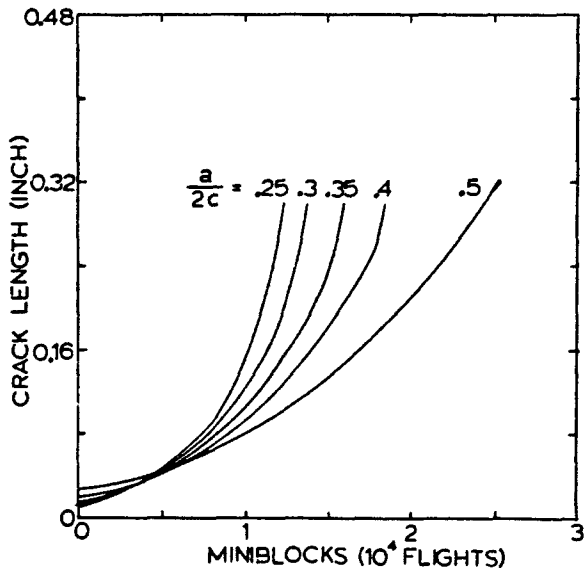

Figure 2. Crack growth as a function of aspect ratio for 3rd stage turbine disk in the TF-33 engine.

At first glance it might appear that we have identified all the parameters which must be measured by our quantitative NDE techniques; however this is not the case. Figures 1 and 2 are idealizations in the sense that they are valid for elliptical cracks. While real cracks may be elliptical, in many cases they have rather ragged boundaries. This is especially true in coarse grained materials where relatively large cracks can form as a result of the link-up of many small ones. As our NDE techniques improve, it is anticipated that through an iterative procedure with developments in fracture mechanics the essential details of crack geometry needed for remaining life calculations may be identified and the needed techniques developed.

Now let us take a look at how NDE fits into the overall Retirement for Cause stragegy. This illustrated in Figure 3 whre the current and proposed maintenance flow charts are shown. As was mentioned before, the present system retires the disk after one design life even if no flaws are detected in the part. It has been estimated that at least 85% of the disks in one of our newest engines could go for more than 10 design lifetimes without failure. For the retirement for cause program to succeed, the required NDE and analytical techniques which are necessary to separate this long life 85% from the 15% which would fail earlier must be developed.

DISK RETIREMENT FOR CAUSE STRATEGY

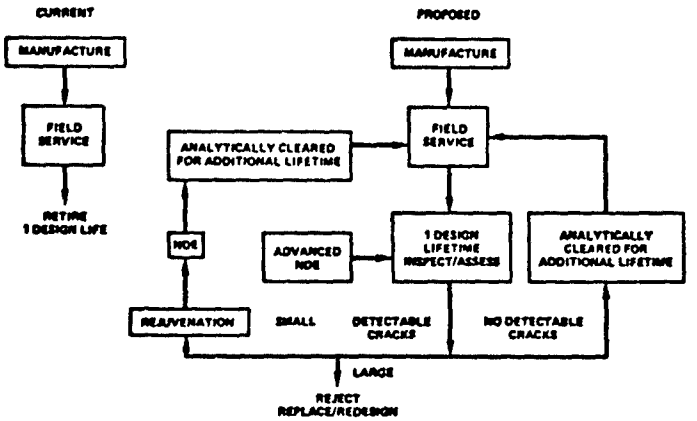

Figure 3.

In the proposed program, NDE comes into the disk evaluation process in two very important places. The first is the initial evaluation of the disk at one design lifetime. Here, the disk is examined for the presence of cracks. If no flaws (cracks, changes in microstructure, etc.) are found, it may be put back into service for an additional lifetime. I should mention at this point that it may be necessary to also inspect for non-discrete defects such as abnormal residual stresses in the part, which may also cause premature failure. Unfortunately, present residual stress measurement techniques are extremely poor except for near surface stress measurements. A great deal of progress would be necessary in this area before we could say we had an acceptable method for measuring bulk stresses.

In the case where a crack is found, accept/reject criteria for the part must be developed. For cracks above a certain size, the disk will have to be rejected, for very small cracks it could be put back into service with no attempt at repair. In the intermediate range, if the techniques are sufficiently developed, the part could be repaired or rejuvenated. After this stage NDE must again be used to determine if the rejuvenation has been successful and no additional damage has been introduced.

Now that we have established the need for a quantitative capability, let us look at how far we have gotten toward the achievement of the goal. The major thrust of the DARPA/AFML program at the start was the quantitative measurement of the size and orientation of bulk flaws. Since the range of flaw sizes encountered in practice is rather large, different approaches were selected for flaws with dimensions greater than the wavelength of the ultrasonic signal than were used for flaws with smaller dimensions (long wavelength regime). In the high frequency, short wavelength regime, the approach was to image the flaw using a transducer array and digital signal processing techniques. An instrument is currently in the prototype development stage which should provide an opportunity to test this concept on practical part geometries. Laboratory results indicate that there is a high probability of success in this area.

Due to the difficulty of theoretically calculating scattered fields from real defects, it was decided to begin in the low frequency, long wavelength regime with simple shapes such

exactly and the approximate theories should be extendable to more general (crack-like) shapes. The Born approximation and integral equation techniques were used to calculate the scattered acoustic fields from the simple shapes. The theoretical results were experimentally verified using titanium samples which had spherical and ellipsoidal voids diffusion bonded into the center of the sample. The next step was to perfect inversion techniques (procedures by which the flaw size, shape and orientation are inferred from the scattered ultrasonic fields). This phase of the program has reached the completion stage and the dimensions of the model flaws can be measured with good accuracy. Current efforts involve the extension of the models to more crack-like defects as well as an investigation from the point of view of fracture mechanics as to the amount of detailed information required to assess the effect of a defect on component performance and service life.

In addition to the investigations at the high and low frequency limits, a special approach was needed for the intermediate regime where the flaw dimensions become comparable to the acoustic wavelength. Here the scattering theories are not valid and imaging also does not work. An empirical signal processing approach was used to extract those parameters from acoustic waves reflected from defects which were related to the defect size. Learning networks which adaptively sort these parameters were trained on data generated both theoretically and experimentally. Spectral and amplitude information from waves scattered at several angles was required to size the defect. Results on the simple shapes indicate that most dimensions can be measured with an accuracy of 30% or better, depending on flaw orientation. When the theoretical results for irregular shapes become available, an attempt will be made to extend the validity of the results into the intermediate wavelength regime using the learning networks as well as estimation theories which are presently being evaluated.

While most of the emphasis in the program has been on bulk flaws, many of the defects which can lead to failure are surface or near surface flaws. An effort was begun in the last year to extend the procedures developed for the ultrasonic measurement of bulk flaws to the surface case. Techniques ranging from measurement of the scattered fields at various angles in analogy to the bulk flaw case to a simple attempt to separate signals in time from extreme dimensions of the flaw are being evaluated.

It is presently too early to know if the apparently promising results will prove practical for real inspection problems. There should be a definitive answer by the spring of 1980, however. A program was begun in June 1978 to attempt the reduction to practice of the various quantitative ultrasonic techniques developed in the DARPA/AFML program. A test bed is being constructed which will include a contour following scanning capability as well as the signal processing capabilities needed for flaw measurement. Upon completion of the system, it will be tested on several problems of practical interest. One of these will be an inspection of the bolt holes in a TF-33 third stage turbine disk which has been shown to have a severe cracking problem in these holes. This should prove to be a severe test of our capabilities, since this is one of the more difficult geometries to inspect ultrasonically.

In addition to the research directed at providing techniques to quantitatively measure flaws, an effort has been underway to detect, size and identify defects in silicon nitride, a ceramic material which would allow gas turbines to be operated at higher temperatures and perform more efficiently. At the present time this material's low fracture toughness has prevented its use in the hot sections of practical gas turbine engines. Inspection difficulties arise from the small critical flaw size (on the order of 200 microns). This requires the use of ultrasonic frequencies in the range of hundreds of megahertz to ensure a high probability of detection. There is also a requirement that the nature of the defect be identifiable since it was found that tungsten carbide inclusions do not affect the strength while the lighter inclusions degrade the material considerably.

To provide the high frequency transducers needed, a special indium bonding technique was developed to couple lithium niobate transducers to a silicon nitride buffer rod. Since operation is in the 200-300 HMz range, normal liquid coupling techniques would produce unacceptably large losses. Thus, a direct pressure contact between the rounded ended of the buffer rod and the specimen to be inspected was tried and appears to be suitable for most cases. It remains to be shown that this contact method will be equally effective under the various surface roughness and curvature conditions encountered in service components. One additional question to be answered is can an inspection be done in a cost effective manner when a pressure contact is used. Apart from these concerns, these new transducers have been shown to be more reproducible than typical low frequency devices and quite efficient. The second need for identification of flaw type was satisfied when it was recognized that the nondeleterious tungsten carbide inclusion had a greater acoustic impedance than the host, while the strength affecting inclusions had a lower impedance. Thus, the relative phase of the reflection from the front surface of the defect is sufficient information for the sorting. Sizing is done using the same techniques developed for lower frequencies.

Summary

It has been shown that ultrasonic inspection of engine components is presently a little used tool due to the cost of its use and the effectiveness of other techniques such as eddy current and penetrants. Research programs currently under way aimed at developing a quantitative capability show promise to change this situation if the quantitative information can be used by those in fracture mechanics to produce a service life prediction capability. If such a development occurs and the quantitative techniques are implemented

in a cost effective way, then ultrasonics will become a very important inspection tool in the future for both manufacturing and field use.

References

1. Thompson, A. L., Weismantel and Comassar, D. M., "The Test Bed Concept as a Means of Introducing New Technology" Air Force Materials Laboratory Technical Report, AFML-TR-78-205 (1978) pp. 17-22.

2. For a detailed discussion of the work being done under this contract, see the following Air Force Materials Laboratory Technical Reports: AFML-TR-78-205, AFML-TR-78-55, AFML-TR-77-44 and AFML-TR-75-212 and the references contained therein. Each report consists of the proceedings of an annual meeting held under the auspices of this contract wherein the individual researchers working on the program report the results of their efforts in the past year and selected outside researchers report on related efforts.

NON-DESTRUCTIVE METHODS FOR THE EARLY DETECTION OF FATIGUE DAMAGE IN AIRCRAFT COMPONENTS

by
Robert E. Green, Jr.
Mechanics and Materials Science Department
The Johns Hopkins University
Baltimore, Maryland 21218
U.S.A.

SUMMARY

The present paper will describe and discuss the various non-destructive techniques which have been used or which are potentially useful for detection of fatigue damage in aircraft components. Included among the non-destructive techniques which will be considered are radiography, penetrant inspection, eddy current, ultrasonics, acoustic emission, magnetic particle and Barkhausen noise analysis, and more exotic techniques such as exoelectron emission, positron annihilation, and other atomic, nuclear, or solid state physics reactions.

It will be shown that the present state-of-the-art is such that some non-destructive testing methods can detect fatigue damage at a very early stage of the fatigue life only with sophisticated equipment in a carefully controlled research laboratory environment, while others can be successfully used under field or even in-service conditions. Suggestions will be made as to how some techniques currently used only in the laboratory can be transferred to actual practice. Consideration will be given to non-destructive methods for early detection of fatigue damage in aircraft components in general, including methods which are suitable for inspection of propulsion systems.

INTRODUCTION

Since aircraft of current design are complex, expensive structures and this trend will undoubtedly continue in the future, there is an ever increasing demand to assure longer safe service life of components prior to maintenance disassembly, inspection, and replacement. Unnecessary time spent on the ground is uneconomical from a commercial viewpoint and can be disasterous from a military viewpoint. Therefore, it is extremely important that present non-destructive testing methods be optimized and new techniques be developed to permit both in-service inspection and rapid out-of-service inspection of aircraft components.

Fatigue damage resulting in microcrack and subsequent macrocrack formation constitutes one of the primary mechanisms for loss of structural integrity leading to failure of aircraft components. It has been well documented for all types of fracture that nucleation of cracks in metals occurs as a result of inhomogeneous plastic deformation in microscopic regions. This inhomogeneous plastic deformation can be in the form of twinning, slip bands, deformation bands, or localized concentrations at grain boundaries, precipitates, dispersed particles, and inclusions. Moreover, the mechanisms responsible for these regions of inhomogeneous plastic deformation are all based on dislocation interactions. In particular, dislocation interactions with point defects, with other dislocations, with stacking faults, with grain boundaries, and with volume defects are known to create regions of severe localized plastic deformation, which develop into microcracks, and these, in turn, either coalesce or grow into macrocracks leading to ultimate fracture.

The ideal non-destructive testing technique would permit very early detection of fatigue damage so that proper assessment of the severity and rate of severity increase of the structural damage leading to failure can be made. Thus the most sensitive systems would be capable of detecting motion and pile-up of dislocations; the next most sensitive systems would be capable of detecting microcracks; the least sensitive systems would be only capable of detecting macrocracks. It is practically expedient to have non-destructive testing techniques which can successfully detect fatigue damage in each of these regimes since some components can tolerate larger regions of fatigue damage or larger crack sizes than others without serious concern for the structural integrity of the component.

CRACK DETECTION SURVEY

Historically, non-destructive testing techniques have primarily been exploited to detect the existence of cracks in structural materials. Of prime concern in this regard is the size of the smallest flaw which can be detected by each of the non-destructive testing methods. In 1974, Rummel et al.(1) conducted a comprehensive statistical analysis of the detectability of artificially induced fatigue cracks in aluminum alloy test specimens. They evaluated 118 test specimens containing a total of 328 fatigue cracks. The cracks ranged in length from 0.018 to 1.27 cm and in depth from 0.003 to 0.451 cm. The test specimens were evaluated in the "as-milled" surface condition, in the "etched" surface condition, and after proof loading, in a randomized inspection sequence. The non-destructive test methods used were x-radiographic, penetrant, eddy current, and ultrasonic. The 984 non-destructive observations taken using each method served as a sample base for establishment of high confidence levels. A probability of 95% at a 95% confidence level was selected for processing all combined data, and analysis was based on these conditions.

Figure 1 (upper row) shows the results of their statistical analysis for the x-radiographic inspection method where crack detection probability is plotted as a function of actual crack length. Figure 1 (lower row) shows the results they obtained for the x-radiographic inspection method where crack detection probability is plotted

as a function of actual crack depth. The condition of the test specimens is indicated on each figure. Figures 2, 3, and 4 show similar plots of their results obtained using the penetrant, eddy current, and ultrasonic inspection methods, respectively.

Rummel et al.(1) pointed out that the beneficial effects of etching and proof loading on crack detection are evident in the respective data plots. They attributed the benefits of etching to both the removal of flowed material from the crack opening and to the selective attack of the cracks at the crack edge. They attributed the beneficial effects of proof loading to a larger crack opening and to plastic flow of material around the crack. An analysis of the data based on material thickness and surface finish variations did not reveal any large effects. Based on the results plotted in Figs. 1 through 4, it was concluded that x-radiography is the least reliable of the four test methods for detection of tight cracks and should not be considered as a sensitive, reliable method for detection of tight cracks. On the other hand, the ultrasonic method was shown to be the most reliable for crack detection as well as to be the most accurate in measuring crack dimensions.

RADIOGRAPHY

With regard to the relative insensitivity of the radiographic technique to crack detection, it is interesting to note that an Advisory Circular(2) published by the U.S. Federal Aviation Administration in 1973 states that the sensitivity of radiographic inspection to a small crack is not as good as ultrasonics or eddy current methods. Nevertheless, radiographic techniques are still currently used for non-destructive inspection of various aircraft components including engines. Thus, Bunce(3) stated that "The general structure of an airframe or the internal assemblies of an engine are usually obvious applications of radiography and rarely lend themselves to either an ultrasonic or eddy current inspection." However, the same year Ruescher(4) studied the effect of variations in radiographic parameters on crack detection by x-ray and concluded that x-ray film readers were not able to detect all of the crack indications shown by penetrant inspection. On the other hand, he pointed out this detection limitation applies to cracks and similar tight defects only, while spherical discontinuities, such as porosity and inclusions, are more easily detected.

In 1974, Pullen(5) reported on high energy radiography which permits measurement of seal clearances between rotating and static components and the position and shape of various static components in a full range of static and dynamic engine conditions. Clarkson,(6) in 1975, pointed out that the use of radiographic techniques to inspect or monitor defects in inaccessible areas of airframes is a recurring requirement. He cited examples where radiographic inspection had proven valuable for non-destructive detection of stress corrosion cracking in spar booms, stringer sections, skin panels, welded tubular structures, and wing fuel tanks.

The same year, Halmshaw and Hunt(7) published a paper in which they discussed the limitations and the capabilities of radiography for detecting cracks. They showed that the ability to detect a crack with x-rays and gamma-rays depends principally on the crack opening and on the angle of the crack to the radiation beam. The size of the crack (crack depth) and the radiographic technique used are also important factors. They warned that it is completely misleading to specify sizes or length of detectable cracks without specifying the crack opening width and the angulation. They regarded cracks with openings less than 0.013 mm (0.0005 in) as unlikely to be detected under any circumstances except in very thin specimens, while cracks with openings of the order of 0.025 mm (0.001 in) can be detected at up to 10° inclination to the x-ray beam depending on their size (depth) and the technique used. They further pointed out that the radiographic situation is completely different from ultrasonic crack detection using pulse-echo methods, where, except for extremely tight cracks, the crack opening is not a significant factor in crack detectability. In ultrasonic testing, the important parameters for crack detection are the dimensions of the crack (length and depth), the angle of the crack to the ultrasonic beam, and the roughness of the crack faces. They continued by emphasizing that the important point of difference between radiographic and ultrasonic crack detection is the dependence of radiography on having a respectable crack opening. They stated that the detection of tight cracks less than 0.02 mm wide is always going to be difficult by radiography, with a low probability of success, even when the probable direction of the crack is known. Finally, they warned that the use of radiography in the hope of detecting tight cracks, when their approximate angle is not known, or the x-ray beam cannot be used at the suitable direction, is bad non-destructive testing and a misuse of radiography.

Stafford et al.(8) reported the use of proton radiography as the first non-destructive method capable of detecting microporosity in high-temperature nickel-base alloy castings. Since the technique requires a uniform thickness of sample, in order to extend the region of sensitivity to the whole of a blade aerofoil an anti-blade was made, of such a shape that when placed in contact with a blade it equalized the thickness. Stewart(9) presented a paper in which he described the development of a high energy radiation system which possesses the ability to penetrate the thick metal systems existing on aero gas turbines so that when used in conjunction with a suitable imaging system, the small movements of components can be revealed, recorded, and analysed. In 1976, Guillen(10) reported that the types of defects detectable by isotope inspection of jet engines could be categorized as cracks and fractures, wear and tear, and distortion or deformation.

Also in 1976, a number of investigators reported the use of neutron radiography for the examination of various aircraft structures. Dance(11) evaluated adhesive bonds in metal honeycomb and phenolic fiberglass-to-metal structures. Adhesive flaws in a variety of bonded assemblies, including a set of test panels with built-in adhesive voids and unbonds, were detected. In addition, he showed that detection of corrosion hidden within metal aircraft assemblies appears to be a promising application of neutron radiography. Edenborough(12) developed a technique for using neutron radiography for improved detection of residual ceramic core in investment cast turbine airfoils. John(13) reported the superiority of neutron radiography over all other NDT techniques in its ability to detect surface and subsurface corrosion in aircraft structures. He applied the neutron radiographic technique to successfully detect corrosion in aircraft wing tanks, rear stabilators, spars, wings, fuselage skin, nose landing gear, and helicopter rotary blades and tail flaps. Underhill and Newacheck(14) reported the use of neutron radiography to inspect for residual wax material in liquid rocket fuel and oxidizer injector assemblies and nozzle cooling passages. They also reported detection of extruded, ruptured, or out-of-position O-rings in valves, lack of epoxy cement in epoxy-bonded helicopter rotor blades, and determination of internal cracks and flaws in objects of low attenuating materials using a gadolinium-tagged penetrating solution.

In 1977, Parish and Cason(15) described an x-radiographic method which employed an image enlargement technique to permit high definition radiography of cast turbine blades as a method of detecting and evaluating the incidence of microporosity. They used an x-ray microfocus unit possessing a focal spot size of about 15 μm (0.015 mm) and were able to detect individual pores as small as 0.03 mm. Since Mr. Parish is scheduled to present a paper in this lecture series on high resolution radiography, I am certain that we will be brought up to date on the capabilities of such systems.

Before concluding discussion of radiographic systems, mention should be made of the potential usefulness of flash radiographic systems(16,17) although to the best of the present author's knowledge these systems have not been used for aircraft inspection.

Thus, the present state of radiography is such that although x-ray, gamma ray, neutron and proton radiography can be usefully exploited for various aspects of non-destructive testing as related to aircraft components, it is apparent that all radiographic techniques are better suited to detection of missing or misplaced components and to dimensional measurements, than to crack detection or to detection of pre-crack fatigue damage.

PENETRANTS

Penetrant non-destructive testing techniques are useful for detecting surface cracks in aircraft components. In the static production and service inspection of components penetrant inspection is very good, but by its very nature cannot be used for dynamic measurements. In 1973, Alburger(18) presented a paper in which he discussed in detail a revised military specification for penetrant inspection being prepared for the U. S. Air Force. He pointed out that penetrant inspection has been used for many years in high volume testing of critical aircraft parts including castings, forgings, structural members, and turbine blades. The revised military specification reflects not only the modern technology of penetrant materials, but also many new concepts of penetrant behavior, and new techniques for evaluating the performance of penetrant materials. It should be noted that, according to the statistical survey conducted by Rummel et al.,(1) although penetrant inspection is superior to radiography for the detection of the smallest cracks, it is inferior to eddy current and ultrasonic inspection techniques.

EDDY CURRENT

Eddy current inspection techniques are somewhat superior to penetrant inspection techniques for the detection of cracks in aircraft components, since they cannot only detect surface cracks but also near surface cracks. They are particularly useful for detecting cracks in holes or tubing. Eddy current techniques are more often used for static rather than dynamic testing. In 1967, Smith and McMaster(19) described the use of an eddy current inspection system, called a magnetic reaction analyzer, which used a Hall element in place of a pickup coil for its detector. This system was reported to be finding use in a variety of applications throughout the aerospace industry including definition of type, orientation, and location of defects. In 1971, Dodd et al.(20) presented sets of curves based on theoretical calculations which permit optimization of eddy current tests for detecting discontinuities. Reeves,(21) in 1973, described a mechanized eddy current defect detection system used for examination of aircraft landing gear components.

In 1974, Lang(22) reported the development of two single-coil eddy current techniques for the surface inspection of aluminum aircraft skin, parts and structures. These techniques were developed to replace liquid penetrant and eddy current methods which were then in use for the inspection of aircraft surfaces. He stated that use of these two new eddy current techniques reduced the workload from over 100 to 1 manhour per inspection on a Lockheed C-130 airplane. Using the new eddy current techniques, known cracked areas on various airplanes were readily detectable, and new cracks could be easily found. In some cases the new eddy current techniques located significant bead seat cracking which had been previously passed over as acceptable by penetrant inspection. This could be done without removing the layer of paint and zinc chromate, which had to be removed for penetrant inspection. The same year Truluck(23) noted that eddy current testing has been one of the growth areas of NDT, with a current requirement to develop techniques to detect, reliably, cracks as small as 0.1 mm (0.004 in) in boltholes. He further stated that it

was desirable to develop eddy current conductivity measurement techniques to determine the accurate heat-treatment state of light alloys and to develop phase-sensitive eddy current equipment to detect small areas of corrosion. In this regard, Clarkson(6) pointed out that the nucleus of a fatigue crack can easily be a minute corrosion pit a few thousandths of an inch deep. He reminded that in a number of cases where highly-stressed and "fatigue-critical" items have been concerned, an eddy current technique has been successfully employed to ensure that the surfaces involved are free of corrosion pits or minute fatigue cracks.

In 1976, in a paper devoted to a general review of the major non-destructive inspection activities in the U.S. Air Force, Forney(24) noted that although the problem of detecting cracks under installed fasteners in the outer layer of structural joints appears well in hand with the use of a new portable pulse echo shear wave spanner device, the location of cracks around fasteners in interior layers remains an elusive task. He reported that a new multifrequency eddy current technique is being investigated which has shown in feasibility studies to be capable of detecting cracks as small as 3 mm (0.125 in) long in a second plate at a depth of nearly 10 mm (0.4 in) from the top plate outer surface. He described how a special low-frequency test coil was centered over the installed fastener and energized simultaneously with a number of sinusoidal current waveforms, each having a different frequency. Return signals associated with each frequency undergo computerized analysis to form a composite signal particularly sensitive to the small cracks in the interior locations of interest. The same year, Smith and Beech(25) presented a paper which describes the principles of eddy current testing and the potential benefits of the method applied to manufactured components and raw materials. Although no applications to inspection of aircraft components are considered, insight into advantages and limitations are presented which should prove useful to aircraft inspection. Forster(26) presented a paper in which he discussed the limits of nondestructive indication of small and smallest flaws on and under the surface of workpieces by electromagnetic and magnetic techniques. He noted that fatigue cracks start at "weak points" such as slag inclusions, slag streaks, or other material inhomogenieties which cause heavy local stress concentrations under service conditions. He further noted that while fatigue cracks are usually considered to start on the surface of the workpiece, in materials subjected to certain stress states cracks can start at some depth beneath the surface, e.g. roller bearings. Of particular significance in this paper was the observation that superposition of a constant magnetic field increased considerably the depth at which meaningful eddy current measurements could be made for a given eddy current frequency. Kiplinger(27) presented a paper in which he discussed the design of several special coils and fixtures which permitted reliable eddy current measurements to be made on turbine engine parts.

ULTRASONICS AND ACOUSTIC EMISSION

As concluded by Rummel et al.(1) in their statistical survey, ultrasonic techniques presently constitute the most reliable methods for crack detection, as well as being the most accurate for measuring crack dimensions. It should also be noted that two papers in the present lecture series are devoted to ultrasonic techniques and a third, on acoustic emission, is closely related to ultrasonics. As will be shown in the following sections, not only are ultrasonic techniques suitable for surface and sub-surface crack detection and sizing, but are also sensitive detectors of pre-crack formation fatigue damage.

There are four different basic ultrasonic techniques which have been used to detect the onset of fatigue damage in cyclically loaded structural materials.

(1) Body Wave Reflection: A transducer, longitudinal or shear wave, generates an ultrasonic pulse which propagates through the body of the test specimen. Upon striking a crack, due to the impedance mismatch, part of the acoustic energy contained in the incident pulse is reflected back to the transducer. The transducer now acts as a receiver and detects that portion of the pulse reflected from the crack.

(2) Surface Wave Reflection: A transducer generates an ultrasonic pulse which propagates along the surface of the test specimen. Upon striking a crack, acoustical impedance mismatching causes a portion of the incident pulse to be reflected back to the transducer where it is detected.

(3) Ultrasonic Attenuation: A transducer generates an ultrasonic pulse which propagates either through the body of the specimen or along its surface. As a result of various mechanisms (in the case of fatigue severely plastically deformed regions or microcracks) energy is lost from the incident pulse. Hence, the pulse which is reflected from the opposite side of the test specimen from which it was transmitted is detected to have a decreased amplitude in comparison with the incident pulse. Alternatively, a second transducer, affixed to the side of the test specimen opposite the sending transducer, can serve as a receiver, or for the surface wave case, a receiving transducer can be affixed to the same surface of the test specimen as the generating transducer.

(4) Acoustic Emission: Elastic waves, some of which possess ultrasonic frequencies, are internally generated when a test specimen is subjected to a sufficiently high state of stress. A transducer affixed to the surface of the test specimen detects these internally generated waves.

Each of these four techniques has certain advantages and disadvantages as regards their usefulness for the detection of the onset of fatigue damage.

ULTRASONIC ATTENUATION

The first ultrasonic technique used to study the development of fatigue damage during stress cycling was the ultrasonic attenuation technique. As early as 1956, Truell and Hikata(28) observed changes in ultrasonic attenuation in the early stages of fatigue cycling on a polycrystalline aluminum specimen. In subsequent publications, Truell and co-workers(29-32) reported results of experiments where ultrasonic attenuation measurements were made during fatigue tests up to fracture of the test specimens. They used cycling rates of 400 cycles per minute to 1900 cycles per minute and in every case the attenuation changed as a function of the number of cycles. For tests carried out to fracture there was a marked increase in attenuation just prior to failure. Although only a small number of fatigue tests were performed and all of these used aluminum specimens, the results indicated the usefulness of such measurements for prediction of fatigue failure.

In 1962, Bratina and Mills(33) used ultrasonic attenuation to study fatigue damage in plain high-carbon steel and two alloy steels. They used a slow cycling rate of approximately one cycle per minute and found that at this low rate the ultrasonic attenuation decreased with increasing numbers of stress cycles. They attributed these results to strain-ageing effects caused by pinning of dislocation loops by diffusing carbon atoms.

The same year, Ponomarev(34) measured the ultrasonic attenuation in metallic and nonmetallic cylindrical samples during repetitive loading. The metallic samples, steel, copper, and duraluminum were subjected to torsional loading, while the nonmetallic samples, glass, plexiglass, quartzite, and quartz were subjected to periodic impact loads. He established that the moment of failure onset of a part due to fatigue damage can be determined from the character of the change in ultrasonic attenuation curve.

Pawlowski,(35,36) in 1963, measured ultrasonic attenuation during fatigue cycling of specimens of low carbon steel, an alloy steel, an aluminum alloy, and grey cast iron. Using a cyclic loading rate of 25 Hz he found that all the materials tested showed an increase in attenuation with increasing number of fatigue cycles. His change in attenuation versus number of cycles curves exhibited two distinct regions. The first region was nearly linear and showed a relatively gradual increase in attenuation with increasing number of cycles. The second region which occurred in the final stage of the fatigue life of the specimen showed a more rapid increase of attenuation with increasing number of cycles and terminated with fracture of the specimen. Pawlowski concluded that an irreversible increase in attenuation can be regarded as an indicator of damage accumulation developing gradually in the process of fatigue. These irreversible changes he attributed to microcrack formation which coalesce to form macrocracks and eventual fracture.

In 1967, Herlescu et al.(37) recorded the change in ultrasonic attenuation as well as velocity of propagation of a Rayleigh wave in mild steel subjected to fatigue deformation. They reported that both attenuation and velocity tended to increase slightly at the early stage of fatigue, dropped considerably and became somewhat constant as cycling proceeded. Finally, there was a pronounced increase in attenuation attributed to scattering by microcrack formation. They observed relatively little change in velocity at this stage.

Cole and Zoiss,(38) in 1969, used a through transmission ultrasonic attenuation method to determine the location and criticality of fatigue induced damage in filament wound fiberglass cylinders. They correlated the measured ultrasonic attenuation to the residual life remaining to the material.

In 1971, Moore et al.(39) attempted unsuccessfully to relate ultrasonic surface wave measurements of attenuation and velocity to fatigue damage in five specimens of 1100 aluminum which had undergone fatigue deformation for 30, 50, 70, 80 and 90 percent of the specimen life. A possible reason for their lack of success was apparent interference effects between some unspecified wave and the surface wave of interest.

In 1972, Green and Pond(40) reported the results of experiments which used change in ultrasonic attenuation measurements as a continuous monitor of fatigue damage during high cycle testing of aluminum and steel specimens. Green and his co-workers(41-52) have continued to make such measurements since that time; the results of this work will be described in more detail in a later section of the present article.

Owston,(53) in 1973, measured the attenuation of ultrasonic waves transmitted through carbon fiber reinforced polymer specimens at various stages of the fatigue life of the test specimens. He reported that the specimens showed considerable variations in ultrasonic attenuation even before fatigue testing, and that the mean value of the attenuation also varied markedly from specimen to specimen. Fatigue failures accompanied by large areas of delamination were easily detected and identified. Failures which were the result of more discrete cracks or excessive micro-cracking of the matrix and fibers were easily detected, but not always easily distinguished from one another.

In 1975, Tsuchida and Okada(54) measured the attenuation of ultrasonic surface waves and noted an incremental change in attenuation at about 60 to 70 percent of the fatigue life.

Also in 1975, Pouliquen and Defebvre(55) measured the ultrasonic attenuation of continuously generated and detected surface waves during fatigue cycling of a steel specimen. The specimen placed between two piezoelectric quartz crystals, on which interdigital combs

were deposited, comprised a composite ultrasonic delay line. Three phases of the attenuation versus number of fatigue cycle curves were observed. In the first phase (0 - 40,000 cycles) the attenuation varied rapidly; in the second phase (40,000 - 80,000 cycles) the attenuation remained practically constant; in the third phase (above 80,000 cycles) the attenuation increased rapidly once again. Pouliquen and Defebvre concluded that the attenuation variation with the test specimen at its position of maximum bending appeared to be the most sensitive for studying fatigue.

In 1977, MacDonald,(56) in a survey of the use of ultrasonics to investigate the state of fatigue in metals, emphasized the view that the rate of change of ultrasonic attenuation correlated better with fatigue life than does the applied stress amplitude.

Most recently, Green and Duke(52) conducted an exhaustive review of ultrasonic and acoustic emission detection of fatigue damage, a portion of which is reproduced in the present paper.

SURFACE WAVE REFLECTION

In 1960, Brosens et al.(57) first attempted to detect fatigue damage by the reflection of ultrasonic Rayleigh surface waves. Apparently, their lack of success was chiefly due to poor efficiency of the plastic wedge for conversion of longitudinal waves to surface waves.

The first successful use of surface wave reflection to detect the development of surface cracks during fatigue cycling was reported by Rasmussen(58) in 1962, who carried out tests on an electropolished aluminum alloy. He claimed detection of fatigue damage as early as 39 percent of the specimen life, but pointed out that the surface finish of the specimen played a primary role in the ability to record such early warning signals.

Since fatigue damage is generally viewed as originating at the surface of an originally flawless material, and since surface waves normally possess an effective penetration depth of approximately one wavelength, such waves have been used to detect fatigue damage continuously up to the present time.(59-76)

Leonard,(63) in 1969, used ultrasonic surface and longitudinal waves with conventional pulse-echo and pitch-catch techniques for detection of fatigue cracks near the tenon base region of turbine engine compressor discs. A most significant result of this inspection method was the detection of a minute crack not detectable by macroscopic or penetrant inspections. In 1973, Bunce(68) reported that a requirement arose to inspect for cracks in turbine blades in a jet engine on a routine basis in situ in the aircraft. Since this requirement ruled out any possibility of using radiography, the choice lay between ultrasonic and eddy current inspections. Access to the blades was through the jet pipe at the rear of the engine from where, by reaching forward through the final stator section, the leading edge of the blades, where the cracks were known to occur, could be reached. An attempt to use an eddy current probe was unsuccessful because the combination of material type, material mass change in the radius and accurate location of the probe proved to be insurmountable problems and so a surface wave ultrasonic technique was investigated. When perfected, the surface wave ultrasonic technique proved to be capable of finding cracks which, after removal of the blade from the engine, could not be seen visually even using high power magnification. The full value of the inspection technique was that it not only effectively prevented in-service blade failure, but as the crack propagation rate was very rapid, the inspection could be, and was carried out on aircraft turnarounds that were just long enough to allow the engine to cool sufficiently for a technician to enter the jetpipe, thus enabling inspections to be repeated at intervals of only a few days.

In a somewhat similar situation, Lake et al.,(71) in 1975, developed a stress enhanced ultrasonic surface wave technique for inspection of gas turbine compressor blades. They pointed out that a number of factors complicate the problem of adequately examining compressor blades to determine structural integrity or freedom from fatigue cracks during overhaul inspections. The factors they listed are: (a) the great number of parts requiring examination -- in the larger engines, upwards of 1000 blades are used in each engine, (b) the presently used methods, namely, magnetic particle and penetrants, are essentially visual examinations, and, (c) perhaps, most importantly, the presently used methods are fundamentally incapable of detecting very early fatigue cracks. They also noted that in addition to fatigue cracks, it is important to examine compressor blades for corrosion and erosion pits, and also foreign object damage, since fatigue cracks may be initiated at such discontinuities. Their prototype system consisted of four transducer arrays, one for the convex side, and one for the concave side of blades in the first stage and two similar arrays for the second stage blades. After inspection of the blades in the no-load condition, a bending load of approximately one-half the yield stress was applied by pinching two adjacent blades together and the inspection repeated. They substantiated that their prototype stress enhanced ultrasonic surface wave inspection system could be semi-automated and could be used to successfully inspect first and second stage blades with the rotor installed in the engine and by means of a suitable fixture, the blades could be examined during overhaul without removing blades from the rotor.

Although surface wave reflection techniques have been used quite successfully to detect fatigue cracks which were undetectable by other non-destructive testing methods, surface wave reflection techniques are not sensitive to material changes which give warning of fatigue damage prior to macrocrack formation, i.e. prior to a surface crack becoming large enough to reflect back to the transducer an easily detectable amount of ultrasonic energy. The condition of the workpiece surface and proper transducer

attachment are special problems associated with the use of surface waves. Moreover, in many real materials internal stress concentrations cause cracks to form in the interior of the material and not at the surface where they can be detected by surface waves. Surface wave reflection techniques are better suited to detection of surface breaking macrocracks and crack surface length measurement than to early detection of pre-crack fatigue damage.

BODY WAVE REFLECTION

Body wave reflection techniques as applied directly to the fatigue process itself were first reported by Socky(77) in 1964 and also have continued up to the present time.(63,64,68,69,72,73,75,78-102). Bunce(68) described the design of a special ultrasonic probe for inspection of attachment lugs containing a bushed hole. He noted that use of such an ultrasonic probe requires no dis-assembly, beyond that required for access, in order to accomplish the inspection, whereas an eddy current inspection of the same hole would need the removal or dis-attachment of the component involved and removal of the bushes which might in itself cause damage.

In 1974, Sugg and Kammerer(90) reported the results of a study which demonstrated that an ultrasonic system, properly designed and using bonded-in-place transducers, can monitor multiple structural areas for fatigue crack growth. Packman et al.,(93) in 1975, reported the development of an ultrasonic shear wave probe for characterization and measurement of defects in the vicinity of fastener holes. In 1976, Couchman et al. (98) described the development of a computerized system designed to detect cracks by rotating a shear wave transducer around installed fasteners or bolt holes. The same year, Forney(100) described a new portable pulse echo scanner device also designed to detect fatigue cracks in highly stressed fastener holes. Most recently, Doyle and Scala (101) published a review article summarizing the status of crack depth measurement by ultrasonics.

Beginning in 1975 and continuing up to the present time a series of reports(102) has been published by the Center for Advanced NDE at the Science Center of Rockwell International, which contains many papers dealing with quantitative flaw definition by ultrasonic techniques.

Body wave reflection techniques have experienced considerable success, particularly with regard to crack detection and sizing. They offer a big advantage over penetrant, eddy current, and surface wave reflection techniques in that they can locate and measure flaws at large depths in most materials. However, body wave reflection techniques are also not sensitive to material changes which give warning of fatigue damage prior to macrocrack formation. The main reason for this is that in order for an easily detectable fraction of the incident ultrasonic energy to be reflected from a crack back to the transducer, the crack must be relatively large, and often the workpiece will be already well on the way to fracture.

ACOUSTIC EMISSION

Even though Kaiser(103) is generally credited with "discovering" acoustic emission in 1950, it was not until 1964 when Dunegan et al.(104) initiated work in the ultrasonic range of frequencies that acoustic emission actually became an engineering tool. The amount of work performed in this field since that time is enormous,(105-108) and many investigators have monitored acoustic emission successfully during fatigue testing, despite the difficulty encountered in separating the acoustic emission signals from background noise.

In 1967 and 1968, Hartbower et al.(109-111) monitored acoustic emission associated with slow crack growth during low-cycle fatigue testing of precracked steel specimens possessing different heat treatments and of aluminum and titanium alloys. For this low-cycle fatigue work an accelerometer in conjunction with a filter apparently eliminated the noise problem. It should be noted here that such low-cycle fatigue tests present no greater noise problems than those associated with simple tensile tests and hence elimination of noise in these tests is relatively easy.

Hutton,(112-114) in 1969, reported measuring acoustic emission during low-cycle tension-compression fatigue testing of a high nickel alloy steel at 1000°F and noted that at least three peaks in the emission curve were evident prior to failure. He considered the first to be due to an initial high density of mobile dislocations, which became pinned in a limited number of cycles. The second and third peaks he regarded as due to micro-cracking and macro-cracking, respectively. He also recorded acoustic emission data during high cycle tension-tension fatigue testing of notched aluminum and carbon steel specimens. The latter test in particular gave evidence that macro-crack nucleation caused sharp increases in acoustic emission prior to detection of a visible crack. The emission data also showed a more gradual increase which he attributed to micro-crack formation. Hutton eliminated the background noise problem by working with a frequency bandpass window.

Also in 1969, Dunegan et al.(115-117) proposed a method of detecting fatigue damage by intermittently stopping the fatigue cycling and proof testing the specimen by overstressing while monitoring the acoustic emission. This method has the advantage of elimination of most of the background noise, but the disadvantage that it is not a continuous on-line technique. Nevertheless, it is informative to note that for steel and aluminum alloy test specimens and for steel and aluminum pressure vessels similar experimental results were obtained. In all cases, both the total acoustic emission count and the count per cycle increased slowly with the increasing number of fatigue cycles and then

increased rapidly just prior to failure.

In 1971 Nakamura(118) reported an acoustic emission monitoring system which can be used successfully in the presence of the heavy background noise usually encountered in the fatigue testing of a large complex structure. The method consists essentially in surrounding one or more master acoustic emission sensors, located in the critical region to be monitored, with an array of slave sensors. When a noise signal originates outside the critical region, an electronic gate is closed which prevents the master sensor from detecting the noise signal. An actual acoustic emission originating within the critical region is detected by the master sensor provided the gate is open. There are several major problems associated with Nakamura's technique. A steady noise external to the critical region will keep the gate constantly closed and hence no signals will ever be detected by the master sensor. Even an intermittent external noise can cause problems because the gate may again be closed just at the moment an important acoustic emission occurs in the critical region. Finally, a noise source located in the critical region will not be eliminated by the slave sensors and hence will mask detection of actual emission sources by the master sensor.

Also in 1971, Rollins(119) reported monitoring acoustic emission during fatigue testing of boron-aluminum composites. He used a bandpass filter (50 to 500 kHz) and an FET switching transistor in front of the digital counter in order to discriminate between the acoustic emission signal and background noise. The FET transistor was gated open for a short period of time which coincided with the maximum tensile stress of the fatigue load cycle which in turn coincided with the time interval when most of the boron filaments broke. Signals that occurred at other times were blocked. His experimental results showed that for a cantilever bend fatigue test no significant acoustic emission was observed until about one-half of the total fatigue life. The emission counts increased slowly thereafter until at about 95% of the total fatigue life the counting rate increased rapidly until failure. For a tension-tension fatigue test some acoustic emission was produced during the tensile preloading. Upon addition of the cyclic load the emission rate was rather high for several hundred cycles, and then decreased and remained low for most of the fatigue life with a sharp rise just prior to failure.

The same year, Moore et al.(39) monitored acoustic emission counts during fatigue cycling of 1100-0 aluminum specimens. They observed that the cumulative number of acoustic emission counts changed slowly in the early part of the fatigue process and then changed by several orders of magnitude. A relationship was observed between the significant change in the slope of acoustic emission curve and the percent of fatigue life. The change was observed to occur at less than 50 percent of the fatigue life and, as such, offered a possible early fatigue damage warning.

In 1972, Hartbower et al.(120,121) demonstrated that acoustic emission can be used as a precursor of imminent failure for low-cycle, high-stress-intensity fatigue as well as for the case of environmentally assisted fatigue. Plots of cumulative stress-wave count versus cycle number consistently showed a marked increase in count rate several (10-20 or more) cycles before fracture.

Kusenberger et al.,(122) in 1972, monitored crack growth in stress cycled specimens of 4340 steel and 7075-T6 aluminum. Periodically, cycling was stopped, the crack length at the surface was measured, and a constant proof load was applied to the specimen. During proof loading, the specimen was monitored for acoustic emission. The results obtained with the 4340 steel specimens were puzzling in that essentially no acoustic emission above the nominal background level was recorded until the last cycle prior to failure. Such results were obtained even though on several occasions proof loads were raised nearly to yield. The results of the experiments with the 7075-T6 aluminum specimens indicated a strong dependence of the acoustic emission on the state of stress. A much lower count was obtained for plane strain than for plane stress.

Kim, Neto, and Stephens(123) reported the results of some preliminary experiments in which they recorded acoustic emission during continuous tensile cycling of a carbon fiber/epoxy composite. They showed that the acoustic emission energy released per unit time during loading varied during the fatigue cycling and that the Kaiser Effect was apparently not applicable to this composite material.

In 1973, Egle et al.(124-126) reported an acoustic emission system for monitoring high cycle fatigue crack growth. They used a conventional acoustic emission system with a high pass filter between the transducer and preamplifier and a second high pass filter between the preamplifier and digital counter. In addition, an electromagnetic transducer was used to gate the counter every 10 or 100 load cycles. For low cycle fatigue of a notched aluminum plate the number of acoustic emission counts per load cycle first decreased and then increased slowly just prior to failure. For high cycle fatigue of an aluminum specimen in a displacement controlled cantilever beam tester the emission exhibited a relatively high count at the start of the loading followed by a sharp decrease and then an increase. For specimens tested with higher maximum displacements and shorter lives, the emission continued to increase until failure. For specimens tested with lower maximum displacements and longer lives, the emission tended to level off and then to decrease. Egle attributes these results to the fact that the rate of crack propagation decreased for the lower maximum displacements because of the displacement control on the fatigue tester.

Owston(53) recorded acoustic emission counts during fatigue testing of carbon fiber reinforced polymer composite specimens and attempted to correlate acoustic emission and

loss of stiffners (drop in natural resonant frequency). He found a moderate correlation for specimens made from material with a low interlamina shear strength, but none for specimens of high interlamina shear strength. A change in the principal source of emission caused by a change in the properties of the material was suggested as the most likely cause of the loss in correlation.

Harris and Dunegan(127) continuously monitored fatigue crack growth in 7075-T6 aluminum and 4140 steel by acoustic emission techniques. The acoustic emission rate per cycle was consistently observed to be cyclic in nature, i.e. the rate was observed to be high for a few cycles of loading followed by a period of inactivity. This was regarded as strong evidence that crack growth in these materials does not occur by a uniform growth per cycle, but by a burst of growth followed by a stationary period.

Morton et al(128) performed similar investigations in which they monitored acoustic emission and quantitatively correlated it with crack growth rate and the applied range of stress intensity for high cycle fatigue of 2024-T851 aluminum alloy. They concluded that the acoustic emissions observed during fatigue are more closely related to the crack tip plastic volume than to crack extension.

Bailey and Pless(129) used acoustic emission techniques and sound travel time determinations to locate cracks in a structural fatigue test specimen. The specimen was subjected to a spectrum of cyclic load conditions which simulated a total of 150,000 aircraft flight hours. The specimen was monitored for acoustic emission approximately 10 percent of the total fatigue test time. It was found, in agreement with the results of other investigators, that crack growth at a given location was not continuous throughout the fatigue tests. Cracks were observed to grow during some test passes, but apparently remained stationary during other passes. Some cracks did not even appear to grow continuously during a single pass. Crack growth was reported to be rapid or slow for given cracks at different times. A total of 18 crack locations were identified by acoustic emission monitoring, 15 of which were verified during metallurgical investigation.

Vary and Klima(130) reported the results of a preliminary investigation to assess the feasibility of continuously monitoring acoustic emission signals from fatigue cracks during cyclic bend tests. Plate specimens of 6Al-4V titanium, 2219-T87 aluminum, and 18-Ni maraging steel were tested with and without crack starter notches. The investigation indicated that it was possible to extract meaningful acoustic emission signals in a cyclic bend machine environment and that such acoustic emission monitoring is a potentially useful tool for investigating fatigue cracking. Ultrasonic crack growth monitoring was applied simultaneously with acoustic emission monitoring for a few specimens. Although abrupt increases in the acoustic emission count rate were observed, the ultrasonic signals indicated only a smooth increase in crack size.

Smith and Morton(131) reported a "short-time" cross-correlation technique for acoustic emission monitoring during high-cycle fatigue testing, which largely rejected random electronic noise as well as mechanical noise from sources other than the crack. Using their technique they were able to separate the acoustic emission signals due to crack extension from those of crack closing.

Corle and Schliessmann(132) conducted a test program to evaluate acoustic emission techniques for use in detecting flaws during proof testing of rocket motor cases. Steel sheet specimens which contained tight fatigue cracks of various sizes were tested. An acoustic emission signature was recorded for each specimen during proof testing and was found to be a function of the flaw size. By evaluating the signature, unflawed specimens could be distinguished from flawed specimens, and the flawed specimens could be ranked on the basis of flaw size, with flaws as small as 0.9 mm(0.035 in) deep being detected. By comparison, flaws as large as 4.1 mm (0.16 in) deep and 66 mm (2.6 in) long were not detected by radiographic techniques, and surface flaws as large as 2.5 mm (0.1 in) deep and 2.5 mm (0.1 in) long were not detected by magnetic particle inspection.

In 1974, Morton et al.(133) investigated the effect of loading variables on the acoustic emissions observed during fatigue-crack growth. They concluded that the acoustic emission rate near peak load is explicitly related to applied stress intensity for materials of widely different character. They also concluded that varying the fatigue test cyclic frequency can result in a change in the acoustic emission rate without resulting in a change in crack growth rate.

Willertz and Hunter(134) recorded the acoustic emission emitted from a 17-4 PH stainless steel while the specimen was undergoing fatigue testing in the torsional mode. Below the cyclical stress sensitivity limit, defined as the highest stress below which no changes in the damping occur with cycling, no abnormal emissions were detected, while at and above this limit emissions were detected which could be attributed to fatigue damage which resulted in failure of the specimen. They observed that once the crack started to propagate, the emissions tended to occur mainly when the stress went through zero and changed sign in one direction only. Application of stress in the opposite direction did not produce appreciable acoustical noise, for some unknown reason.

Williams and Reifsnider(135) conducted strain and load controlled fatigue tests on boron-aluminum and boron-epoxy angle-plied composite specimens simultaneously with acoustic emission monitoring. By recording the acoustic emission signals only during the top half of the loading cycle where new damage was most likely to occur, rather than during unloading and at low stress levels, specimen fretting and machine noise was effectively rejected. They found good correlation between the amount of specimen damage and totalized

acoustic emission, and the rate of damage development with acoustic emission rate until significant delaminations caused extraneous scrapping and fretting noise.

In 1975 Acquaviva and Chait(136) performed acoustic emission tests on unnotched and notched tension-tension fatigue specimens of a high strength titanium alloy. No acoustic emission was detected from the unnotched fatigue specimens until 30 to 150 cycles before fracture, indicating that the crack initiation and propagation phases were quasi-simultaneous for this high strength material. At 30 Hz, the crack initiation to fracture time would be about 3 sec. The notched specimens produced acoustic emission signals at least 2500 cycles (83 sec) prior to fracture. A measure of the crack area for each of the notched specimens showed that the higher emission counts were associated with the larger crack depths.

Pless and Bailey(137) used an acoustic emission monitoring system to detect crack extensions induced in a large aircraft wing structure through cyclic loading. The crack extensions were induced by tension-tension loadings at specified percentages of design limit load acting on four-inch long crack-starter sawcuts made at well-defined locations on the specimen. Since both audible and inaudible fracture increments were detected, it was concluded that the tests proved the feasibility of the acoustic emission monitoring technique. However, even though the signal-to-noise ratio was high enough to virtually exclude false alarms during these tests, the tests could provide no information about acoustic and other transients resulting from active flight systems.

Mehdizadeh(138) conducted tension-tension fatigue tests on steel specimens exposed to a corrosive saltwater environment. He concluded that periodic proof testing combined with acoustic emission monitoring can be as sensitive a method for assessing the progress of corrosion fatigue damage as the continuous acoustic emission monitoring method. However, the capability of the proof testing - acoustic emission technique to evaluate a well developed corrosion fatigue crack depends upon the geometry and size of the crack relative to the test specimen. Although incipient corrosion fatigue cracks were detected in some cases after 10-30 percent of the fatigue life had elapsed, in other cases test specimens containing well developed corrosion fatigue cracks generated relatively little acoustic emission during proof tests.

Lazarev et al.(139) reported that standard fatigue equipment available in Russia can be used for fatigue testing accompanied by acoustic emission monitoring provided that the background noise level is reduced to a value sufficiently lower than the acoustic emission signals. They presented the results of an acoustic emission monitored fatigue test which showed a sharp rise in acoustic emission counts coincident with crack formation in the test specimen.

Hatano(140) measured acoustic emission during high-cycle fatigue testing of pure aluminum specimens. He detected intermittent burst-type emission in the early stage of fatigue testing before observation of macroscopic crack growth. He also noted that most of the acoustic emission signals were detected during that portion of the fatigue cycle where the cyclic load was a maximum.

Dunegan(141) published an article in which he utilized the results of some prior work in order to show how acoustic emission techniques can be used to estimate the stress intensity factor of a growing crack, and therefore provide predictive ability for determining failure.

Fuwa(142) used acoustic emission to study the damage occurring in unidirectional carbon-fibre-reinforced plastics during cyclic loading and stress relaxation at high stress levels. Their results suggested that true fatigue processes do not occur in carbon-fibre-reinforced plastics and that the damage sustained during cycling is of the same kind as that which occurs in ordinary tensile loading.

In 1976, Kishi et al.(143) studied the acoustic emission generated during cyclic deformation of pure aluminum and reported an acoustic emission peak accompanied by a Bauschinger effect. This peak was observed with the appearance of irreversible plastic strain and the peak height decreased with increase in the number of cycles up to a constant value at the saturation stress.

Carlyle and Scott(144) reported a new method of portraying acoustic emission fatigue data which facilitates the interpretation of dynamical micromechanical failure processes in materials and also proved valuable in the characterization of extraneous testing machine and grip noise. In their technique the location of individual acoustic emission events was plotted within a coordinate system of load versus number of fatigue cycles. Using their method they detected several events which would not have been observed with conventional acoustic emission monitoring.

Shinaishin et al(145) reported additional results of acoustic emission detection of fatigue crack initiation and propagation. The fatigue tests were run in reverse bending and in tensile fatigue on notched and unnotched titanium specimens. The necessity to use notched specimens in the bending fatigue tests was occasioned by the fact that initial tests run on several unnotched specimens resulted in failure of the specimens at a fraction of the expected life without any acoustic emission warning. Similarly, notches were cut in the tensile fatigue specimens, because for tests run on unnotched specimens, acoustic emission cracking was detected only after more than 99 percent of the specimen fatigue life had been expended.

Bailey and colleagues(146-149) expanded upon their earlier work on assessing the possibility of using acoustic emission for in-flight monitoring of aircraft structures. Their Flight Structural Monitoring System (FSMS) was designed to detect the large transient acoustic sound generated by single large crack extensions rather than the lower level signals generated by fatigue crack initiation. Using the FSMS they successfully monitored crack extensions in full-size complex structural components during fatigue testing by a combination of signal processing techniques involving spatial discrimination, frequency filtering, and signal amplitude discrimination. Cracks were initiated and grown on a wing test article at selected fastener holes from sharp-notch sawcuts by subjecting the specimen to a flight-by-flight load spectrum typical of a military transport aircraft. Acoustic emission was detected from 12 of the 15 test holes monitored which experienced crack growth and 3 of 6 extraneous acoustic emission sources were traced to loose fasteners. For 3 of the cracks monitored, the acoustic emission counts showed reasonable correlation with amount of crack growth. The greatest detractor to correlatable data was random noise.

In 1977, Sinclair and Connors(150) monitored acoustic emission during fatigue crack growth in A533B steel, low carbon steel, and H1 weld metal. During loading of the specimens, signal recognition discriminators and location resolution were employed to allow detection of signals in the presence of background noise. All specimens tested either possessed cut notches or previously introduced fatigue cracks of appreciable size. For the most intensively investigated A533B steel the acoustic emission counts were related to the creation of new crack area. The location resolution of the tests was insufficient to permit determination of the acoustic emission mechanisms.

Horak and Weyhreter(151) reported the development of an acoustic emission system for monitoring components and structures in a severe fatigue noise environment. Their system utilized master-slave discrimination, rise time discrimination, and coincidence detection to identify and reject unwanted noise signals from computer processing. Among the discrimination concepts which they found to be unsatisfactory were frequency filtering, computerized data reduction, and mechanical dampening. Since Horak and Weyhreter found that the wave forms of the various transient noises contributed most to false data generation, the only acoustic emission signals reliably detected were those which occurred during the time periods between the transient fatigue noises. Their system indicated 10 false locations in 16 hours on a fatiguing part which had not begun to crack. Thirty-six false locations were indicated in 15 secs when their discrimination system was not used. Crack propagation was not always continuous and sometimes stopped completely for several hundred cycles. Although crack propagation is generally considered to occur during the maximum stress application of the fatigue cycle, their results showed that acoustic emission resulting from crack extension occurs during low, medium, and high parts of the loading curve. These data led them to caution that the exclusive use of time gates to eliminate extraneous noise signals might also eliminate a large portion of the acoustic emission signals also. As a result of the various types of defects and loads involved, crack initiation was detected and located from several minutes to several hours prior to ultimate failure. Since crack initiation occurred within the material, crack initiation size was not determined.

Williams and Reifsnider(152) used a system which incorporated a time gate, variable readout, and filtering to monitor acoustic emission during fatigue loading of boron-epoxy and boron-aluminum composite specimens which contained a circular centered hole. Their normal practice was to look at acoustic emissions generated only during the top half of the loading cycle and to use a frequency band-pass of 10-300 kHz. Correlations were observed between acoustic emission counts, specimen compliance, infrared heat patterns, and structural damage.

RECENT ULTRASONIC ATTENUATION AND ACOUSTIC EMISSION MEASUREMENTS

Survey of the published literature shows that at the present time ultrasonic attenuation and acoustic emission measurements are superior to all other non-destructive testing techniques for the early detection of fatigue damage. Therefore, these two techniques have been the ones selected by the present author and his colleagues for further investigation.

In 1972, Joshi and Green(42) reported the results of experiments which used change in ultrasonic attenuation measurements as a continuous monitor of fatigue damage during high cycle testing of aluminum and steel specimens.

Ultrasonic pulses were generated by an x-cut quartz transducer firmly attached to the clamped end of a polycrystalline aluminum or steel bar using Eastman 910 cement. The specimen shape, transducer size and frequency used insured that the entire specimen was completely filled with ultrasound in a guided wave mode. This mode of operation permitted the ultrasonic waves to detect both bulk and surface alterations in the test specimens.

Each specimen was held in a horizontal plane and was displaced vertically at the opposite end by a fixture attached to the cam of the fatigue machine. In this manner the specimen was fatigued in reverse bending as a cantilever beam to fracture at 30 Hz with a vertical amplitude peak-to-peak which was set at a fixed value in the 7.5 mm to 15 mm.

The specimens were either made from 6061-T6 polycrystalline aluminum or from cold-rolled polycrystalline steel. All specimens tested were made from the same lot of aluminum or steel in order to minimize differences in alloy composition, cold work, heat treatment, and surface finish. Prior to fatigue testing, each specimen was ultrasonically

tested for internal flaws and microscopically examined for any surface defects or scratches.

Figure 5 shows the results of a typical experiment for an aluminum specimen tested at a constant vibration amplitude peak-to-peak of 7.5 mm. It can be seen that the attenuation began to increase at about 2.8 million cycles and proceeded catastropically to fracture at about 3.5 million cycles. The 2.8 million cycle mark occurred at about 26 hours and failure occurred after about 33 hr. Thus the ultrasonic attenuation measurements gave a strong indication of the onset of fatigue failure at approximately 7 hr prior to the occurrence of the fracture itself. Conventional ultrasonic monitoring was unable to detect any additional echoes due to energy reflected from the crack until about 2 hr prior to failure. Thus, for this particular experiment, ultrasonic attenuation indicated that failure was eminent 5 hr before conventional ultrasonic testing could indicate any crack formation.

Figure 6 summarizes the experimental results obtained from ultrasonic monitoring of the fatigue tests with the aluminum specimens. The ordinate axis in this figure corresponds to the maximum stress on the outermost fiber of the bar when bent to the maximum amplitude chosen for the particular test. The upper abscissa axis indicates the test time; the portion of this scale ranging from 22 - 32 hr should be used with the tests run at a maximum fiber stress of 2.29×10^4 psi; the scale ranging from 0 - 12 hr should be used with all other tests. The lower abscissa axis indicates the number of fatigue cycles which elapsed before various events were detected. The portion of this scale ranging from 2.59×10^6 cycles to 3.46×10^6 cycles should be used with the single test run at a maximum fiber stress of 2.29×10^4 psi; the scale ranging from $0-1.296 \times 10^6$ cycles should be used with all other tests. The entries represented by circles indicate the average time elapsed in 5 similar tests before an 0.4 db change in attenuation was observed. The criterion of 0.4 db change was selected as an early warning signal since this amount of change could be clearly distinguished from background fluctuations on the attenuation recording strip chart in all aluminum and all steel tests. The entries represented by triangles indicate the average time elapsed in 5 similar tests before detection of an additional echo in the pulse-echo pattern due to energy reflected from a crack in the test specimen. The entries represented by squares indicate the average time elapsed in 5 similar tests before fracture occurred. It can be clearly seen that in all cases the change in ultrasonic attenuation indicated that failure was eminent before conventional ultrasonic testing could detect an additional echo caused by energy reflected from a crack. Moreover, the smaller the amplitude of vibration and hence the longer the fatigue test, the more absolute time there is between the ultrasonic attenuation warning and fracture of the test specimen.

Figure 7 shows the results of a similar experiment for a steel specimen tested at a constant vibration amplitude peak-to-peak of 7.5 mm. In this case the attenuation began to increase at about 6×10^5 cycles and the increase proceeded catastropically to fracture at about 9×10^5 cycles. The 6×10^5 cycle mark occurred at about 6 hr and failure occurred after about 8 hr. Conventional ultrasonic monitoring was able to detect an additional echo at the 7 hr mark. Thus, ultrasonic attenuation measurements gave warning 1 hr earlier than ultrasonic pulse detection in this case.

Figure 8 summarizes the experimental results obtained from ultrasonic monitoring during the fatigue tests of the steel specimens. The ordinate axis corresponds to the maximum stress on the outermost fiber of the bent bar. The upper abscissa indicates the test time in hours, while the lower abscissa indicates the number of fatigue cycles which elapsed before various events were detected. The entries represented by circles indicate the average time elapsed in 3 similar tests before an 0.4 db change in attenuation was observed. The entries represented by triangles indicate the average time elapsed in 3 similar tests before detection of an additional pulse due to reflection of energy from a crack. The entries represented by squares indicate the average time elapsed in 3 similar tests before fracture occurred. The results are similar to those obtained with aluminum in that ultrasonic attenuation gave early warning of fatigue failure.

Panowicz(46) performed experiments in order to determine whether or not ultrasonic attenuation measurements could also be used to predict fatigue failure in test specimens which had latent defects purposely introduced in them in order to alter the fatigue life and to more realistically simulate actual in-service operating conditions for many cases. The terminology "induced latent defects" was used to indicate artificially created defects which were latent in the sense that they were undetectable by either normal visual inspection or any currently available ultrasonic pulse-echo testing technique.

The test specimens were machined from 1100°F polycrystalline aluminum in the form of bars with dimensions of approximately 1.3 cm by 2.5 cm by 30.5 cm. All specimens were made from the same lot of aluminum in order to minimize differences in alloy composition, grain size, and surface finish.

The latent defects were created in the aluminum specimens in the following manner. A fine saw cut 1.6 cm deep was made in each specimen along the 2.5 cm width, at a distance of 10 cm from one end of the bar. After thorough degreasing and cleaning, the specimen was clamped in a set of steel dies which left exposed a 2.5 cm length in the region of the saw cut. The function of the die set was to reinforce the specimen during loading in order to concentrate the plastic deformation in the area of the cut being welded. In order to promote the plastic welding process, the specimen-die assembly was heated for

one hour at a temperature selected in the hot working range of aluminum. Immediately after heating, the specimen-die assembly was placed in a cylindrical steel protective housing which served as a guide for die movement. The specimen-die assembly was then end loaded in compression to a predetermined load at a rate of 3.6 mm per sec. This rate was found to produce high quality welds with the particular loading configuration and tensile test machine used.

It was established experimentally that any plastic weld produced by heating and loading the specimen above the specified minimum values created a joint in the bar that was undetectable by either visual inspection or ultrasonic pulse-echo testing. The weld joint was made microscopically visible by etching the specimen in a micro-etch consisting of 20% sodium hydroxide solution in water. As the applied load for welding was increased, the micro-etch delineated weld joint transformed from one which appeared to be a continuous line to a series of unconnected microdefects. These observations are consistent with the hypothesis that the induced latent defects consisted largely of oxide particles which were trapped inside the specimen during the welding operation.

Figure 9 shows the results of a typical test where ultrasonic attenuation was measured as a function of number of fatigue cycles for an aluminum specimen heated at a promoting temperature of 750°F (399°C) and plastically welded with an applied load of 15,000 lb (6804 kg). Despite differences in the results of tests run on specimens which were welded using different promoting temperatures and different applied loads, all experiments performed yielded similar results in that ultrasonic attenuation gave early warning of fatigue failure. As in the previous work, an ultrasonic attenuation change of 0.4 dB was selected as an early warning criterion since this amount of change could be clearly distinguished from background fluctuations on the attenuation recording strip chart and since in every test run a crack was detected only after a change in ultrasonic attenuation of 0.4 dB or more had been observed.

Mignogna et al.(49) made continuous measurements of changes in ultrasonic attenuation of a 2.25 MHz wave propagating in plain and "rivet simulated" 1/16 inch thick sheets of 7075-T6 aircraft aluminum alloy during fatigue cycling. The test specimens were held in a horizontal plane and fatigued until failure in reverse bending as a cantilever beam at 30 Hz; the peak-to-peak vertical amplitude was 0.3 in (7.62 mm). All specimens were cut from the same 7075-T6 aluminum sheet in order to minimize differences in alloy composition, cold work and heat treatment. Care was taken to assure the similarity of the surface condition and to note the rolling direction of each specimen. Three basic specimen configurations typical of those which might be encountered in an actual aircraft were considered. The first, or plain, specimen design incorporated no fasteners or fixtures. The other two specimen configurations, however, included rivet simulated regions with fastener hole patterns typical of those used in aircraft construction. Screw fasteners were used rather than rivets to facilitate examination of these regions after failure of the sample.

Pulses from a 0.5 in x 1 in 2.25 MHz longitudinal transducer were introduced into the specimens through a modified mode conversion block of lucite designed to generate shear waves at 45° to the surface normal. The mode conversion block or "wedge" was coupled to the specimen with an ethylene glycol based couplant. This method of introducing the ultrasound into the specimen was necessitated due to their thin cross section.

Figure 10 shows a typical plot of change in ultrasonic attenuation versus percent of fatigue life for a plain aluminum alloy sheet specimen with its length parallel to the rolling direction of the sheet. Although the attenuation increased slowly during the early stages of fatigue, no significant change in attenuation nor any significant additional pulses were observed during the first 85% of the fatigue life of the specimen. An additional echo having an amplitude of 0.03 V was first observed at 5.75×10^5 cycles or 86% of the fatigue life. At the same time the attenuation began to increase significantly. The total fatigue life of the specimen (100%) was 6.69×10^5 cycles. Similar data are shown in Fig. 11 for a specimen having its length perpendicular to the rolling direction. The attenuation changed very little in the first 83% of the fatigue life. It began to increase at 83% of the fatigue life and an additional pulse was observed at approximately 84% or 2.95×10^5 cycles. The total fatigue life (100%) was 3.48×10^5 cycles. As would be expected due to the differences in texture, the fatigue life of the plain specimens whose length were perpendicular to the rolling direction were less than those with the length parallel to the rolling direction.

It was found generally that there was more change in the attenuation in the early portion of the fatigue life for the rivet simulated specimens. Figure 12 shows a typical plot of change in ultrasonic attenuation versus percent of fatigue life for a rivet simulated specimen with screws located at the end farthest from the ultrasonic transducer. The specimen geometry was such that the length was parallel to the sheet rolling direction. There was a small change in the attenuation during the initial portion of the fatigue life, but in the latter portion there was a much more rapid increase beginning at about 91% or 6.50×10^5 cycles; the total fatigue life was 7.24×10^5 cycles. Similarly, Fig. 13 presents the data for another typical rivet simulated specimen having rivets located at the middle. The specimen geometry was such that the length was perpendicular to the sheet rolling direction. At approximately 87% of the fatigue life the attenuation began to change very rapidly; the total fatigue life of this specimen was 3.54×10^5 cycles.

Numerous investigations which involve monitoring the acoustic emission resulting from crack initiation and propagation during cyclic loading have been reported as discussed earlier. The general observed relation between a measure of acoustic emission (e.g. total counts, count rate, etc.,) and the number of fatigue cycles is depicted schematically in Fig. 14. Although different investigators have related the acoustic emission observed during cyclic deformation to a variety of material alterations, nc satisfactory explanation of the mechanism causing fatigue damage resulting in failure has been established.

The extreme sensitivity of both ultrasonic attenuation and acoustic emission monitoring suggest that the greatest potential for discerning the mechanisms responsible for fatigue damage lies in utilizing these two techniques to investigate material alterations during cyclic loading. In order to accumulate as much information as possible, Duke and Green(50) have applied both monitoring techniques simultaneously to the same specimen while it was subjected to fatigue cycling. In order to facilitate the combined monitoring during fatigue cycling it was necessary to modify the basic experimental arrangement previously employed. A variable delay optical trigger was employed in order to synchronize the repetition rate of the ultrasonic pulse with the fatigue cycle. Utilizing this procedure, the pulse could be generated at any point in the fatigue cycle; in the tests reported in this work the pulse was generated during the undeflected portion of the cycle. The remainder of the ultrasonic attenuation monitoring system was essentially the same as that used previously. However, the capability of making reliable acoustic emission measurements during cyclic loading was provided by use of an acoustic emission transducer-cable-amplifier system from the Admiralty Marine Technology Establishment. This system, which combined a multi-shielded Mu-metal and copper screened cable with other special features, has a signal-to-noise ratio at least three orders of magnitude better than conventional acoustic emission monitoring systems.

Prismatic specimens of 7075 aluminum were tested in two different heat treated conditions: as-received 7075-T651 and solution treated. Figure 15 shows the results of a typical experiment for an as-received specimen tested at a constant vibrational amplitude of 9 mm peak-to-peak. In the case of the as-received specimen there was very little change in attenuation during the early portion of the fatigue life. At 80 percent of the fatigue life, however, the change in attenuation increased rapidly, quickly going beyond the sensitivity range monitored. On the other hand, the true root mean square voltage of the acoustic emission signal was observed to fluctuate during the first 20 percent of the fatigue life, followed by a portion in which it remained relatively unchanged, and then at 80 percent of the fatigue life it increased rapidly with only minor fluctuations until failure.

Figure 16 shows the results of a similar experiment for a solution treated specimen also tested at a constant vibrational amplitude of 9 mm peak-to-peak. It can be seen that the ultrasonic attenuation increased slowly from the start until at 90 percent of the fatigue life it rapidly increased beyond the sensitivity range monitored. The true root mean square voltage of the acoustic emission signal exhibited a peak before 5 percent of the fatigue life had occurred. This initial peak was followed by a long period of no activity. At 78 percent of the fatigue life the acoustic emission activity began to increase, though somewhat erratically, and continued to do so until failure. Although both change of ultrasonic attenuation and acoustic emission increased rapidly prior to failure in agreement with the findings of previous investigators, acoustic emission activity was also observed in the early stages of fatigue cycling. The cause of this early emission requires further investigation before its importance relative to fatigue damage can be properly assessed.

Thus, it is clear that body wave and surface wave reflection techniques are inferior to ultrasonic attenuation and acoustic emission techniques for the early detection of fatigue damage, since both reflection techniques require that an appreciable fraction of the available ultrasonic energy be reflected from a crack of sufficient size and correct orientation in order to be detected. Ultrasonic attenuation and acoustic emission techniques can easily detect microcrack formation, and the more sensitive systems can even detect motion and pile-up of dislocations prior to microcrack formation.

OTHER METHODS

In addition to the primary techniques already discussed, other non-destructive test methods have been used with varying degrees of success to detect fatigue damage. Magnetic techniques for crack detection are useful, but relatively insensitive, and are limited to detection of surface cracks in ferromagnetic materials.(26,153) Due to the current application of fracture mechanics concepts to aircraft design, considerable effort has been expended in attempting to non-destructively make quantitative measurement of flaws. Although progress has been made in developing a better fundamental understanding of ultrasonic wave scattering and spectroscopic analysis,(102) neither of these techniques has progressed to the point where it can be used to reliably detect fatigue damage. Ultrasonic second harmonic measurements as proposed by Yermilin et al.(154) and Buck and colleagues (155,156) have met with some success. Batra et al.(157) have demonstrated that ultrasonic Doppler-shift techniques can be used for detecting and sizing radial cracks. Most recently Buck and Alers(158) presented a review of new techniques for detection and monitoring of fatigue damage in which they discussed, in addition to the methods already mentioned, holographic interferometry, photostimulated exo-electron emission, and positron annihilation.

RESIDUAL STRESS (STRAIN) MEASUREMENTS

As mentioned in the INTRODUCTION, the most sensitive systems for early detection of fatigue damage would be capable of detecting motion and pile-up of dislocations. Since such pile-ups would lead to regions of severe residual stress (strain) prior to micro-crack formation, all non-destructive techniques for residual stress (strain) measurements are potential techniques for extremely early detection of fatigue damage. The methods currently being used or under development for non-destructive residual stress (strain) measurements may be broadly grouped into four categories: x-ray diffraction methods, ultrasonic methods, electromagnetic methods, and solid state physics methods.

The x-ray diffraction method consists primarily of measuring the stress induced shift in the peaks of the angular distribution of the intensity of x-rays diffracted from various lattice planes of crystalline materials (line shifts). The peak shifts can be directly related through Bragg's Law to changes in the spacing between the planes of the crystal lattice. A secondary effect of residual stresses is to cause broadening of the intensity angular distribution (line broadening). Although the x-ray diffraction method is the non-destructive technique most often used in actual practice to measure residual stress, it is not optimally suited for many applications partially because the necessary equipment is heavy and bulky, and, more importantly, it suffers from the fact that it only serves to determine the state of stress in a surface layer of a material, while in many practical cases a knowledge of the bulk stresses is desired. A very important advantage of the x-ray diffraction method, however, is that the lattice strain in the stressed material can be measured without prior knowledge of the value in the unstressed state by making two measurements at different angles of incidence of the x-ray beam.

Ultrasonic methods depend on the fact that nonlinear elastic behavior is induced in an otherwise linear elastic solid due to the presence of a residual stress. Most ultrasonic measurements of residual stress have been based on stress-induced acoustical birefringence of an isotropic solid. When transverse waves are propagated through an isotropic solid at right angles to the direction of applied stress, the transverse wave with particle displacement parallel to the direction of applied stress propagates with a faster velocity than the transverse wave with particle displacement perpendicular to the direction of the applied stress. Other features of nonlinear elastic wave propagation such as harmonic generation, temperature dependence of ultrasonic velocity, or ultrasonic dispersion have been proposed for residual stress determinations. The major difficulty associated with reliable ultrasonic residual stress measurement is that the change in elastic wave velocities in solid materials due to residual stress is small and other factors which can cause greater velocity changes may mask residual stress effects. The fact that ultrasonic techniques offer the possibility of measuring bulk residual stresses in thick sections of materials can also lead to problems, since the same section of a material may contain both compressive and tensile stresses whose effects integrated over the path of the ultrasonic wave will cancel.

Electromagnetic methods are based on stress-induced changes in electrical conductivity, magnetic permeability, magnetostriction, coercive force, retentivity, and saturation induction. The method which has drawn most attention to date is Barkhausen noise analysis. The use of Barkhausen noise to measure residual stress is based on the fact that the size, shape, and orientation of magnetic domains changes rapidly during magnetization of ferromagnetic materials inducing noiselike voltage pulses in a coil inductively coupled to the specimen. This noise is a function of the residual stress state in the ferromagnetic material. Other methods include eddy current testing, variable frequency permeability measurements, measurement of the amplitude of electromagnetically generated ultrasonic waves, and direct alternating current measurement of coercive force, retentivity, saturation induction, and magnetostriction. The major problem associated with electromagnetic measurement of residual stress is that the various electrical and magnetic properties are sensitive to other material properties, such as composition, homogeneity, and texture, as well as stress. Moreover, a number of the proposed methods are limited to ferromagnetic materials.

Most of the solid state physics methods proposed for measuring residual stress may be grouped under the category of nuclear hyperfine effects. These methods depend upon the strain dependence of the coupling between nuclear magnetic moments and the surrounding atomic lattice. Some of these methods involve only the nuclear ground state, while others involve the excited states. Of all these methods, the Mössbauer effect has been most extensively directed at residual stress measurement although limited to alloys containing iron-57 nuclei. Other proposed methods include electromagnetic nuclear magnetic and quadrupole resonance, acoustic nuclear magnetic and quadrupole resonance, ferromagnetic nuclear magnetic resonance, perturbed angular correlation, nuclear magnetic resonance diffraction (zeugmatography), lithium nuclear microprobe, and piezoelectricity. Most of these techniques have been limited to research laboratories and require complex, bulky equipment and highly skilled operators. Some techniques require a large homogeneous magnetic field, while others require that the specimen fit inside an encircling coil. Several only work with ferromagnetic or radioactive materials, while in other cases ferromagnetic impurities interfere with testing of nonmagnetic materials. Two of the techniques require a transducer mechanically coupled to the specimen, one requires the presence of interstitial hydrogen, and another requires the presence of permanent electric dipoles in the specimen.

An excellent reference for obtaining more detailed information about all of the above mentioned methods for nondestruction evaluation of residual stress is the proceedings of a workshop held on this subject in 1975.(159)

CONCLUSIONS

1. At the present time, the best non-destructive techniques for detection and possible sizing of fatigue macrocracks are ultrasonics, eddy current, penetrant, and radiography, in order of decreasing sensitivity.

2. The best non-destructive techniques for detection of microcrack formation and possibly pre-microcrack fatigue damage are ultrasonic attenuation and acoustic emission.

3. A large number of non-destructive techniques for residual stress (strain) measurements are candidates for extremely early fatigue damage detection.

In order to transfer some of the techniques from the research laboratory to a field testing situation, the research worker must be better informed as to specific aircraft problems and the field inspector must be more willing to try new techniques. In the opinion of the present author, this communication-cooperation gap is the biggest obstacle to rapid progress in practical implementation of improved non-destructive methods for the early detection of fatigue damage in aircraft components.

ACKNOWLEDGMENTS

This work was supported in part by the Air Force Office of Scientific Research (AFSC), United States Air Force; in this regard we specifically express out thanks to Mr. William J. Walker and to Lt. Col. J. D. Morgan, III. The authors wish to express their gratitude to Dr. Robert Dukes and Mr. Don Birchon of the Admiralty Marine Technology Establishment for the loan of the Low Noise Acoustic Emission System. A special note of thanks is due Mrs. Corinne Harness for her efficient typing of the manuscript.

REFERENCES

1. W. D. Rummel, P. H. Todd, Jr., R. A. Rathke, and W. L. Castner, The Detection of Fatigue Cracks by Nondestructive Test Methods, Materials Eval. 32, 205-212 (1974).

2. Nondestructive Testing in Aircraft, Department of Transportation, Federal Aviation Administration, AC-43-3 (May 1973).

3. H. G. Bunce, NDT in the Aerospace Industry, The State of the Art: Ultrasonics, Brit. J. NDT 15, 55-57 (1973).

4. E. H. Ruescher, The Influence of Some X-ray Parameters on Crack Detection Capability, Materials Eval. 31, 152-154 (1973).

5. D. A. W. Pullen, High Energy Radiography: A new Technique in the Development of Efficiency and Integrity in Aero Gas-Turbine Engines, Materials Eval. 32, 25-30 (1974).

6. V. W. Clarkson, The Requirement for the Non-Destructive Testing of Airframes, Brit. J. NDT 17, 118-121 (1975).

7. R. Halmshaw and C. A. Hunt, Can Cracks be Found by Radiography?, Brit. J. NDT 17, 71-75 (1975).

8. P. Stafford, A. C. Sherwood, and D. West, Proton radiographic detection of microporosity in aero-engine turbine castings, NDT 8, 235-240 (1975).

9. P. A. E. Stewart, Engine testing using advanced techniques, Aeronautical J., 331-343 (August 1975).

10. J. A. Guillen, Jet Engine Isotope Inspection, Paper 5B6, Proceedings of Eighth World Conference on Nondestructive Testing, Cannes, France (1976).

11. W. E. Dance, Neutron Radiographic Nondestructive Evaluation of Aerospace Structures, Practical Applications of Neutron Radiography and Gaging, ASTM STP 586, American Society for Testing and Materials (1976), pp. 137-151.

12. N. B. Edenborough, Neutron Radiography to Detect Residual Core in Investment Cast Turbine Airfoils, Practical Applications of Neutron Radiography and Gaging, ASTM STP 586, American Society for Testing and Materials (1976), pp. 152-157.

13. J. John, Californium-Based Neutron Radiography for Corrosion Detection in Aircraft, Practical Applications of Neutron Radiography and Gaging, ASTM STP 586, American Society for Testing and Materials (1976), pp. 168-180.

14. P. E. Underhill and R. L. Newacheck, Miscellaneous Applications of Neutron Radiography, Practical Applications of Neutron Radiography and Gaging, ASTM STP 586, American Society for Testing and Materials (1976), pp. 252-267.

15. R. W. Parish and D. W. J. Cason, High definition radiography of cast turbine blades as a method of detecting and evaluating the incidence of microporosity, NDT International 10, 181-185 (1977).

16. F. Zamet and G. Thomer, Flash Radiography, Elsevier Scientific Publishing Co., Amsterdam, American Elsevier Publishing Co., New York (1976).

17. Proceedings of the Flash Radiography Symposium, L. E. Bryant, Jr. (Editor), The American Society for Nondestructive Testing, Columbus, Ohio (1977).

18. J. R. Alburger, Instruments and Test Methods as Employed in an Improved Inspection Penetrant Material Specification, Proc. Ninth Symposium on NDE, San Antonio, Texas (1973), pp. 149-180.

19. G. H. Smith and R. C. McMaster, Current Aerospace Applications Using MRA Eddy Current Test Systems, Materials Eval. 25, 283-288 (1967).

20. C. V. Dodd, W. E. Deeds, and W. G. Spoeri, Optimizing Defect Detection in Eddy Current Testing, Materials Eval. 29, 59-63 (1971).

21. C. R. Reeves, A Mechanized Eddy Current Scanning System for Aircraft Struts, Materials Eval. 31, 48-52 (1973).

22. D. J. Lang, Inspection of Aircraft Surfaces Using Two Single-Coil Eddy Current Techniques, Materials Eval. 32, 87-92 (1974).

23. V. G. Truluck, Non-Destructive Testing in the R. A. F. Today, Brit. J. NDT 16, 150-154 (1974).

24. D. M. Forney, Jr., NDI in the United States Air Force, Brit. J. NDT 18, 72-81 (1976).

25. T. P. Smith and H. G. Beech, The Application and Use of Eddy-Currents in Non-Destructive Testing, Brit. J. NDT 18, 137-143 (1976).

26. F. Förster, Limits of Nondestructive Indication of Small and Smallest Flaws on and under the Surface of Workpieces by Electromagnetic and Magnetic Techniques, Paper 1B1, Proceedings of Eighth World Conference on Nondestructive Testing, Cannes, France (1976).

27. L. V. Kiplinger, New Concepts in Eddy Current Inspection of Turbine Engine Parts, Presented at 1976 ASNT Fall Conference, Houston, Texas (1976).

28. R. Truell and A. Hikata, Fatigue in 2S Aluminum as Observed by Ultrasonic Attenuation Methods, Watertown Arsenal Technical Report No. WAL 143/14-47 (1956).

29. R. Truell and A. Hikata, Fatigue and Ultrasonic Attenuation, American Society for Testing and Materials, Special Technical Publication No. 213 (1957).

30. R. Truell, B. Chick, A. Picker and G. Anderson, The Use of Ultrasonic Methods to Determine Fatigue Effects in Metals, WADC Technical Report 59-389 (1959).

31. R. Truell, B. Chick, G. Anderson, C. Elbaum and W. Findley, Ultrasonic Methods for the Study of Stress Cycling Effects in Metals, WADD Technical Report 60-920 (1961).

32. B. Chick, A. Hikata, G. Anderson, W. Findley, C. Elbaum and R. Truell, Ultrasonic Methods in the Study of Fatigue and Deformation in Single Crystals, WPAFB Report No. ASD-TDR-62-186 Pt. II, AD No. 408704 (1963).

33. W. J. Bratina and D. Mills, Study of Fatigue in Metals Using Ultrasonic Technique, Can. Metall. Q. 1, 83-97 (1962).

34. P. V. Ponomarev, Ultrasonic Control of Fatigue Damage to Materials, Zavodskaya Laboratoriya 28, 1345-1346 (1962), English Translation in Ind. Lab. 28, 1429-1431 (1963).

35. Z. Pawlowski, Internal Friction of Metals and the Problem of Damage Cumulation with Static and Variable Loadings, Proc. of Vibration Problems (Warsaw) 4, 43-64 (1963).

36. Z. Pawlowski, Ultrasonic Attenuation During Cyclic Straining, Proc. Fourth International Conference on Nondestructive Testing (1963), Butterworths, London (1964), pp. 192-195.

37. T. Herlescu, A. Bernath and V. Safta, Contribution A L'Etude Du Phenomene De Fatigue Par Le Mesurage De La Variation Des Constantes Physico-Mecaniques, Rev. Roum. Sci. Tech. Serie Metall. 12, 269-284 (1967).

38. C. K. Cole and M. H. Zoiss, Ultrasonics - A Nondestructive Technique for Predicting the Residual Life of Compressively Fatigued Filament Wound Composites, Proc. 15th National Symposium of the Society of Aerospace Material and Process Engineers, Los Angeles, California (May 1969) pp. 923-942.

39. J. F. Moore, S. Tsang and G. Martin, The Early Detection of Fatigue Damage, Technical Report AFML-TR-71-185, AD 730 348 (1971).

40. R. E. Green, Jr., and R. B. Pond, Sr., An Ultrasonic Technique for Detection of the Onset of Fatigue Damage, Air Force Office of Scientific Research, Scientific Report AFOSR-TR-72-1199 (1972).

41. R. E. Green, Jr., Development of an Ultrasonic Attenuation In-Service Inspection Technique for Heavy-Walled Nuclear Reactor Pressure Vessels, Final Technical Report, Middle Atlantic Power Research Committee (1972).

42. N. R. Joshi and R. E. Green, Jr., Ultrasonic Detection of Fatigue Damage, Engr. Fract. Mech. 4, 577-583 (1972).

43. R. E. Green, Jr., and R. B. Pond, Sr., An Ultrasonic Technique for Detection of the Onset of Fatigue Damage, Air Force Office of Scientific Research, Scientific Report AFOSR-TR-73-0901 (1973).

44. R. E. Green, Jr., Ultrasonic Attenuation Detection of Fatigue Damage, Proc. Ultrasonics International 1973 Conference, London, England (March 1973), IPC Science and Technology Press Ltd., Guildford, England (1973), pp. 187-193.

45. N. R. Joshi and R. E. Green, Jr., Ultrasonic Attenuation Monitoring of Fatigue Damage in Nuclear Pressure Vessel Steel at High Temperature, Materials Evaluation 33, 25-29, 36 (1975).

46. W. V. Panowicz, Ultrasonic Detection of Fatigue Damage in Aluminum Specimens Containing Induced Latent Defects, Master's Thesis, Dept. of Mechanics and Materials Science, The Johns Hopkins University, Baltimore, Maryland (1975).

47. R. E. Green, Jr., and R. B. Pond, Sr., An Ultrasonic Technique for Detection of the Onset of Fatigue Damage, Air Force Office of Scientific Research, Final Report AFOSR-TR-76-0811 (1976).

48. R. E. Green, Jr., and R. B. Pond, Sr., Ultrasonic Detection of Fatigue Damage in Aircraft Components, Air Force Office of Scientific Research, Scientific Report AFOSR-TR-77-0658 (1977).

49. R. B. Mignogna, J. C. Duke, Jr., and R. E. Green, Jr., Early Detection of Fatigue Cracks in Aircraft Aluminum Alloy Sheets, Paper presented at National Fall Conference of ASNT, Detroit, Michigan (October 1977), submitted for publication in Materials Evaluation.

50. J. C. Duke, Jr., and R. E. Green, Jr., Simultaneous Monitoring of Acoustic Emission and Ultrasonic Attenuation During Fatigue of 7075 Aluminum, Paper presented at National Spring Conference of ASNT, New Orleans, Louisiana (April 1977), submitted for publication in Materials Evaluation.

51. J. C. Duke, Jr., and R. E. Green, Jr., Capability of Determining Fatigue Mechanisms in 7075 Aluminum by Combining Ultrasonic Attenuation and Acoustic Emission Monitoring, Paper presented and to be published in Proc. of ARPA/AFML Review of Progress in Quantitative NDE Meeting, La Jolla, CA (July 1978).

52. R. E. Green, Jr., and J. C. Duke, Jr., Ultrasonic and Acoustic Emission Detection of Fatigue Damage," to be published in Volume VI International Advances in Nondestructive Testing, W. J. McGonnagle (Editor) Gordon and Breach, New York (1979).

53. C. N. Owston, Carbon Fibre Reinforced Polymers and Non-Destructive Testing, British J. of NDT 15, 2-11 (1973).

54. Y. Tsuchida and K. Okada, Detection of Fatigue Failure Using Ultrasonic Surface Waves, Bulletin Faculty of Engineering Tokushima University, 12, 31-42 (1975).

55. J. Pouliquen and A. DeFebvre, Use of Surface Acoustic Waves for the Detection of Modifications Produced by Deformation Fatigue or Corrosion on Metallic Surfaces, Proc. Ultrasonics International 1975 Conference, London, England (March 1975), pp. 102-106.

56. D. E. MacDonald, Investigation of the State of Fatigue in Metals Using Ultrasonics, Proc. Ultrasonics International 1977 Conference, Brighton, England (June 1977), IPC Science and Technology Press Ltd., Guildford, England (1977), pp. 346-363.

57. P. J. Brosens, N. A. G. Hakima, and G. R. Khabbaz, Detection of Fatigue Damage with Rayleigh Waves, M.I.T. Aeronautical Research Lab. Tech. Rept. 60-307 (1960).

58. J. G. Rasmussen, Prediction of Fatigue Failure Using Ultrasonic Surface Waves, Nondestructive Testing 20, 103-110 (1962).

59. F. N. Kusenberger, B. E. Leonard, J. R. Barton, and W. L. Donaldson, Nondestructive Evaluation of Metal Fatigue, AFOSR-TR-65-0981 (1965).

60. F. N. Kusenberger, J. R. Barton, and W. L. Donaldson, Nondestructive Evaluation of Metal Fatigue, AFOSR-TR-67-1288 (1967).

61. F. N. Kusenberger, P. H. Francis, B. E. Leonard, and J. R. Barton, Nondestructive Evaluation of Metal Fatigue, AFOSR-TR-69-1429 (1969).

62. B. I. Vybornov, Ultrasonic Method for the Early Detection of Failure of the Material in Fatigue Tests, Industrial Laboratory 35, 838-841 (1969).

63. B. E. Leonard, Investigation of Ultrasonic Methods for Detecting Service-Induced Cracks in Aluminum Compressor Discs, Proc. Seventh Symposium on Nondestructive Evaluation of Components and Materials in Aerospace, Weapons Systems, and Nuclear Applications, San Antonio, Texas (April 1969), pp. 10-19.

64. E. B. Norris, S. A. Viaclovsky, and A. R. Whiting, An Ultrasonic Detection System for Determining Crack Initiation and Rate of Crack Propagation in Low Cycle Fatigue Testing, Proc. Seventh Symposium on Nondestructive Evaluation of Components and Materials in Aerospace, Weapons Systems, and Nuclear Applications, San Antonio, Texas (April 1969), pp. 32-36.

65. F. N. Kusenberger, L. Lankford, Jr., P. H. Francis, and J. R. Barton, Nondestructive Evaluation of Metal Fatigue, AFOSR-TR-70-1206 (1970).

66. F. N. Kusenberger, L. Lankford, Jr., P. H. Francis, and J. R. Barton, Nondestructive Evaluation of Metal Fatigue, AFOSR-TR-71-1965 (1971).

67. J. R. Barton, F. N. Kusenberger, P. H. Francis, W. L. Ko, and J. Lankford, Jr., Nondestructive Evaluation of Metal Fatigue, AFOSR-TR-74-0820 (1973).

68. H. G. Bunce, NDT in the Aerospace Industry, The State of the Art: Ultrasonics, Brit. J. NDT 15, 55-57 (1973).

69. W. D. Rummel, P. H. Todd, Jr., R. A. Rathke, and W. L. Castner, The Detection of Fatigue Cracks by Nondestructive Test Methods, Materials Evaluation 32, 205-212 (1974).

70. C. L. Ho, H. L. Marcus, and O. Buck, Ultrasonic Surface-Wave Detection Techniques in Fracture Mechanics, Experimental Mechanics 14, 42-48 (1974).

71. W. W. Lake, J. Thorp, J. R. Barton, and W. D. Perry, Development of Stress Enhanced Ultrasonic Compressor Blade Inspection Equipment, Proc. Tenth Symposium on NDE, San Antonio, Texas (April 1975), pp. 181-193.

72. M. G. Silk, Accurate Crack Depth Measurements in Welded Assemblies, Paper 2B16, Proceedings of Eighth World Conference on Nondestructive Testing, Cannes, France (1976).

73. H. S. Silvus, Jr., Advanced Ultrasonic Testing Systems, A State-of-the-Art Survey, NTIAC-77-1 (1976).

74. F. N. Kusenberger, G. A. Matzkanin, J. R. Barton, P. H. Francis, J. Lankford, and C. M. Teller, Nondestructive Evaluation of Metal Fatigue, AFOSR-TR-1313 (1977).

75. M. G. Silk, Sizing Crack-like Defects by Ultrasonic Means, Chapter 2, Vol. 3, Research Techniques in Nondestructive Testing, R. S. Sharpe (Editor) Academic Press, New York (1977), pp. 51-99.

76. B. R. Tittmann, F. Cohen-Tenoudji, M. deBilly, A. Jungman, and G. Quentin, A Simple Approach to Estimate the Size of Small Surface Cracks with the Use of Acoustic Surface Waves, Appl. Phys. Lett. 33, 6-8 (1978).

77. R. B. Socky, The Use of Ultrasonics in Fatigue Testing, Materials Evaluation 22, 509-515 (1964).

78. Y. A. Rublev and S. Y. Danilov, Ultrasonic Detection of Fatigue Cracks During Repeated Static Tests, Industrial Laboratory 29, 1306-1309 (1964).

79. P. Reti, J. Kalman, and G. Barna, Ultrasonic Detection of Initial Material Fatigue Cracks under Operating Condition, Gep (Hungarian) No. 1, 11-16 (1964). Wright-Patterson AFB Translation AD 460317 (1965).

80. S. J. Klima, D. J. Lesco, and J. C. Freche, Ultrasonic Technique for Detection and Measurement of Fatigue Cracks, NASA Technical Note D-3007 (1965).

81. S. J. Klima, D. J. Lesco, and J. C. Freche, Application of Ultrasonics to Detection of Fatigue Cracks, Experimental Mechanics 6, 154-161 (1966).

82. C. E. Lautzenheiser, A. R. Whiting, and R. E. Wylie, Crack Evaluation and Growth During Low-Cycle Plastic Fatigue-Nondestructive Techniques for Detection, Materials Evaluation 24, 241-248 (1966).

83. W. G. Clark, Jr., and L. J. Ceschini, An Ultrasonic Crack Growth Monitor, Materials Evaluation 27, 180-184 (1969).

84. S. J. Klima and J. C. Freche, Ultrasonic Detection and Measurement of Fatigue Cracks in Notched Specimens, Experimental Mechanics 9, 193-202 (1969).

85. D. M. Corbly, P. F. Packman, and H. S. Pearson, Accuracy and Precision of Ultrasonic Shear Wave Flaw Measurements as a Function of Stress on the Flaw, Materials Evaluation 30, 103-110 (1970).

86. F. Jeglic, P. Niessen, and D. J. Burns, Ultrasonic Detection of High-temperature Fatigue-crack Growth, Experimental Mechanics 11, 82-85 (1971).

87. J. R. Barton, J. R. Birchak, J. D. King, J. A. Birdwell, F. N. Kusenberger, A. Leone, and C. H. McGogney, A new System for Inspecting Steel Bridges for Fatigue Cracks, Proc. Ninth Symposium on NDE, San Antonio, Texas (April 1973), pp. 132-148.

88. F. H. S. Chang, J. C. Couchman, and B. G. W. Yee, The Effects of Stress on the Detection of Fatigue Cracks by Ultrasonic Techniques, Proc. Ninth Symposium on NDE, San Antonio, Texas (April 1973), pp. 424-433.

89. D. E. Pettit and D. W. Hoeppner, The Influence of Nondestructive Inspection Parameters on the Preproof and Postproof Fatigue Crack Detection Limits for Fracture Mechanics Applications, Proc. Ninth Symposium on NDE, San Antonio, Texas (April 1973), pp. 434-441.

90. F. E. Sugg and C. C. Kammerer, On-Board Ultrasonic Structural Surveillance, Materials Eval. 32, 157-162 (1974).

91. B. G. W. Yee, J. C. Couchman, J. W. Hagemeyer, and F. H. Chang, Stress and the Ultrasonic Detection of Fatigue Cracks in Engineering Metals, Nondestructive Testing 7, 245-250 (1974).

92. B. G. W. Yee and J. W. Hagemeyer, The Effects of Relaxation and Closure Stresses on the Detection of Fatigue Cracks in 2219-T87 Aluminum, Proc. Tenth Symposium on NDE, San Antonio, Texas (April 1975), pp. 247-256.

93. P. F. Packman, R. M. Stockton, and J. M. Larsen, Characterization and Measurement of Defects in the Vicinity of Fastener Holes by Nondestructive Inspection, AFOSR-TR-76-0400 (1975).

94. Ultrasonic Testing for Aircraft, Department of Transportation, Federal Aviation Administration, AC-43-7 (1975).

95. D. Hagemaier, Ultrasonic Maintenance Inspection of Aircraft Structures, Materials Eval. 34, 9-19 (1976).

96. R. Shankar, A. N. Mucciardi, D. Cleveland, W. E. Lawrie, and H. L. Reeves, Adaptive Nonlinear Signal Processing for Characterization of Ultrasonic NDE Waveforms Task 2: Measurement of Subsurface Fatigue Crack Size, AFML-TR-76-44 (1976).

97. J. R. Birchak and C. G. Gardner, Comparative Ultrasonic Response of Machined Slots and Fatigue Cracks in 7075 Aluminum, Materials Evaluation 34, 275-280 (1976).

98. J. Couchman, J. Bell, and P. Noronha, Computerized Signal Processing for Detecting Cracks under Installed Fasteners, Ultrasonics 14, 256-262 (1976).

99. B. H. Lidington, M. G. Silk, P. Montgomery, and G. Hammond, Ultrasonic Measurements of the Depth of Fatigue Cracks, British J. of NDT 18, 165-170 (1976).

100. D. M. Forney, Jr., NDI in the United States Air Force, Brit. J. NDT 18, 72-81 (1976).

101. P. A. Doyle and C. M. Scala, Crack Depth Measurement by Ultrasonics: A Review, Ultrasonics 16, 164-170 (1978).

102. (a) Interdisciplinary Program for Quantitative Flaw Definition, Special Report First Year Effort (1975)

(b) Interdisciplinary Program for Quantitative Flaw Definition, Third Quarterly Report, SC595.8QITR (1975).

(c) Proceedings of the ARPA/AFML Review of Quantitative NDE, AFML-TR-75-212 (1976)

(d) Interdisciplinary Program for Quantitative Flaw Definition, Semi-Annual Report, SC595.14SA (1976)

(e) Proceedings of the ARPA/AFML Review of Progress in Quantitative NDE, AFML-TR-77-44 (1977).

(f) Interdisciplinary Program for Quantitative Flaw Definition, Semi-Annual Report, SC595.21 SA (1977).

(g) Interdisciplinary Program for Quantitative Flaw Definition, Semi-Annual Report, SC 595.32 SA (1978).

(h) Proceedings of the ARPA/AFML Review of Progress in Quantitative NDE, AFML-TR-78-55 (1978).

D. O. Thompson, Program Manager, Center for Advanced NDE, Science Center, Rockwell International, Thousand Oaks, California.

103. J. Kaiser, Untersuchungen uber das auftreten Geraushen beim Zugversuch. Ph.D. Thesis, Technische Hochschule, Munich (1950), Arkiv fur das Eisenhuttenwesen, AREIA 24 (Jan. - Feb. 1953), pp. 43-45.

104. H. L. Dunegan, C. A. Tatro, and D. O. Harris, Acoustic Emission Research. Lawrence Radiation Laboratory, Livermore, California Report UCID-4868, Rev. 1 (1964).

105. Acoustic Emission, R. G. Liptai, D. O. Harris, and C. A. Tatro (editors), American Society for Testing and Materials, Special Technical Publication No. 505 (1972).

106. J. C. Spanner, Acoustic Emission Techniques and Applications, Intex Publishing Co., Evanston, Illinois (1974).

107. Monitoring Structural Integrity by Acoustic Emission, J. C. Spanner and J. W. McElroy (editors), American Society for Testing and Materials, Special Technical Publication No. 571 (1975).

108. Acoustic Emission, R. W. Nichols (editor), Applied Science Publishers Ltd., London (1976).

109. W. W. Gerberich and C. E. Hartbower, Some Observations on Stress Wave Emission as a Measure of Crack Growth, International J. of Fract. Mech. 3, 185-192 (1967).

110. C. E. Hartbower, W. W. Gerberich, and H. Liebowitz, Investigation of Crack-Growth Stress-Wave Relationships, J. of Eng. Fract. Mech. 1, 291-308 (1968).

111. C. E. Hartbower, W. W. Gerberich, and P. P. Crimmins, Monitoring Subcritical Crack Growth by Detection of Elastic Stress Waves, The Welding Journal WEJUA 47, 1-18s (1968).

112. P. H. Hutton, Use of Acoustic Emission to Study Failure Mechanics in Metals, ASME Paper No. 69-Met-8 (1969).

113. P. H. Hutton, Acoustic Emission - A new Tool for Evaluating Structural Soundness, Proc. Seventh Symposium on Nondestructive Evaluation of Components and Materials in Aerospace Weapons Systems and Nuclear Applications, San Antonio, Texas (April 1969), pp. 165-171.

114. P. H. Hutton, Acoustic Emission Applied to Determination of Structural Integrity, Automotive Engineering 79, 33-37 (1971).

115. H. L. Dunegan, D. O. Harris, and A. S. Tetelman, Detection of Fatigue Crack Growth by Acoustic Emission Techniques, Proc. Seventh Symposium on Nondestructive Evaluation of Components and Materials in Aerospace Weapons Systems and Nuclear Applications, San Antonio, Texas (April 1969), pp. 20-31. Materials Evaluation 28, 221-227 (1970).

116. D. O. Harris, H. L. Dunegan, and A. S. Tetelman, Prediction of Fatigue Lifetime by Combined Fracture Mechanics and Acoustic Emission Techniques, Lawrence Radiation Laboratory Report, UCRL 71760, (October 1969).

117. D. O. Harris and H. L. Dunegan, Verification of Structural Integrity of Pressure Vessels by Acoustic Emission and Periodic Proof Testing, Dunegan Research Corporation, Livermore, California, Technical Report DRC-71-2 (May 1971).

118. Y. Nakamura, Acoustic Emission Monitoring System for Detection of Cracks in a Complex Structure, Materials Evaluation 29, 8-12 (1971).

119. F. R. Rollins, Jr., Acoustic Emission from Boron-Aluminum Composites During Tensile Fracture and Fatigue, Midwest Research Institute, Kansas City, Missouri, Technical Report No. 6 to Office of Naval Research (1971).

120. C. E. Hartbower, C. F. Morais, W. G. Reuter, et al., Development of a Non-destructive Testing Technique to Determine Flaw Criticality, AFML-TR-71-218 (1972).

121. C. E. Hartbower, C. F. Morais, W. G. Reuter, and P. P. Crimmins, Acoustic Emission from Low-Cycle High-Stress-Intensity Fatigue, Engr. Fract. Mech. 5, 765-789 (1973).

122. F. N. Kusenberger, J. Lankford, Jr., P. H. Francis, J. R. Barton, Nondestructive Evaluation of Metal Fatigue, AFOSR-TR-72-1167 (1972).

123. H. C. Kim, A. P. R. Neto, and R. W. B. Stephens, Some Observations on Acoustic Emission During Continuous Tensile Cycling of a Carbon Fibre/Epoxy Composite, Nature Phys. Sci. 237, 78-80 (1972).

124. D. M. Egle, J. R. Mitchell, K. H. Bergey, and F. J. Appl, Acoustic Emission for Monitoring Fatigue Crack Growth, Instrument Soc. Amer. Trans. 12, 368-374 (1973).

125. D. M. Egle, Detecting High Cycle Fatigue Crack Growth Using Acoustic Emission, Presented at the Fracture and Flaws Symposium, Albuquerque, New Mexico, (March 1973).

126. J. R. Mitchell, D. M. Egle, and F. J. Appl, Detecting Fatigue Cracks with Acoustic Emission, Proc. Okla. Acad. Sci. 53, 121-126 (1973).

127. D. O. Harris and H. L. Dunegan, Continuous Monitoring of Fatigue Crack Growth by Acoustic Emission Techniques, Dunegan-Endevco Technical Report DE-73-2 (Feb. 1973), Exp. Mech. 14, 71-81 (1974).

128. T. M. Morton, R. M. Harrington, and J. G. Bjeletich, Acoustic Emissions of Fatigue Crack Growth, Engr. Fract. Mech. 5, 691-697 (1973).

129. C. D. Bailey and W. M. Pless, Acoustic Emissions Used to Nondestructively Determine Crack Locations in Aircraft Structural Fatigue Specimen, Proc. Ninth Symposium on NDE, San Antonio, Texas (April 1973), 224-232.

130. A. Vary and S. J. Klima, A Potential Means of Using Acoustic Emission for Crack Detection under Cyclic-Load Conditions, Proc. Ninth Symposium on NDE, San Antonio, Texas (April 1973), pp. 258-266.

131. S. Smith and T. M. Morton, Acoustic-Emission Detection Techniques for High-Cycle-Fatigue Testing, Exp. Mech. 13, 193-198 (1973).

132. R. R. Corle and J. A. Schliessmann, Flaw Detection and Characterization Using Acoustic Emission, Materials Eval. 31, 115-120 (1973).

133. T. M. Morton, S. Smith, and R. M. Harrington, Effect of Loading Variables on the Acoustic Emissions of Fatigue-crack Growth, Exp. Mech 14, 208-213 (1974).

134. L. E. Willertz and D. O. Hunter, An Acoustical Emission-Damping Fatigue Study of a 17-4 PH Steel, J. of Testing and Evaluation 2, 190-195 (1974).

135. R. S. Williams and K. L. Reifsnider, Investigation of Acoustic Emission During Fatigue Loading of Composite Specimens, J. Composite Materials 8, 340-355 (1974).

136. S. J. Acquaviva and R. Chait, Monitoring Fatigue Failure of a High Strength Titanium Alloy by Acoustic Emission Techniques, Proc. Tenth Symposium on NDE, San Antonio, Texas (April 1975), pp. 1-7.

137. W. M. Pless and C. D. Bailey, Detection of Large Crack Extensions in Aircraft Wing Structure by Acoustic Peak Detectors, Proc. Tenth Symposium on NDE, San Antonio, Texas (April 1975), pp. 30-43.

138. P. Mehdizadeh, Assessment of Corrosion Fatigue Damage by Acoustic Emission and Periodic Proof Tests, Proc. Tenth Symposium on NDE, San Antonio, Texas (April 1975), pp. 286-302, Materials Evaluation 34, 55-63 (1976).

139. A. M. Lazarev, I. V. Gulevskii, and L. Y. Odnopozov, Use of Standard Equipment for Fatigue Testing by the Acoustic-Emission Method, Soviet J. of NDT 11, 383-385 (1975).

140. H. Hatano, Acoustic Emission During High Cycle Fatigue Testing, J. Soc. of Materials Science Japan 24, 48-53 (1975).

141. H. L. Dunegan, Using Acoustic Emission Technology to Predict Structural Failure, Metals Engineering Quarterly, February 1975, pp. 8-16.

142. M. Fuwa, B. Harris, and A. R. Bunsell, Acoustic Emission During Cyclic Loading of Carbon-Fibre-Reinforced Plastics, J. Phys. D. : Appl. Phys. 8, 1460-1471 (1975).

143. T. Kishi, Y. Obata, H. Tanaka, Y. Sakakibara, R. Horiuchi, and K. Aoki, Acoustic Emission Peak Under Cyclic Deformation, J. Japanese Inst. of Metals 40, 492-498 (1976).

144. J. M. Carlyle and W. R. Scott, Acoustic-Emission Fatique Analyzer, Exp. Mech. 16, 369-372 (1976).

145. O. A. Shinaishin, M. S. Darlow, and S. J. Acquaviva, Acoustie Emission Detection of Fatigue Crack Initiation and Propagation in Notched and Unnotched Titanium Specimens, Materials Evaluation 34, 137-143 (1976).

146. C. D. Bailey, Acoustic Emission for In-Flight Monitoring on Aircraft Structures, Materials Evaluation 34, 165-171 (1976).

147. C. D. Bailey, J. M. Hamilton, and W. M. Pless, AE Monitoring of Rapid Crack Growth in a Production-Size Wing Fatigue Test Article, NDT International 9, 298-304 (1976).

148. C. D. Bailey and W. M. Pless, Acoustic Emission Structure-Borne Background Noise Measurements on Aircraft During Flight, Materials Evaluation 34, 189-195, 201 (1976).

149. W. M. Pless, C. D. Bailey, and J. M. Hamilton, Acoustic Emission Detection of Fatigue Crack Growth in a Production-Size Aircraft Wing Test Article Under Simulated Flight Loads, Materials Evaluation 36, No. 5, 41-48 (1978).

150. A. C. E. Sinclair and D. C. Connors, Acoustic Emission Analysis During Fatigue Crack Growth in Steel, Materials Science and Engr. 28, 263-273 (1977).

151. C. R. Horak and A. F. Weyhreter, Acoustic Emission System for Monitoring Components and Structures in a Severe Fatigue Noise Environment, Materials Evaluation 35, No. 5, 59-63, 68 (1977).

152. R. S. Williams and K. L. Reifsnider, Real-Time Nondestructive Evaluation of Composite Materials During Fatigue Loading, Materials Evaluation 35, No. 8, 50-54 (1977).

153. J. E. Nuti, T. Erber, and S. A. Guralnick, Magnetic Detection of Crack Initiation and Propagation, Phys. Lett. 57A, 357-358 (1976).

154. K. K. Yermilin, L. K. Zarembo, V. A. Krasil'nikov, Y. D. Mezintsev, V. M. Prokhorov, and K. V. Khilkov, Variation in the Second Harmonic of a Shear Ultrasonic Wave in Metals Under Cyclic Alternating Load, Phys. Met. Metallogr. 36, 174-176 (1973).

155. O. Buck, Harmonic Generation for Measurement of Internal Stresses as Produced by Dislocations, IEEE Transactions SU-23, 346-350 (1976).

156. O. Buck, W. L. Morris, and J. M. Richardson, Acoustic Harmonic Generation at Unbonded Interfaces and Fatigue Cracks, Appl. Phys. Lett. 33, 371-373 (1978).

157. N. K. Batra, J. M. Raney, and R. M. Panos, Detection of Radial Bolt-Hole Cracks Using Sampled CW Ultrasonic Doppler-Shift Techniques, Presented at ARPA/AFML Review of Progress in Quantitative NDE, La Jolla, California (July 1978).

158. O. Buck and G. A. Alers, New Techniques for Detection and Monitoring of Fatigue Damage, Presented at American Society for Metals Seminar on Fatigue and Microstructure, St. Louis, Missouri (October 1978).

159. Proceedings of a Workshop on Nondestructive Evaluation of Residual Stress, Nondestructive Testing Information Analysis Center, Southwest Research Institute, San Antonio, Texas, NTIAC-76-2 (1976).

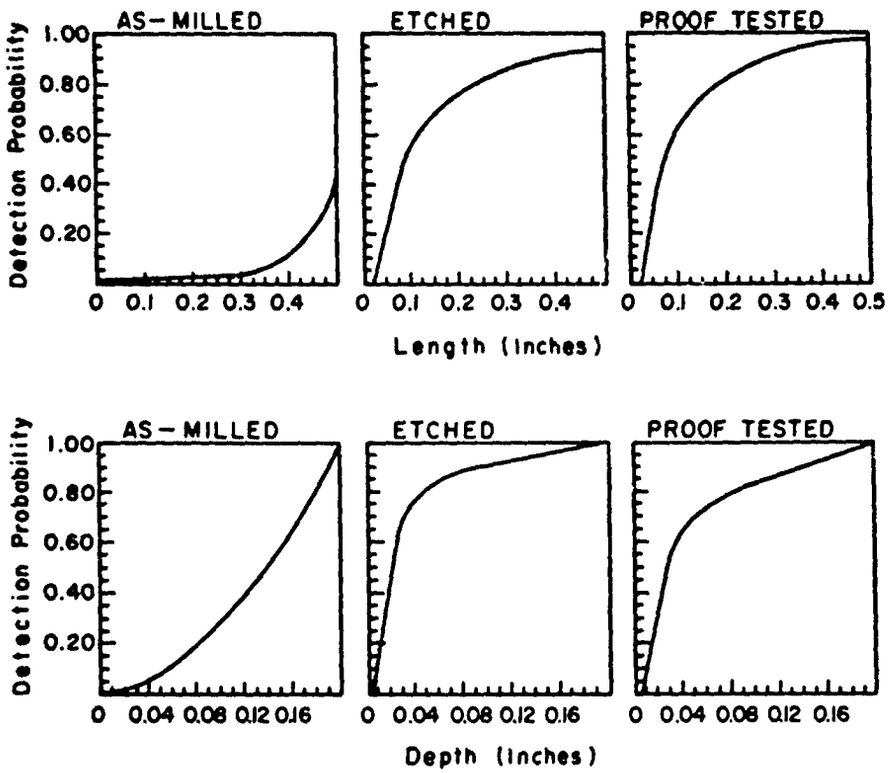

Fig. 1. Crack detection probability of the x-radiographic inspection method [after Rummel et al.(1)].
upper row: as a function of actual crack length
lower row: as a function of actual crack depth

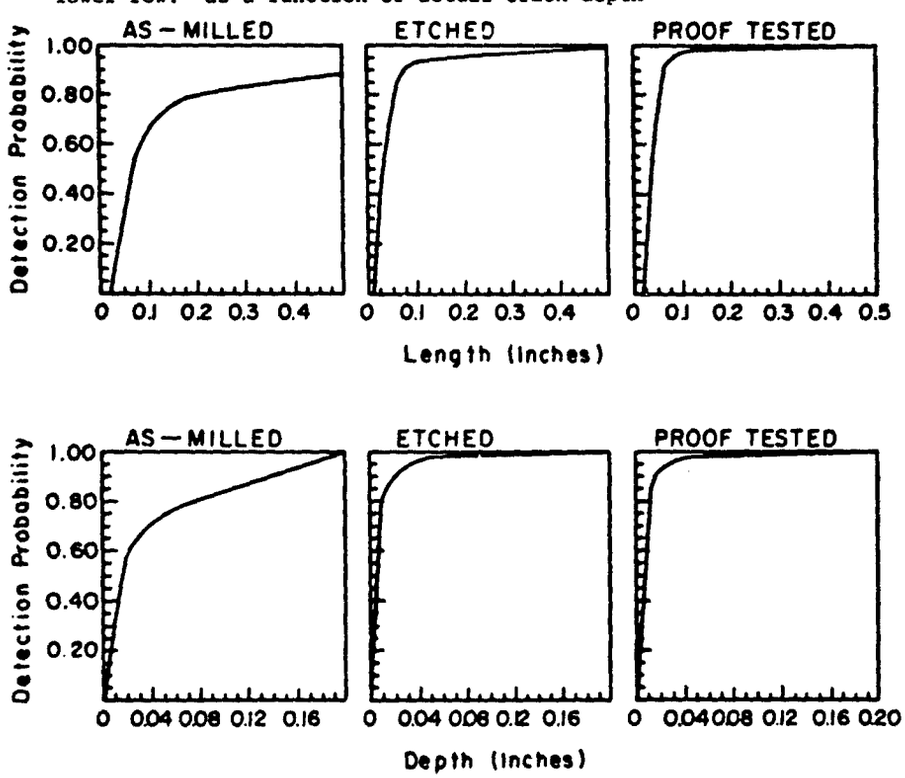

Fig. 2. Crack detection probability of the penetrant inspection method [after Rummel et al.(1)].
upper row: as a function of actual crack length
lower row: as a function of actual crack depth

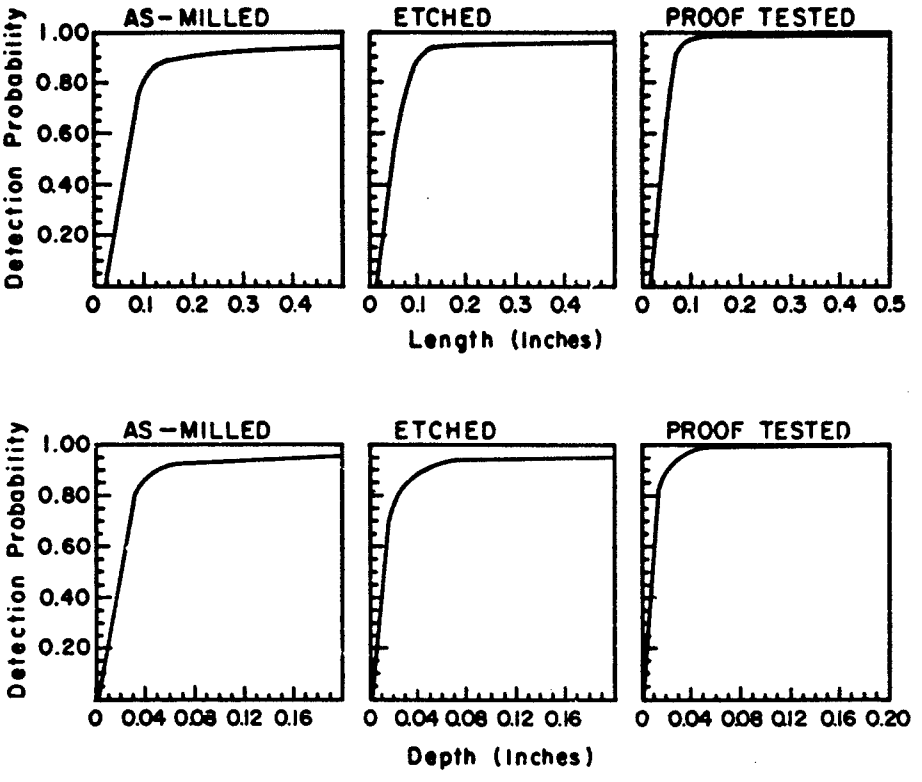

Fig. 3. Crack detection probability of the eddy current inspection method [after Rummel et al.(1)].
upper row: as a function of actual crack length
lower row: as a function of actual crack depth

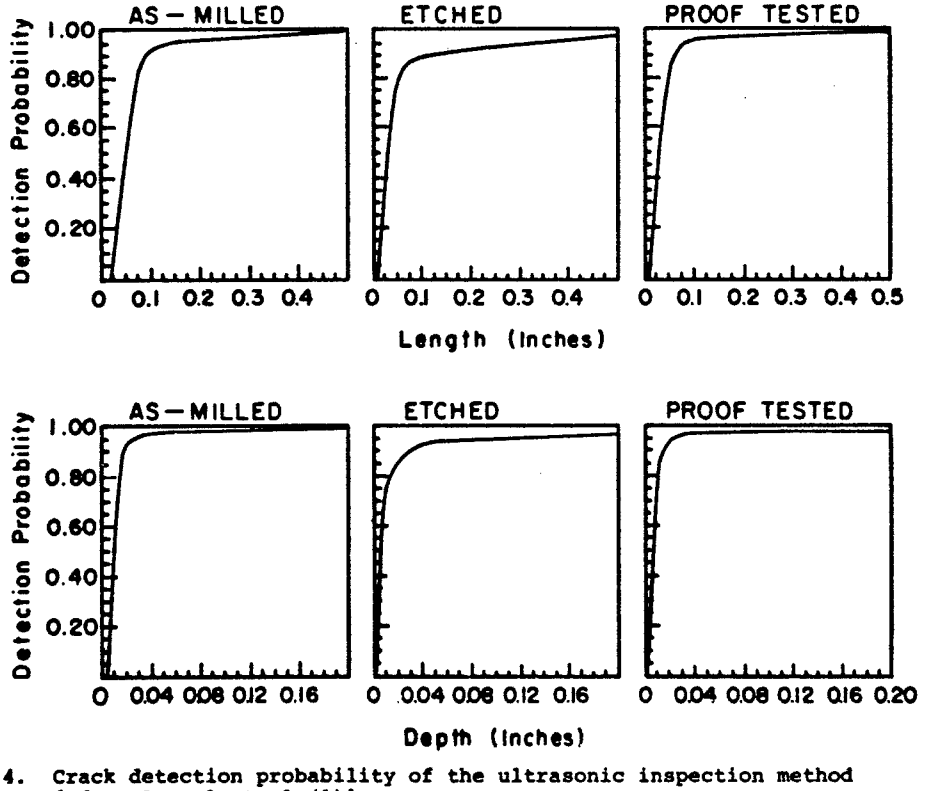

Fig. 4. Crack detection probability of the ultrasonic inspection method [after Rummel et al.(1)].
upper row: as a function of actual crack length
lower row: as a function of actual crack depth

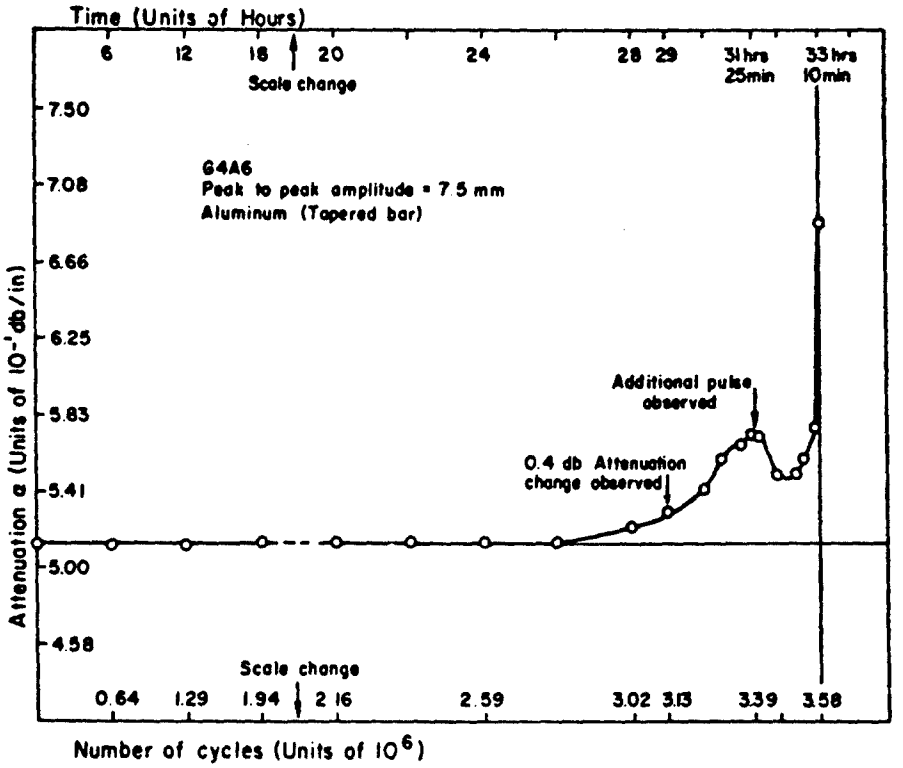

Fig. 5. Typical plot of ultrasonic attenuation versus number of fatigue cycles for aluminum [after Joshi and Green(42)].

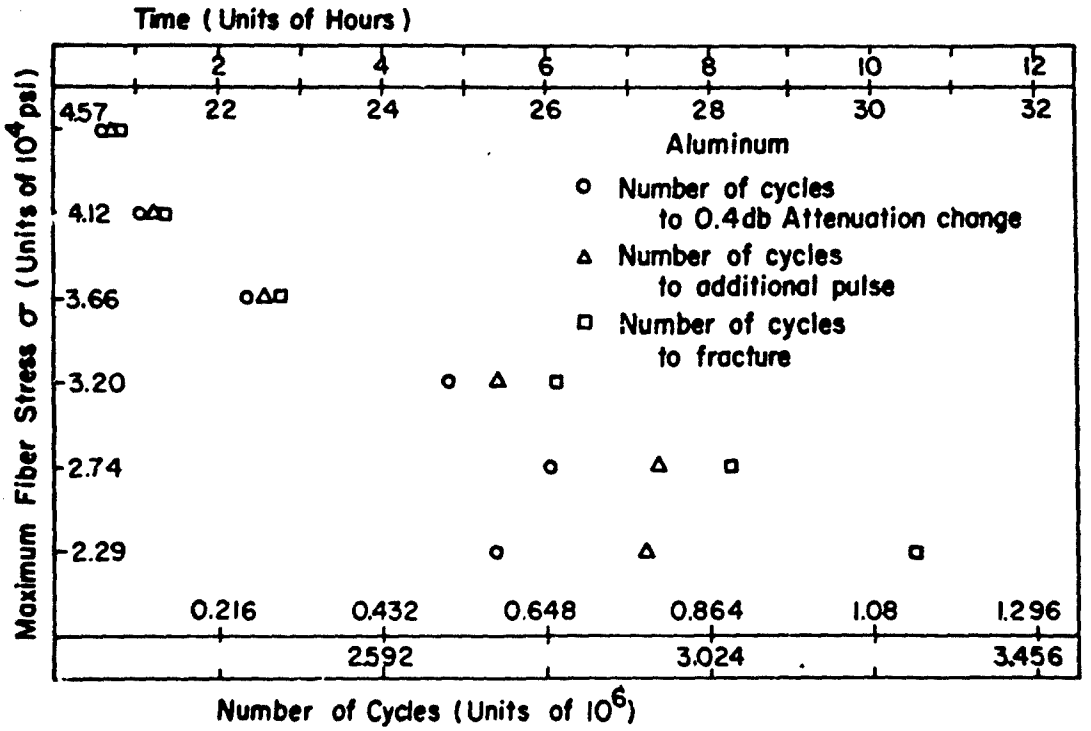

Fig. 6. Summary of experimental results obtained with aluminum specimens [after Joshi and Green(42)].

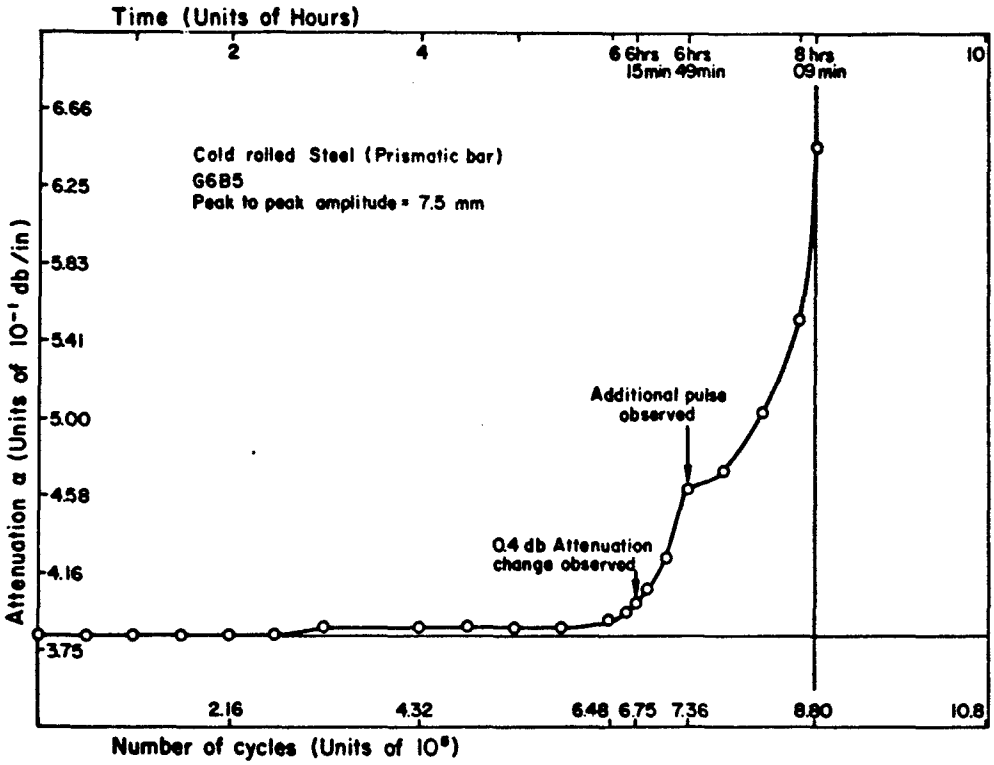

Fig. 7. Typical plot of ultrasonic attenuation versus number of fatigue cycles for steel [after Joshi and Green(42)].

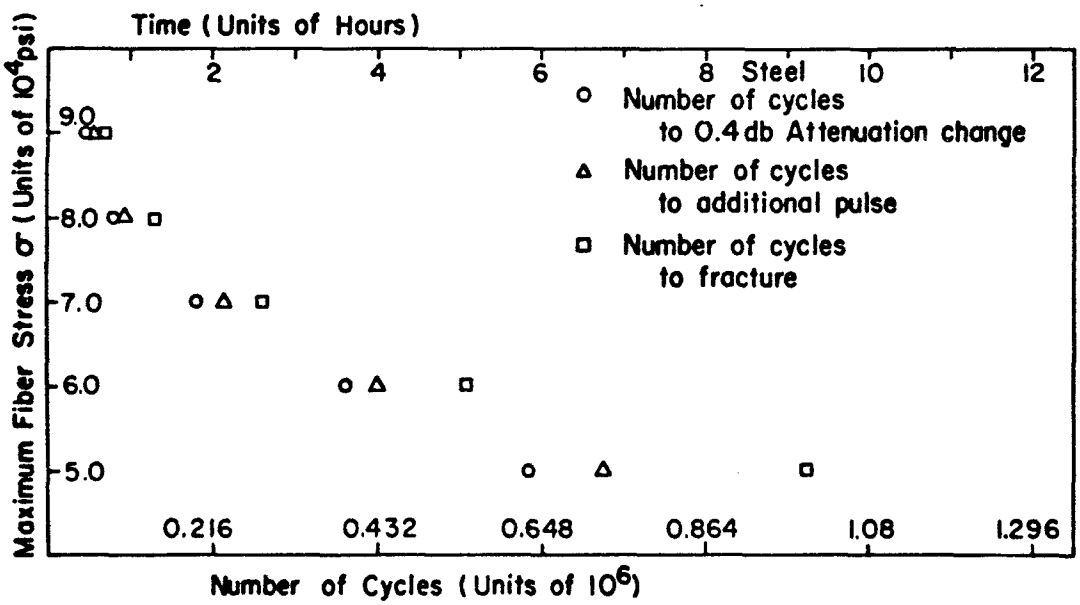

Fig. 8. Summary of experimental results obtained with steel specimens [after Joshi and Green(42)].

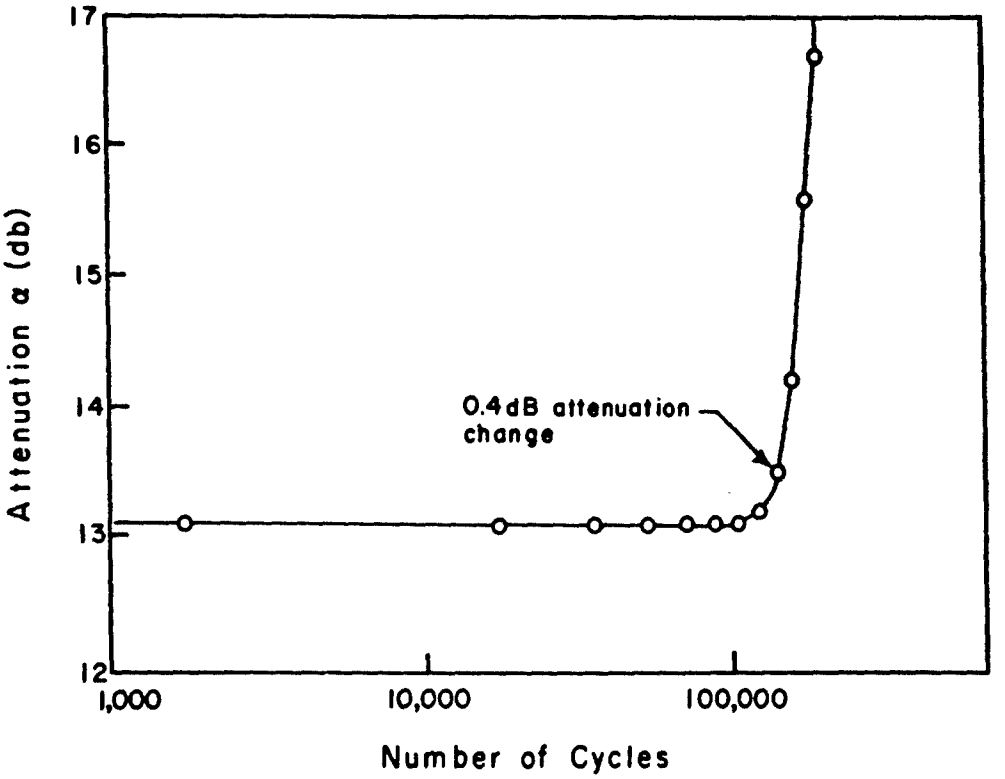

Fig. 9. Ultrasonic attenuation versus number of fatigue cycles for an aluminum specimen containing an induced latent defect [after Panowicz(46)].

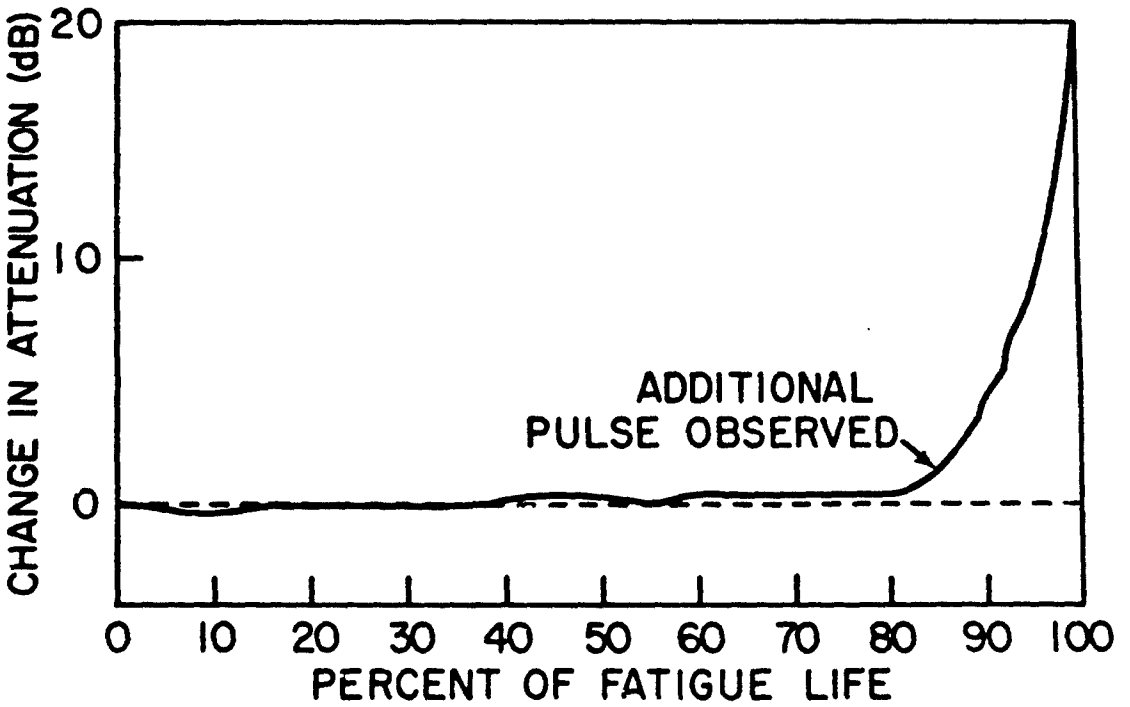

Fig. 10. Typical plot of change in ultrasonic attenuation versus percent of fatigue life for plain aluminum alloy sheet, rolling direction parallel to specimen length [after Mignogna et al.(49)].

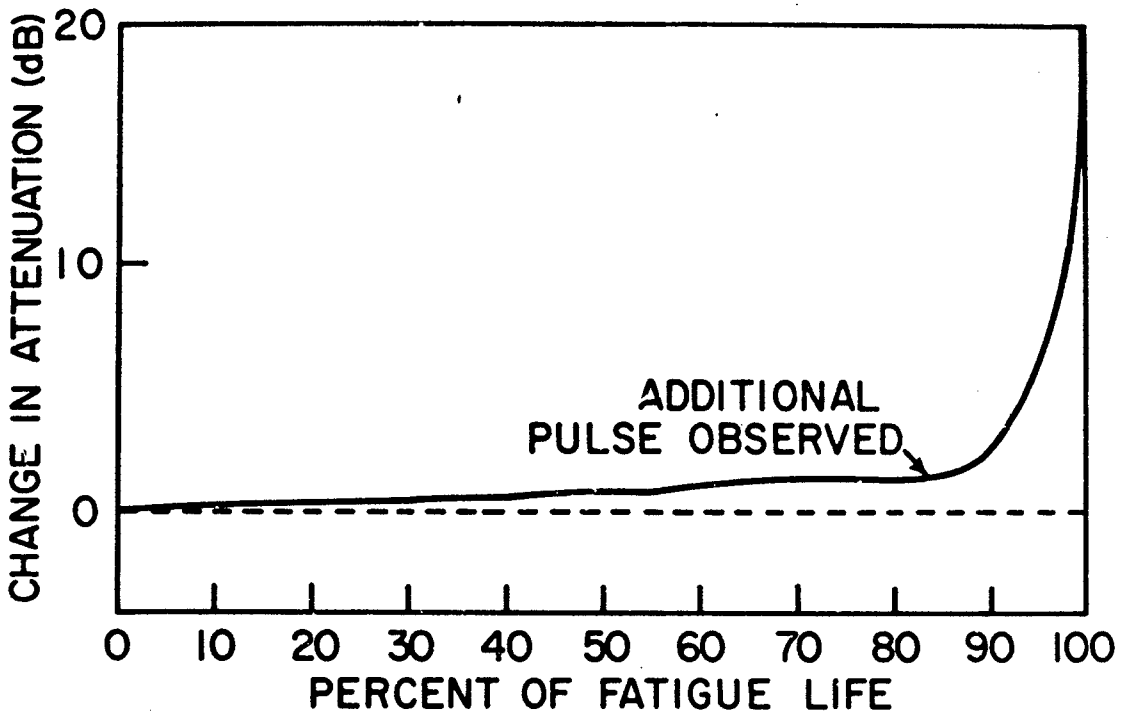

Fig. 11. Typical plot of change in ultrasonic attenuation versus percent of fatigue life for plain aluminum alloy sheet, rolling direction perpendicular to specimen length [after Mignogna et al.(49)].

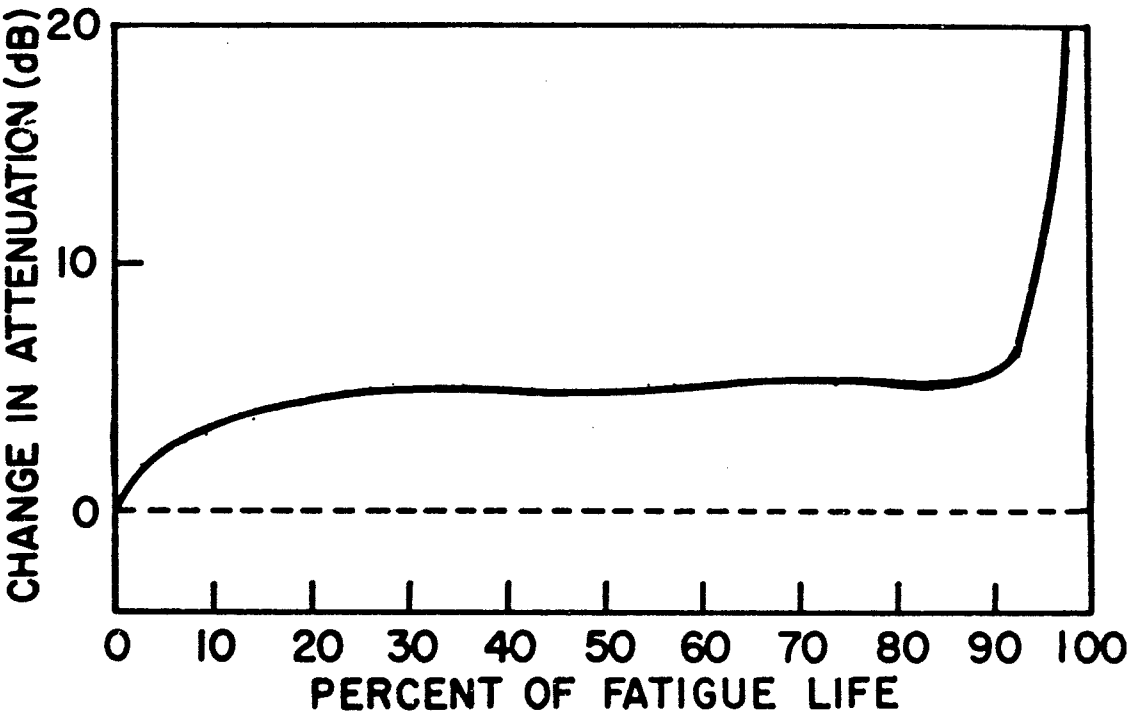

Fig. 12. Typical plot of change in ultrasonic attenuation versus percent of fatigue life for aluminum alloy sheet, rolling direction parallel to specimen length, screws at end [after Mignogna et al.(49)].

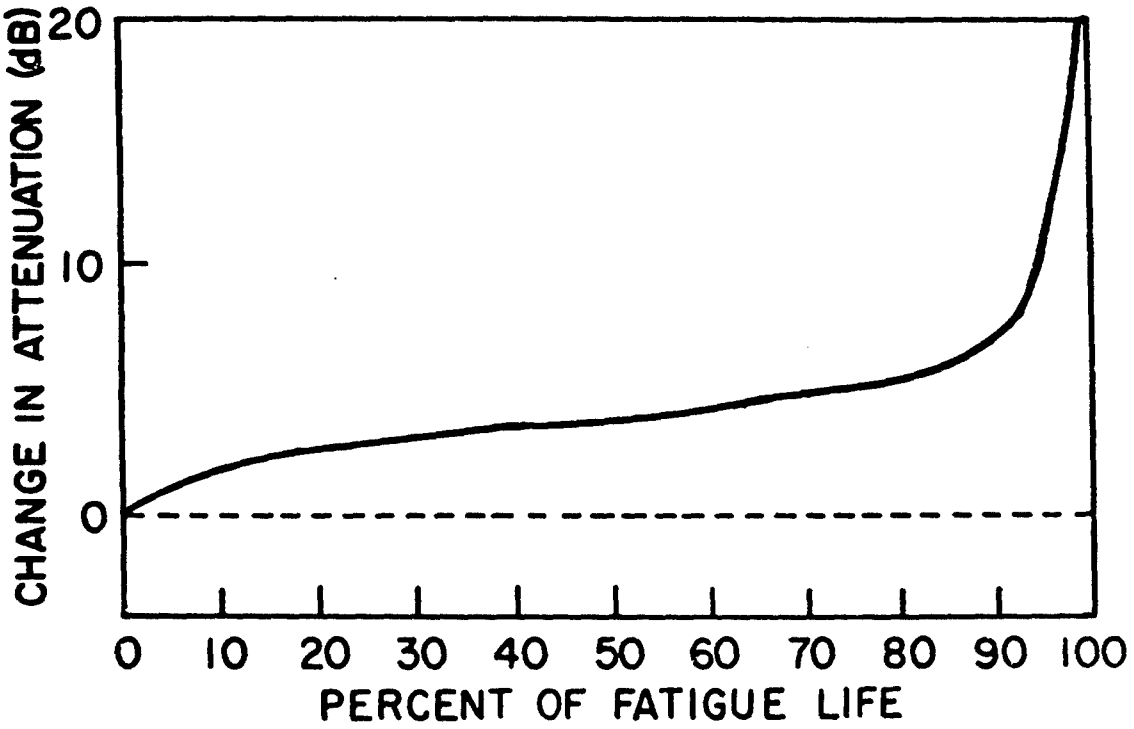

Fig. 13. Typical plot of change in ultrasonic attenuation versus percent of fatigue life for aluminum alloy sheet, rolling direction perpendicular to specimen length, screws at end [after Mignogna et al.(49)].

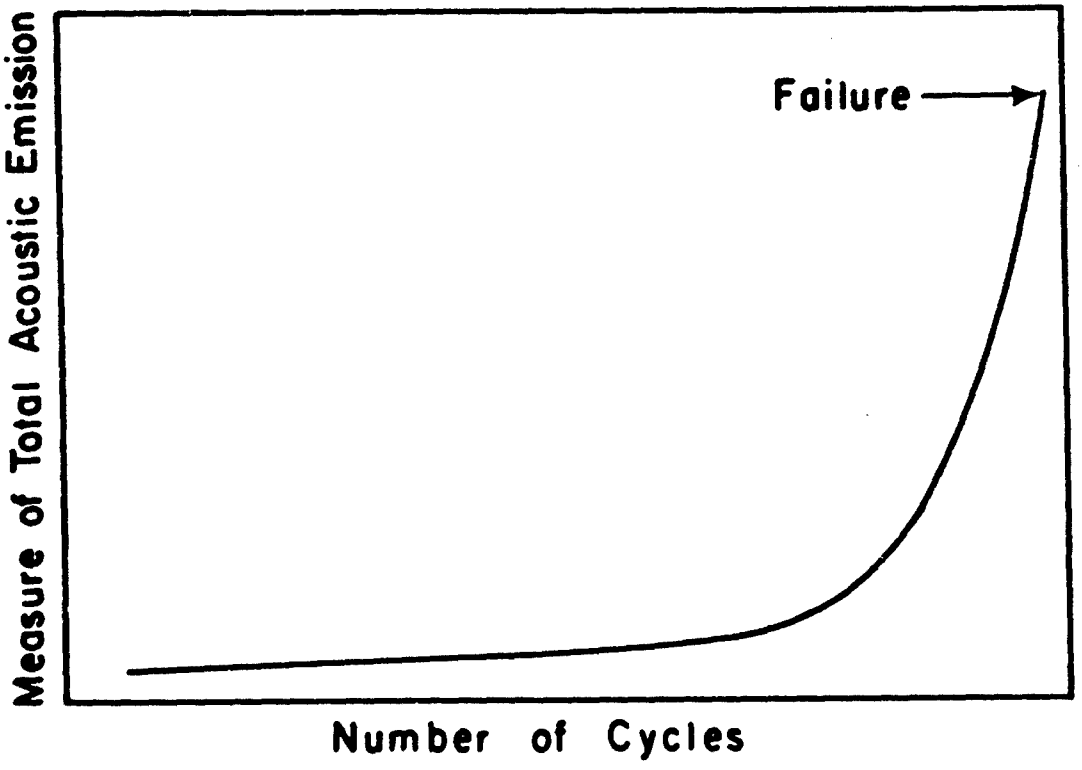

Fig. 14. Schematic plot of acoustic emission versus number of fatigue cycles

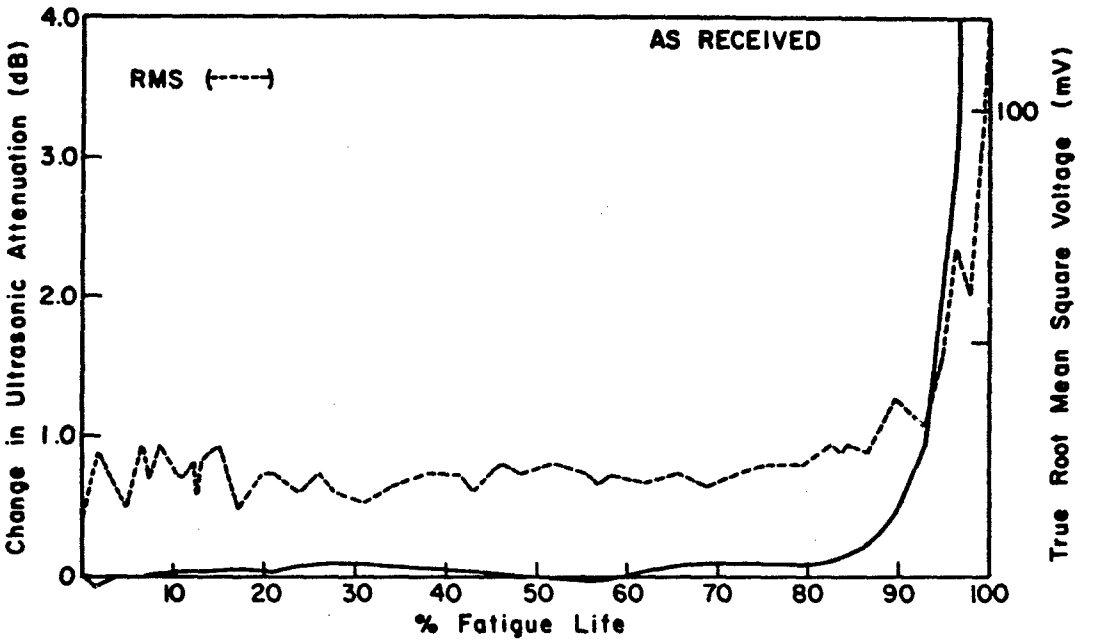

Fig. 15. Typical plot of change in ultrasonic attenuation and true root mean square voltage of acoustic emission versus fatigue life for as-received 7075-T651 aluminum [after Duke and Green(50)].

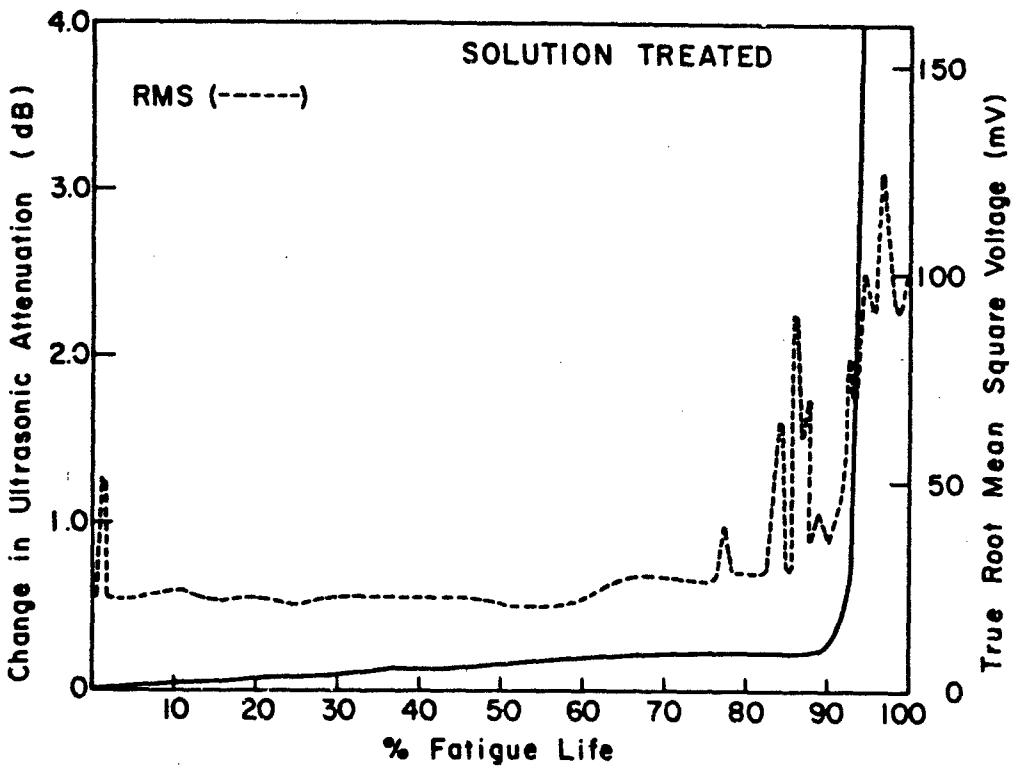

Fig. 16. Typical plot of change in ultrasonic attenuation and true root mean square voltage of acoustic emission versus fatigue life for solution treated 7075 aluminum [after Duke and Green(50)].

CONTROLE IN SITU PAR EMISSION ACOUSTIQUE DE SOUDAGES PAR BOMBARDEMENT ELECTRONIQUE

IN SITU INSPECTION OF ELECTRON BEAM WELD BY ACOUSTIC EMISSION

P.P. DUMOUSSEAU - CENTRE TECHNIQUE DES INDUSTRIES MECANIQUES - (C.E.T.I.M.)
52, Avenue Félix-Louat - 60304 - SENLIS (France)

ABSTRACT

The lecture is mainly devoted to discussion of Acoustic Emission (A.E.) applicability to Non-Destructive Inspection particularly to welding control.

A general presentation of the technique emphasizes instrumentation and signal processing aspects. Interest is devoted to specific methods : localization, spatial and temporal discrimination...

Application of A.E. to welding control is reviewed. Advantages (sensitivity, real time monitoring of crack formation, localization of emissive sites...) but also difficulties (environmental conditions, material influence, interpretation of signals...) are discussed.

Experimental work performed to check feasibility of applying this control to E.B. Welding of Gas Turbine Components is detailed. Emissive behaviour of various materials is considered referring to their crack susceptibility. It concerns annealed steel (grade XC 80), stainless steel (grades Z10 CNT 18 and Z12 CND V12), titanium alloy (TA6V), Inconel 718 (grade NC 19 FeNb). Results of tests conducted on linear and circular welds of specimens and real components are presented and discussed. Finally, the practical problems involved in industrial application are considered.

I/ PRESENTATION GENERALE DE L'EMISSION ACOUSTIQUE

L'émission acoustique (E.A.) consiste en la libération d'énergie mécanique sous forme d'ondes élastiques transitoires. Elle accompagne en particulier toute variation locale rapide de l'état de déformation d'un matériau soumis à contraintes.

Dans la pratique, elle englobe les phénomènes suivants :

- Déformation plastique : mouvement des dislocations, bandes de Lüders, effet Portevin-Le Chatelier ;
- Rupture : initiation et propagation de fissures, fatigue, corrosion, corrosion sous tension ;
- Transformation martensitique ;
- En milieu fluide : ébullition et cavitation.

L'émission acoustique suscite, pour des raisons évidentes, l'intérêt des services industriels de contrôle. Par rapport aux autres méthodes de contrôle non destructif, elle présente cependant certains traits distinctifs :

- Elle est d'une extrême sensibilité puisque la limite inférieure actuelle de détection des capteurs est de l'ordre de 10^{-12} J. On a ainsi constaté l'aptitude à déceler des microcriques de l'ordre de 10^{-3} mm^2. En contrepartie se posent des problèmes délicats de sensibilité à l'ambiance industrielle et de fiabilité ;
- Contrairement aux autres méthodes de CND ce n'est pas une méthode d'imagerie mais une méthode de détection en temps réel des évolutions. La principale difficulté est l'interprétation correcte de l'information perçue. A moyen terme on pense toutefois que l'Emission Acoustique engendrera de nouvelles méthodes d'évaluation de la nocivité des défauts et de prévision de rupture ;
- La propagation des ondes n'impose pas l'interaction directe du capteur avec le défaut. Pour des raisons d'accessibilité, d'état de surface, de température, ce peut être une commodité pour l'opérateur. Cela permet surtout la localisation du site émissif par des méthodes de triangulation ;
- On rencontre une extrême diversité dans les comportements émissifs. L'énergie détectée est notamment influencée par la microstructure et les propriétés mécaniques du matériau, la vitesse de sollicitation, les conditions physiques de l'essai, etc... En simplifiant grossièrement, les structures hétérogènes, les mécanismes de type fragile, les caractéristiques mécaniques élevées sont très favorables. A l'autre extrême le comportement très ductile de certains aciers d'usage courant peut parfois poser des problèmes de détection. En règle générale l'utilisateur devra toujours prendre cet aspect en considération pour la faisabilité de la méthode.

.../...

II/ ASPECTS EXPERIMENTAUX

II.1/ Généralités

Le synoptique d'une chaîne d'émission acoustique est schématisé figure 1. Les fonctions suivantes sont représentées :

. Détection - Elle est communément réalisée par un capteur piézoélectrique résonnant dont la fréquence nominale est de l'ordre de 10^5 - 10^6 Hz ;

. Amplification - Elle est de l'ordre de 60 à 100 dB pour amener les µV ou mV délivrés par le capteur à un niveau exploitable. En sortie du capteur le préamplificateur joue un rôle supplémentaire d'adaptation des impédances ;

. Filtrage - L'élimination des bruits parasites liés à l'environnement mécanique ou acoustique est réalisée par un filtrage passe-haut dont la fréquence de coupure est au moins égale à 40 kHz ;

. Traitement - La méthode la plus couramment adoptée dans les chaînes actuellement commercialisées est un comptage du nombre d'arches du signal dépassant un seuil réglé au dessus du bruit de fond. Le comptage peut être cumulé ou relatif à une base de temps (taux d'émission acoustique). On discutera plus loin des limites de cette méthode et de celles qu'il est également possible de mettre en oeuvre.

La conception d'une telle chaîne est essentiellement liée aux particularités du signal d'émission acoustique.

Les énergies mécaniques mises en jeu dans la déformation plastique et la rupture s'étendent de 10^{-14} J (mouvement accéléré de dislocations) à 10^{-8} J (empilement de dislocations - rupture d'un grain) voire 10 J (rupture macroscopique). De plus, selon les matériaux, des phénomènes semblables se caractérisent par des énergies très différentes. Nous avons ainsi mis en évidence des écarts de 40 dB entre acier maraging et acier inox lors de la progression stable d'une fissure [1]. La méthode a donc des exigences particulières en ce qui concerne la sensibilité du détecteur et la dynamique de l'électronique associée.

On a proposé divers modèles physiques, aussi réalistes qu'on voudra, des mécanismes générateurs d'émission acoustique. Leur transformée de Fourier conduit toujours à des spectres large bande dont l'étendue est grosso-modo égale à l'inverse du temps de production de l'évènement initial. Ceci est conforme à l'expérience qui détecte l'émission acoustique du domaine audible jusqu'à plusieurs dizaines de MHz.

En définitive, la méthode n'est devenue réellement applicable en milieu industriel que par le choix de capteurs de fréquence $\sim 10^5$ - 10^6 Hz et par adoption du filtrage passe-haut. Les premiers prélèvent seulement une fraction de la densité spectrale énergétique mais permettent d'en suivre l'évolution. Le second élimine le domaine des basses fréquences où le bruit d'origine industrielle prédomine.

II.2/ Détection

L'élément clé de la chaîne instrumentale est le capteur. Les céramiques piézoélectriques sont seules susceptibles de détecter des déplacements de l'ordre de 10^{-2} Å [2]. En contrepartie leur sélectivité spectrale est sévère car les coefficients de surtension sont de l'ordre de 10^1 - 10^2. La fréquence nominale du capteur est essentiellement définie par sa géométrie. Pour les fabrications usuelles on utilise le P.Z.T. (Titano-zirconate de plomb) dont le Point de Curie (370°C) et les constantes piézoélectriques ($g_{33} \sim 10^{-2}$ V/m/N/m^2 ; $k \sim 0,7$) sont parmi les plus élevés. A haute température on peut faire appel au niobiate de lithium dont le Point de Curie est à 1.210°C mais qui est moins sensible et très onéreux.

Les capteurs résonnants ont une sensibilité de l'ordre de - 75 dB re 1 V/µbar. On peut, par adaptation mécanique ou électronique, aboutir à des capteurs piézoélectriques "large bande" mais avec des pertes de sensibilité voisines de 15 dB. L'utilisation de capteurs capacitifs [3], de l'effet électret [4], de capteurs électromagnétiques [5] conduit effectivement à des récepteurs large bande mais moins sensibles d'au minimum 30 dB.

L'étalonnage des capteurs nécessite un rapide effort d'unification et de normalisation. Les méthodes utilisées sont en effet de trois ordres [6] :

. Caractérisation intrinsèque de l'élément sensible (méthodes de l'IRE - méthodes impulsionnelles) ;

. Méthodes comparatives (réciprocité - jet d'hélium) ;

. Sources standard d'émission acoustique (laser - générateur piézoélectrique d'impulsions - étincelles - cassure d'un capillaire de verre ou d'un stylet fragile).

II.3/ Traitement du signal

Les méthodes de traitement numérique sont l'avenir mais posent encore, en raison des fréquences considérées, des problèmes d'échantillonnage et surtout de capacité de stockage.

Le comptage, hérité des techniques nucléaires, souffre d'inconvénients majeurs qui à notre

.../...

avis justifieraient son abandon. Il est en effet tributaire de paramètres expérimentaux tels que fréquence, seuil du discriminateur, amortissement du capteur. Il introduit une pondération défavorable aux signaux énergétiques. Il ne rend pas compte explicitement de la répartition des amplitudes. Par dessus tout, le comptage ne peut être associé à aucune grandeur de référence.

Une approche énergétique est physiquement plus séduisante. On peut procéder par intégration analogique ou numérique des signaux impulsifs délivrés par le capteur, par mesure de la RMS des signaux continus. Ces mesures définissent en réalité la densité spectrale énergétique au voisinage de la résonance principale du capteur. Par étalonnage on peut espérer remonter à l'énergie mécanique réellement libérée.

L'approche énergétique permet d'obtenir certains résultats masqués lors d'une approche par comptage et permet en particulier la distinction entre phénomènes de plasticité et rupture [7].

L'analyse spectrale fait l'hypothèse que les durées de certains processus sont différentes et/ou peuvent évoluer. Ce traitement présente de grandes difficultés en raison du filtrage opéré par l'ensemble structure-capteur et de la non-stationnarité du signal. Dans la littérature les résultats d'ordre pratique sont donc rares. Pour certains aciers on a toutefois identifié des caractéristiques spectrales de déformation plastique et de rupture différentes [8] [9].

L'analyse statistique est une des méthodes les plus prometteuses. L'analyse d'amplitude permet par exemple de caractériser les processus de rupture des matériaux composites, d'identifier des phases différentes dans l'acheminement à rupture d'éprouvettes métalliques [10]. Pour notre part nous avons mis au point une méthode extrêmement puissante de traitement statistique mais aussi chronologique ou paramétrique des informations contenues dans chaque évènement d'émission acoustique : amplitude maximale, énergie, durée, temps de montée, intervalle entre signaux [11]. Il constitue à notre connaissance un des instruments les plus avancés actuellement pour traiter les problèmes industriels d'émission acoustique.

II.4/ Localisation

La localisation est simple dans son principe. Des capteurs répartis sur la structure permettent de mesurer les différences de temps d'arrivée Δt_{ij} des signaux provenant de la source émissive. Des méthodes générales de triangulation hyperbolique ou des algorithmes plus simples, particuliers à certaines mailles (par exemple triangle équilatéral centré ou losange), permettent de calculer les coordonnées de la source.

La localisation sous forme simplifiée est un moyen d'analyse et de contrôle extrêmement fructueux. Sa mise en oeuvre à l'échelle des structures industrielles (capacités à pression lors de l'épreuve hydraulique par exemple) pose par contre de nombreux problèmes mathématiques et physiques dont nous avons fait la revue par ailleurs [12]. C'est une méthode "lourde" car elle nécessite un nombre élevé de voies de mesure, leur gestion par miniordinateur, un personnel averti.

En localisation, l'importance des problèmes posés par la nature du matériau tient à la maîtrise, encore imparfaite à l'heure actuelle, de la détection d'une progression ductile stable de fissure. Or la plupart des aciers industriels courants sont ductiles et présentent dans certains cas un comportement défavorable à l'usage de la méthode. De plus il n'y a pas nécessairement de lien étroit entre émissivité et nocivité d'un défaut.

La propagation s'effectue généralement sous forme d'ondes de LAMB. Les composantes longitudinales et transversales du mouvement y sont couplées. Comme les ondes de LAMB sont dispersives, cela se traduit par une pluralité des modes et par la dépendance des vitesses de propagation et des amortissements du produit fréquence (du capteur) x épaisseur (de la structure).

Quelle que soit la maille adoptée des considérations géométriques [12] montrent que la précision de localisation n'est pas homogène. Elle dépend fortement de la position relative de la source comme on le voit figure 2.

II.5/ Méthodes particulières

L'effet KAISER met en évidence le caractère irréversible des phénomènes générateurs d'émission acoustique. Si l'on charge, décharge et recharge de nouveau une structure, celle-ci n'émet pas tant que l'on n'a pas dépassé le niveau précédent. L'effet KAISER s'applique en principe à la déformation plastique mais on peut l'utiliser pour vérifier la progression d'une fissure entre deux mises en charge statiques. Il est par suite possible d'utiliser ce phénomène pour déterminer les dépassements de contrainte ou la croissance d'un endommagement.

Pour surmonter les problèmes posés par l'environnement mécanique ou électromagnétique, séparer les signaux utiles de signaux provenant de sources concurrentes, des techniques particulières ont été développées : discrimination en fréquence, en amplitude, temporelle, spatiale.

La discrimination de fréquence est systématiquement utilisée pour éliminer les phénomènes vibratoires ou mécaniques. Elle peut aussi distinguer les processus de rupture des composites.

La discrimination d'amplitude est opérée dans toute chaîne d'émission acoustique pour éliminer le bruit de fond électronique. Plus concrètement le tri des signaux par rapport à deux niveaux d'amplitude a été utilisé au contrôle des soudures par points. On sépare ainsi les signaux provenant de la formation du noyau de ceux provenant de l'expulsion du matériau en fusion.

.../...

La discrimination temporelle est utilisée lors d'essais cycliques pour exclure les phases où le rapport signal/bruit est défavorable. De même dans un processus de soudage séquentiel des "fenêtres" peuvent isoler telle phase utile. La durée du signal peut aussi servir à son identification.

La discrimination spatiale permet de ne prendre en compte que des signaux provenant d'une aire donnée. Les systèmes "maître-esclave" valident les signaux selon l'ordre d'arrivée. Les méthodes par coïncidence, imposent aux signaux un décalage dans le temps prédéterminé. Pour éliminer les signaux provenant de sources lointaines on peut utiliser une discrimination selon le temps de montée. Les systèmes de localisation multi-capteurs sont évidemment équipés de systèmes d'exclusion spatiale soit par le matériel, soit par le logiciel. Des exemples particulièrement spectaculaires d'utilisation de ces techniques de discrimination sont donnés en [13] (soudage de tuyauteries nucléaires), [14] [15] (détection de fissures de fatigue dans un environnement aéronautique particulièrement sévère). Soulignons enfin que l'adoption de méthodes de traitement numérique accroît considérablement les possibilités d'identification et de discrimination des signaux.

III/ APPLICATION DE L'EMISSION ACOUSTIQUE AU CONTROLE NON DESTRUCTIF

L'utilisateur potentiel espère tirer profit de la méthode principalement pour les raisons suivantes :

- Sensibilité de détection des défauts et anomalies ;
- Transmissibilité des ondes et possibilité de localisation ;
- Aptitude à déceler les évolutions à l'aide de procédures simples : effet KAISER, inspection par surcharge périodique... ;
- Accès à des informations éventuellement significatives du caractère critique du défaut ;
- Possibilités extrêmement importantes offertes par le traitement du signal.

En contrepartie il doit tenir compte des sujétions et limitations suivantes :

- Nécessité de solliciter la pièce en réalisant un champ de contraintes proche de la réalité ;
- Sensibilité aux bruits et parasites ;
- Dépendance de l'émissivité envers le matériau, le mode de fabrication, la nature du défaut, etc... ;
- Complexité, dans certains cas, de l'interprétation de l'information perçue ;
- Coût élevé du matériel et recours à un personnel qualifié.

Avant de nous attacher plus particulièrement au soudage nous allons passer brièvement en revue certains types de contrôles pouvant concerner l'aéronautique.

III.1/ Contrôle de fin de fabrication

Il repose sur un principe simple : toute pièce défectueuse émettra lorsqu'elle sera sollicitée tandis qu'une pièce saine restera silencieuse. Il est alors possible de concevoir des procédures industrielles d'acceptation ou rejet. Le C.E.T.I.M. a appliqué avec succès un tel contrôle basé sur l'émissivité des pièces défectueuses à la détection des tapures de trempe de barres de dévers (figure 3), à la détection de fissures dans des chapes de frein...

Il est possible que les méthodes basées sur l'émissivité soient insuffisantes. On peut alors faire appel à des procédures de traitement plus élaborées. Ainsi, par exemple, la répartition statistique des amplitudes a permis de distinguer (figure 4) des assemblages soudés correctement d'assemblages défectueux.

Souvent aussi, l'appoint de la localisation est nécessaire pour authentifier la présence d'un défaut.

III.2/ Contrôle des matériaux spéciaux : Composites - Céramiques

Les études de faisabilité concernant ce type de contrôle connaissent actuellement un développement impétueux.

Tous les composites renforcés par dispersion, particules ou fibres sont concernés. Les mécanismes de déformation plastique ou rupture de la matrice, de déformation ou rupture de l'élément renforçateur, de délamination à l'interface de deux phases sont émetteurs. Toutefois les émissions prédominantes sont observées à la rupture des fibres de renforcement (whiskers, verre, métal, polymère, céramique). La proportion de fibres rompues peut être établie en fonction de la déformation.

On connaît la faible résistance à la fatigue des matériaux renforcés ; le contrôle de ceux-ci par la technique des surcharges périodiques permet de suivre leur endommagement.

.../...

Pour les céramiques on s'efforce d'obtenir des indications de bonne tenue mécanique en service à partir des microfissurations détectées en réception.

III.3/ Contrôle des assemblages

Les qualités d'adhérence des assemblages collés sont mises en évidence par émission acoustique [16] [17] [18]. Le C.E.T.I.M. a obtenu des résultats similaires.

La méthode est aussi applicable aux assemblages nids d'abeilles. Le contrôle des assemblages soudés peut s'effectuer par mise sous contrainte mécanique ou thermique. Ainsi lors de l'épreuve de boites d'engagement sur armes automatiques [19] l'émission acoustique est le seul moyen susceptible de qualifier en réception, la tenue ultérieure d'assemblages soudés par résistance électrique.

III.4/ Contrôles de réception des récipients à pression

La première application connue remonte à 1963 (épreuve des enveloppes moteur de la fusée Polaris).

A titre d'illustration nous présentons l'application à deux cas pratiques du dispositif de localisation mis en place au C.E.T.I.M. Ce sont :

- Détection et localisation d'un défaut ayant conduit à la rupture d'une capacité en AG_3. La fissure a été détectée très longtemps avant de devenir débouchante (figure 5) et a pu être localisée à moins de 5 cm de la position réelle (figure 6) ;

- Détection sur cuve en acier E24 de défauts réalisés artificiellement et devant conduire à rupture. Comme le montre la figure 7 la précision obtenue est bonne puisque le barycentre des positions calculées est à quelques cm du défaut ou sur lui à la précision des reports près. La dispersion observée sur les localisations individuelles est inévitable car elle reflète l'influence de la répartition d'amplitude des signaux. Par contre la cohérence et la précision de localisation s'améliorent au fur et à mesure de la progression des défauts. Ceci constitue une preuve indirecte de leur caractère critique croissant.

Dans certains cas les résultats sont plus inégaux car tributaires de conditions d'application défavorables : structure mal détensionnée ou oxydée, matériau ductile, défauts peu émissifs.

III.5/ Contrôle des circuits hydrauliques ou pneumatiques - Contrôle d'étanchéité

L'émission acoustique permet le contrôle d'ensembles hydrauliques : fonctionnement de pompes, vannes, servovalves, endommagement par cavitation [20] [21]. Ce contrôle d'étanchéité a l'avantage de pouvoir s'effectuer à distance. Compte tenu de la nature non impulsive du signal la localisation des fuites s'effectue par des méthodes non conventionnelles : comparaison d'amplitude, corrélation. La limite inférieure de détection en contrôle d'étanchéité de systèmes hydrauliques semble se situer à environ 2 bars/l/h [22]. Pour les systèmes pneumatiques elle est d'environ 0,2 cm^3/atm/sec [21].

Signalons enfin que le C.E.T.I.M., à la demande d'E.D.F., a mis au point l'appareillage de contrôle d'étanchéité du circuit primaire des centrales nucléaires lors des épreuves hydrauliques règlementaires.

III.6/ Contrôles de composants électroniques

On a signalé récemment [23] que le contrôle de fabrication à 100 % de certains composants (PTRC) était déjà appliqué dans la grande industrie. De même les défectuosités de circuits électroniques sont détectées à l'aide des microdécharges aux points chauds des résistors et transistors, aux fuites des condensateurs ou des circuits intégrés [24]. On recherche également les particules perdues dans les assemblages électroniques scellés.

III.7/ Contrôle du fonctionnement (diagnostic acoustique)

Avec l'avantage d'une grande sensibilité aux fréquences élevées l'émission acoustique peut être intégrée à l'ensemble des méthodes de diagnostic acoustique des mécanismes. Elle est employée pour roulements à billes, paliers [24] etc... Souvent l'endommagement est suffisamment révélé par l'élévation du niveau de bruit de fonctionnement. Sinon on doit faire appel aux méthodes dites de "signature acoustique".

IV/ APPLICATION DE L'EMISSION ACOUSTIQUE AU CONTROLE DU SOUDAGE

IV.1/ Généralités

Les forts gradients thermiques de la zone fondue ou de la zone affectée thermiquement (ZAT) créent ou sollicitent les défauts engendrés par l'opération de soudage : fissures, manques de pénétration, collages, inclusions, porosités, etc... Ceux-ci, à des degrés divers, provoquent de l'émission acoustique. L'information peut être acquise soit en cours de soudage ou immédiatement après (fissuration à chaud) soit en différé (fissuration à froid). Cette dernière peut d'ailleurs intervenir après plusieurs dizaines d'heures dans certains aciers à haute ténacité et il n'existe pratiquement pas d'autre moyen que l'émission acoustique pour connaître le délai de stabilisation de la soudure.

.../...

Les avantages escomptés de la méthode sont multiples : sensibilité (parfois surabondante), localisation même sans accès direct, temps réel donc possibilité de réparation immédiate. La principale difficulté d'application réside dans l'élimination éventuelle des bruits propres à l'opération de soudage (parasites électromagnétiques, changements de phase du matériau, craquement du laitier...). Une autre difficulté réside dans le comportement du capteur à température élevée. L'emploi de céramiques piézoélectriques à haut Point de Curie ou l'usage de guides d'ondes permettent de la surmonter. De même température et conductivité thermique peuvent influencer l'émissivité du matériau et la propagation des ondes. La vitesse de celles-ci décroît en effet avec la température tandis que leur atténuation croît. Par suite, la localisation peut s'avérer parfois délicate.

A notre connaissance les premiers travaux sur le contrôle du soudage par émission acoustique ont été menés au Battelle Northwest par JOLLY [25]. Celui-ci a ainsi prouvé la sensibilité de la méthode en détectant dans l'inox 304-L des défauts non décelés par rayons X mais confirmés par examen métallographique. Il a indiqué la corrélation, dans ce cas, entre longueur de fissure et énergie libérée par émission acoustique.

Depuis, l'intérêt des milieux industriels s'est principalement manifesté pour le contrôle des soudages multipasses [26] [27] et des soudages par résistance [28]. Dans le premier domaine l'intérêt économique est évident en raison de la possibilité de réparation immédiate. Dans le second le contrôle est possible à 100 % et l'émission acoustique est la seule méthode qui apporte des informations sur la tenue mécanique ultérieure. L'application très spéciale à des soudages impérativement étanches mérite une mention particulière : tubes de gainage de combustible nucléaire [29], capuchons de conteneurs à déchets radioactifs [30].

La littérature portant sur l'applicabilité de la méthode aux divers modes de soudage fait ressortir la spécificité de chaque cas notamment pour ce qui concerne l'émissivité des matériaux ou des défauts et le traitement des signaux le plus adéquat. Nous allons en faire succinctement la revue en ne retenant que les conclusions les plus générales. Le lecteur se reportera aux références indiquées pour obtenir les détails concrets d'application.

IV.2/ Soudages avec flux gazeux (TIG-MIG-MAG) [Réf. 29 à 34]

Ces modes de soudage sont favorables à l'application industrielle car le flux gazeux n'introduit pas de bruit perturbateur. Les essais montrent que non seulement la formation et l'extension des fissures peuvent généralement être révélées mais aussi dans certains cas les manques de pénétration, soufflures et porosités. De plus l'examen peut se poursuivre longuement durant la phase de refroidissement.

Les matériaux testés sont nombreux. Citons en particulier l'inox (inox 316 et inox 304-L respectivement, pour les gaines de combustible nucléaire et les conteneurs mentionnés plus haut), le titane, l'inconel, l'aluminium et ses alliages... Pour les aciers au carbone, il faut tenir compte de l'intense bruit perturbateur engendré par les transformations martensitiques.

IV.3/ Soudages avec flux solide [Réf. 25 à 27 - 33 à 35]

Le soudage automatique sous flux solide (arc submergé) concerne principalement les aciers de construction parfois de forte épaisseur. L'émission acoustique est alors très sensible à l'influence perturbatrice du laitier pendant son refroidissement. Les défauts détectés avec le plus de fiabilité sont les fissures et les inclusions de flux de soudage. Les porosités et manques de pénétration sont décelés s'ils s'accompagnent de fissurations secondaires. Enfin les conformations défectueuses (cratères, caniveaux...) peuvent être distinguées des conformations soignées.

Le contrôle du soudage à l'arc sous électrode enrobée, qui s'apparente au précédent, présente les mêmes difficultés d'application en raison du craquement du laitier.

IV.4/ Soudages par résistance [Réf. 28 - 31 - 34 - 36 à 38]

Le contrôle des soudages utilisant ce principe, notamment par point et par étincelage, a donné des résultats très prometteurs. Le soudage à la molette pose des problèmes plus délicats car il s'agit de séparer le bruit produit par l'accroissement du volume fondu des bruits de positionnement des tôles et d'usure de l'électrode.

On constate généralement qu'il existe une bonne corrélation entre volume fondu et intensité de l'émission acoustique. Comme la qualité de la soudure dépend de la taille du noyau l'importance de l'émission acoustique traduit donc paradoxalement une soudure de qualité et non un défaut. De même on a confirmé aussi bien avec du zircalloy [36], du monel ou du laiton [37] qu'il existe une nette corrélation entre ampleur de l'émission et résistance mécanique de la soudure au "déboutonnage"...

Le contrôle industriel de masse par cette méthode a déjà débuté. Les appareillages utilisent généralement un double système de discrimination temporelle et de discrimination d'amplitude pour identifier et caractériser la phase significative du soudage.

IV.5/ Brasage et soudages spéciaux

L'application à la recherche du manque d'édhérence des brasages entre électrode métallique et culot céramique de tubes électroniques a été effectuée avec succès [39].

.../...

Pour le soudage par plasma des essais concluants ont été effectués sur des alliages aviation et de l'inox. De même pour le soudage laser [40]. De plus nous allons consacrer un développement particulier au contrôle du soudage par bombardement électronique.

V/ ETUDE PARTICULIERE : FAISABILITE DU CONTROLE IN SITU DE SOUDAGES PAR BOMBARDEMENT ELECTRONIQUE * **

Le constructeur mentionné utilise l'Inconel 718 forgé pour certaines pièces tel l'arbre de turbine de la photo 8. Ce matériau offre en effet de nombreux avantages mécaniques à chaud (550°C) en particulier pour la fatigue oligocyclique. Par contre son soudage par bombardement électronique est particulièrement délicat.

Le couple de matériau à souder est ici l'Inconel 718 (NC 19 FeNb) et l'inox Z12 CNDV12. Le soudage peut introduire les criques longitudinales que l'on voit sur la photo 9a. Celles-ci sont contrôlables par les moyens classiques. Il peut surtout introduire dans l'Inconel une microfissuration initiée dans la zone affectée thermiquement et qui peut, dans certains cas, pénétrer dans le cordon (Photos 9b à 9d). Ces fissures sont transversales, ne débouchent pas en surface et sont de taille limitée à quelques 1/100ème ou 1/10ème de mm. Compte tenu de la géométrie particulière de la pièce les moyens conventionnels ne permettent pas à ce jour de les déceler.

V.1/ Mécanismes générateurs possibles pour l'émission acoustique

La formation des défauts lors du soudage des viroles cylindriques considérées dépend de l'apport thermique dans le cordon, de la génération des contraintes internes et des phénomènes métallurgiques associés. Un examen succinct va montrer la liaison de ces facteurs avec la génération d'émission acoustique.

Le bruit d'impact proprement dit du faisceau est peu important. Par contre la fusion du métal s'accompagne dans le volume liquéfié de mouvements turbulents, d'ébullitions locales, de vaporisations, d'éjections. On sait que ces mécanismes sont générateurs d'une émission acoustique assimilable à un "bruit blanc" [41]. Les projections peuvent en outre créer des impacts parasites.

La solidification entraîne des modifications locales rapides de volume et éventuellement des transformations de phase aptes à engendrer une émission acoustique que nous nommerons "de solidification". Ainsi on a montré que le retrait à la solidification des métaux fondus entraîne une émission acoustique notablement influencée par l'importance de la contraction en volume [42]. De même le réarrangement et la contraction accompagnant la transformation martensitique produisent de l'émission acoustique [43]. On a enfin montré expérimentalement [44] que la déformation plastique à haute température d'alliages à base nickel, tels le waspalloy, s'accompagne d'une émission de forte intensité, car le mouvement des dislocations est alors facilité.

La zone affectée thermiquement subit un échauffement très localisé faisant apparaître plusieurs phénomènes. Du côté NC 19 FeNb au chauffage il y a redissolution des précipités et grossissement du grain. La rapidité du refroidissement ne permet pas la reprécipitation complète mais est suffisante pour provoquer vers 950°C la précipitation d'un film de carbure de Niobium aux joints de grains de l'Inconel 718. Ceux-ci sont rendus incohérents donc fragiles. Du côté Z 12 CNDV12, au chauffage il y a austénitisation avec grossissement du joint de grain. Au refroidissement il y a transformation martensitique (voir plus haut). Dans le cordon la solidification s'effectue perpendiculairement aux isothermes et engendre une cristallisation allongée dans le sens du gradient de température. Les limites de croissance des dendrites constituent un cheminement privilégié pour toute propagation d'une fissuration.

La formation de fissures à chaud ou à froid dépend de l'état de contrainte local aux points faibles de la structure solidifiée. La fissuration longitudinale apparaît, sous l'influence des contraintes de retrait, dans le plan médian du cordon à l'endroit où les grains de solidification créent une discontinuité de structure. La formation de fissures dans la ZAT est liée aux gradients thermiques et aux concentrations de contraintes dues à la forme du bain. L'apparition, aux joints de grains les plus faibles et/ou les plus sollicités, des deux types de fissuration qui viennent d'être décrits engendre de l'émission acoustique. Contrairement à l'émission acoustique de "solidification", cette émission acoustique de "fissuration" peut se prolonger pendant le refroidissement de la soudure.

Pour être complets sur l'émission acoustique accompagnant la formation des défauts de soudage nous indiquerons que l'émission acoustique déjà signalée qui accompagne les mouvements du bain liquide peut indirectement révéler la formation de soufflures, porosités... De plus les contraintes s'exerçant sur la cavité où le gaz est emprisonné peuvent produire à chaud des déformations plastiques du type de celles mentionnées plus haut et à froid conduire à des fissurations différées.

V.2/ Essais de faisabilité

Ce qui vient d'être exposé montre la multiplicité des mécanismes générateurs possibles pour l'émission acoustique accompagnant le soudage par bombardement électronique. Si l'on veut effectuer le contrôle lors du soudage proprement dit, il est impératif que les signaux significatifs d'une émission acoustique de "fissuration" se distinguent du bruit de fond inévitablement lié aux phénomènes annexes de solidification, transformation de phase, etc... Comme ce bruit cesse à la fin du soudage il semble commode d'essayer de détecter, si elle existe, l'émission acoustique engendrée par le développement des fissures pendant le refroidissement. De même pour le cas de la fissuration à froid.

* ** Etude supportée financièrement par la Société TURBOMECA

.../...

Pour démontrer la réalité de l'émission acoustique associée à la formation des défauts on a procédé à une première série d'essais comparatifs. On a effectué des tirs linéaires sur plaquettes d'un matériau facilement criquable (acier XC 80 recuit) et d'un alliage peu fissurant (TA 6 V). L'émission acoustique a été surveillée pendant le refroidissement.

Pour TA 6 V on obtient une référence de silence absolu en l'absence de toute fissuration. Pour XC 80 recuit l'émission acoustique a très clairement décelé les fissurations longitudinales du cordon. L'activité pour ce type de défaut peut se prolonger jusqu'à 6 mn après le soudage. On a aussi décelé des fissures à froid de taille inférieure à 2/10ème mm prenant naissance au niveau de soufflures internes (photo 10). De manière connexe les essais ont montré la possibilité de localiser les défauts avec une précision acceptable et suggéré une relation croissante entre émissivité et taille des défauts (figure 11).

Dans une deuxième série d'essais on a considéré l'émissivité des matériaux concernés dans le problème industriel posé : Inconel 718 et inox (ici Z 10 CNT 18). On a procédé par tirs linéaires. On constate sur la planche photo 12 une première différence entre les niveaux du "bruit de fond" pendant le soudage et une seconde différence dans l'activité lors du refroidissement. Une concordance qualitative a été mise en évidence entre cette dernière et la présence de fissures.

Les deux matériaux considérés sont austénitiques γ (c.f.c). Leur comportement de fusion-solidification est donc à priori voisin. La différence principale se situe au refroidissement où des précipités apparaissent dans la solution solide d'Inconel 718. Parmi ceux-ci, comme l'atteste l'examen métallographique, le carbure de niobium se fixe aux points de grains et cause la fissuration. Il ne semble pas illogique de rapprocher cette explication des différences observées dans l'émission acoustique des deux matériaux au refroidissement. De même le passage par un maximum d'émissivité de l'Inconel 718 lors du refroidissement paraît lié à l'évolution de la température. Un phénomène semblable a d'ailleurs été observé lors de la fissuration de l'acier 304 L [25]. D'un point de vue pratique on constate que la phase d'émission acoustique post-soudage est relativement brève. Sur pièce réelle il paraît donc impératif d'exercer le contrôle pendant le soudage proprement dit.

Dans la troisième partie de l'étude on a soudé des viroles cylindriques d'Inconel 718 et d'inox martensitique Z 12 CNDV 12 pour simuler la fabrication de l'arbre de turbine réel. On s'est attaché à l'étude de l'émission acoustique produite pendant le soudage. (Voir le montage photo 13).

Les indications données plus haut sur les origines possibles de l'émission acoustique ont été confirmées. La présence d'un "bruit de solidification" a été nettement révélée. On voit photo 14 qu'il se compose de signaux impulsifs extrêmement rapprochés. On a de plus constaté qu'il est relié à la puissance introduite par unité de volume et qu'il croît avec elle. Lorsqu'il y a fissuration les signaux impulsifs correspondants sont engendrés. On le voit sur la planche photo 15 qui compare, toutes choses égales d'ailleurs, deux cas dont le contrôle métallographique s'est révélé pour l'un positif (fissuration du type C - Cf. photo 9d), pour l'autre négatif. La différence d'émissivité apparaît nettement.

L'existence de signaux liés à la fissuration lors de la phase de soudage étant établie, on peut s'orienter vers la recherche de solutions pratiques pour le soudage considéré. Il est nécessaire que les signaux de fissuration émergent du "bruit de solidification". C'est donc l'ampleur de celui-ci, en dernier ressort les paramètres de soudage et le matériau, qui fixent le rapport signal/bruit et la faisabilité du soudage. Accessoirement le niveau de "bruit" peut servir à vérifier la continuité des conditions de soudage.

Compte tenu de la sensibilité naturelle de l'émission acoustique à des hétérogénéités locales du matériau ou à de légères variations des paramètres de tir on ne peut uniquement opérer, comme il est classique, par des méthodes de seuil. On doit adopter des méthodes complémentaires de traitement statistique aptes à distinguer l'existence de deux populations de signaux. Pour certains cas spécifiques où le soudage est bref, l'appareillage peut être simplifié puisqu'il y a émissivité lors du refroidissement.

L'expérience montre qu'on ne peut éviter la microfissuration de la ZAT dans l'Inconel 718, quelles que soient les conditions de soudage et l'état métallurgique du matériau. Ceci est mis en évidence en poussant les grossissements de l'examen métallographique. Le contrôle doit donc se fixer une taille limite des défauts acceptables, ne compromettant pas la tenue de la pièce en service. L'émission acoustique engendrée par la fissuration à chaud d'un tel défaut de référence doit surpasser le "bruit de solidification". Comme ce dernier est essentiellement commandé par la puissance thermique et le matériau considéré on voit que la méthode ne peut s'appliquer qu'à des cas spécifiques. Les problèmes de reproductibilité et fiabilité doivent également être examinés avec soin.

VI/ CONCLUSION

L'émission acoustique est une technique encore au stade de la recherche et du développement. Ce n'est pas une technique d'imagerie mais une technique de détection. Ses performances dépendent des phénomènes physiques se produisant dans le matériau et de la valeur du traitement de l'information perçue. Elle est seule par contre à pouvoir accéder à l'évolution et à l'éventuelle estimation de la nocivité des défauts. Il n'y a donc pas concurrence mais complémentarité de l'émission acoustique et des autres techniques (R. X, Ultrasons, ...).

L'émission acoustique se développe dans un contexte scientifique et technologique favorable : développement de matériaux à hautes caractéristiques mécaniques, performances accrues des maté-

.../...

riels électroniques, progrès des techniques de traitement du signal, développement des systèmes informatiques.

Un travail important reste à accomplir pour amener l'utilisation industrielle au niveau des possibilités virtuelles. Il faut en effet considérer, à côté des avantages intrinsèques, les facteurs qui limitent actuellement la diffusion : délicatesse de mise en oeuvre, interprétation des résultats nécessitant un personnel averti, coût...

Le contexte industriel est cependant favorable à terme car les performances demandées et les exigences d'économie et sécurité s'accroissent. Ainsi, pour se limiter au domaine aéronautique, l'US Air Force souhaite développer pour la flotte des avions cargos C5 les dispositifs déjà utilisés pour détecter les fissures dans les ailes et réservoirs du C 135. Elle espère ainsi une économie de maintenance de l'ordre de $ 35 millions. De même l'émission acoustique a déjà remplacé rayons X, ultrasons et techniques électromagnétiques pour la détection des corrosions de l'empennage de l'avion F 111.

Les études prospectives [45] estiment qu'elle sera une des méthodes de Contrôle Non Destructif dont le taux de développement sera le plus rapide et qu'à long terme elle atteindra un niveau d'utilisation comparable à celui des moyens actuels.

BIBLIOGRAPHIE

[1] P. DUMOUSSEAU & Col. -- Recherche CETIM 15H090 Rapport final (Mars 1978)

[2] C.H. PALMER & R.E. GREEN -- Applied Optics - 16 n° 9 (Sept. 77) - p. 23-33

[3] N.N. HSU - JA. SIMMONS & J.C. HARDY -- Materials Evaluation - 31 n° 10 (Oct. 77)

[4] G. CURTIS -- Non Destructive Testing (Avril 1974) - p. 82-91

[5] B.N. MAXFIELD & R. COCHRAN -- Materials Evaluation - 31 n° 2 (Fév. 73) - p. 17-20

[6] C. DRUHET & J. ROGET -- Recherche CETIM 15H150 Rapport partiel n° 3 (Oct. 78)

[7] N. MIRABILE -- Conference on Fracture Mechanics Technology - Hong-Kong (Mars 77)

[8] L.J. GRAHAM & G.A. ALERS -- Materials Evaluation - 32 n° 2 (Fév. 74) - p. 31-36

[9] B. WOODWARD & R.W. HARRIS -- Acustica - 37 n° 3 (1975) - p. 190-197

[10] J.C. LENAIN -- Cast INSA Lyon (Nov. 77) - p. X.1 - X.17

[11] B. FUCHS -- Recherche CETIM 15H200 Rapport partiel n° 1 (Mai 78)

[12] P. DUMOUSSEAU -- 2ème Colloque Technologie des Appareils à Pression Paris (Oct. 77) - p.225-239

[13] D.W. PRINE -- N.D.T. International (Déc. 76) - p. 281-284

[14] C.D. BAILEY -- Materials Evaluation - 34 n° 8 (Août 76) - p. 165-171

[15] C.R. HORAK & A.P. WEYRETER -- Materials Evaluation - 35 n° 5 (Mai 77) - p. 59-64

[16] J.B. BEAL -- NASA SP 5802 (1967)

[17] A.A. POLLOCK -- British Journal of N.D.T. (Mai 71) - p. 85-89

[18] G.J. CURTIS -- AERE Report R 7684 (Mars 74)

[19] P.H. HUTTON -- B.N.W.L. SA 4576 (Janvier 73)

[20] H.P. BLOCH -- Hydrocarbon Processing (Mai 77) - p. 213-215

[21] H.L. BALDERSTON -- 8th Reliability and Maintainability Conference - Denver (Juillet 67)

[22] P. DUMOUSSEAU & Col. -- Recherche CETIM 15H160 Rapports partiels n° 6 (Juil. 76) et 7 (Juil. 77)

[23] J.M. DREW & W.P. SCHUHMAN -- Communication 7th EWGAE Meeting Manchester (Oct. 78)

[24] R.A. COLLACOT -- Tribology International (Juin 75) - p. 123-126

[25] W.D. JOLLY -- Materials Evaluation - 28 n° 6 (Juin 70) - p. 135-139 et 144

[26] A.E. WEHRMEISTER -- Materials Evaluation - 35 n° 6 (Juin 77) - p. 45-47

[27] D.W. PRINE -- NDT International (Déc. 76) - p. 281-284

.../...

[28] TRODYNE -- Engineering Note n° 10019 (Déc. 71)

[29] D.M. ROMRELL -- Materials Evaluation - 30 n° 12 (Déc. 72) - p. 254-258

[30] R.C. CROWE -- B.N.W.L. SA 3758 (Avril 71)

[31] W.D. JOLLY -- B.N.W.L. SA 817 (Sept. 68)

[32] C.K. DAY -- B.N.W.L. SA 902 (Janvier 69)

[33] W.D. JOLLY -- Welding Journal - 48 n° 1 (Janv. 69) - p. 21-27

[34] W.D. JOLLY -- B.N.W.L. SA 2727 (Sept. 69)

[35] C.E. HARTBOWER & Col. -- A.S.T.M. STP 505 (Mai 72) - p. 187-221

[36] E.B. SCHWENK & G.D. SHEARER -- Non Destructive Testing - 6 n° 1 (Fév. 73) - p. 29-33

[37] S.J. VAHAVOLIOS & Col. -- Materials Evaluation - 36 n° 3 (Mars 78) - p. 41-44 et 51

[38] R.B. STEEL & C.C. POPADICK -- Materials Evaluation - 34 n° 3 (Mars 76) - p. 64-66

[39] J.H. GIESKE -- B.A. Transactions - 11 n° 9 (Janvier 72) - p. 24-30

[40] M.A. SAIFI & J.J. VAHAVOLIOS -- I.E.E.E. Journal of Quantum Electronics - 12 n° 2 (Fév. 76) p. 129-136

[41] H.A. CROSTACK-- Proceedings 3rd EWGAE Meeting - Ispra (Sept. 74) - p. 28-47

[42] H. BORCHERS & H.M. TENSI - Metall - 17 (1963) - p. 784-788

[43] G.R. SPEICH & R.M. FISHER -- A.S.T.M. STP 505 (1972) - p. 140-151

[44] E. DICKHAUT & J. EISENBLATTER -- Journal of Engineering for Power - 97-A n° 1 (Janv. 75)-p.47-52

[45] D. BALLARD -- Materials Evaluation - 31 n° 12 (Déc. 73) - p. 15-A - 21-A

FIGURES

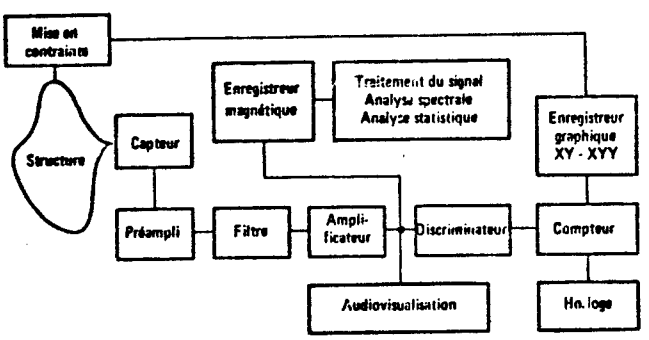

Figure 1 - Synoptique de la chaîne d'émission acoustique

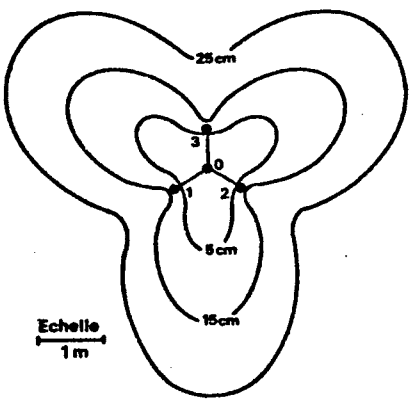

Figure 2 - Tracé des zones d'incertitude de la maille triangle équilatéral centré pour une erreur de 5 % sur la mesure des Δ t (programme CILS - Les lignes "isoerreur" indiquent la borne supérieure de l'incertitude dans l'aire délimitée)

.../...

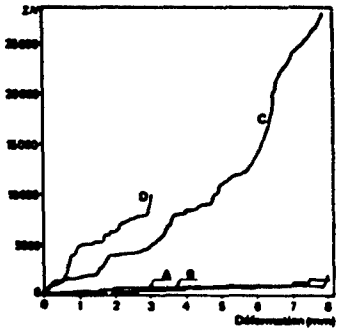

Figure 3 - Détection de tapures de trempe par émission acoustique. Les pièces avec tapures (C-D) se distinguent des pièces saines (A-B) par une émissivité nettement plus prononcée

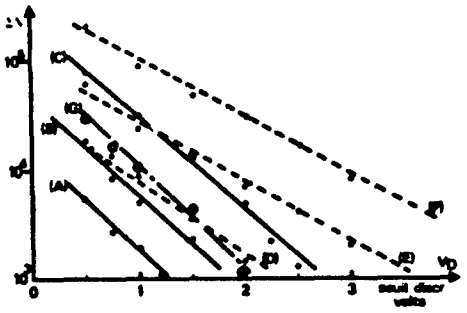

Figure 4 - Contrôle d'assemblages soudés au moyen d'une analyse d'amplitude - Assemblages corrects A, B, C, G - Assemblages défectueux D, E, F

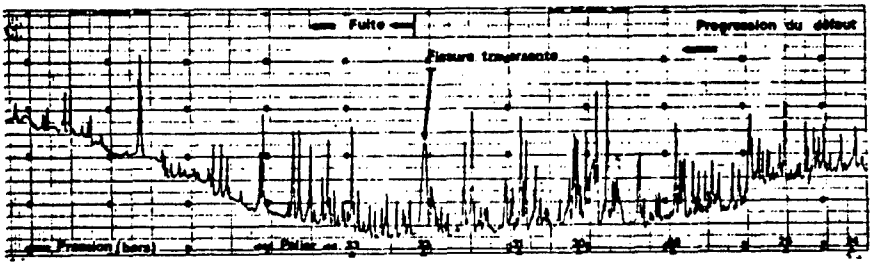

Figure 5 - Evolution de la valeur efficace (RMS) du signal d'émission acoustique lors de l'essai d'éclatement d'une capacité à pression en AG_3

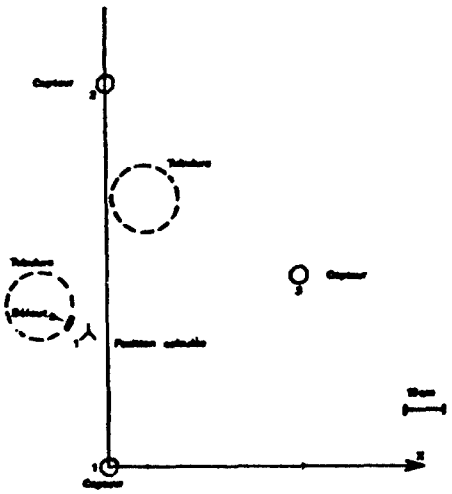

Figure 6 - Localisation lors de l'essai d'éclatement d'une capacité à pression en AG_3

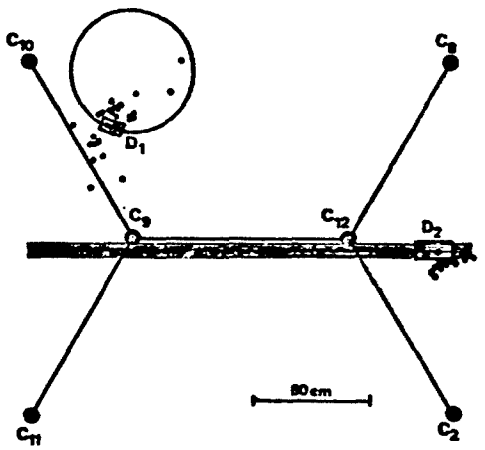

Figure 7 - Localisation, évènement par évènement, de défauts réalisés dans une capacité à pression en acier E24

.../...

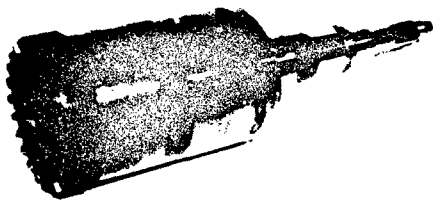

Figure 8 - Photographie de l'arbre de turbine à contrôler (soudage Inconel 718 - Z 12 CNDV 12)

Photo 9a - G x 25

Photo 9b - G x 14

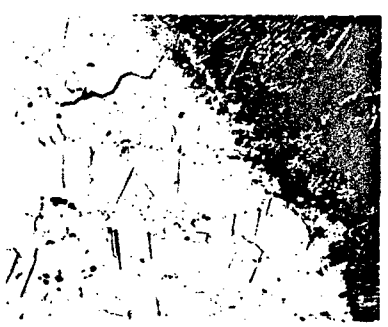

Photo 9c - G x 100

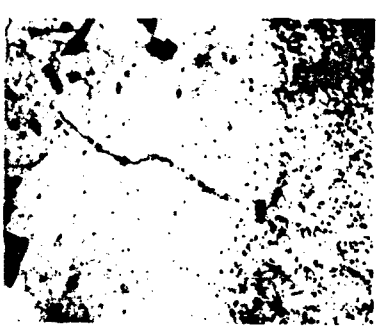

Photo 9d - G x 500

Figure 9 - Photographie 9a : Fissuration longitudinale du cordon - Photographies 9b à 9 d : Fissuration transversale du cordon à divers grossissements

.../...

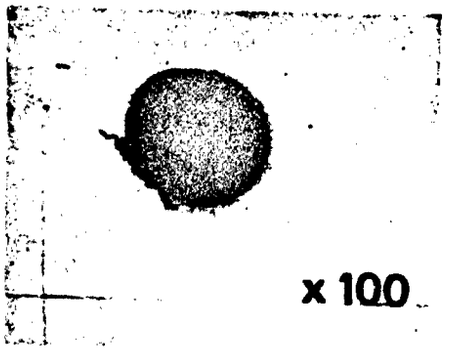

Figure 10 - Fissuration initiée par une soufflure interne

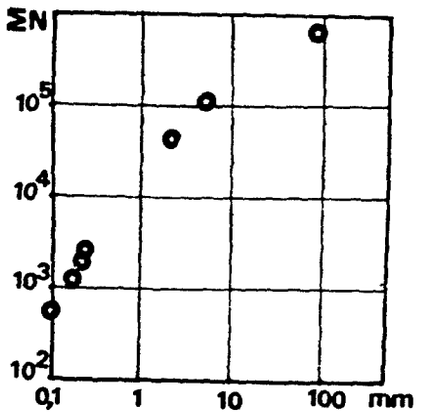

Figure 11 - Mise en évidence de la relation qualitative entre émissivité et taille des défauts

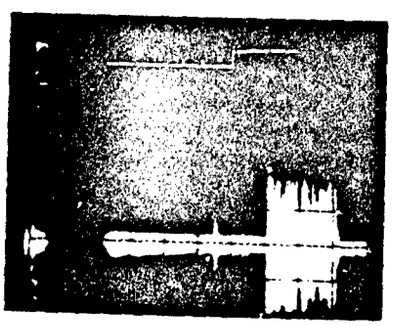

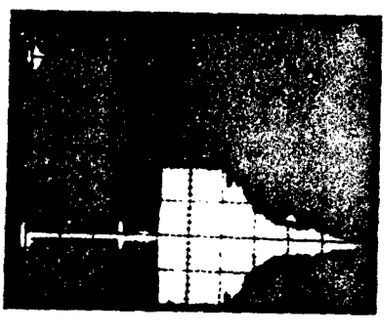

Figure 12 - Comparaison du comportement d'émission acoustique pendant et immédiatement après soudage

A gauche : inox — A droite : Inconel 718

Noter le niveau plus élevé de ce dernier pendant soudage et l'activité immédiatement postérieure

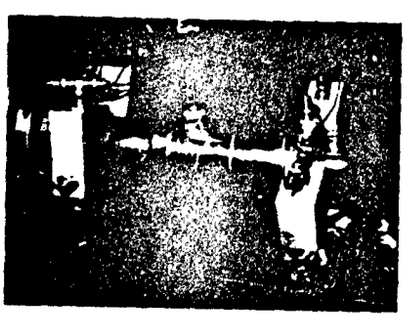

Figure 13 - Photographie du montage expérimental pour le contrôle lors du soudage (système à 2 capteurs)

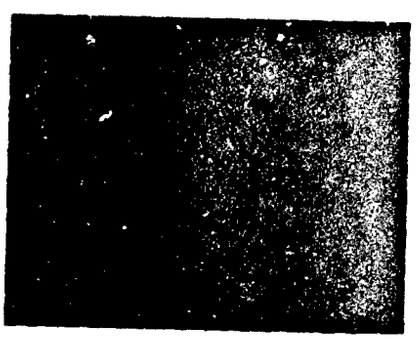

Figure 14 - Mise en évidence des signaux d'émission acoustique liés à la solidification du bain

.../...

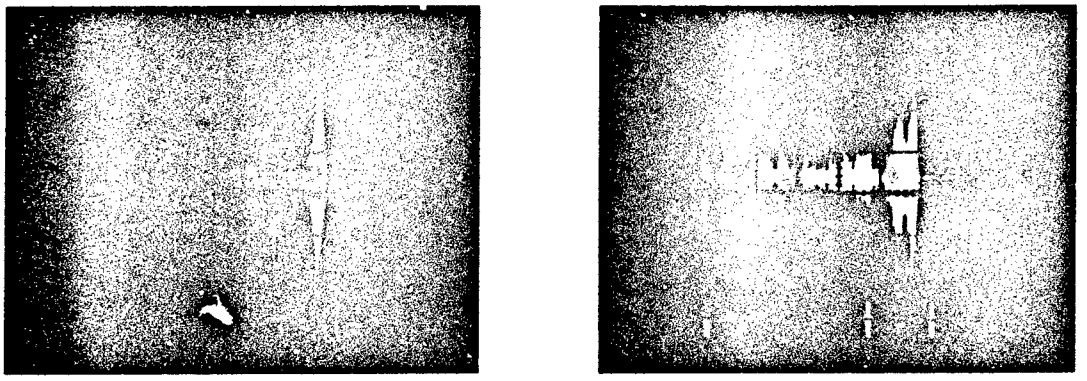

Figure 15 - Mise en évidence de la différence d'émissivité de 2 soudages
A gauche : non fissurant A droite : fissurant

TRANSDUCTEURS ULTRASONORES À LARGE BANDE POUR LE CONTRÔLE NON DESTRUCTIF DE PIÈCES AÉRONAUTIQUES

par Jean-François de BELLEVAL

Office National d'Etudes et de Recherches Aérospatiales (ONERA)
92320 Châtillon (France)
et Université de Technologie de Compiègne

♦

Résumé

Le contrôle non destructif de pièces aéronautiques par ultrasons nécessite de détecter des défauts de plus en plus petits et de plus en plus près de la surface de ces pièces. L'évaluation quantitative de ces défauts, permettant une prévision plus précise de leurs conséquences mécaniques, doit aussi être améliorée. Ceci exige l'utilisation de transducteurs ultrasonores plus sensibles et présentant une plus large bande passante.

La principale méthode utilisée à présent pour augmenter la bande passante de transducteurs piézoélectriques entraîne une réduction importante de leur sensibilité ; elle est fondée sur l'amortissement de la lame piézoélectrique par sa face arrière. On propose d'utiliser au contraire un amortissement par une face avant à plusieurs couches, qui permet l'augmentation simultanée de la sensibilité et de la bande passante. Pour étudier la faisabilité de ce procédé, un logiciel d'ordinateur a été mis au point pour calculer la propagation d'une onde à travers des couches d'épaisseurs différentes. Ce programme permet d'optimiser les caractéristiques (impédance et épaisseur) des diverses couches constituant le transducteur. Des comparaisons avec des transducteurs réels ont permis de valider ce modèle théorique.

BROAD-BAND ULTRASONIC TRANSDUCERS FOR NON-DESTRUCTIVE INSPECTION OF AERONAUTICAL COMPONENTS

Summary

For ultrasonic non-destructive inspection of aeronautical components, it is mandatory to detect defects both smaller and smaller, and nearer and nearer the surface of these components. The quantitative evaluation of these defects, allowing a definition of their mechanical consequences, must also be improved. This requires the use of more sensitive ultrasonic transducers, with a larger bandwidth.

The main method used at present to increase the bandwidth of piezoelectric transducers entails an important decrease of their sensitivity : it is based on the damping of the piezoelectric wafer on its rear face. We suggest to use instead damping by a multilayer front face, which allows a simultaneous increase of both sensitivity and bandwidth. In order to study the feasibility of this process, a computing programme has been developed to calculate the propagation of a wave through several layers of different thicknesses. This programme makes it possible to optimize the characteristics (impedance and thickness) of the various layers making up the transducer. Comparisons with actual transducers allowed the validation of this theoretical model.

1. INTRODUCTION

L'évolution des techniques de fabrication et des qualités mécaniques exigées pour les pièces aéronautiques requiert un contrôle non destructif de plus en plus sévère. Les techniques de contrôle doivent donc s'affiner dans les prochaines années. En ce qui concerne les pièces maîtresses d'un turboréacteur que sont les disques de turbines et de compresseurs, la principale méthode utilisée est le contrôle par ultrasons en immersion (échographie). Les principales améliorations susceptibles d'être apportées à cette technique sont les suivantes :

(a) augmenter la résolution près de la surface des pièces à contrôler,

(b) détecter des défauts plus petits,

(c) améliorer l'évaluation quantitative des défauts détectés,

(d) rendre le contrôle plus automatique à la fois pour augmenter la productivité et pour s'affranchir de l'erreur humaine.

Actuellement de manière industrielle en ondes longitudinales, on ne détecte pas les défauts dans une zone de 3 à 4 mm d'épaisseur à partir de la face d'entrée des ultrasons. Ceci est dû à l'écho très important lié à la face d'entrée

qui masque pendant un certain temps (environ 1 μs) les échos liés aux défauts susceptibles de se trouver dans cette zone. Pour les pièces importantes des turboréacteurs (disques de turbines et de compresseurs par exemple), cette zone est enlevée au cours de l'usinage ce qui garantit que la pièce finale est sans défaut. Les nouvelles techniques de fabrication faisant appel à la métallurgie des poudres (hot isostatic pressing (HIP) and isothermal forging) peuvent produire des disques de dimensions plus proches des dimensions finales ce qui pourra réduire considérablement les coûts d'usinage et les quantités de matières utilisées. Il sera alors nécessaire de détecter des défauts beaucoup plus près des surfaces des pièces.

Parallèlement une amélioration du rapport de la poussée au poids d'un turboréacteur dépend de l'augmentation possible des efforts demandés aux pièces, laquelle est évidemment liée à l'amélioration de la connaissance de la répartition des contraintes mais aussi à la possibilité de détection de défauts plus petits et à leur meilleure évaluation quantitative.

2. LES CAUSES DES LIMITATIONS ACTUELLES

2.1. Résolution près de la surface

Le principe de l'échographie ultrasonore est schématisé sur la figure 1. Les ultrasons émis par un transducteur excité par une impulsion électrique sont transmis par de l'eau jusqu'à la surface de la pièce où ils sont partiellement réfléchis et partiellement transmis à travers l'interface. Les lois régissant la réflexion et la transmission sont parfaitement connues. Le fait important est que, pour l'angle du faisceau ultrasonore le plus favorable (incidence normale), moins de 15% de l'énergie est transmise à travers l'interface. Après la traversée de l'interface le faisceau ultrasonore peut interagir avec un défaut. L'énergie ultrasonore réfléchie par le défaut va de nouveau devoir traverser l'interface et seulement 15% sera encore transmise pour être finalement détectée par le transducteur. Globalement il existe un rapport de l'ordre de 10^{-6} entre le signal correspondant au plus petit défaut que l'on veut pouvoir détecter et le signal correspondant à la réflexion sur l'interface de la pièce.

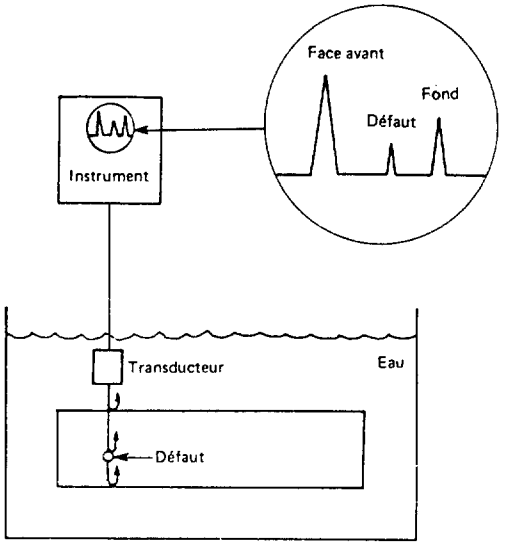

Fig. 1 – Schéma représentant un système d'échographie ultrasonore.

Pour avoir une bonne résolution en profondeur (dans la direction de propagation des ultrasons) il faut pouvoir distinguer les différents trains d'onde correspondant aux différents échos (échos d'interface et échos de défauts), il faut donc que ces trains d'onde soient les plus brefs possible. En particulier tant que le niveau du signal correspondant à l'écho sur l'interface n'est pas inférieur à celui du signal correspondant au plus petit défaut que l'on veut pouvoir détecter, ce type de défaut est masqué. On a ainsi une zone au voisinage de la surface des pièces où l'on ne peut détecter les défauts, l'épaisseur de cette zone dépend de la brièveté du signal détecté, laquelle est elle-même liée à celle du train d'onde.

La figure 2 illustre ce phénomène. Elle représente les signaux d'échographie détectés pour deux transducteurs ultrasonores de caractéristiques différentes en fonction du temps ou, ce qui revient au même, en fonction de la profondeur de pénétration des ultrasons dans la pièce. Le premier pic (dépassant le cadre de la figure) de chaque courbe correspond à l'écho d'interface, le deuxième à l'écho lié à un trou de 0,5 mm de diamètre visé perpendiculairement à sa génératrice. Pour la figure 2 a ce trou est à 5 mm de profondeur par rapport à la surface d'entrée des ultrasons alors que pour la figure 2 b il est à 10 mm. Nous observons que l'écho d'interface dans le cas (a) masque les défauts dans une zone d'environ 3 mm de profondeur alors que dans le cas (b) il masque une zone de l'ordre de 6 mm, c'est ce qui explique qu'il n'a pas été possible dans ce cas de détecter le trou situé à 5 mm de profondeur.

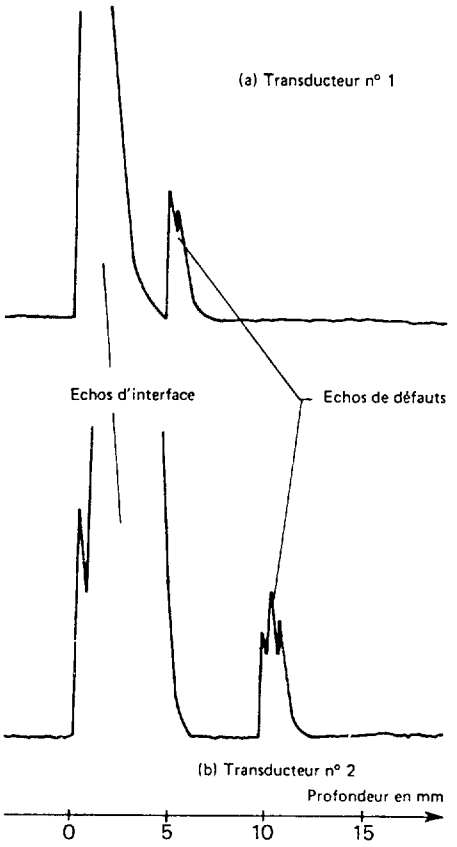

Fig. 2 – Signaux d'échographie pour deux transducteurs de caractéristiques différentes.

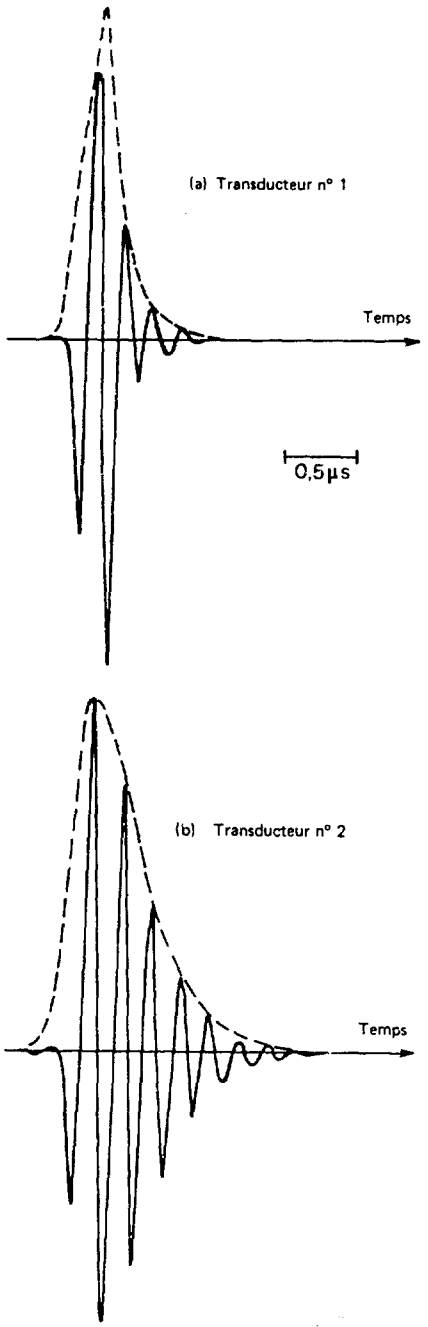

Fig. 3 – Réponses impulsionnelles mesurées des deux transducteurs (échographie sur un plan réflecteur).

Nous avons remarqué précédemment que l'épaisseur de la zone où les défauts sont masqués dépend de la durée du train d'onde ultrasonore émis. L'excitation électrique créant cette onde étant une impulsion, cette durée est liée à la réponse impulsionnelle du transducteur utilisé. Nous caractériserons expérimentalement cette réponse impulsionnelle en excitant le transducteur par une impulsion électrique très brève puis en détectant au moyen de ce même transducteur l'onde réfléchie par une surface plane perpendiculaire au train d'onde émis. Sur la figure 3 sont représentées les réponses impulsionnelles des deux transducteurs utilisés pour tracer les échogrammes représentés sur la figure 2. Nous remarquons que la réponse du premier transducteur (fig. 3 a) est beaucoup plus brève que celle du deuxième transducteur (fig. 3 b) qui était moins performant sur le plan de la résolution au voisinage de la surface (fig. 2 b). Sur cette figure est également tracée l'enveloppe du signal (signal détecté), laquelle est seule représentée sur les appareils utilisés en contrôle industriel : c'est cette enveloppe qui est représentée sur la figure 2.

Il est bien connu que la durée de la réponse impulsionnelle d'un système quelconque est inversement proportionnelle à sa bande passante : c'est ce que nous observons sur la figure 4 où est présentée la réponse spectrale de chacun des deux transducteurs utilisés. Notons cependant que la condition de large bande passante ne suffit pas, la forme de la réponse spectrale est importante ; suivant cette forme des rebondissements de la réponse impulsionnelle peuvent se produire. Un exemple très théorique est donné sur la figure 5 correspondant à une forme de réponse spectrale en créneau. Nous observons des rebondissements de la réponse impulsionnelle. Remarquons que ce cas particulier ne peut absolument pas représenter la réponse réelle d'un transducteur car un système ayant ces caractéristiques n'obéirait pas au principe de causalité. Cet exemple est une simple illustration du phénomène décrit. La forme idéale (minimisant les rebondissements) de la réponse spectrale pour une bande passante donnée est une courbe de Gauss avec une caractéristique de phase linéaire [1].

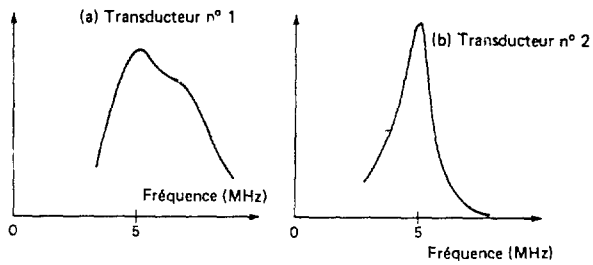

Fig. 4 – Réponses spectrales de ces mêmes transducteurs (échelle linéaire).

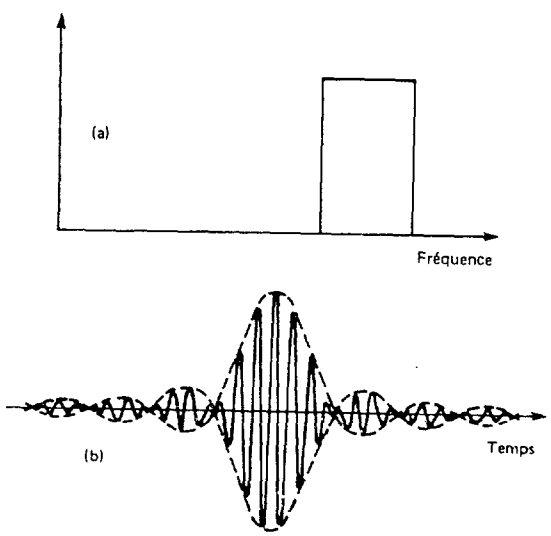

Fig. 5 – Exemple purement théorique d'une forme de réponse spectrale non optimale (a) réponse spectrale ; (b) réponse impulsionnelle.

2.2. Evaluation des défauts

Le contrôle non destructif a pour but de détecter tous les défauts dans une pièce, qui entraîneront une perte de performances mécaniques la rendant inapte à l'utilisation prévue. Suivant la zone de la pièce ou suivant la pièce elle-même, les efforts seront plus ou moins grands, on pourra donc tolérer des défauts plus ou moins importants. Il est donc nécessaire d'évaluer le défaut ou de le caractériser pour en déduire les conséquences mécaniques sur la pièce. Actuellement cette évaluation se fait par comparaison de l'amplitude de l'écho ultrasonore lié au défaut avec celle de l'écho lié à un défaut-type (fond plat d'un trou ou trou cylindrique visé perpendiculairement à sa génératrice) dans un échantillon de composition identique. Le choix d'un échantillon de composition identique a pour but de s'affranchir de toutes les variations d'énergie qui dépendent de la transmission de l'onde ultrasonore au niveau de l'interface eau-matériau. Cette transmission est fonction des propriétés acoustiques du matériau (impédance). Remarquons qu'il est théoriquement possible de tenir compte de ces variations de transmission d'un matériau à l'autre et donc de faire l'étalonnage sur des défauts-type dans un autre matériau. Finalement la seule grandeur mesurée dans ce contrôle est l'amplitude de l'onde ultrasonore rétrodiffusée par le défaut. On conçoit aisément que cette amplitude dépend d'un très grand nombre de paramètres du défaut (orientation, forme, état de surface, ...), qui pour certains n'ont aucune relation avec les conséquences mécaniques de la présence de ce défaut. De nouvelles méthodes sont à l'étude qui permettront de beaucoup mieux caractériser les défauts. Elles font appel à l'analyse spectrale d'une onde ultrasonore diffusée (dans une ou plusieurs directions) par le défaut. Présentons comme exemple (fig. 6) un résultat extrait de [2]. Les courbes de cette figure sont les spectres des ondes rétrodiffusées par une cible circulaire de 3,2 mm de diamètre, la cible étant placée sous différents angles par rapport à l'onde incidente. Nous notons une très grande variation de la forme du spectre en fonction de l'angle, cette variation de forme s'accompagne évidemment d'une variation de niveau qui n'est pas représentée sur la figure. Une variation de niveau pourrait être interprétée comme une variation de l'importance du défaut alors que le spectre nous donne des renseignements supplémentaires qui permettent dans ce cas de déterminer l'angle d'incidence. L'interprétation de telles mesures est évidemment très complexe et loin d'être résolue actuellement.

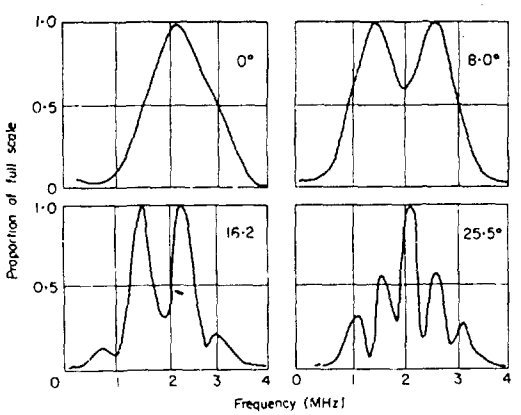

Fig. 6 – Densité spectrale pour un réflecteur de 3,2 mm de diamètre à différentes valeurs de l'angle d'incidence.

Il nous suffit cependant de comprendre que la caractérisation d'un défaut nécessite une très grande quantité d'informations au sens de la théorie du traitement des signaux. Cette importante quantité d'informations fournie par les signaux détectés à partir de la diffusion d'ondes ultrasonores dans une ou plusieurs directions devra subir un traitement complexe (analyse spectrale, reconnaissance de formes, ...), qui permettra de classer les défauts dans le but de les caractériser. Rappelons qu'un signal contient une quantité d'informations proportionnelle à la largeur de son spectre, on peut en déduire que l'évaluation d'un défaut au moyen des techniques ultrasonores ne sera possible qu'au moyen de transducteurs à large bande. Rappelons aussi cependant qu'une autre amélioration des techniques demandée est la détection de défauts plus petits, ce qui entraîne qu'il est nécessaire simultanément à l'augmentation de la bande passante des transducteurs d'augmenter leur sensibilité.

Nous pouvons conclure que l'amélioration des techniques faisant appel aux ultrasons nécessite l'augmentation de la bande passante des transducteurs sans perte de sensibilité, aussi bien pour augmenter la résolution près de la surface des pièces que pour obtenir une évaluation quantitative des défauts.

3. CONCEPTION DE TRANSDUCTEURS A LARGE BANDE

En échographie (fig. 1) le même transducteur est utilisé pour générer l'onde ultrasonore et pour détecter les ondes réfléchies par les défauts, on utilise donc pour cela des transducteurs réversibles. Pour simplifier l'exposé on s'intéressera principalement à leur fonctionnement en émetteur sachant que le fonctionnement en récepteur est analogue.

Les transducteurs ultrasonores utilisés en contrôle non destructif utilisent une lame piézoélectrique comme élément de couplage électromécanique (c'est l'élément qui transforme l'énergie électrique en énergie vibratoire et inversement). Ils sont constitués principalement de (fig. 7) :

– la lame piézoélectrique (souvent une céramique) métallisée sur ses deux faces pour la connexion électrique,

– un matériau sur la face arrière de la lame piézoélectrique (son rôle est d'amortir la vibration de la lame et d'absorber l'onde acoustique émise vers l'arrière),

– une face avant (ses deux rôles possibles sont : assurer la protection mécanique de la lame piézoélectrique et améliorer le transfert acoustique entre cette lame et le milieu de couplage),

– un boitier enfermant le tout.

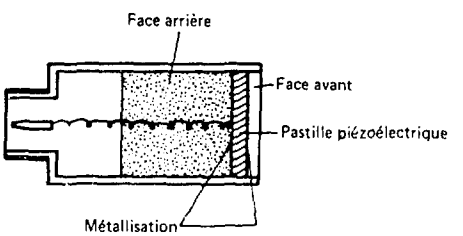

Fig. 7 – Constitution d'un transducteur piézoélectrique.

Considérons pour commencer un transducteur composé uniquement d'un élément piézoélectrique d'impédance Z_c et d'une face arrière d'impédance Z_o (fig. 8). Supposons ce transducteur immergé dans un milieu (le milieu de propagation des ultrasons ou milieu de couplage) d'impédance Z_∞. Si l'on excite l'élément piézoélectrique par une impul-

sion électrique, l'énergie fournie par le générateur va être transformée en énergie acoustique (ou vibratoire) ; sous certaines hypothèses, il sera créé aux niveaux des interfaces quatre impulsions de pression représentées sur la figure 8 [3, 4] :

- impulsion (0) proportionnelle à $Z_o/(Z_o + Z_c)$ se propageant vers l'arrière, cette impulsion devra être absorbée par la face arrière,
- impulsion (1) proportionnelle à $Z_c/(Z_o + Z_c)$ se propageant vers l'avant,
- impulsion (2) proportionnelle à $Z_c/(Z_c + Z_\infty)$ se propageant vers l'arrière,
- impulsion (3) proportionnelle à $Z_\infty/(Z_c + Z_\infty)$ se propageant vers l'avant.

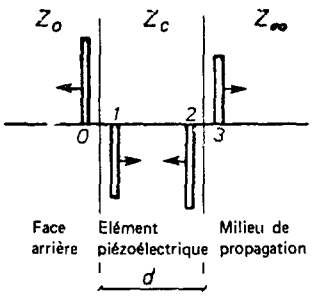

Fig. 8 – Génération d'impulsions mécaniques par effet piézoélectrique.

Après réflexion et transmission au niveau des deux interfaces de l'élément piézoélectrique, les impulsions (1), (2) et (3) donnent au niveau de la face avant du transducteur, en fonction du temps, une pression acoustique représentée sur la figure 9. On constate que la variation de pression est quasi-périodique (de périodicité égale au double du temps de propagation dans l'élément piézoélectrique et constituant la période nominale : $T_N = 1/f_N$). La durée de cette variation dépend des coefficients de réflexion aux interfaces.

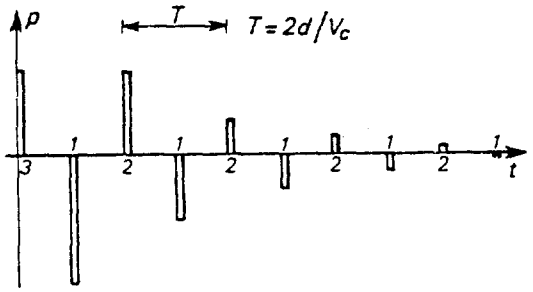

Fig. 9 – Pression acoustique en fonction du temps.

On peut considérer que l'élément piézoélectrique se comporte comme un résonateur mécanique excité par l'impulsion électrique. La dissipation d'énergie de ce résonateur est principalement due au rayonnement acoustique par la face arrière (énergie perdue parce que dissipée dans le matériau constituant cette face) et par la face avant (énergie utile). On peut en conclure que :

(i) l'efficacité du transducteur dépend du coefficient piézoélectrique (ou du facteur de couplage électromécanique) et du rapport entre l'énergie acoustique transmise par la face avant à l'énergie acoustique transmise par la face arrière,

(ii) la bande passante dépend du rapport de l'énergie rayonnée à l'énergie mécanique (ou vibratoire) emmagasinée dans la lame piézoélectrique au moment où est produite l'impulsion électrique.

Ces considérations permettent d'envisager d'augmenter la bande passante des transducteurs en créant un amortissement de l'élément piézoélectrique au niveau de sa face arrière ou/et de sa face avant.

3.1. Amortissement par la face arrière

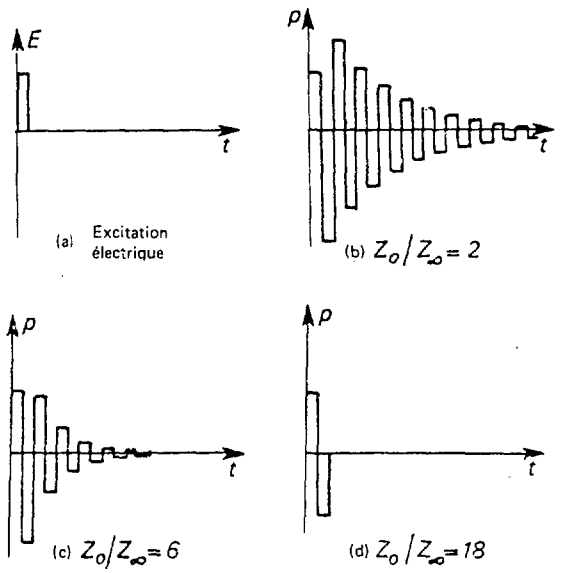

Fig. 10 – Réponses de transducteurs (amortissement par la face arrière).

La méthode la plus classique consiste à augmenter le rayonnement d'énergie par la face arrière. Il suffit pour cela d'augmenter le rapport Z_o/Z_c, le rapport optimal pour l'élargissement de la bande passante étant 1. Cette méthode a cependant l'inconvénient de diminuer l'énergie rayonnée vers l'avant donc l'efficacité du transducteur, compte-tenu du fait que les impédances de l'élément piézoélectrique et du milieu de propagation sont généralement fixées. Pour illustrer ce phénomène, nous présentons sur la figure 10 la réponse en pression de transducteurs excités par une impulsion électrique de durée égale au temps de propagation d'une onde acoustique dans l'épaisseur de l'élément piézoélectrique (fig. 10 a). Le choix de cette excitation électrique a été effectué pour minimiser dans le calcul l'effet des très hautes fréquences, qui dans la réalité sont beaucoup plus vite atténuées que les basses fréquences. Nous observons que pour des impédances de la face arrière élevées le signal est plus bref (donc la bande passante plus grande) mais son amplitude est plus faible. Ce phénomène est encore accentué en échographie quand le transducteur est utilisé en émetteur puis récepteur après réflexion de l'ordre ultrasonore sur un obstacle (interface de la pièce ou défaut). Le signal détecté (s'il y a eu réflexion parfaite de l'onde ultrasonore, par exemple sur un plan perpendiculaire au faisceau) est alors proportionnel au produit de convolution de la fonction précédemment calculée (fig. 10) par elle-même. La figure 11

présente la simulation d'un tel cas pour les mêmes impédances que celles utilisées dans la figure 10. La figure 12 représente la réponse spectrale des mêmes transducteurs que précédemment également dans les conditions d'utilisation de l'échographie. Ces réponses sont chacune normalisées en amplitude pour permettre une comparaison plus aisée des bandes passantes. Nous observons évidemment une bande passante beaucoup plus étroite pour les transducteurs dont les impédances des faces arrières sont faibles.

Notons que la réponse spectrale d'un transducteur au sens rigoureux du terme est en fait proportionnelle à la racine carrée de celle représentée sur la figure 12. Nous avons choisi cette représentation car elle correspond aux conditions expérimentales utilisées (par exemple pour le résultat de la figure 4), donc facilite la comparaison entre la théorie et l'expérience.

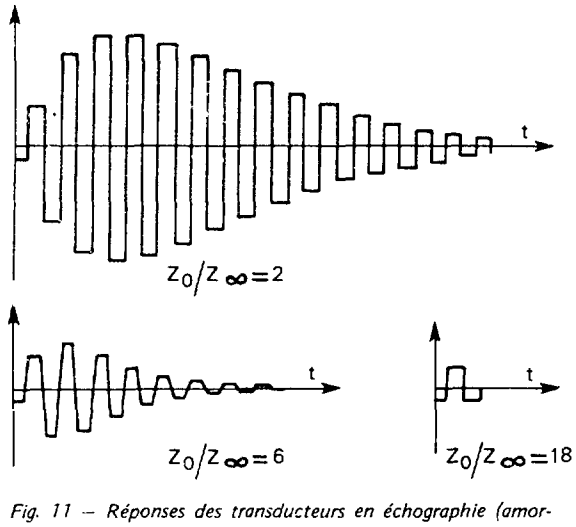

Fig. 11 – Réponses des transducteurs en échographie (amortissement par la face arrière) $Z_c/Z_\infty = 18$.

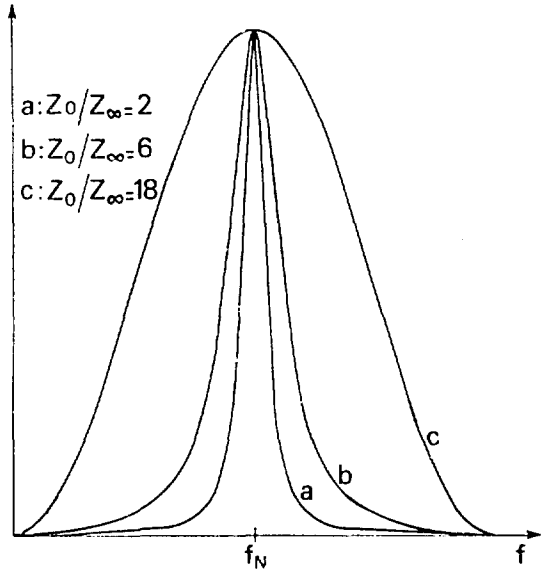

Fig. 12 – Réponses spectrales des transducteurs en échographie (amortissement par la face arrière) - $Z_c/Z_\infty = 18$ - les courbes ont été normalisées par rapport à leurs maximums.

3.2. Amortissement par la face avant

On peut également augmenter le rayonnement d'énergie vers l'avant par l'utilisation de couches adaptatrices d'impédance entre l'élément piézoélectrique et le milieu de propagation. On sait que pour une onde monochromatique, on peut augmenter la transmission entre deux milieux en intercalant une lame entre ces deux milieux. La transmission sera maximale pour une lame d'impédance égale à la moyenne géométrique des impédances des deux milieux et d'épaisseur égale au quart de la longueur d'onde. C'est un principe bien connu et largement utilisée en optique par exemple où le traitement des lentilles par de telles couches permet une bien meilleure transmission. Le problème est cependant plus complexe pour les transducteurs ultrasonores pour deux raisons :

(i) parce que les rapports des impédances des milieux entre lesquels on veut améliorer la transmission est beaucoup plus grand (dans le cas que l'on étudie il est de l'ordre de 20, alors que en optique il est de l'ordre de 1,5),

(ii) parce que l'on veut améliorer la transmission dans un domaine de fréquence des ultrasons étendu (transducteur à large bande).

Dans ce cas le principe exposé précédemment n'est plus valable ; pour optimiser de telles couches adaptatrices d'impédance, on est obligé de calculer la réponse impulsionnelle d'un transducteur en comportant. Plusieurs auteurs [5, 6, 7] ont abordé ce problème au moyen de l'analogie électromécanique des transducteurs ultrasonores; nous avons préféré [8] étudier la propagation de chaque impulsion de pression générée aux interfaces de la lame piézoélectrique dans un milieu stratifié pouvant comporter jusqu'à cinq couches (le milieu constituant la face arrière d'impédance Z_0, la lame piézoélectrique d'impédance Z_c, deux couches constituant la face avant d'impédance Z_1 et Z_2 et le milieu de propagation d'impédance Z_∞). Ce sont ces impulsions qui après propagation dans ces différentes couches créent le champ ultrasonore du transducteur. Nous pourrons ainsi optimiser théoriquement la conception d'un transducteur à face avant multicouche.

4. CALCUL DE LA RÉPONSE D'UN TRANSDUCTEUR

4.1. Principe du calcul

Comme nous l'avons exposé précédemment une excitation électrique impulsionnelle crée aux interfaces de la lame piézoélectrique quatre impulsions de pression représentées sur la figure 13 schématisant le transducteur. Nous supposerons toujours que la face arrière est très absorbante et donc que l'impulsion (0) qui y est créée est complètement absorbée et ne peut revenir vers l'avant. Par contre les impulsions (1), (2) et (3) vont être transmises et réfléchies à chacune des interfaces entre les différentes couches et produiront une variation de pression dans le milieu de propagation. A un instant donné la pression produite par le transducteur sera donc égale à la somme des impulsions qui auront mis le même temps pour se propager depuis leur lieu de création jusqu'au point considéré. Il est donc nécessaire de dénombrer tous les trajets possibles de propagation de chaque impulsion à travers les différentes couches, de calculer pour chacun d'eux le coefficient de transmission et le temps de propagation. Par une sommation à chaque instant de ces différentes impulsions on obtient la réponse impulsionnelle du transducteur. Le

détail de la modélisation de ce calcul est exposé en [8]. La principale difficulté du programme de calcul provient du nombre très important de trajets possibles, lequel s'accroît de manière exponentielle en fonction de la longueur des trajets pris en compte (ou ce qui revient au même en fonction du temps de propagation). Pour donner un ordre de grandeur de ce nombre, il suffit de préciser que pour calculer le temps de réponse d'un tel transducteur sur un intervalle de temps égal à dix fois la période nominale du transducteur, nous avons pris en compte plus de 10^6 trajets différents.

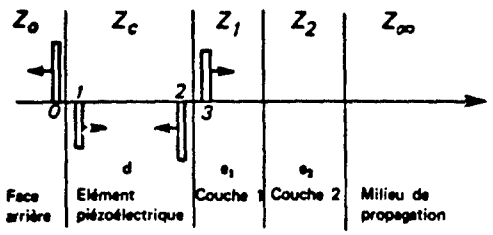

Fig. 13 – Schéma d'un transducteur à face avant à deux couches.

4.2. Présentation de quelques résultats

La figure 14 permet la comparaison des réponses de transducteurs à la même excitation que dans le cas de la figure 10. Les transducteurs simulés par ce calcul ont une face arrière d'impédance $Z_o/Z_\infty = 2$ et une lame piézoélectrique d'impédance $Z_c/Z_\infty = 18$. Nous constatons que le fait de rajouter une lame d'impédance $Z_1/Z_\infty = 2$ et d'épaisseur $e_1 = \lambda_1/4$ (où λ_1 est la longueur d'onde dans le matériau constituant la lame pour la fréquence nominale du transducteur) permet d'améliorer à la fois le temps de réponse, et l'efficacité du transducteur d'un rapport au moins égal à 2. Une face avant à deux couches ($Z_1/Z_\infty = 6$, $Z_2/Z_\infty = 2$) améliore encore le résultat tant en temps de réponse qu'en sensibilité (fig. 14 d). Nous pouvons également observer sur la figure 15 l'effet de ces couches sur la réponse spectrale des transducteurs dans les mêmes conditions que celles de la figure 12. Comme nous le verrons par la suite l'impédance $Z_1 = 2{,}7 \times Z_\infty$ pour une face avant à une seule couche est l'impédance optimale. La forme de la réponse spectrale de la figure 15 c peut nous faire supposer que les valeurs des impédances Z_1 et Z_2 ne sont pas les valeurs optimales.

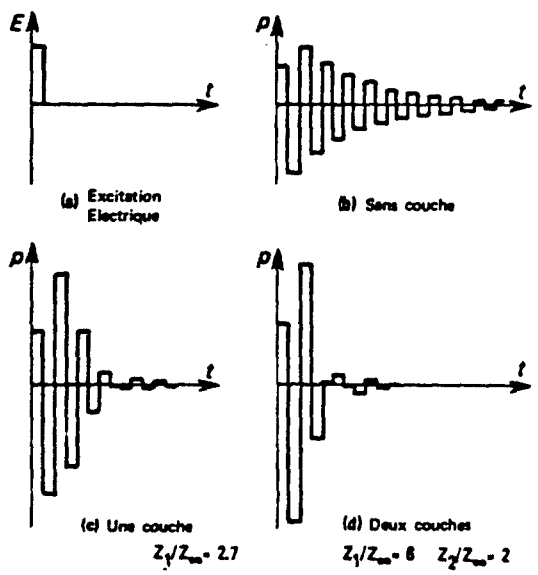

Fig. 14 – Résultats de calcul ($Z_c/Z_\infty = 18$, $Z_o/Z_\infty = 2$).

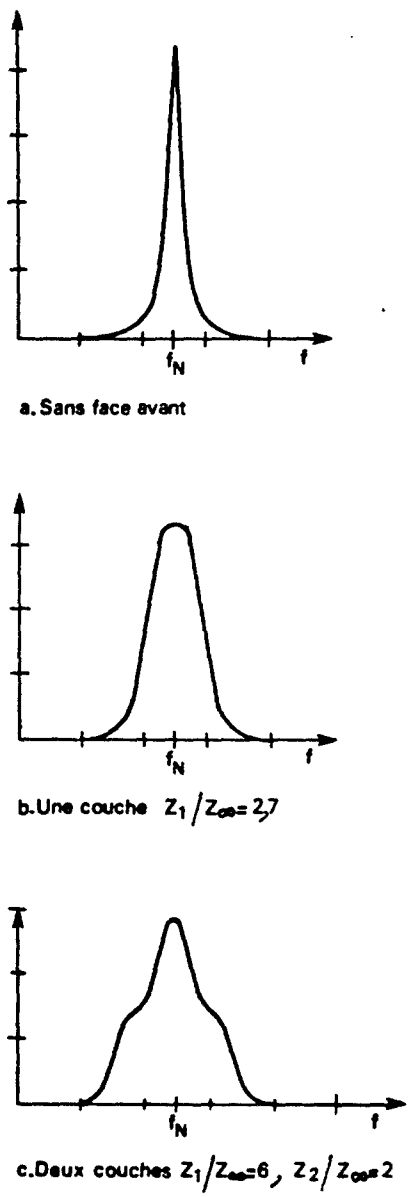

Fig. 15 – Réponse spectrale des transducteurs en échographie ($Z_c/Z_\infty = 18$, $Z_o/Z_\infty = 2$).

4.3. Optimisation des transducteurs

Ce programme de calcul permet d'optimiser les impédances et les épaisseurs des différentes couches dont est revêtu un transducteur, en fonction de l'utilisation qui en sera faite. La figure 16 nous permet de déterminer l'impédance optimale d'une couche unique d'adaptation au niveau de la face avant du transducteur dans le cas où l'on s'intéresse à une réponse impulsionnelle la plus courte possible. On peut remarquer que cette impédance optimale dans le cas étudié ($Z_g/Z_\infty = 2$, $Z_c/Z_\infty = 18$) est égale à 2,7 × Z_∞, les impédances plus faibles entraînant une réponse impulsionnelle insuffisamment amortie et les impédances plus fortes entraînant une réponse impulsionnelle ayant des rebondissements qui peuvent être très néfastes, par exemple pour détecter des défauts près de la surface d'une pièce. L'épaisseur de la couche est égale dans ce cas à $\lambda_1/4$, où λ_1 est la longueur d'onde dans le matériau constituant la couche pour la fréquence nominale du transducteur. Nous pouvons remarquer que l'optimisation ainsi obtenue ne correspond pas à celle de la transmission pour une onde monochromatique : cette optimisation serait en effet obtenue pour $Z_1/Z_\infty = 4$.

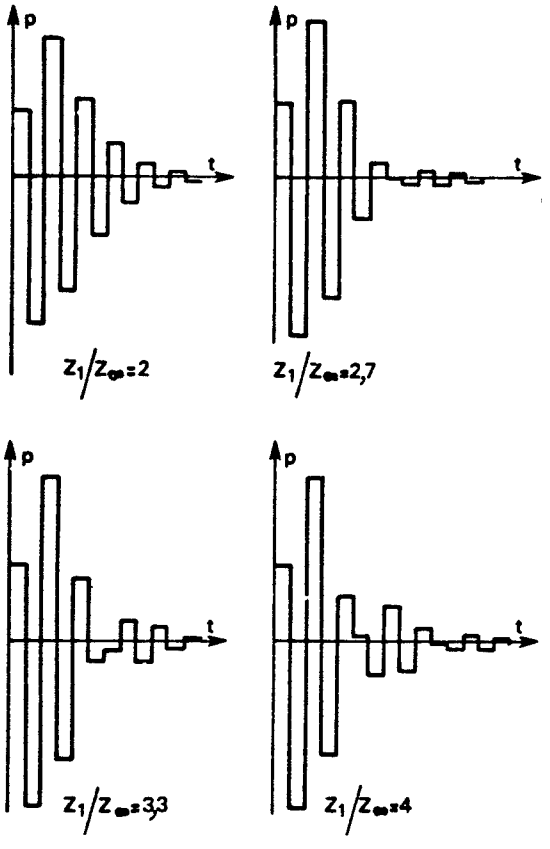

Fig. 16 – Optimisation de l'impédance d'une couche unique. ($Z_g/Z_\infty = 2$, $Z_c/Z_\infty = 18$).

De la même manière, l'épaisseur de la couche d'adaptation a une importance primordiale sur la réponse du transducteur. On sait que pour une onde monochromatique la transmission est optimale pour une épaisseur de cette couche de $\lambda_1/4$, $3\,\lambda_1/4$, $5\,\lambda_1/4$, ...; ce n'est plus vrai pour une onde impulsionnelle. Nous pouvons en effet observer sur les figures 17 et 18 les réponses temporelles et spectrales dans le cas d'une couche d'impédance $2{,}7 \times Z_\infty$ d'épaisseur $\lambda_1/4$ et $3\,\lambda_1/4$. Nous constatons un rétrécissement important de la bande passante correspondant à un amortissement moins bon et des rebondissements de la réponse temporelle dans

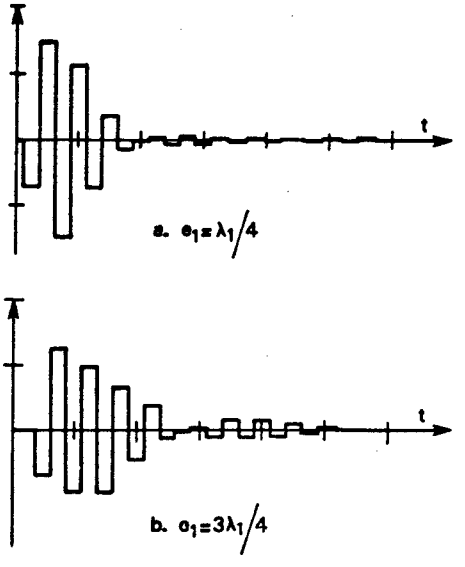

Fig. 17 – Réponse d'un transducteur dont la face avant comporte une couche d'impédance $Z_1/Z_\infty = 2{,}7$ ($Z_g/Z_\infty = 2$; $Z_c/Z_\infty = 18$) ; (a) $e_1 = \lambda/4$; (b) $e_1 = 3\,\lambda/4$ (même condition d'excitation que figure 10).

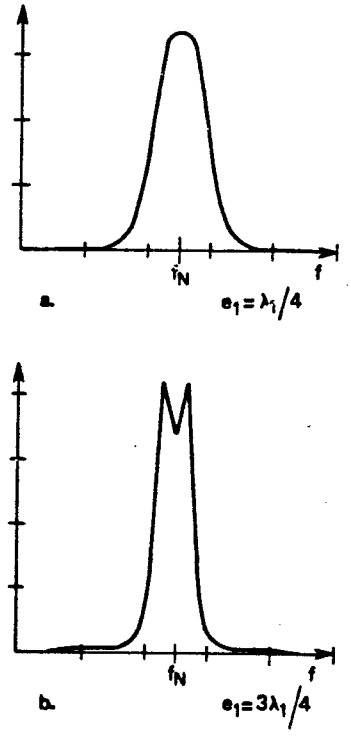

Fig. 18 – Réponse spectrale dans le même cas que la figure 17 (mêmes conditions que figure 12).

le cas où l'épaisseur est égale à 3 $\lambda_1/4$.

Un autre exemple d'optimisation qu'il est possible d'effectuer est présenté sur la figure 19. Pour une face avant imposée par des contraintes de fabrication (dans l'exemple choisi cette face avant est constituée d'une lame de verre et d'une lame de résine époxy), il peut être intéressant d'optimiser l'impédance de la face arrière pour obtenir une forme de la réponse spectrale adaptée à l'utilisation qui sera faite du transducteur. Pour certaines applications où il est nécessaire d'avoir une très bonne sensibilité, la réponse de la figure 19 a sera la plus intéressante. Si l'on veut une réponse spectrale plus régulière, on sera par contre obligé d'augmenter l'impédance de la face arrière. On obtient alors la réponse spectrale présentée sur la figure 19 c.

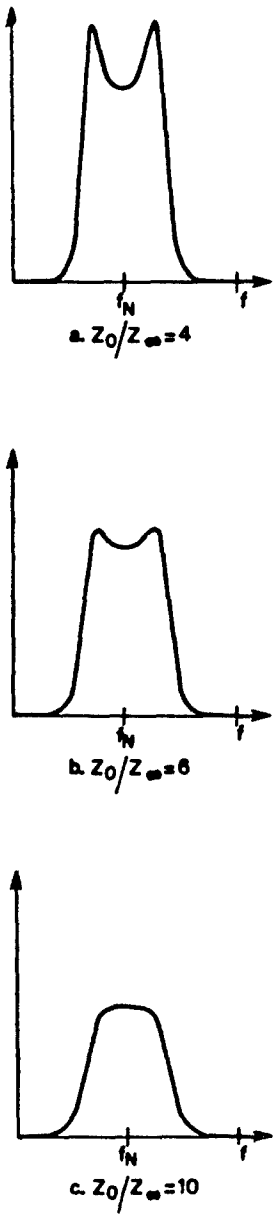

Fig. 19 – Réponse spectrale de transducteurs à face avant à deux couches en fonction de l'impédance de la face arrière.

5. COMPARAISON AVEC DES TRANSDUCTEURS RÉELS

Des transducteurs ayant des faces avant composées d'une ou deux couches ont été fabriqués. Leur réponse a été mesurée en échographie (comme pour la figure 3). La figure 20 permet de comparer les résultats théoriques aux mesures correspondantes. Nous observons un accord satisfaisant compte tenu des phénomènes négligés (effet piézoélectrique inverse par exemple).

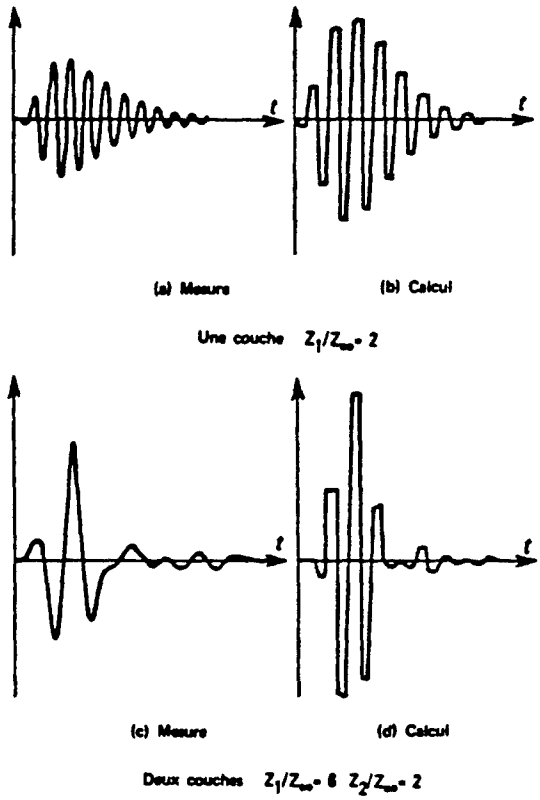

Fig. 20 – Comparaison entre les résultats du calcul et de la mesure.

Cette méthode de calcul peut de plus donner des indications sur les défauts de fabrication des transducteurs. Nous présenterons un seul exemple de ce cas : après fabrication d'un transducteur à face avant à deux couches quart-d'onde ($Z_0/Z_\infty = 6$, $Z_1/Z_\infty = 10$, $Z_2/Z_\infty = 2$ et $Z_c/Z_\infty = 18$, $e_1 = \lambda_1/4$ et $e_2 = \lambda_2/4$) nous avons mesuré sa réponse spectrale en échographie, qui est présentée sur la figure 21. Nous observons deux pics d'inégales hauteurs alors que le calcul prévoit deux pics d'égales hauteurs (fig. 22 a). Un deuxième calcul effectué avec les mêmes paramètres excepté l'épaisseur de la couche (1) qui a été prise 20% plus faible donne une réponse spectrale présentée sur la figure 22 b. Nous observons une diminution importante du deuxième pic comme sur la réponse expérimentale. Nous pouvons ainsi attribuer cette irrégularité de la réponse spectrale du transducteur réalisé à une imprécision de l'épaisseur d'une des couches de la face avant.

Remarque - Signalons pour donner une idée de la difficulté de fabrication de tels transducteurs que la couche (1) dans le cas étudié est une couche de verre de 300 µm d'épaisseur

et la couche (2) une couche de résine époxy de 130 μm d'épaisseur, ce qui explique l'imprécision obtenue sur les épaisseurs de ces couches.

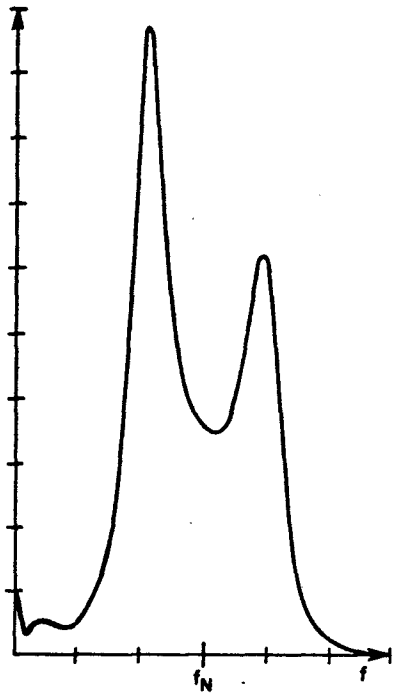

Fig. 21 – Réponse spectrale mesurée d'un transducteur à face avant à deux couches (Z_e/Z_{co} = 6, Z_1/Z_{co} = 10, Z_2/Z_{co} = 2, Z_c/Z_{co} = 18 ; $e_1 = \lambda_1/4$, $e_2 = \lambda_2/4$).

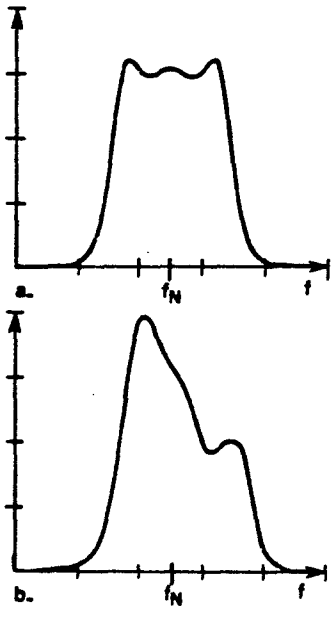

Fig. 22 – Réponse spectrale calculée : (a) transducteur de caractéristiques identiques à figure 21 ; (b) transducteur de mêmes caractéristiques sauf e_1 = 0,8 ($\lambda_1/4$).

6. CONCLUSIONS

Les résultats obtenus tant par le calcul que par les premières réalisations de transducteurs ultrasonores à face avant multicouche permettent de conclure que de tels transducteurs auront une meilleure efficacité et une meilleure bande passante que les transducteurs de conception classique. Ceci permettra de résoudre un certain nombre de problèmes qui se posent en contrôle non destructif par ultrasons (augmentation de la résolution près de la surface des pièces, détection de défauts plus petits, ...).

La méthode de calcul présentée permet de guider la réalisation de tels transducteurs qui seront adaptés aux applications envisagées, d'une part en fournissant par une étude paramétrique les caractéristiques de fabrication et d'autre part en permettant l'interprétation de leurs réponses mesurées, en fonction des défauts de fabrication.

REFERENCES

[1] F.K. SITTIG – High speed ultrasonic delay line design : A restatement of some basic considerations. *Proc. IEEE* 56-7, p. 1194-1202 (1968).

[2] L. ADLER, K.V. COOK et W.A. SIMPSON – Ultrasonic frequency analysis. *Research Techniques in Non Destructive Testing*, vol. 3, Academic Press, 1977.

[3] E.G. COOK – Transient and steady-state response of ultrasonic piezoelectric transducers. *IRE Convention Record* 1956, part 9, p. 61-69.

[4] M. REDWOOD – A study of waveforms in the generation and detection of short ultrasonic pulses. *Applied Materials Research*, April 1963, p. 76-84.

[5] J.P. SIMANSKI, J. POULIQUEN et A. DEFEBVRE – Loading transducers for non-destructive testing and signal processing by acoustic bulk waves. *Ultrasonics*, May 1974, p. 100-105.

[6] P.J. HIGHMORE – Impedance matching at ultrasonic frequencies using thin transition layers. *Ultrasonics International 1973 Conference Proceedings.*

[7] C.S. DESILETS, J.D. FRASER et G.S. KINO – The design of efficient broad-band piezoelectric transducers. *IEEE Trans.* SU-25, No. 3 (May 1978).

[8] J.-F. de BELLEVAL et D. LECURU – Improvement of ultrasonic transducers by using a multilayer front face. 1978 *IEEE Ultrasonics Symposium Proceedings - T.P. ONERA* n° 1978-114.

SELECTIVE BIBLIOGRAPHY

The bibliography which follows has been prepared by the AGARD Technical Information Panel and is a compilation of references selected specially to suit this particular Lecture Series : it is not intended to be comprehensive. It is regretted that AGARD cannot undertake to provide copies of the documents listed. These should be sought from the organizations which published them.

I	MOTEURS D'AVIONS	B-1
II	MOTEURS NON EXPLICITEMENT D'AVIONS	B-5

I. MOTEURS D'AVIONS

C-74-F01328 CA-TLSE
LA FIABILITE VECUE DANS LA PRATIQUE A AIR FRANCE.
Ravier (Mo), FRY(Fo), CYPKIN (Ro).
Air France
Aéronaut. et Astronaut. : (Fr.), N° 42 (1973-4), pp. 17-37, 18 fig. 3 tabl.

Présentation d'une série de trois exposés sur la fiabilité : théorie et pratique de la fiabilité des équipements : importance des moyens de surveillance d'état des moteurs ; fiabilité avion et systèmes (ACA-DA).
Fiabilité avion. Fiabilité. Equipement de bord. Entretien maintenance aéronef. Moteur aéronef. Méthodes statistiques. Opération compagnie aérienne. Détection défauts. Surveillance.
Air France. Temps moyen entre pannes. Contrôle non destructif. Intervention Etat. 01 02. 14 04.

C-78-006341 MD
CRITICAL INSPECTION OF BEARINGS FOR LIFE EXTENSION
(Inspection critique de paliers en vue de la prolongation de leur durée de vie).
Barton(J.R.) , Kusenberger (F.N.), Smith (R.T.).
Advisory Group for Aerospace Research and Development
AGARD Conference Proceedings, vol CP-234, N°12 (3/78), pp. 1-29, 26 réf. bibl. 1 fig. 1 tabl., 22 phot. Voss (27-29/9/77), ISBN 92-835-0213-2. Me.372-15

Recherches effectuées pour le développement de méthodes de contrôle non destructif plus sûres (en particulier contrôle magnétique)
Palier. Fiabilité. Contrôle qualité. Durée vie matériel. Essai non destructif. Moteur aéronef.
Propriété magnétique. Domaine magnétique. Détection défaut. Contrainte résiduelle. Installation essai.
Signature magnétique. Roulement bille.
Contrôle non destructif. Programme fiabilité. Pratt Whitney J57 moteur.

C-77-03395 MD
ACCEPTABLE METHODS TECHNIQUES AND PRACTICES. AIRCRAFT INSPECTION AND REPAIR
(Inspection et réparation d'un avion. Méthodes, techniques et pratiques acceptables).
Federal Aviation Administration (US),
FAA-AC-43-13-1A
Advisory Circular (1972), 333 p. , nombr. fig., tabl. et Phot. (Comprend l'Amendement du 5/12/75).

Cet ouvrage comporte 16 chapitres traitant de l'inspection de la réparation des aéronefs. Réparation des structures, des revêtements, du câblage, des équipements, des systèmes électriques, radio et électroniques de rotors, hélices et moteurs. Protection contre la corrosion (CAEN/GM).
Entretien maintenance aéronef. Réparation. Norme. Etats Unis. Inspection. Accessoire aéronef. Cellule aéronef. Equipement électrique aéronef. Structure aéronef. Moteur aéronef. Protection corrosion. Essai non destructif.

C-78-006674 MD
X-RAY DIFFRACTION : FROM STRUCTURAL X-RAY DIFFRACTOGRAPHY TO X-RAY OSCILLOGRAPHIC DIFFRACTOSCOPY
(La diffraction des rayons X : de la diffractographie à la diffractoscopie oscillographique des structures).
TRONCA (A.).
Advisory Group for Aerospace Research and Development,
AGARD Conference Proceedings, vol. CP-234, N°8(3/78), pp. 1-12, 3 réf. bibl., 3 tabl. , 12 phot.
Voss (27-29/9/77), ISBN 92-835-0213-2.
Me. 372-15

Résultats obtenus par trois méthodes d'inspection rapide d'aubes de compresseurs de moteurs à réaction: diffractographie classique de rayons X ; inspection oscillographique rapide.
Rayon X. Diffraction. Essai non destructif. Film radiographique. Oscillographe. Détection défaut.
Aube compresseur. Moteur réaction. Alliage aluminium. Acier. Courant Foucault. Analyse diffraction rayon X. Contrôle non destructif.

C-78-006411 MD
SURFACE CORROSION EVALUATION BY RELATIVE MAGNETIC SUSCEPTIBILITY MEASUREMENTS
(Analyse de la corrosion de surface par des mesures de susceptibilité magnétique relative).
Walther (H.).
Advisory Group for Aerospace Research and Development.
AGARD Conference Proceedings, vol. CP-234,N°6(3/78), pp. 1-11, 1 réf, bibl., 11 fig. Voss (27-29/9/77),
ISBN 92-835-021 3-2.
Me. 372-15

Etudes d'aubes de turbines d'avions en In-100, d'aubes de turbines de centrales et d'échantillons de fluage en INCONEL X-750 : principe de la méthode,
Susceptibilité magnétique. Résistance corrosion. Propriété surface. Essai non destructif.
Superalliage. Alliage nickel. Acier inoxydable. Mesure expérimentale. Transformation phase.
Oxydation. Carbonisation. Aube turbine. Détection défaut.
Contrôle non destructif. Oxydation alliage. Inconel alliage.

A-77-011606 MD
MAGNETIC PARTICLE INSPECTION OF AVIATION ENGINS VANES
Aleksandrov (A.G.), Shelikhov (S.G.)
Soviet Journal of Nondestructive Testing, vol. 12, N°1, Nov. 1976, p. 62-65

Translation. Magnetic Measurement. Jet Vanes. Nondestructive Tests. Powder Particles. Aircraft Engines. Cracking Fracturing.

A-77-011603 MD
SIGNAL-TREATMENT METHODS DURING AIRCRAFT-ENGINE INSPECTION BASED ON VIBROACOUSTIC NOISES.
Izokh (V.V.), Mikulovich (V.I.)
Soviet Journal of Nondestructive Testing, vol.12, N°1, Nov 1976, p. 29-34. 15 refs.

Engine Design. Acoustic Measurements. Aircraft Engines. Spectrum Analysis. Signal to noise ratios. Nondestructive Tests. Translation.

AD-A036 000/8SL MD
EVALUATION OF CALIFORNIUM-252-BASED NEUTRON RADIOGRAPHY AND PHOTON SCATTERING TECHNIQUES FOR THE INSPECTION OF HOT ISO-STABICALLY PRESSED COMPONENTS OF T-700 . AIRCRAFT ENGINE. FINAL REPT.
Harper H. , Young (J.C.), Baltgalvis (J.), Weber (H.), John (J.).
Irt Corp San Diego Calif.
Contract DAAJ01-75-0-0895.
Aug. 76, .84p. Rept n°. IRT-6102-003

The Evaluation of two non destructive gas turbines. Turboshaft engines. Neutron radiography. Nondestructive testing. Isostatic pressing. Hot pressing. Gages. Compton scattering. Photons. Scattering. Three dimensional. High resolution. Helicopter engines. Californium. Radioactive Isotopes. 14 02. 21 05.81 04.
T-700 engines. NTISDODXA

AD-A035 181/7SL MD
FEASIBILITY DEMONSTRATION OF USING PULSE LASER HOLOGRAPHIC TECHNIQUES TO INSPECT NAVAL AIRCRAFT ENGINE COMPONENTS. FINAL TECHNICAL REPT...
Jacoby (J.L.), Wright (J.E.).
TRW Systems Group Redondo Beach Calif Space Vehicles Div,
Contract N° 0156-74-C-1580. Proj. F4140l. Task WF41461400.
27 Jun 75, 34p. Rept N° TRW-AT-SVD-TR-75-9

The feasibility of employing pulsed laser holographic int.
Non destructive testing. Turbine blades. Pulsed lasers. Holography. Interferometry. Aircraft entines. Airfoils. Cracks. Inspection. Transients. Vibration. Feasibility studies. Dynamic loads. Turbine wheels. 14 02.21 05.01 03.81 04.82 01.
T-56 engines. TF-41 engines. NTISDODXA

AD-904 725/9SL MD
AIRBORNE ENGINE CONDITION ANALYSIS INSTRUMENTATION (AECAI). FINAL REPT.,.
Harris W.J., Minnear (J.). Chang (J.D.), Ziebarth (H.K.).
Airesearch Mfg CB Los Angeles Calif,
Contract N° 0019-71-C-0304. Distribution limitation now removed.
Jul 72, 262p. Rept N° 72-8518.

Aircraft engines. Monitors. Turbofan engines. Monitors. Jet bombers. Attack bombers. Performance Engineering. Aircraft equipment. Detectors. Instrumentation. Airborne. Degradation. Fuel systems. Oils. Lubricants. Sampling. Control systems. Data processing. Recording systems. Display systems. Non destructive testing. Real time. Acoustic detectors. Vibration. Analysis. 21 05.01 03.

AD/A-000 660/1SL MD
SOME QUESTIONS ON THE CREATION OF AN OPEN STAND FOR ACOUSTIC INVESTIGATIONS OF DTRD'S.
Balmakov (A.I.), Enenkov (V.G.).
Foreign Technology Div Wright-Patterson AFB Ohio,
18. Edited machine trans. of Rizhskii Institut Inzhenervov Gradzhanskoi Aviatsii. Trudy (USSR) n° 174 p. 135-152 1971 by James R. Moore.
22 Oct 74, 25p. Rept n° FTD-MT-24-863-74.

Contemporary methods of experimental research on the acoustic characteristics of DTRD's are examined in the article. Primary attention is given to the full scale experiment on an open stand. The purposes of acoustic investi. Turbofan engines. Test stands. Acoustic emissions. Acoustic fields. Acoustic equipment. Test facilities. USSR. Translations. 21 05.20 01.
NTISDODAF.

AE77-00427 CA-TLSE
PRODUCTION INSPECTION OF NEAR NET SHAPE TURBINE DISKS.
(Méthode de contrôle de Fabrication de disques de turbine forgés pratiquement aux "cotes finies").
Doherty (J.), Lagrotta (J.M.), Wheeler (E.).
AIAA Paper ; N° 77-882 (7/77), 5p. 4réf. bibl. 6 fig. (IAA-A77-38572).
Me 300-1

Contrôle qualité. Moteur aéronef. Turboréacteur. Turbine gaz. Rotor turbine. Disques. Métallurgie poudre.
Contrôle fabrication. Contrôle non destructif. Essai ultrasonique. Cotation fabrication.

AD-A007 850/1SL MD
NONDESTRUCTIVE HOLOGRAPHIC TECHNIQUES FOR STRUCTURES INSPECTION. FINAL TECHNICAL REPT.
1 Jul 71- 30 Apr 74.
Erf (R.K.), Gagosz R.M., Waters 'J.P.), Stetson (K.A.), Aas (H.G.)
United Aircraft Research Labs East Hartford Conn Air Force Materials Lab.
Wright Patterson AFB, Ohio.
Contract F33615-71-C-1874. Proj. AF-7351. Task 735109.
Oct 74, 181p. Rept n° UARL- N991208-36

The theoretical and experimental work, performed during a three year study concerned
Holography. Nondestructive testing. Airframes. Structures. Surface roughness. Compressor blades. Adhesive bonding. Cracks. Detection. Strain Mechanics. 14 02.14 05.01 03.73 04.82 01.51 03.
NTISDODAF

Radiography. Fluorescent screens. Nondestructive testings X ray photography. Photographic materials. Photographic contrast. Photographic images. Aluminium alloys. Titanium alloys. Honeycomb cores. Fractography. Turbine blade.

N78-22101/7SL. CA-TLSE
IN-PLACE RECALIBRATION TECHNIQUE APPLIED TO A CAPACITANCE-TYPE SYSTEM FOR MEASURING ROTOR BLADE TIP CLEARANCE
Earranger (J.P.).
National Aeronautics and Space Administration. Lewis Research Center, Cleveland, Ohio
Apr 78, 35p. NASA-TP-1110, E-9395.

The rotor blade tip clearance measurement system consists of a capacitance sensing probe with self contained tuning elements, a connecting coaxial cable, and remotely located electronics. Tests show that the accuracy of the system suffers from a strong dependence on probe tip temperature
Blade tips. Clearances. Rotor blades Turbomachinery. Capacitance. Calibrating. Coaxial cables. Jet engines. Nondestructive tests. Sensors. Transducers. 21 05.81 04
NTISNASA

N78-11991/4SL CA-TLSE
LA RECHERCHE AEROSPATIALE Bi-Monthly Bulletin N° 1977-2.
European Space Agency, Paris (France)
Tran-Transl. into English of Ic Rech. Aerospatiale, Bull. bimestriel (Paris).
N° 1977-2, Mar. Apr 1977 p. 67-132. Misc-original French Report Available from ONERA, Paris, FF 30.
SeF 77. 181 p. ESA-TT-408
No abstract

Acoustic emission. Boundary layer transition. Holographic interferometry. Thermosetting resins. Trajectory optimization. Cascade flow. Compressibility effects. Fluid mechanics. Incompressible boundary layer. Structural analysis. Switching theory. Turbine blades. Turbulent jets. 01 01.22 03.11 09.05 01.51 01.84 04.71 15.
Translations. France. NTISNASAT.

N74-121 87/2 MD
FLIGHT MONITOR FOR JET ENGINE DISK CRACKS AND THE USE OF CRITICAL LENGTH CRITERION OF FRACTURE MECHANICS
Barranger (J.P.).
National Aeronautics and Space Administration. Lewis Research Center, Cleveland, Ohio.
Nov 73. 21 p. NASA-TN-D- 7483, B-7570.

A disk crack detector is discussed which is intended to operate under flight conditions. It monitors the disk rim for surface cracks emanating from the blade root interface. An eddy current type sensor, with a remotely located capacitance/conductance bridge and signal analyzer, can reliably detect a simulated crack 3mm long.
Crack propagation. Eddy currents. Non destructive tests. Rotating disks. Fracture mechanics. Jet engines. Surface cracks. Turbocompressors.
NASA.

M-76-221487
MAGNETIC POWDER MONITORING OF AIRCRAFT ENGINE BLADES
Aleksandrov (A.G.) , Shellikhov (G.S.)
Defektoskopiya, Jan. Feb. 1976 (1) , 81-85 (Russian)

Turbine blades. Nondestructive testing. Magnetic particle testing.

II. MOTEURS NON EXPLICITEMENT D'AVIONS

A-77-046815 CA-TLSE
HOLOGRAPHIC TESTING IN THE INDUSTRIAL ENVIRONMENT.
Nicholls (D.W.)
Society for Experimental Stress Analysis,
Spring Meeting, Dallas, Tex. May 15-28 1977, Paper. 18 p.

Non destructive tests. Engine parts. Structural Members. Turbines. Holography.

A-77-037645
ADVANCED NONDESTRUCTIVE INSPECTION TECHNIQUES AS APPLIED TO FRACTURE MECHANICS DESIGN FOR TURBINE ENGINE COMPONENTS.
Packman (P.F.)
American Society of Mechanical Engineers, New York.
Fatigue life technology, Proceedings of the Symposium, Philadelphia, Pa. March 27-31 1977, p. 95-116, 19 ref. Contract N° F44626-76-0-0042.

Nondestructive tests. Gas Turbine Engines. Fracture Strength. Engine Tests. Engine parts.

A-77-030173 CA-TLSE
JET ENGINE ISOTOPE INSPECTION
Guillen (J.A.)
World Conference on Nondestructive Testing, 8th , Cannes, France, September 6-11 1976, Proceedings.
Paris, Institut de Soudure, 1976, Section 58, Paper 58-6. 8 p.

Nondestructive tests. Radiography. Radioactive isotopes. Engine tests. Jet engines. Iridium isotopes.

A-76-032141 MD
DEVELOPMENT OF STRESS ENHANCED ULTRASONIC COMPRESSOR BLADE INSPECTION EQUIPMENT
Lake (W.W.), Thorp (J.), Barton (J.R.), Perry (W.D.)
Southwest Research Institute, San Antonio, Tex,
Symposium on Nondestructive Evaluation, 10th, San Antonio, Tex. April 23-25, 1975, Proceedings
p. 181-193, 8refs. Grant N° DAAJ01-73-C-0881.

Gas turbine engines. Ultrasonic tests. Compressor blades. Engine tests.

A-75-046564
PROTON RADIOGRAPHIC DETECTION OF MICROPOROSITY IN AERO-ENGINE TURBINE CASTINGS.
Stafford (P.), Sherwood (A.C.), West (D.)
Non destructive Testing
Vol 8 Oct 1975, p. 235-240

Heat resistant alloys. Turbine blades. Cast alloys. Nondestructive tests. Microporosity. Proton irradiation.

A-74-043166
TURBINE BLADE INSPECTION
Erf (R.K.)
New York , Academic Press, Inc.
1974, p. 343-354, 7 ref. (A74-43151 22-14). Contract N° N00019-69-C-0271.

Turbine blade inspection via holographic interferometry.
Turbine blades. Nondestructive tests. Vibration measurement. Holographic interferometry.

A-74-027452 MD
PARAMETER SELECTION FOR MULTIPLE FAULT DIAGNOSTICS OF GAS TURBINE ENGINES.
Urban (L.A.)
American Society of Mechanical Engineers, Gas Turbine Conference and Products Show, Zurich, Switzerland, Mar 30 Apr 4, 1974, Paper 74-GT-62, 6p.
Parameter selection for multiple fault diagnostics of gas turbine engines. 5ASME paper 74-GT-620

Gas turbine engines. Thermodynamic cycles. Engine monitoring instruments. Nondestructive tests. Engine analyzers.

A-74-027444 MD
RESIDUAL STRESSES IN GAS TURBINE ENGINE COMPONENTS FROM BORKHAUSEN NOISE ANALYSIS.
Barton (J.R.), Kusenberger (F.N.)
American Society of Mechanical Engineers, Gas Turbine Conference and Products Show, Zurich, Switzerland
Mar 30, Apr 4, 1974, Paper 74-GT-51, 9 p. 22 ref.
Residual stresses in gas turbine engine components from Borkhausen noise analysis. 5ASME Paper 74-GT-510

Gas Turbine Engines. Stress Measurement. Nondestructive tests. Residual stress. Engine parts. Engine noise.

A-74-027417 MD
DIAGNOSTIC SONICS FOR GAS TURBINE ENGINES
Zabriskie (C.J.)
American Society of Mechanical Engineers. Gas Turbine Conference and Products Show, Zurich, Switzerland
Mar 30 Apr 4, 1974, Paper 74-GT-18, 10 p.
Diagnostic sonics for gas turbine engines 5ASME Paper 74-GT-180.

Sonograms. Gas turbine engines. Engine monitoring instruments. Nondestructive tests. Acoustic measurements.

A-74-016480 TLSE
NON DESTRUCTIVE INSPECTION OF TITANIUM JET ENGINE DISKS
Vicki (F.J.)
Proceedings of the Second International Conference, Cambridge, Mass.
May 2-5 1972, Volume 1 (A74-16444-05-17) New York, Planum Press, p. 733-741
Non destructive inspection of titanium jet engine disks.

Jet engines. Non-destructive tests. Titanium alloys. Engine parts.

AD-A043 959/6SL CA-TLSE
ULTRASONIC INSPECTION OF CERAMICS CONTAINING SMALL FLOWS. Final Technical Rept.
19 Feb 76 18 Feb 77
Derkacs (T.). Matay (I.M.), Brentnall (W.D.)
TRW Inc Cleveland Ohio, Contract N° 622269-76-C-0148
Mar 77, 77 p. Rept n° TRW-ER-7867-F

A 45 MHz ultrasonic shear wave technique was developed and evaluated for detection of small defects.
Ceramic materials. Defects Materials. Ultrasonic tests. Nondestructive testing. High Frequency. Gas turbines. Silicon carbides. Silicon nitrides. Boron. Doping. Hot pressing. Sintering. Fracture Mechanics. Flexural strength. Shear stresses. Surface finishing. Fractography. 11 02.21 05.14 02.71 04.94 10.81
Ceralloy 147A. NTISDODXA

AD-A040 333/7SL CA-TLSE
A COMPARISON OF VARIOUS NON-DESTRUCTIVE INSPECTION PROCESSES USING HOT ISOSTATICALLY PRESSED POWDER TURBINE PARTS.
Final rept. Jun 75 - Jun 76
Nulk (D.E.)
General Electric Co Lynn Mass Aircraft Engine Group
Contract DAAJ01-75-C 0894
Dec 76. 173 p.
Four emerging NDE (non destructive evaluation) processes.

Non destructive testing. Turbine parts. Powder metallurgy. Hot pressing. Isostatic pressing. Gas turbines. Turboshaft engines. Cracks. Defects materials. Surface analysis. Parasity. Ultrasonic Inspection. Fluorescence. Holography. Acoustic detection. Neutron radiography. Campton scattering. 14 02.21 05.54 10.81 04.
T-700 engines. Nicket alloy Rene 95 . NTISDCDXA

AD-A028 246/7SL MD
WELDED ROTOR INSPECTION DEVELOPMENT PROJECT T55-J-827
Final rept. 1 Jun 75 15 Mar 76
Jain Sushiel, Strautman Victor, Jodon Paul
Avcc Lycoming Div Stratford Conn
Contract DAAJ01-75-C-0339
15 Mar 76. 64 p . Rept n° LYC-76-16

The results of this project show that the pulse-echo techniques used in ultrasonic testing offers the best resolution and flow detectability on a welded rotor shaft. Based on these results, detailed procedures have been established defining acceptance criteria and equipment used. This project also covered
Ultrasonic tests. Nondestructive testing. Gas turbine rotors. Welds. Acoustic emissions. Welded joints. Gas turbines. Electron beam welding. Inertia 21 05.14 02.81 04.73 01
NTISDODXA

AD-A027 357/3SL MD
NONDESTRUCTIVE EVALUATION OF CERAMICS
Final technical rept. 20 Jan 75 19 Apr 76
Derkacs (T.). Matay (I.M.) , Brentnall (W.D.)
TRW Inc Cleveland Ohio , Contract N° 0019-75-C- 0238
19 May 76, 124 p. Rept n° TRW-ER-7798-F

An ultrasonic nondestructive evaluation (UNDE) techniques was developed to successfully detect small defects in gas turbine quality ceramic materials. A high frequency (25-45 MHz), longitudinal wave mode, pulse-reflection.
Gas turbines. Ultrasonic tests. Silicon carbides. Silicon nitrides. Nondestructive testing. High frequency. Ultrasonics. Flexural strength. Hot pressing. Defects materials. Fracture mechanics. Bonding. Sintering. 11 02.71 04.73 01
Refractory materials . NTISDODXA

AD-A008 273/5SL MD
DEVELOPMENT OF NONDESTRUCTIVE INSPECTION EQUIPMENT FOR JET ENGINE COMPRESSOR BLADES
Final Rept. 21 Aug 73 - 31 Jan 75.
Perry (W.D.) , Silvus (H.S.), Barton (J.R.)
Southwest Research Inst San Antonio Tex Army Aviation Systems Command, St. Louis, Mo
Contract DAAJ01-73-C-0881.
Feb. 75, 60 p. Rept N° SWRI-15-3707

The report presents the results of a program to develop a prototype system to semi-automatically inspect compressor blades using the "stress enhanced ultrasonic method" .
Non destructive testing. Compressor blades. Ultrasonic tests. Ultrasonic inspection. Jet engines. Cracks. Fatigue mechanics. Test equipment. 13 08.21 05.14 02.73 01.94 02.81 04.
T-53 engines. NTISDODA

AD-769 317/9 MD
PROBLEMS OF DYNAMICS AND DURABILITY.
Number 229, 1972 (selected articles)
Pallei (Z.S.); Pivovarov (V.A.)
Foreign Technology Div Wright-Patterson AFB, Ohio,
18. Edited machine trans. of Voprosy Dinamiki i Prochnosti (USSR) n° 229 p. 1-74 1972, by Robert Allen Potts.
27 Sep 73, 74 p. Rept n° FTD-MT-24-660-73.

Predicting the service life of the rotor blades of turbines on the basis of equivalent bench tests, Predicting the service life of turbine rotor blades, Analysis of the failures of turbine rotor blade.
Gas turbine blades. Performance Engineering. Life Durability. Rotor blades Turbomachinery. Gas turbines. Failure. Thermal properties. Oscillation. Nondestructive testing. USSR. Translations.
AF.

77-32471/3SL CA-TLSE
HOLOGRAPHY AND APPLICATIONS(GENERALITES SUR L'HOLOGRAPHIE ET SES APPLICATIONS)
Smigielski (P.)
Institut Franco-allemand de recherches, St Louis (France).
Conf-presented at the conf. On inform. sur les Appl. de l'Holographie au controle non destructif, Paris 22 Jun 1976. Language in French
30 Aug 76, 44 p. ISL-CO-209/76

A review of the history and physical principles of holography is presented.
Applications using interferometric holography are discussed with regard to nondestructive tests, dimensional control, dynamic measurement of deformation.
Holographic interferometry. Non destructive tests. Holography. Deformation.
Hydrodynamics. Turvine blades. 14 05.21 05.14 02.82 01.94 10
France. NTISNASAE

N76-33526/4SL MD
INSPECTION OF COMPOSITES USING A COMPUTER-BASED REAL TIME RADIOGRAPHIC FACILITY
Roberts (E.J), Vary (A.)
National Aeronautics and Space Administration. Lewis Research Center, Cleveland, Ohio
Conf-Presentdd at the 2D Conf. on Automated Inspection and Product Control, Chicago, 19-21 Oct 1976
1976 12p. NASA-TM-X-73504

A radiographic inspection facility was developed at the NASA Lewis
Composite materials. Gas turbine engines. Radiography. Research facilities. Digital computers. Epoxy resins. Imaging techniques. Real time operation. Ring structures. Ultrasonic rests. X ray analysis. 21 05.11 04.14 02.81 04.71 06.84 10
Non destructive testing. Diagnostic equipment. NTISNASA

ANL-MSD-78-5 CA-TLSE
NON DESTRUCTIVE EVALUATION TECHNIQUES FOR HIGH TEMPERATURE CERAMIC COMPONENTS
Quarterly Report, January- March 1978
Argonne National Lab. 111 Department of Energy.
Contract W-31-109-ENG-38.
Mar 78, 19p.

The use of holographic interferometry techniques for the nondestructive evaluation of ceramic heat exchanger tubes and ceramic rotors for high temperature (avove 1200 exp O C).
Fossil-fuel power plants. Heat exchangers. Tubes. Ceramics. Gas turbines. Holography. Interferometry. Nondestructive testing. Research programs. Very high temperature. 10 02.14 02.11 02.10 01.21 05.13 11.94 10.97 09.94 09.97 12.81 04. ERDA/200104. ERDA/420500. Electric power plants. Gas turbine rotors. NTISDE.

UCRL-78280 ARC
FLASH RADIOGRAPHIC TECHNIQUE APPLIED TO FUEL INJECTOR SPRAYS
Bahl(K.L.), Vantine (H.C.)
California Univ. Livermore, Lawrence Livermore lab. Energy Research and Development Administration. Contract W.7405-eng-48. American Society for Nondestructive Testing Flash X-Ray Symposium, Houston, Texas, United States of America (USA), 27 Sep 1976. Jun 76 17 p. CONF-760914-4

A flash radiographic technique, using 50 ns exposure times, was used to study the pattern and density dis Fuel injection systems. Furnaces. Gas turbines. Internal combustion engines. Density. Distribution. Droplets. Sprays. X-ray raciography. 21 05.21 07.87 04.81 10
ERDA/330100. ERDA/420500. ERDA/421000. NTISERDA

M-78-220792
USE OF A SEMI-AUTOMATED EDDY CURRENT INSPECTION SYSTEM ON AN INCOLOY 901 MATERIAL
Lewis (R.R.)
ASNT 37th National Fall Conference. ASNT, Columbus, Ohio. 1977, 410-421. (English).

Nickel base alloys. Nondestructive testing. Superalloys. Eddy current testing. Jet engines. Turbines. Cracks, Incoloy 901 NI. SP

M-78-220764
ACOUSTIC EMISSION FLOW DETECTION IN TURBINE COMPRESSOR BLADES
Green (A.T.), Fricker (R.), Weir (D.B.)
ASNT 37th National Fall Conference. ASNT, Columbus, Ohio 1977, 19-21 . (English).

Turbine Blades. Nondestructive testing. Acoustic emission.

M-78-220761
CRACK DETECTION BY HOLOGRAM INTERFEROMETRY
Zarutskii (M.A.)
Sov. Phys. Tech. Phys. May 1977, 47, (5) , 641-642 (English).

Holography. Crack propagation. Turbine blades. Flow detection.

M-78-220588
COMPOSITE FAN BLADES CAN BE INSPECTED HOLOGRAPHICALLY
Delgrosso (E.J.); Carlson (C.E.)
Automot. Eng. Dec. 1977, 85 (12) , 62-65 (English).

Turbine blades. Nondestructive testing. Titanium base alloys. Composite materials. Baron. Aluminium Holography. Ti-6Al-4V. TI.

M-78-220240
POSSIBILITIES OF LOW TEMPERATURE RADIOGRAPHY
Kaor (P.)
Br. J. Non-destr. Test. Sep 1977, 19 (5) , 239-241. (English).

Turbine blades . Nondestructive testing. Radiography. Low temperature.

M-77-221371
INSPECTION OF JET ENGINES WITH ISOTOPES
Martinez (J.A.G.)
Nondestructive Testing. Asoc Espanolo Paro el Control de la Calidad, Bilbao.1976- 121-125 (Spanish).

Jet engines. Nondestructive testing. Inspection. Radiography. Radioisotopes.

M-77-221375
INSPECTION OF JET ENGINES WITH THE BOROSCOPE
Rubio (J.)
Nondestructive testing. Asoc Espanola Paro el Control de la Calidad, Bilbao 1976, 157-163 (Spanish).

Jet engines. Nondestructive testing. Inspection. Maintenance

M-77-220985
INSPECTION OF WELDS BY AN ACOUSTIC-EMISSION METHOD DURING ELECTRON-BEAM WELDING.
Bolotin (Y.I.) , Belov (V.M.)
Svar. Proizvod. Apr 1976 (4), 29-31 (Russian).

Chromium steels. Welding. Electron beam welding. Welded joints. Nondestructive testing. Turbine blades. Acoustic emission.

M-77-220033
PROVOCATIVE TECHNIQUES IN THERMAL NDT IMAGING.
Trezek (G.J.), Balk (S.)
Mater. Eval. , Auf. 1976, 34, (8), 173-176 (English).

Turbine blades. Nondestructive testing. Thermal radiation. Flow detection.

M-76-220981
TESTING COMPLEX-SHAPED PARTS BY THE ULTRASONIC ECHO METEODS
Shraiber (D.S.)
Defektoskopiga. Nov.- Dec 1975 (6) 17-25 (Russian)

Turbine blades. Nondestructive testing. Ultrasonic testing.

M-76-220292
APPARATUS FOR MEASURING BLADE DISPLACEMENTS IN FULL-SCALE TURBODYNAMO DISCS.
Ostopchuk (II)
Probl. Prachn. Sep 1975 (9) 100-101 (Russian)

Stainless steels. Dimensional analysis. Nickel base alloys. Testing equipment . Design. Nondestructive testing. Turbine blades.

M-76-220269
NON DESTRUCTIVE TESTING ON INCONEL TURBINE BLADES USING SMALL ANGLE NEUTRON SCATTERING.
Cherubini G. , Olivi A. , Pizzi F. , Walther H.
Metall. Ital. June 1975, 67 (6) , 315-319 (Italian).

Superalloys. Nondestructive testing. Nickel base alloys. Turbine blades. Neutron radiography. Inconel X750. SP. NI. Inconel 700

M-76-220064
ULTRASONIC TESTING OF METAL-METAL SOND IN INTERNAL COMBUSTION ENGINE CYLINDERS
Deputat (J.) Pawlowski (Z) , Rulka (R.)
Paper N° C-49, 7th International Conference on Nondestructive testing, Warsaw, Poland. 1973, 9p. (Pamphlet) . (English).

Engine cylinders. Nondestructive testing. Cast iron. Aluminium. Ultrasonic testing. Adhesive bonding.

M-75-220377
SHARP FOCUS IMPROVES X-RAY ANALYSIS
Spaulding (W.H.)
Met. Prog. Dec 1974, 106 (7) , 86-88 (English)

Jet Engines, Nondestructive testing. Welded Joints. Titanium base alloys. Radiography.

M-75-220012
SIGNAL TO NOISE RATIO IN THE INSPECTION PENETRANT PROCESS
Alburget (J.R.)
Mater. Eval. Sep 1974 22, (9), 193-200 (English).

Fluid penetrant testing. Penetrants. Acoustic measurement. Turbine blades. Nondestructive testing.

M-74-510500
INCREASING THE SOUNDNESS OF TURBINE BLADE CASTINGS BY THE LOST WAX PROCESS.
Shpindler (S.S.), Portnoy (YP) Kalashnikova (K.N.) , Grigorash (E.P.)
Liteino. Proizv, Feb 1974 (2) , 2-3 (Russian).

Turbine blades. Casting. Heat resistant alloys. Investment casting. Casting defects. Non destructive testing.

M-74-220333
HIGH ENERGY RADIOGRAPHY - A NEW TECHNIQUE IN THE DEVELOPMENT OF EFFICIENCY AND INTEGRITY IN AERO C.S TURBINE ENGINES.
Pullen D.A.W.
Mater. Eval. Feb. 1974, 32 (2) 25-30 , 37. (English).

Jet Engines. Nondestructive testing. Radiography. Linear accelerators.

REPORT DOCUMENTATION PAGE

1. Recipient's Reference	2. Originator's Reference	3. Further Reference	4. Security Classification of Document
	AGARD-LS-103	ISBN 92-835-0237-X	UNCLASSIFIED

5. Originator Advisory Group for Aerospace Research and Development
North Atlantic Treaty Organization
7 rue Ancelle, 92200 Neuilly sur Seine, France

6. Title NON-DESTRUCTIVE INSPECTION METHODS FOR PROPULSION SYSTEMS AND COMPONENTS

7. Presented on 23–24 April 1979 in London, UK, and on 26–27 April 1979 in Milan, Italy.

8. Author(s)/Editor(s)	9. Date
Various	April 1979
10. Author's/Editor's Address	**11. Pages**
Various	156

12. Distribution Statement This document is distributed in accordance with AGARD policies and regulations, which are outlined on the Outside Back Covers of all AGARD publications.

13. Keywords/Descriptors

Nondestructive tests
Turbines
Compressors
Turbine components
Engines
Ultrasonic tests
Magnetic tests
Eddy current tests
Holography

14. Abstract

This Lecture Series No.103 on the subject of Non-Destructive Inspection Methods for Propulsion and Components is sponsored by the Propulsion and Energetics Panel of AGARD and implemented by the Consultant and Exchange Programme.

The safety in use of mechanical systems is dependent on the identification of possible defects in their component parts. This particularly applies to turbine engines, certain components of which, especially turbine and compressor discs and blades, are subjected to particularly severe stresses; creep, low cycle fatigue, thermal fatigue.

These potential defects must be detected, on the one hand when the parts are at the manufacturing stage and, on the other, during periodic inspections in service.

It is, therefore, essential to have available non-destructive inspection methods which, while they are accurate and sensitive, can be used in the workshop for the detection of even minor defects and cracks.

A considerable amount of research work has been done throughout the world in this field and has led to the development of various methods; ultrasonic, magnetometer, X-ray. New procedures, which are complementary to these now conventional methods, are in process of development or optimization; acoustic emission, laser holography, eddy current etc.

The aim of this Lecture Series is to survey the means currently available, with particular emphasis on the intrinsic possibilities and present limitations of the non-destructive inspection methods most widely applied to turbine engines, and to describe the state of progress of research on more recent methods.

AGARD Lecture Series No.103
Advisory Group for Aerospace Research and Development, NATO
NON-DESTRUCTIVE INSPECTION METHODS FOR PROPULSION SYSTEMS AND COMPONENTS
Published April 1979
156 pages, including Bibliography of 54 items

This Lecture Series No.103 on the subject of Non-Destructive Inspection Methods for Propulsion Systems and Components is sponsored by the Propulsion and Energetics Panel of AGARD and implemented by the Consultant and Exchange Programme.

The safety in use of mechanical systems is dependent on the identification of possible defects in their component parts. This particularly applies to turbine engines, certain components of which, especially turbine and compressor discs and blades, are subjected to particularly severe stresses; creep, low cycle fatigue, thermal fatigue.

P.T.O.

AGARD-LS-103

Nondestructive tests
Turbines
Compressors
Turbine components
Engines
Ultrasonic tests
Magnetic tests
Eddy current tests
Holography

AGARD Lecture Series No.103
Advisory Group for Aerospace Research and Development, NATO
NON-DESTRUCTIVE INSPECTION METHODS FOR PROPULSION SYSTEMS AND COMPONENTS
Published April 1979
156 pages, including Bibliography of 54 items

This Lecture Series No.103 on the subject of Non-Destructive Inspection Methods for Propulsion Systems and Components is sponsored by the Propulsion and Energetics Panel of AGARD and implemented by the Consultant and Exchange Programme.

The safety in use of mechanical systems is dependent on the identification of possible defects in their component parts. This particularly applies to turbine engines, certain components of which, especially turbine and compressor discs and blades, are subjected to particularly severe stresses; creep, low cycle fatigue, thermal fatigue.

P.T.O.

AGARD-LS-103

Nondestructive tests
Turbines
Compressors
Turbine components
Engines
Ultrasonic tests
Magnetic tests
Eddy current tests
Holography

AGARD Lecture Series No.103
Advisory Group for Aerospace Research and Development, NATO
NON-DESTRUCTIVE INSPECTION METHODS FOR PROPULSION SYSTEMS AND COMPONENTS
Published April 1979
156 pages, including Bibliography of 54 items

This Lecture Series No.103 on the subject of Non-Destructive Inspection Methods for Propulsion Systems and Components is sponsored by the Propulsion and Energetics Panel of AGARD and implemented by the Consultant and Exchange Programme.

The safety in use of mechanical systems is dependent on the identification of possible defects in their component parts. This particularly applies to turbine engines, certain components of which, especially turbine and compressor discs and blades, are subjected to particularly severe stresses; creep, low cycle fatigue, thermal fatigue.

P.T.O.

AGARD-LS-103

Nondestructive tests
Turbines
Compressors
Turbine components
Engines
Ultrasonic tests
Magnetic tests
Eddy current tests
Holography

AGARD Lecture Series No.103
Advisory Group for Aerospace Research and Development, NATO
NON-DESTRUCTIVE INSPECTION METHODS FOR PROPULSION SYSTEMS AND COMPONENTS
Published April 1979
156 pages, including Bibliography of 54 items

This Lecture Series No.103 on the subject of Non-Destructive Inspection Methods for Propulsion Systems and Components is sponsored by the Propulsion and Energetics Panel of AGARD and implemented by the Consultant and Exchange Programme.

The safety in use of mechanical systems is dependent on the identification of possible defects in their component parts. This particularly applies to turbine engines, certain components of which, especially turbine and compressor discs and blades, are subjected to particularly severe stresses; creep, low cycle fatigue, thermal fatigue.

P.T.O.

AGARD-LS-103

Nondestructive tests
Turbines
Compressors
Turbine components
Engines
Ultrasonic tests
Magnetic tests
Eddy current tests
Holography

These potential defects must be detected, on the one hand when the parts are at the manufacturing stage and, on the other, during periodic inspections in service.

It is, therefore, essential to have available non-destructive inspection methods which, while they are accurate and sensitive, can be used in the workshop for the detection of even minor defects and cracks.

A considerable amount of research work has been done throughout the world in this field and has led to the development of various methods; ultrasonic, magnetometer, X-ray. New procedures, which are complementary to these now conventional methods, are in process of development or optimization; acoustic emission, laser holography, eddy current etc.

The aim of this Lecture Series is to survey the means currently available, with particular emphasis on the intrinsic possibilities and present limitations of the non-destructive inspection methods most widely applied to turbine engines, and to describe the state of progress of research on more recent methods.

The material in this publication was assembled to support a Lecture Series under the sponsorship of the Propulsion and Energetics Panel and the Consultant and Exchange Programme of AGARD and presented on 23–24 April 1979 in London, UK, and on 26–27 April 1979 in Milan, Italy.

ISBN 92-835-0237-X

These potential defects must be detected, on the one hand when the parts are at the manufacturing stage and, on the other, during periodic inspections in service.

It is, therefore, essential to have available non-destructive inspection methods which, while they are accurate and sensitive, can be used in the workshop for the detection of even minor defects and cracks.

A considerable amount of research work has been done throughout the world in this field and has led to the development of various methods; ultrasonic, magnetometer, X-ray. New procedures, which are complementary to these now conventional methods, are in process of development or optimization; acoustic emission, laser holography, eddy current etc.

The aim of this Lecture Series is to survey the means currently available, with particular emphasis on the intrinsic possibilities and present limitations of the non-destructive inspection methods most widely applied to turbine engines, and to describe the state of progress of research on more recent methods.

The material in this publication was assembled to support a Lecture Series under the sponsorship of the Propulsion and Energetics Panel and the Consultant and Exchange Programme of AGARD and presented on 23–24 April 1979 in London, UK, and on 26–27 April 1979 in Milan, Italy.

ISBN 92-835-0237-X

These potential defects must be detected, on the one hand when the parts are at the manufacturing stage and, on the other, during periodic inspections in service.

It is, therefore, essential to have available non-destructive inspection methods which, while they are accurate and sensitive, can be used in the workshop for the detection of even minor defects and cracks.

A considerable amount of research work has been done throughout the world in this field and has led to the development of various methods; ultrasonic, magnetometer, X-ray. New procedures, which are complementary to these now conventional methods, are in process of development or optimization; acoustic emission, laser holography, eddy current etc.

The aim of this Lecture Series is to survey the means currently available, with particular emphasis on the intrinsic possibilities and present limitations of the non-destructive inspection methods most widely applied to turbine engines, and to describe the state of progress of research on more recent methods.

The material in this publication was assembled to support a Lecture Series under the sponsorship of the Propulsion and Energetics Panel and the Consultant and Exchange Programme of AGARD and presented on 23–24 April 1979 in London, UK, and on 26–27 April 1979 in Milan, Italy.

ISBN 92-835-0237-X

These potential defects must be detected, on the one hand when the parts are at the manufacturing stage and, on the other, during periodic inspections in service.

It is, therefore, essential to have available non-destructive inspection methods which, while they are accurate and sensitive, can be used in the workshop for the detection of even minor defects and cracks.

A considerable amount of research work has been done throughout the world in this field and has led to the development of various methods; ultrasonic, magnetometer, X-ray. New procedures, which are complementary to these now conventional methods, are in process of development or optimization; acoustic emission, laser holography, eddy current etc.

The aim of this Lecture Series is to survey the means currently available, with particular emphasis on the intrinsic possibilities and present limitations of the non-destructive inspection methods most widely applied to turbine engines, and to describe the state of progress of research on more recent methods.

The material in this publication was assembled to support a Lecture Series under the sponsorship of the Propulsion and Energetics Panel and the Consultant and Exchange Programme of AGARD and presented on 23–24 April 1979 in London, UK, and on 26–27 April 1979 in Milan, Italy.

ISBN 92-835-0237-X

AGARD
NATO ⊕ OTAN
7 RUE ANCELLE · 92200 NEUILLY-SUR-SEINE
FRANCE
Telephone 745.08.10 · Telex 610176

DISTRIBUTION OF UNCLASSIFIED AGARD PUBLICATIONS

AGARD does NOT hold stocks of AGARD publications at the above address for general distribution. Initial distribution of AGARD publications is made to AGARD Member Nations through the following National Distribution Centres. Further copies are sometimes available from these Centres, but if not may be purchased in Microfiche or Photocopy form from the Purchase Agencies listed below.

NATIONAL DISTRIBUTION CENTRES

BELGIUM
Coordonnateur AGARD – VSL
Etat-Major de la Force Aérienne
Quartier Reine Elisabeth
Rue d'Evere, 1140 Bruxelles

CANADA
Defence Scientific Information Service
Department of National Defence
Ottawa, Ontario K1A 0Z2

DENMARK
Danish Defence Research Board
Østerbrogades Kaserne
Copenhagen Ø

FRANCE
O.N.E.R.A. (Direction)
29 Avenue de la Division Leclerc
92 Châtillon sous Bagneux

GERMANY
Zentralstelle für Luft- und Raumfahrt-dokumentation und -information
c/o Fachinformationszentrum Energie, Physik, Mathematik GmbH
Kernforschungszentrum
7514 Eggenstein-Leopoldshafen 2

GREECE
Hellenic Air Force General Staff
Research and Development Directorate
Holargos, Athens, Greece

ICELAND
Director of Aviation
c/o Flugrad
Reykjavik

ITALY
Aeronautica Militare
Ufficio del Delegato Nazionale all'AGARD
3, Piazzale Adenauer
Roma/EUR

LUXEMBOURG
See Belgium

NETHERLANDS
Netherlands Delegation to AGARD
National Aerospace Laboratory, NLR
P.O. Box 126
Delft

NORWAY
Norwegian Defence Research Establishment
Main Library
P.O. Box 25
N-2007 Kjeller

PORTUGAL
Direcção do Serviço de Material da Força Aerea
Rua da Escola Politecnica 42
Lisboa
Attn: AGARD National Delegate

TURKEY
Department of Research and Development (ARGE)
Ministry of National Defence, Ankara

UNITED KINGDOM
Defence Research Information Centre
Station Square House
St. Mary Cray
Orpington, Kent BR5 3RE

UNITED STATES
National Aeronautics and Space Administration (NASA)
Langley Field, Virginia 23365
Attn: Report Distribution and Storage Unit

THE UNITED STATES NATIONAL DISTRIBUTION CENTRE (NASA) DOES NOT HOLD STOCKS OF AGARD PUBLICATIONS, AND APPLICATIONS FOR COPIES SHOULD BE MADE DIRECT TO THE NATIONAL TECHNICAL INFORMATION SERVICE (NTIS) AT THE ADDRESS BELOW.

PURCHASE AGENCIES

Microfiche or Photocopy
National Technical
Information Service (NTIS)
5285 Port Royal Road
Springfield
Virginia 22161, USA

Microfiche
Space Documentation Service
European Space Agency
10, rue Mario Nikis
75015 Paris, France

Microfiche
Technology Reports
Centre (DTI)
Station Square House
St. Mary Cray
Orpington, Kent BR5 3RF
England

Requests for microfiche or photocopies of AGARD documents should include the AGARD serial number, title, author or editor, and publication date. Requests to NTIS should include the NASA accession report number. Full bibliographical references and abstracts of AGARD publications are given in the following journals:

Scientific and Technical Aerospace Reports (STAR)
published by NASA Scientific and Technical
Information Facility
Post Office Box 8757
Baltimore/Washington International Airport
Maryland 21240, USA

Government Reports Announcements (GRA)
published by the National Technical
Information Services, Springfield
Virginia 22161, USA

Printed by Technical Editing and Reproduction Ltd
Harford House, 7–9 Charlotte St, London W1P 1HD

ISBN 92-835-0237-X